

Photosensitizers and natural compounds attenuate the Tau aggregation and restore the signalling cascades of Tau

by

Tushar Dubey
10BB15A26043

**A thesis submitted to the
Academy of Scientific & Innovative Research
for the award of the degree of
DOCTOR OF PHILOSOPHY
In
SCIENCE**

**Under the supervision of
Dr. Subashchandrabose Chinnathambi**



**CSIR-National Chemical Laboratory,
Pune**



**Academy of Scientific and Innovative Research
AcSIR Headquarters, CSIR-HRDC campus
Sector 19, Kamla Nehru Nagar,
Ghaziabad, U.P. – 201002, India**

April - 2022

Certificate

This is to certify that the work incorporated in this Ph.D. thesis entitled, “**Photosensitizers and natural compounds attenuate the Tau aggregation and restore the signalling cascades of Tau**”, submitted by **Tushar Dubey** to the Academy of Scientific and Innovative Research (AcSIR) in fulfillment of the requirements for the award of the Degree in Sciences, embodies original research work carried-out by the student. We, further certify that this work has not been submitted to any other University or Institution in part or full for the award of any degree or diploma. Research material(s) obtained from other source(s) and used in this research work has/have been duly acknowledged in the thesis. Image(s), illustration(s), figure(s), table(s) etc., used in the thesis from other source(s), have also been duly cited and acknowledged.



(Signature of Student)

Tushar Dubey

Date: 11/04/2022



(Signature of Supervisor)

Dr. Subashchandraboze Chinnathambi

Date: 11/04/2022

STATEMENTS OF ACADEMIC INTEGRITY

I **Tushar Dubey**, a Ph.D. student of the Academy of Scientific and Innovative Research (AcSIR) with Registration No. **10BB15A26043** hereby undertake that, the thesis entitled **“Photosensitizers and natural compounds attenuate the Tau aggregation and restore the signalling cascades of Tau”** has been prepared by me and that the document reports original work carried out by me and is free of any plagiarism in compliance with the UGC Regulations on *“Promotion of Academic Integrity and Prevention of Plagiarism in Higher Educational Institutions (2018)”* and the CSIR Guidelines for *“Ethics in Research and in Governance (2020)”*.



Signature of the Student

Date : 11/04/2022

Place : Pune

It is hereby certified that the work done by the student, under my guidance, is plagiarism-free in accordance with the UGC Regulations on *“Promotion of Academic Integrity and Prevention of Plagiarism in Higher Educational Institutions (2018)”* and the CSIR Guidelines for *“Ethics in Research and in Governance (2020)”*.



Signature of the Advisor/ Supervisor

Acknowledgements

The journey of my PhD. was always gifted me innumerable challenges, which sometimes broke me and sometimes made me stronger. The completion of this journey would have been impossible without the kind help of many people whom I met along this journey. The journey along with its people have transformed me into a more confident and capable individual.

The first person, whom I should acknowledge is certainly the one who granted me opportunity to work under his guidance and showed faith on me that no matter how many blunders I do, I will do something better in Science. I am highly obliged to my research mentor Dr. Subashchandrabose Chinnathambi for granting the opportunity to work with him and for his immense patience with me and my research work. I would like to thank him for his constant support throughout my tenure. Whenever I faced any challenge, I used to have confidence that "Sir" is there he will help me to come out of this situation. In each and every discussion he encouraged the scientific thinking in me. I always used to bring crazy ideas but he always supported me. He has provided his valuable and critical comments, which has aided in improving the quality of work.

I am grateful to Director, CSIR-National Chemical Laboratory for the opportunity to do my doctoral work and Chair, Biochemical Sciences for providing divisional facilities. I wish to convey my regards to Dr. Dhanasekaran Shanmugam and Dr. Mahesh Kulkarni for helping us to utilize the animal cell culture lab. I would like to thank university grant commission (UGC) and CSIR for providing the financial aid to our laboratory. I am thankful to Academy of Scientific and Innovative Research (AcSIR) for the academic proceedings for PhD. I would like to thank CSIR healthcare, DBT Neuroscience, National microglia mission project, DST-Health Sciences for supporting us for the lab facilities.

I would like to extend my gratitude to my Doctoral Advisory Committee members, Dr. Suresh Bhat, Dr. Dhanasekaran Shanmugam and Dr. Mahesh Dharne for constantly monitoring my research progress and providing essential suggestions to improve the work.

I sincerely thank all the labs and members of the Biochemical Sciences Division for their help in using their lab facilities. I am thankful to Dr. Dhanasekaran and his lab members Dr. Anurag, Dr. Meenakshi, Dr. Rahul, Dr. Rupali, Parag, Sindhuri, Tejashri and Ajinkya. I would like to thank Dr. Sureshkumar Ramasamy and his lab members Dr. Manu, Dr. Deepak, Dr. Ameya, Dr. Yashpal, Dr. Vijay, Dr. Deepanjan and Debjyoti for allowing me to use the instrumental facilities.

I would sincerely like to thank the people who made this journey feasible and interesting, my lab mates. Thank you Dr. Nalini Gorantla, Dr. Shweta Sonawane, Dr. Abhishek Balmik, Rashmi, Smita, and Hari, without you guys I possibly wouldn't have made it this far. My special thanks to Dr. Nalini who helped and in my work from the beginning of my journey in this lab. I learned several techniques from her and she was always a strong support for me throughout my journey. These people are more like a family to me. I thank them for always being there and encouraging me during my rough times. I would like to thank my trainees Dhey Vyas, Anouska and Preksha their contributions in my studies.

I would like to thank my collaborators Dr. Thulsiram for the purification and characterization of various herbal extracts. I would like to extend my sincere thanks to Dr. Chandreshekhra from university of Mysore for the *Drosophila* studies.

I would extend my gratitude to Central to Central Electron Microscopy facility and Mr. Gholap from Centre for Material Characterization for the access to the T20 electron microscope. I thank Venkatesh for his immense help in scanning the TEM samples. I thank Dr. Moneesha Fernandes, Organic Chemistry Division, for giving me access to her Circular Dichroism facility.

I am highly obliged to my parents Mrs. Manjula Dubey, Mr. Ashutosh Dubey and my grandmother Dr. Vidhya Dubey. I thank them for always standing strong with me, supporting and having faith in all my decisions. They have been the strongest pillars of my life.

Thank You

List of Abbreviations

Aβ	Amyloid-β
AD	Alzheimer's disease
PDT	Photodynamic treatment
PS	Photosensitizer
PD	Parkinson's disease
APP	Amyloid-precursor protein
BBB	Blood-brain-barrier
Nrf-2	Nuclear factor erythroid 2-related factor 2
CD	Circular Dichroism
EB1	End-binding protein 1
BME	<i>Bacopa monnieri</i> extract
HD	Huntington's disease
MTT	(3-(4,5-Dimethylthiazol-2-yl)-2,5-Diphenyltetrazolium Bromide)
GSK-3β	Glycogen synthase kinase-3
Nup358	Nucleoporins 358
RB	Rose Bengal
TB	Toluidine Blue
NDs	Neurodegenerative diseases
PHFs	Paired helical filaments
PTMs	Post-translational modifications
ROS	Reactive oxygen species
SEC	Size-exclusion chromatography
TEM	Transmission electron microscopy
ThS	Thioflavin S

List of figures

Figure No.	Title	Page No.
Figure 1	The physiological role of Tau	13
Figure 2	The domain organization of natively unfolded Tau	14
Figure 3	The pathological role of Tau	15
Figure 4	The screening of Tau aggregation inhibitors	16
Figure 5	The principle and components of photodynamic therapy	17
Figure 6	Introduction to Ayurveda	21
Figure 7	The nootropic property of <i>Bacopa monnieri</i>	23
Figure 8	The <i>in-vitro</i> Tau aggregation inhibition by TB	39
Figure 9	Disaggregation of Pre-formed Tau aggregates by PE-TB	40
Figure 10	TB inhibited the aggregation of repeat Tau <i>in vitro</i>	41
Figure 11	PE-TB disaggregated pre-formed mature repeat Tau aggregates	42
Figure 12	The biocompatibility of TB	43
Figure 13	TB modulated tubulin cytoskeleton of neurons	44
Figure 14	Modulation of actin cytoskeleton by TB and PE-TB	45
Figure 15	TB and PE-TB modulated EB1 level in neuronal cells	45
Figure 16	TB and PE-TB improved the longevity and learning behavior of UAS E-14 Tau mutant of <i>Drosophila</i>	46
Figure 17	RB inhibits the aggregation of Tau <i>in vitro</i>	48
Figure 18	PE-RB disaggregates mature Tau fibrils <i>in vitro</i>	49
Figure 19	The effect of RB and PE-RB on neuroblastoma cells	50
Figure 20	RB and PE-RB modulate the Tubulin cytoskeleton	50
Figure 21	RB and PE-RB modulate the actin cytoskeleton	51
Figure 22	RB and PE-RB induces Podosome-like structures	51
Figure 23	RB and PE-RB show neuroprotection in UAS E-14 Tau mutant of <i>Drosophila</i>	52
Figure 24	The phytochemical extraction of <i>Bacopa Monnieri</i>	54
Figure 25	BME attenuated the aggregation of soluble Tau <i>in vitro</i>	55
Figure 26	BME disaggregated the mature pre-formed aggregates	56
Figure 27	BME rescues the neuron from Tau-mediated toxicity	57
Figure 28	BME modulated the Nrf2 level in cells	58
Figure 29	BME restored the Nup358 arrangement	59

Figure 30	BME modulated the GSK-3 β phosphorylation	59
Figure 31	BME reduced the Tau phosphorylation	60
Figure 32	The photo-excited dyes disaggregates the protein aggregates	64
Figure 33	Cytoskeleton modulation by photo-excited dyes	65
Figure 34	The <i>Bacopa monnieri</i> extract (BME) have neuroprotective property against Tau toxicity	70
Figure 35.	The schematic diagram demonstrating further aspects of study	72

List of Tables

Table No.	Title	Page No.
Table 1	The clinically approved photosensitizers	19
Table 2	LC-HRMS analysis of <i>Bacopa monnieri</i> extract (BME)	60
Table 3	The herbs prescribed in Ayurveda for neurological disorders	67

Contents

	Page No.
Chapter 1 Introduction	12
1.1 Alzheimer's disease and protein aggregation	12
1.2 Tau protein	12
1.3 Tau aggregation inhibitors	14
1.4 The introduction to Photodynamic therapy	16
1.4.1 The principle of Photodynamic therapy	16
1.4.2 The introduction to Photosensitize	17
1.4.3 Dyes in diagnosis and therapeutics against neurodegenerative disease	18
1.4.4 Photo-excited dyes: novel approach against AD	20
1.5 Ayurveda and its role in neuroprotection	20
1.5.1 Introduction to Ayurveda	20
1.5.2 Neuroprotective herbs in Ayurveda	21
1.5.3 <i>Bacopa monnieri</i>: Nootropic herb in Ayurveda	22
1.5.4 The neuroprotective property of <i>Bacopa monnieri</i>	23
Aims of the Study	25
Chapter 2 Materials and methods	26
2.1.1 List of chemicals and cell growth media	27
2.1.2 List of antibodies	27
2.1.3 Laboratory Instruments and Equipment	28
2.2 Sodium dodecyl sulphate–polyacrylamide gel electrophoresis	29
2.3 Protein purification	29
2.3.1 Expression of protein in bacteria	29
2.3.2 Purification of protein by cation-exchange chromatography	29
2.3.3 Purification of protein by size-exclusion chromatography	29
2.3.4 Estimation of protein concentration	30
2.3.5 Tau aggregation	30
2.3.6 ThS fluorescence assay	30
2.3.7 Transmission electron microscopy	30
2.3.8 Sedimentation assay	31
2.3.9 CD spectroscopy	31
2.4 Photodynamic treatment assay	32
2.5 Cytotoxicity assay	32
2.6 ROS Production	32
2.7 Western Blotting	33
2.7.1 Protein extraction form cells	33
2.7.2 The western Blotting	33
2.7.3 Stripping procedure	33
2.8 Immunofluorescence microscopy	33
2.9 Drosophila experiments	34

2.9.1 Fly Stocks and Genetics	34
2.9.2 Fly husbandry	34
2.9.3 Preparation of TB/RB-supplemented diet	34
2.9.4 Larval feeding behaviour assay	34
2.9.5 Fecundity assay	34
2.9.6 Negative geotaxis assay	34
2.9.7 Viability of fly from egg to adult	35
2.9.8 Larval olfactory behaviour	35
2.10 Preparation of ethanolic extract of <i>Bacopa monnieri</i>	35
2.10.1 The preparation of <i>Bacopa monnieri</i> extract	35
2.10.2 HPLC and TLC Conditions	36
2.10.3 UPLC–ESI (+)-MS condition	36
2.11 Statistical data analysis	36
Chapter 3 Photo-excited Toluidine Blue Inhibits Tau Aggregation in Alzheimer’s disease	37
3.1 Background	37
3.2 Results	38
3.2.1 Toluidine Blue inhibited the aggregation of full-length Tau <i>in vitro</i>	38
3.2.2 Photo-excited Toluidine Blue disaggregates full-length Tau aggregates <i>in vitro</i>	39
3.2.3 TB inhibited the aggregation of repeat Tau <i>in vitro</i>	40
3.2.4 Photo-excited TB potentially disaggregated the pre-formed repeat Tau aggregates	41
3.2.5 The biocompatibility of Toluidine Blue in neuronal cells	41
3.2.6 Toluidine Blue and photo-excited Toluidine Blue modulate the cytoskeleton of neuronal cells	43
3.2.7 TB modulates the EB1 levels in neuronal cells	44
3.2.8 Toluidine Blue and photo-excited Toluidine Blue modulate the longevity and learning in UAS E-14 Tau mutant of <i>Drosophila</i>	45
3.3 Summary	46
Chapter 4 Photodynamic exposure of Rose-Bengal inhibits Tau aggregation and modulates cytoskeletal network in neuronal cells	47
4.1 Background	47
4.2 Results	47
4.2.1 Attenuation of <i>in vitro</i> Tau aggregation by RB	47
4.2.2 Photo-excited RB disaggregates the pre-formed Tau aggregates	47
4.2.3 RB induces no adverse effect of neuronal viability	48
4.2.4 RB and PE-RB modulate the tubulin cytoskeleton	49
4.2.5 RB and PE-RB modulate actin cytoskeleton	50

4.2.6 RB and PE-RB ameliorate the longevity and memory in UAS E-14 Tau mutant of <i>Drosophila</i>	51
4.3 Summary	52
Chapter 5 Ethanol extract of <i>Bacopa monnieri</i> attenuates the in-vitro Tau aggregation, Tau phosphorylation, and Tau-mediated toxicity	53
5.1 Background	53
5.2 Results	53
5.2.1 Phytochemical extraction and characterization of <i>Bacopa monnieri</i>	53
5.2.2 BME potentially modulated the aggregation of full-length Tau	54
5.2.3 The disaggregation of pre-formed Tau fibrils by BME	54
5.2.4 The rejuvenating property of BME in neuronal cells	55
5.2.5 BME modulated the Nrf2 levels in neurons	56
5.2.6 BME restores the nuclear transport in neuronal cells	57
5.2.7 BME modulates GSK-3β phosphorylation in neurons	57
5.2.8 BME reduced the formaldehyde-mediated Tau phosphorylation	58
5.3 Summary	61
Chapter 6 Discussion	62
6.1 The diverse role of Tau in neuron	62
6.2 Tau phosphorylation and Neurotoxicity	62
6.3 The effect of photo-excited molecules on protein aggregates	63
6.4 Cytoskeleton deformities and PDT	65
6.5 Ayurveda and neurodegeneration	67
6.6 The rejuvenating effect of BME	69
6.7 The antioxidant property of BME	69
6.8 BME recued Tau phosphorylation	69
Future directions	72
Bibliography	73
Abstract	85
List of publications in SCI journals	86
List of poster presentation in various conferences	87
Publications	89

Abstract

Name of the Student: Tushar Dubey	Registration No. : 10BB15A26043
Faculty of Study: Biological Sciences	Year of Submission : 2022
CSIR Lab: CSIR-National Chemical laboratory	Name of the Supervisor: Dr. Subashchandrabose Chinnathambi

Title of the thesis: Photosensitizers and natural compounds attenuate the Tau aggregation and restore the signalling cascades of Tau

Abstract

The intracellular Tau aggregates are known to be associated with Alzheimer's disease. The inhibition of Tau aggregation is an important strategy for screening of therapeutic molecules in Alzheimer's disease. Various compounds of natural and synthetic origins have been screened for the potency against Tau aggregation. The photo-excited dyes showed inhibitory effect on amyloid protein aggregation and toxicity. In the present work, we studied the effect of two acknowledged photosensitizers Toluidine Blue (TB) and Rose Bengal (RB) against Tau aggregation. The aim of this work was to study the protective role of these dyes against Tau aggregation and cytoskeleton modulations. The studies carried out with help of ThS fluorescence, circular dichroism, and electron microscopy suggested that TB and RB attenuated the *in vitro* Tau aggregation. Whereas, the PE-TB and PE-RB disaggregated the mature Tau fibrils. In our studies, we observed that PE-RB and PE-TB Bengal modulated the cytoskeleton network. The Neuro2a cells exposed to PE-RB and PE-TB were having extended neurite, which indicated the modulation of tubulin network. Similarly, the treatment of photo-excited dyes modulated actin structures in cells. Neuro2a cells exposed to PE-RB and PE-TB had increased actin-rich filopodia and lamellipodia. The behavioural studies on *Drosophila* transgenic models suggested that exposure to these dyes improved the longevity and egg laying capacity of flies. Similarly the negative geotaxis assay suggested that flies exposed to PE-RB and PE-TB were having improved locomotor function. The treatment of PE-RB and PE-TB improved memory and learning of UAS E-14 Tau mutant of *Drosophila*.

Bacopa monnieri is a nootropic herb described in Ayurveda. In our work the ethanolic extract of *Bacopa monnieri* was studied for its potency to inhibit Tau aggregation and rescue of viability of Tau stressed cells. *Bacopa monnieri* was observed to inhibit the Tau aggregation *in vitro*. The cells exposed to *Bacopa monnieri* were also observed to have low level of ROS and caspase-3 activity. The western blot and immunofluorescence analysis showed that the *Bacopa monnieri* elevated the Nrf2 levels and downregulated phospho-Tau level in cells. NUP358 are the key proteins involved in nuclear transport. It was observed that *Bacopa monnieri* treatment restored NUP358 arrangement in formaldehyde stressed cells.

The overall results of our studies suggested that PE-TB and PE-RB have potency against Tau aggregation and Tau-mediated toxicity. Whereas, *Bacopa monnieri* showed potency against Tau phosphorylation and Tau aggregation. Hence these compounds could be considered for further studies in treatment of Alzheimer's disease.

Chapter 1

Introduction

1.1 Alzheimer's disease and protein aggregation

Neurodegenerative disorders are characterized by progressive loss of neurons, memory deprivation, language dysfunction, impaired problem solving, thinking skills, and motor nerves dysfunction¹. Parkinson's disease, Huntington's disease, Creutzfeldt - Jakob disease, Frontotemporal dementia, and Alzheimer's disease are examples of neurodegenerative disorders². Neurodegenerative diseases have been reported to be associated with misfolding, oligomerization, and accumulation of protein aggregates. The proteinaceous aggregates of α -synuclein lead to the generation of Lewy bodies, which are considered a cause of the progression of Parkinson's disease³. Several studies suggest that mutation in the α -synuclein gene leads to the familial Parkinson's disease⁴. Similarly, the misfolded prion protein leads to the generation of sporadic Prp^{sc}, resulting in the Creutzfeldt-Jakob disease⁵. The tri nucleotide disorder such as Huntington's disease involves the aggregation of Huntingtin protein⁶. Intracellular Tau aggregates and extracellular senile plaques are known to be the hallmarks of Alzheimer's disease (AD). AD is the neurodegenerative disease characterized by progressive memory loss and behavioural impairments. The major causes of AD include genetic factors, acetyl choline imbalance and accumulation of protein aggregates. The genetic factors of AD involve the multifactorial genetic dysfunction (APP, PS1, PS2, and TAU), mutations in *Presenilin 1 (PS1)*, and *Presenilin 2 (PS2)* genes considered to be primarily involved in onset of familial AD. Similarly, the mutation in *APOE4* gene is also considered as a genetic cause of late-onset of AD^{7,8}. Apart from genetic factors, the imbalance of the cholinergic system is considered to cause AD. Acetylcholine is one of the critical neurotransmitters of central nervous system. Several studies have indicated that the degeneration of cholinergic neurons leads to impairment in acetylcholine transport resulting in dementia. The treatment of choline esterase inhibitors restores the acetylcholine level in neurons, which is one of the therapeutic strategies for AD patients⁹. Among all these suggested causes for AD, the accumulation of protein aggregates is the main neuropathological feature of AD¹⁰. The extracellular senile plaques led to toxicity in neurons¹¹. The action of gamma-secretase on amyloid precursor protein (APP) results in the formation of amyloid β -42 ($A\beta$ -42) peptides, leading to accumulation of extracellular senile plaques. The impaired clearance of APP from cells leads to the generation of $A\beta$ -42 peptides. The accumulation of $A\beta$ results in the formation of heterogeneous population of oligomers and proto filaments, which ultimately accumulate, as extracellular $A\beta$ fibrils¹². The $A\beta$ -42 aggregates induce neurotoxicity in various manners viz; generation of oxidative stress, induction of caspase activity, loss of synaptic function and induction of several kinases¹³. Similarly, another protein involved in AD is Tau, which stabilizes the microtubules. In the pathological state, Tau detaches from the microtubules and leads to the formation of intracellular neurofibrillary tangle NFTs (Fig. 1)¹⁴.

1.2 Tau protein

Tau protein maintains the assemblies and stability of microtubules. The TAU gene is present at chromosome 17q21, which results in the generation of six isoforms by alternative splicing. This initial 120 amino acid residue long region of Tau has an acidic character. The microtubule-binding region has basic charge on it. On the contrary 40 residues of carboxyl-terminal have a neutral charge overall Tau protein is basic charge protein. The 90 amino acid extended

region adjacent to the repeat region (150-240 AA) contains proline motifs which are known to be the target of various proline-directed Ser/Thr kinases¹⁵.

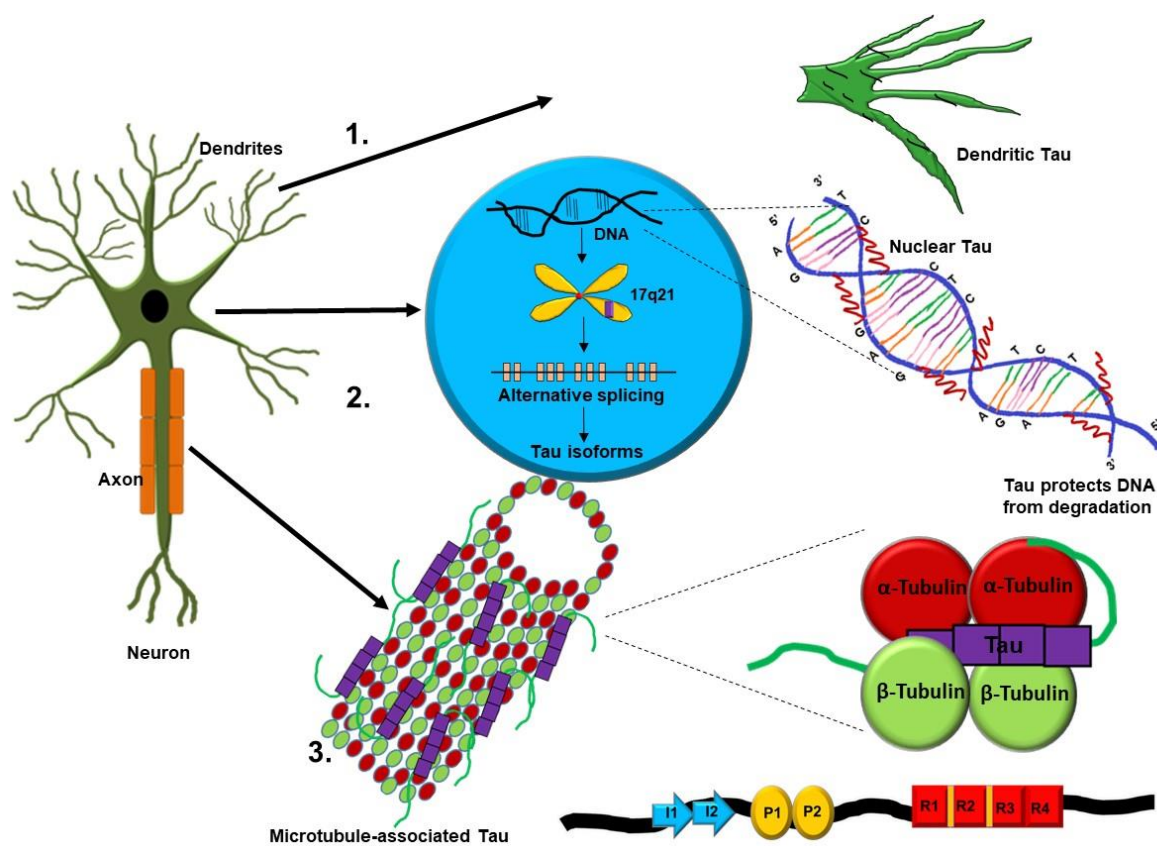


Figure 1. The physiological role of Tau. Tau protein associates with microtubules which aids to maintain the stability of microtubules. Tau is known to be localized in the axonal cytoplasm, but the presence of Tau in the dendrites is reported. The role of nuclear Tau is still needs to be studied but preliminary studies have suggested the role of nuclear Tau in the maintenance of DNA stability and DNA repair.

The four repeat region (244-368), which is mainly responsible for its aggregation. VQIINK in R2 and VQIVYK of R3 are the sequences that initiates Tau aggregation. Under physiological conditions, Tau stabilizes the protein, but in diseased state Tau undergoes several post-translational modifications such as phosphorylation, glycation, glycosylation, and ubiquitination, which lead to the pathological Tau species¹⁶. Among all PTMs of Tau phosphorylation is the principle cause, which leads to Tau aggregation. Studies addition of phosphate leads to charge compensation on Tau protein, which induces its aggregation (Fig. 2)¹⁷. Tau is a natively unfolded and dynamic protein, due to its hydrophilicity the Tau does not acquire any tertiary structure. The FTIR and CD spectroscopy evidenced that the Tau aggregates have β -sheet-rich structure¹⁸. Tau is predominantly an axonal protein, but the studies have also suggested the presence of dendritic Tau. Tau is considered as majorly localized in the cytoplasm, but presence of nuclear Tau is also being evidenced. Nuclear Tau is known to protect DNA from degradation by involving DNA damage response¹⁹. The nuclear Tau is associated with chromosome relaxation, although the mechanism is yet to be explained²⁰.

Under pathological conditions, Tau detaches from microtubules and form heterogeneous oligomers. These oligomers further form proto-filaments, which ultimately result in paired helical filaments (PHFs)²¹.

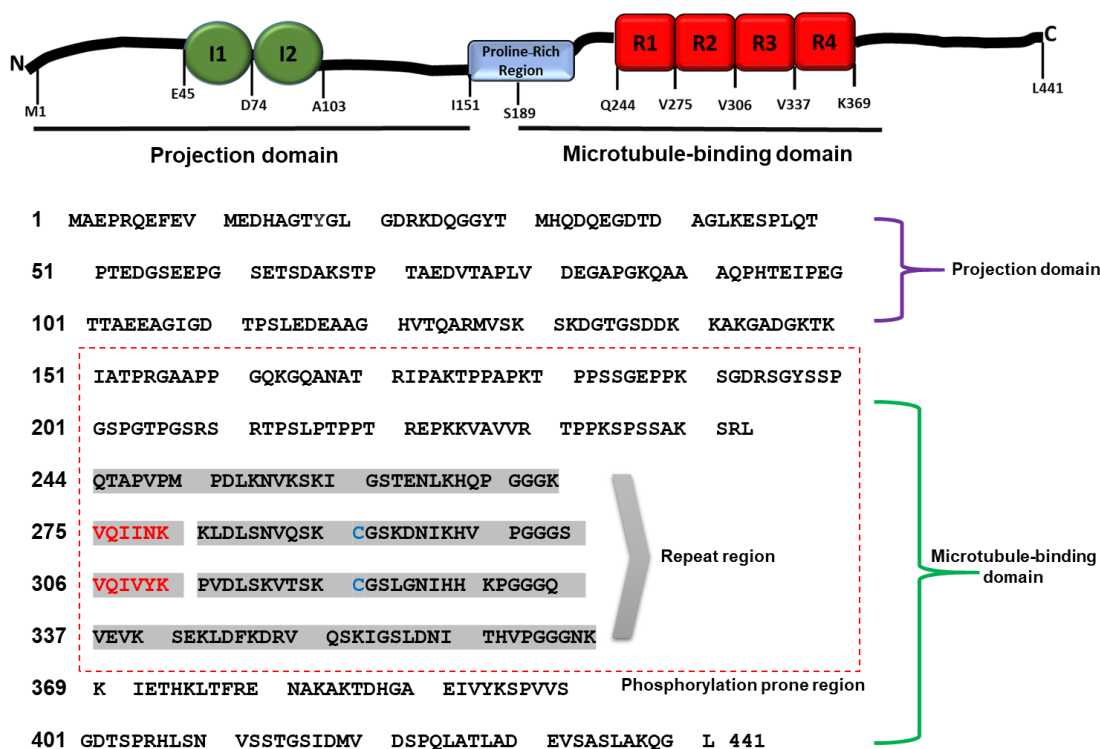


Figure 2. The domain organization of natively unfolded Tau. The 441 amino acid long full-length Tau has two domains, the projection domain and microtubule-binding domain. Further, the microtubule-binding domain has 4 repeat region, which is considered to be responsible for Tau aggregation. The proline-rich region and repeat region have several site(s) prone for various post-translational modifications e.g. phosphorylation. The alternative splicing of the Tau gene led to the generation of six different Tau isomers.

In addition to AD, several other diseases such as progressive supranuclear palsy, corticobasal syndrome, pick's disease, and chronic traumatic encephalopathy are also known to be associated with Tau, which are cumulatively termed as Tauopathies²². The post-translational modifications e.g. phosphorylation are known to be associated with Tau pathology. Tau protein has several sites, which are phosphorylated by various Tau specific kinases. Some kinases have a serine/threonine kinase activity, while others target tyrosine²³. GSK-3 β and CDK5 are the key Ser/Thr kinases, while Src family kinases (SFKs), FYN, and the ABL family kinases phosphorylate tyrosine²⁴. Tau aggregates are involved in generation of various neuronal dysfunctions. The presence of intracellular Tau aggregates lead to the generation of oxidative stress in cells leading to neurotoxicity²⁵. The presence of Tau aggregates is known to initiate neuroinflammation²⁶. Neurodegenerative disorders have been associated with impaired nucleocytoplasmic transport. The transport of transcription factors and Ran gradient across the nucleus and the arrangement of nucleoporins are known to be disturbed in case of neurodegenerative diseases. The recent studies have suggested that Tau protein disrupts the nucleocytoplasmic transport by interfering with Ran protein transport²⁷. Thus, Tau protein is involved in various neuronal impairment it is considered as a prime target for studying several therapeutic strategies against AD (Fig. 3).

1.3 Tau aggregation inhibitors

The pathology of AD is closely associated with Tau aggregation, various molecules have been screened for their potency to inhibit Tau aggregation. The Tau aggregation inhibitors include the molecules extracted from a natural sources as well as synthetic origin²⁸.

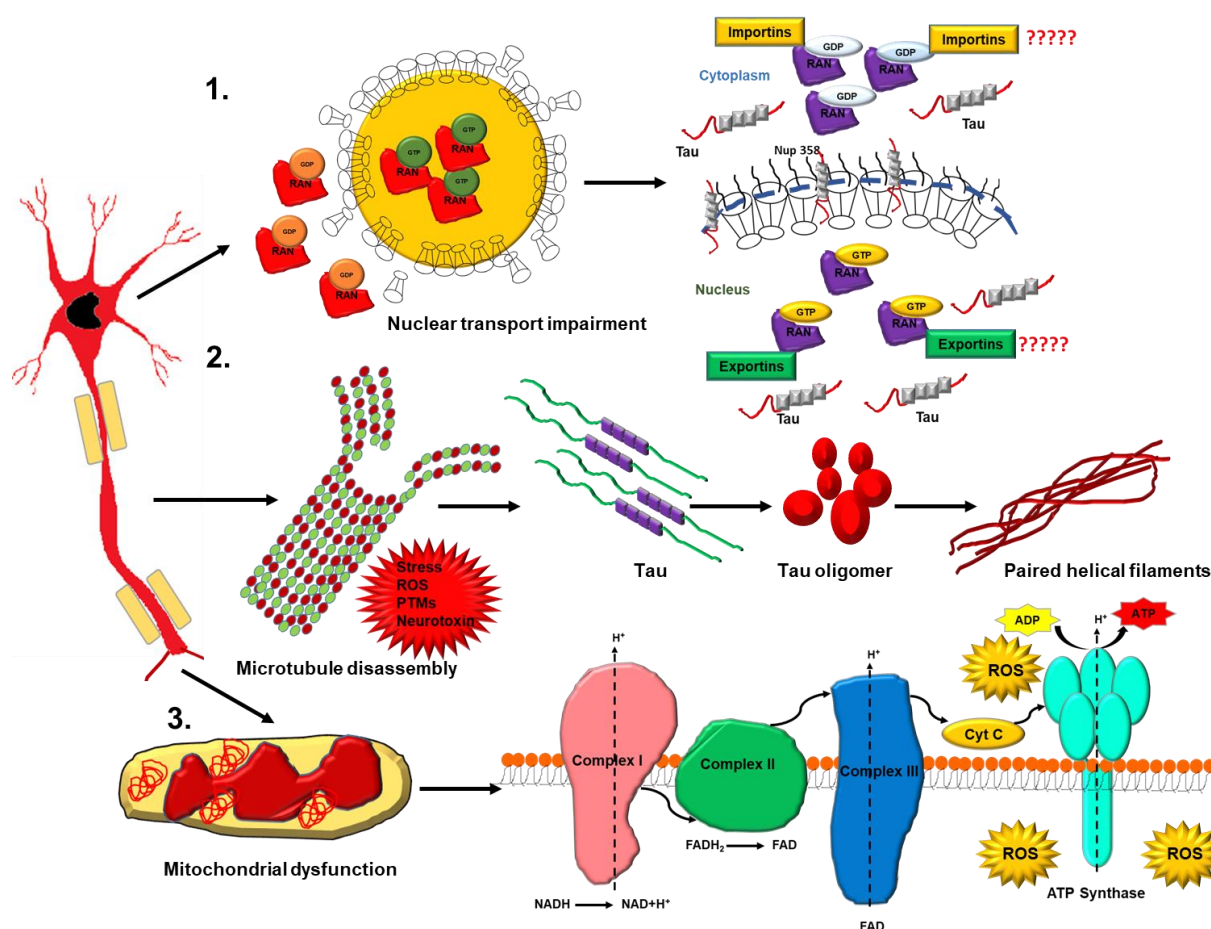


Figure 3. The pathological role of Tau. Under pathological conditions, Tau detaches from microtubules and self-aggregates to form intracellular aggregates. These aggregates led to the generation of various neuronal impairments. The detachment of Tau from the microtubule result in the destabilization of microtubules which causes various cytoskeletal deformities. Ran and Nups play a crucial role in nucleocytoplasmic transport. The presence of Tau aggregates reduced the Ran level and disrupted the arrangement of Nups. Tau aggregates increase the oxidative stress in neuron and lead to dysfunction of the mitochondrial electron transport chain.

The Curcumin is a polyphenol extracted from the roots of *Curcuma Longa*, the studies suggested that Curcumin disintegrates the Tau fibrils and oligomers formation. Curcumin is known to inhibit the β - sheet formation during the initial stages of Tau aggregation. Furthermore, the Cinnamaldehyde, isolated from *Cinnamomum zeylanicum* is known to inhibit Tau aggregation. The polyphenolic extract of grape seed disaggregated Tau fibres leading to reduction in neurotoxicity²⁹. In recent studies in our lab, the limonoids nimbin and salannin extracted from *Azadirachta indica* inhibit *in-vitro* Tau aggregation³⁰. Further the limonoids including gedunin, epoxyazadiradione, azadirone and azadiradione observed to have potency in inhibiting Tau aggregation. These limonoids affected the proteostasis by modulating the Hsp 70 level in cells³¹. The quinone derivatives such as the anthraquinones, daunorubicin and adriamycin isolated from the bacterium *Streptomyces peucetius* are also reported to dissolve the Tau fibrils³². The flavonoid Baicalein (5,6,7-trihydroxyflavone) isolated from the roots of *Scutellaria baicalensis* is known to inhibit the Tau fibrillization. The studies suggest that Baicalein sequesters the oligomers, ultimately leading to a reduction in Tau aggregation³³. Epigallocatechin gallate (EGCG) is the polyphenol isolated from green tea is known to inhibit the formation of toxic oligomers of K18 Δ K280 Tau. The biochemical, biophysical, and docking studies revealed that EGCG interact(s) with Tau leading to modulation of its aggregation potency³⁴. The compounds of synthetic origins are also have potency against Tau aggregation

B4AD5 and B4A1 are the N-phenylamine-derived compounds that are known to inhibit Tau aggregation. The organometallic compounds such as porphyrins are known to inhibit Tau aggregation. The cobalt-based metal complexes are reported to inhibit Tau aggregation; studies have also suggested that these metal complexes reduce the okadiadic acid-induced phosphorylation of Tau in neuronal cells³⁵. Methylene blue (MB) was observed to have potency to attenuate the Tau assembly. Along with MB, perhenazine, thionin and quinaxoline also reported to inhibit Tau aggregation³⁶. Thiazole and hydrazine-containing structure BSC3094 has shown potency against Tau aggregation with a DC of 0.7 μM ³⁷ (Fig. 4).

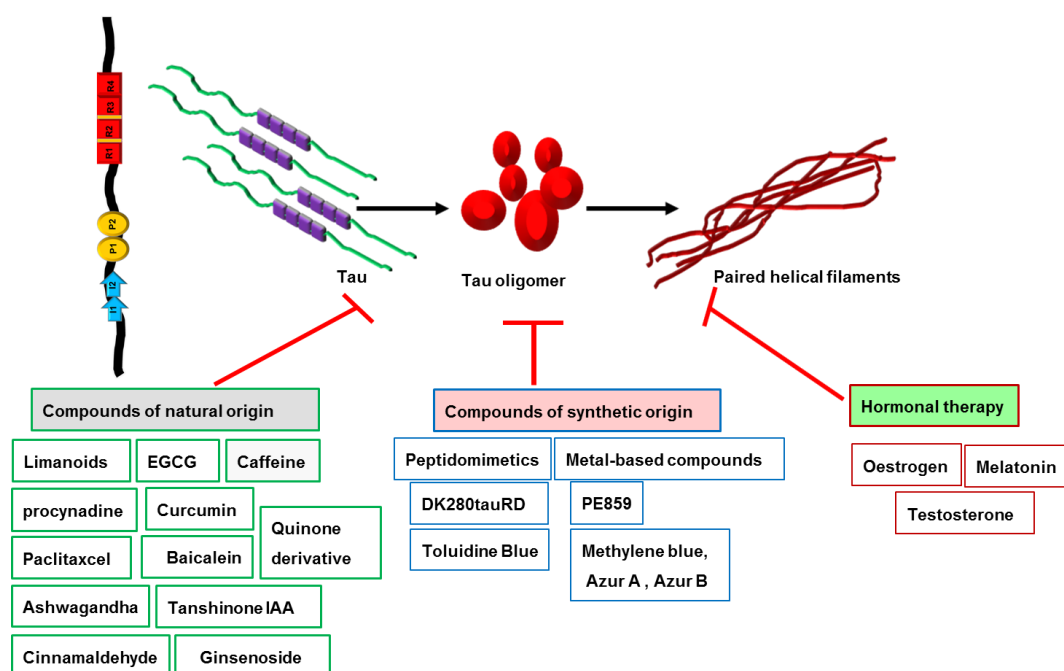


Figure 4. The screening of Tau aggregation inhibitors. Various studies have been carried out for screening of Tau aggregation inhibitors. Tau aggregation inhibitors contain compounds of natural origin, which have various alkaloids, phenols, polyphenols etc. The synthetic Tau inhibitors have peptidomimetics, dyes and metal-based compounds. Hormonal therapy is also found to be effective for the inhibition of Tau aggregation.

1.4 The introduction to Photodynamic therapy

1.4.1 The principle of Photodynamic therapy

Photodynamic therapy (photo+dynamic therapy) (PDT), involves the application of photo-excited molecules to the target. The two step mechanism of PDT includes absorption of light by the photosensitizer as first step followed by the transfer of energy by the excited state of photosensitizer molecule to the molecular oxygen. In the first step the photosensitizer acquires the excited state by absorption of light energy. As this high energy state is short lived the singlet state gets converted to triplet state *via* a process known as “intersystem crossing”. This triplet state having more half-life participates in two types of reaction called as type I and type II reaction. In type I reaction, it reacts with a substrate and molecular oxygen to form free radicals. In type 2 reaction, the triplet state transfers it’s energy to oxygen directly and converts it into a singlet state (Fig. 5)^{38,39}. The application of light as therapy was used from ancient times. In the modern era, the process of PDT was first examined in 1898⁴⁰. Furthermore, in 1904 the significance of singlet oxygen in PDT was established and the term “photodynamic therapy” was introduced⁴¹. The first clinical approval for PDT was done in 1993, and since then, PDT has emerged as a promising therapy for the treatment of various disorders⁴².

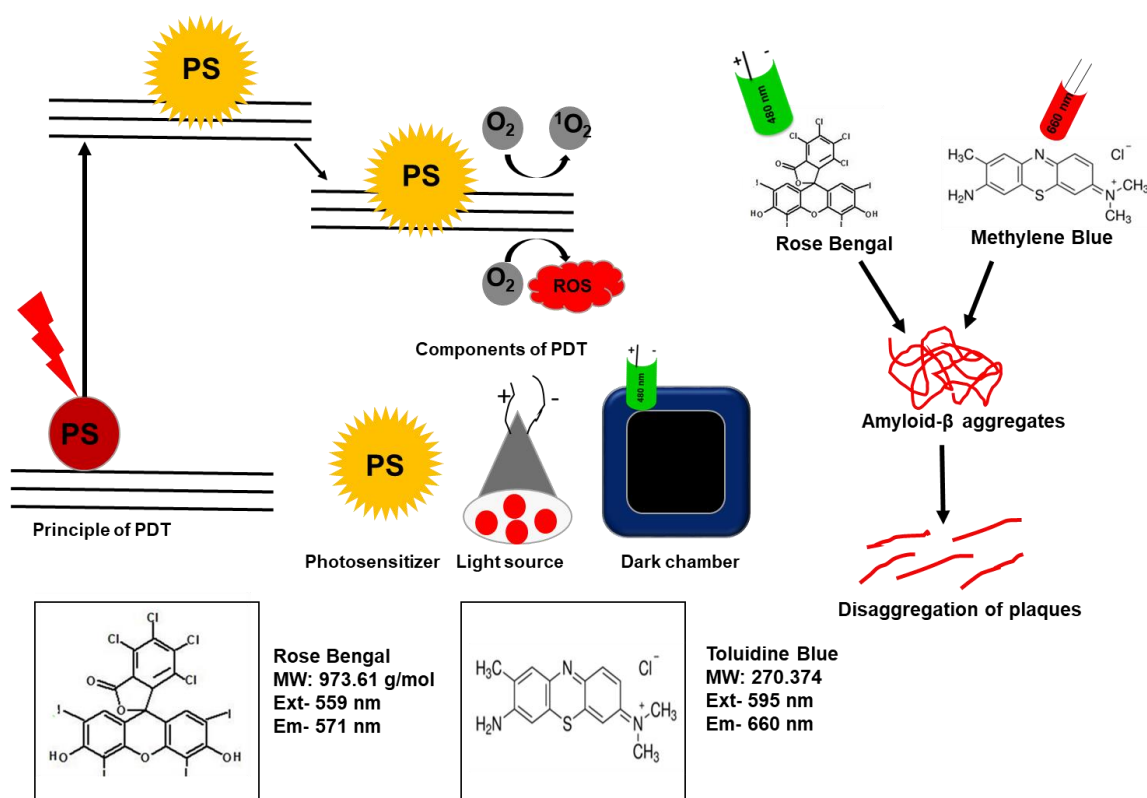


Figure 5. The introduction to Photodynamic therapy (PDT). PDT involves the application of photo-excited dyes against target tissues. The main components of PDT involve light source, photo-sensitive molecules and dark chamber. The exposure of photo-excited dyes to A β fibrils results in disintegration of A β aggregates. The PDT has been observed to be effective in disintegrating the AD-related A β fibrils.

1.4.2 The introduction to Photosensitizers

The light-sensitive molecules used for PDT are termed photosensitizers (PS)⁴³. Various light-sensitive molecules have been reported in the literature but the ideal PSs should have properties such as-

High quantum yield: The PSs should produce high singlet oxygen species, which lead administration of lower doses of PSs.

Target specificity: The PS should target-specific, application of PSs must not have any adverse effect on surrounding healthy tissues.

Minimum dark toxicity: The toxicity generated by non-photo-excited PS is known as dark toxicity. The PS should not have any adverse effect on cell viability in un-excited form.

Rapid clearance from the body: One of the important aspects of the choice of PS is the retention time in the body. The PS should be excreted from the body without causing any side effect.

Availability and cost effective: The molecules are chosen as PS should be easy to synthesize, and the cost of preparation should be low.

The first-generation PSs have several drawbacks such as low quantum yield, dark toxicity and less specificity⁴⁴. To resolve these issues, second and third-generation PSs were introduced. The second-generation PSs mainly include porphyrin-derived compounds such as benzoporphyrins, purpurins, texaphyrins, phthalocyanines, naphthalocyanines, and protoporphyrin IX (PpIX)⁴⁵. The

porphyrin compounds such as meta-tetra(hydroxyphenyl) porphyrin, the meta isomer of 5,10,15,20-tetra(hydroxyphenyl)porphyrin, and 5,10,15,20-tetrakis(4-sulfonatophenyl)-21H, 23H-porphyrin (TPPS4) are the second-generation photosensitizers^{46,47}. The second-generation PSs include some non-porphyrin compounds belonging to anthraquinones, phenothiazine, xanthene, cyanine, and curcuminoids⁴⁸. Phenothiazine dyes including Methylene Blue and Toluidine Blue have λ_{\max} at 666 nm and 630 nm respectively. The cationic dye TB is known to have a high affinity for sulphates, carboxylates, and phosphate radicals of mammalian tissues, hence it's being widely used for histological purpose⁴⁹. TB has a phenothiazine structure, which imparts the property of photo-excitation. The potency of photo-excited TB has been reported against pathological microbes such as *Candida albicans*, *Pseudomonas aeruginosa*, *Acinetobacter baumannii* and *Staphylococcus epidermidis*⁵⁰⁻⁵². Rose Bengal is another photosensitizer belonging to xanthene dye. Chemically Rose Bengal is widely used as fluorochrome and a histological dye. The dye is readily soluble in water and have a molecular mass of 973.67 g/molecular mass. Rose Bengal is known to have the potency of photo-excitation at λ_{\max} of 546 nm. Rose Bengal has been known for the inhibitory properties against several carcinoma and microbial infections. Silica nanoparticles decorated with Rose Bengal is reported to inactivate the methicillin-resistant *Staphylococcus aureus*⁵³. The gold nanorods conjugated with Rose Bengal have been proven to be effective against the oral carcinoma⁵⁴. The treatment of photo-excited Rose Bengal was observed to inhibit the *Pseudomonas aeruginosa keratitis* isolates⁵⁵. Several compounds belonging to the chlorin family have been applied as photosensitizer. Meta-tetra (hydroxyphenyl)chlorin, tin ethyl etiopurpurin, N-aspartyl chlorin e6 are the examples of chlorin-based photosensitizer isolated from chlorophyll A^{56,57}. Pheophorbides are another class of pyrrole-based photosensitizer, which is also derived from chlorophyll⁵⁸. WST09 and WST11 are the bacterial origin pyrrole-based photosensitizer-derived from bacteriochlorophyll A⁵⁹. The recent studies instructed the development of third-generation of photosensitizers, which include PSs immobilized on nanoparticles. Chlorin E6 (Ce6)+nanoparticles, Gold-Nanoclustered Hyaluronan Nano-Assemblies, Ce6+tumor-targeting nanogel, Ce6+ChitoUDCA nanoparticles are the examples of some of the emerging third-generation PSs, which showed appreciable potency against various cancerous cells^{60,61}. The combinatorial therapy using PSs is emerging as a promising therapeutic strategy (Table 1). The platinum (IV) complex-based prodrug monomer (PPM) and 2-methacryloyloxy ethyl phosphorylcholine (MPC), improved the drug delivery and assisted in resolving the challenge of multidrug resistance in tumours⁶². Similarly, the doxorubicin and chlorin e6 Dox@MSNs-Ce6 complex loaded on silica nanoparticles was found to have imposed potency of drug⁶³. Hence, the application of PSs is emerging as potential strategy for treatment.

1.4.3 Dyes in diagnosis and therapeutics against neurodegenerative disease

The application of dyes for the diagnosis of Tau aggregation is considered to be a sensitive, reliable technique. Congo red and it's derivative (trans,trans)-1-fluoro-2,5-bis(3-hydroxycarbonyl 4-hydroxy) styrylbenzene (FSB) were used to detect the Tau aggregates in animal models such as P301S Tau transgenic mice. The curcumin derived near-infrared fluorescent probes (NIRF) (4-dimethylamino-2,6-dimethoxy)phenyl that alters its colour after conjugating with Tau⁶⁴

Table 1.

S.No.	Name of photosensitizer	Target	Year of Clinical approval
1.	Photofrin	Head and neck carcinoma and lung cancer	1993 in Canada, 1995 in USA, 1998 in UK
2.	Temoporfin	Oesophageal cancer	2001 in China
3.	Talaporfin	Lung cancer	2003 in Japan
4.	Chlorin e6	Ladder cancer	2006 in Russia
5.	ALA	Brain tumour	2017
6.	Padeliporfin	Prostate cancer	2018 in Mexico

Table 1. The clinically approved photosensitizers and their application. (Adapted from *Dubey, T and Chinnathambi, S; Small GTPase, 2021*)

Similarly, isobutyl-substituted difluoroboron β -ketonate with a π -conjugated 1,4-butadienyl linker is a Tau-specific NIRF used for diagnosis of Tau aggregates⁶⁴. 1,7-Bis(4'-hydroxy-3'-trifluoromethoxyphenyl)-4-methoxycarbonyl-ethyl-1,6-heptadiene-3,5-dione(FMeC1), CARNAD -58, CARNAD-28, CARNAD-3, BMAOI-14 are examples of some curcumin-derived fluorescence probes, which are specific for A β aggregates⁶⁵. One of the derivatives of BODIPY, "Quinoxaline", is known to emit fluorescence after binding to Tau fibrils⁶⁶. Crystal violet, Hoffman's violet, Methyl green, Toluidine blue are examples of dyes, which change colour upon binding to the protein aggregates⁶⁶. The binding of Thioflavin S and Thioflavin T lead to restriction in their rotational freedom, which results in the generation of elevated fluorescence. Hence, these dyes are proved to be an essential tool in tracing the protein aggregation^{34,66}. Coumarin-quinoline (CQ) has an affinity for A β and Tau aggregate, the CQ has the potency to cross blood-brain-barrier, which facilitates the *in vivo* diagnosis of Tau and A β aggregate³⁴. Indocyanine green and IR-780 are cyanine-based dyes, which have the potency to bind the extracellular A β plaques⁶⁷.

Various classes of dyes have been known to be effective against Tau/A β aggregation and their pathology. In recent years, the tricyclic phenothiazine dye Methylene Blue (MB) has been studied extensively for its potency against Tau aggregation and Tau-mediated neurotoxicity⁶⁸. The treatment of MB downregulated the activity of MARK4/PAR1, which ultimately results in the reduction of Tau phosphorylation and Tau toxicity⁶⁹. The N-demethylated derivatives of MB azure A and azure B are known to be effective against Tau aggregation. The azure A and azure B crosslink C291 and C322, which attenuated the Tau aggregation⁷⁰. However, it was observed that MB inhibited the formation of long fibrils of Tau, whereas Tau oligomers were not affected by MB⁷¹. The *in vivo* studies supported the potency of MB against Tauopathy. The administration of MB to Transgenic mice expressing full-length human Tau (2N4R Tau- Δ K280, termed Tau Δ K) improves their cognitive behaviours^{72,73}. Furthermore, the *in vivo* studies indicated that cyanine dye 3,3'-diethyl-9-methyl-thiacarbocyanine iodide (C11) modulated the Tau aggregation in transgenic mice model⁷⁴. The xanthene dye Erythrosine B (ER) treatment attenuated the *in vitro* aggregation of A β , ER reduced the A β -mediated cytotoxicity of neuroblastoma cells SH-SY5Y cells⁷⁵. The natural dye Haematoxylin which extracted from *Caesalpinia sappan*, potentially inhibited A β fibrillization⁷⁶. The inhibition of A β fibrillization was resulted from the interaction of dye with A β at N-terminal region, S8GY10 region, turn region, and C-terminal region *via* hydrogen bonding. Curcumin is reported to attenuate the aggregation of A β and Tau⁷⁷. Curcumin downregulates the Tau-mediated toxicity in various aspects, studies suggested that treatment of curcumin inhibited the

oligomerization of Tau protein and modulated the phosphorylation of Tau that ultimately resulted in reduction of Tau-mediated neurotoxicity⁷⁸. Hence the recent studies suggested that dyes could be considered as a potent therapeutic molecules against Tau aggregation.

1.4.4 Photo-excited dyes: novel approach against AD

The advancements in field of PDT are widening the probability of application photo-excited dyes. The studies have indicated the potency of photo-excited dyes against the AD-related protein aggregates. The A β aggregates are neurotoxic, recent results have supported the concept of disintegration of A β fibrils *via* photo-excited dyes⁷⁹. The photo-excited xanthene dye Rose Bengal attenuated the *in vitro* aggregation of monomeric A β and conformational transition in A β secondary structures. The exposure of PE-RB reduced the degree of toxicity in the A β stressed PC-12 cells⁸⁰. Similarly, the micelle prepared by coating with Chlorin e6 and Tanshinone irradiated with 655 nm light disintegrated the mature A β fibrils and reduced the A β -mediated toxicity⁸¹. The treatment of photo-excited ThT attenuated aggregation of A β by oxidizing Y10, H13, H14, and M35 amino acids of A β which resulting in the reduction of aggregation rate⁸². The photo-excited MB disintegrated the A β fibrils *in-vitro*; *in vivo* studies indicated that PE-MB modulated the neuromuscular junction in *Drosophila*⁸². The preliminary studies suggested that photo-excited dyes could have potency against AD- related pathology.

1.5 Ayurveda and its role in neuroprotection

1.5.1 Introduction to Ayurveda

Ayurveda is considered to be one of the ancient science for therapeutic practices. The philosophy of Ayurveda deals with the improvement of human health by the application of natural resources. "Ayur " is a word representing life, and veda represents science or knowledge, hence the word Ayurveda has meaning the science for the improvement of life. The three principle braches of Ayurveda are "Roga Vigyan" (the science of diseases), "Vikriti vigyan" (the science of disease process), Chikitsa vigyan (science of therapeutics). The Ayurveda is divided in eight divisions *viz*, Kayachikitsa (medicine), Salakya (dealing with diseases of the supra-clavicular region), Salyapahartrka (dealing with extraction of foreign bodies), Visagara Vairodhika-Prasamana (dealing with alleviation of poisons, artificial poisons and toxic symptoms due to intake of antagonistic substances), Bhutavidya (dealing with spirits or organisms), Kaumarabhrtya (Pediatrics), Rasayana (dealing with promotive measures) and Vajikarana (dealing with aphrodisiacs)⁸³. Ayurvedic medicines mainly involves polyherbal formulations. The collection of medicinal herbs is a very important event in the preparation of medicines. The various formulations include "Asava", which is synthesized by fermentation of fresh herbal extracts," Kwath ", synthesized by boiling the herbs and collecting the decoction. "Vati", is polyherbal the formulation in form of tablet and churna means powdered form of herbs, "Bhasma" is the fine power subjected to high temperature. In recent years modern analytical techniques such as TLC, HPLC, HPLC-MS, GC-MS, NMR *etc.*, have been used for the chemical profiling of Ayurvedic formulations. The Ayurvedic formulations are characterized on the basis of the mechanism of action. The naimittika rasayana is the formulation for improvement of general weakness, vajikarana rasayana is for the improvement of vitality and vigour, pranakamyra rasayana improves the vitality and longevity, shrirasayana is prepared for skin disorders, while "medhya rasayana" is for the improvement of neuronal health of a person. (Fig. 6).

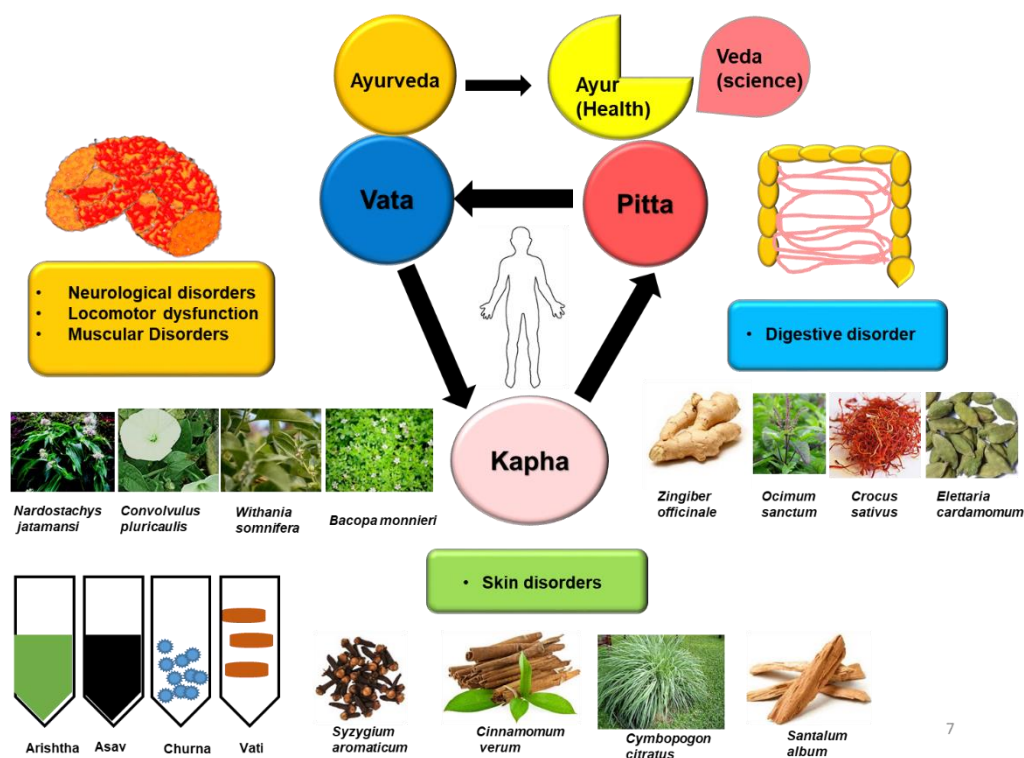


Figure 6. Introduction to Ayurveda. The Ayurveda is a traditional medicinal system which includes therapeutic application of natural resources. The imbalance of three components (Dosha) of body viz, vata, pitta and kapha led to generation of diseased condition. The mental health and neurological disorders are believed to be related to imbalance of “Vata” component. Various herbal formulations have been prescribed in Ayurveda which are known to have neuroprotective properties. These formulations include Asav, kwath, vati and chruna which are administered based on the disease symptoms.

1.5.2 Neuroprotective herbs in Ayurveda

Various herbs have been suggested in Ayurveda for the treatment of memory and cognitive disorders. *Convolvulus pluricaulis* is a perineal creeping plant belonging to the family Convolvulaceae. Traditionally *C. pluricaulis* has been given in various formulation for treatment of anxiety, memory loss and cognitive disorders. Recent studies have supported the neuroprotective property of *C. pluricaulis*. The methanolic extract of *C. pluricaulis* leaves showed neuroprotective property in *3-Nitropropionic acid (3-NP) stressed rat model*⁸⁴. The treatment of methanolic extract of *C. pluricaulis*, reduced the malondialdehyde, nitrite levels and restored the activity of antioxidant enzymes e.g. superoxide dismutase, which indicated the antioxidant property of *C. pluricaulis*⁸⁵. The active components of *C. pluricaulis* such as scopoletin, ayapanin and scopolin were observed to ameliorate the scopolamine-induced amnesia in mice⁸⁶. The administration of *C. pluricaulis* extract modulated the synaptic plasticity in hippocampus, which resulted in improving the memory of mice⁸⁷. Thus, the studies indicated *C. pluricaulis* has a neuroprotective property.

Withania somnifera, commonly known as “Ashwagandha” or Indian Ginseng is the evergreen shrub belonging to solanaceae family. Traditionally, *W. somnifera* is widely prescribed for the treatment of mental stress, general weakness, diarrhoea, anxiety and depression. The studies have demonstrated the various aspects of the neuroprotective property of *W. somnifera*. The ethanolic extract of *W. somnifera* showed the inhibition of pro-inflammatory enzymes lipoxygenase and cyclooxygenases⁸⁸. The oral dose of “Withanone”, a bioactive component of *W. somnifera*, improved memory and cognition in old wistar rats by inhibiting the A β

aggregation. Similarly, the extract of *W. somnifera* showed neuroprotective activity in 6-Hydroxydopamine (6-OHDA) stressed rats. 6-OHDA elevated the oxidative stress resulting in generation of Parkinson's disease-like symptoms. The oral administration of *W. somnifera* to 6-OHDA stressed rats, restored the glutathione peroxidase, superoxide dismutase and catalase activity and attenuated the lipid peroxidation in rat brain⁸⁹. Thus, the recent studies clearly advocated the neuroprotective property of *W. somnifera*.

Centella asiatica (CA) is another essential herb that is considered to be neurotonic. *C. asiatica* is commonly known as "Gotu kola", "mandukparni" and jalbrahmi. It has been used from ancient times for the treatment of neuronal disorders, skin diseases, diarrhoea, fever, genitourinary disorders. *C. asiatica* is a creeping plant belongs to Umbellifere family, which is found in marshy areas throughout India⁹⁰. The administration of *C. asiatica* extract rescues the wistar rats from colchicine-mediated memory impairment and oxidative stress⁹¹. The *PSAPP mice* bearing M146L presenilin 1 mutations, results in spontaneous aggregation of A β in brain. The administration of *C. asiatica* extract modulated the A β aggregation and ROS generation in mice brain⁹². Moreover, *C. asiatica* extract reduced A β -mediated toxicity in PC-12 cells⁹³.

Curcuma longa, has a significance in diet as well as in medicines, The *Curcuma longa* is known for its anti-bacterial, analgesic, antipyretic and neuroprotective property⁹⁴. Curcumin is the participle bioactive component of *Curcuma longa*, the bright yellow coloured compound curcumin is chemically a diarylheptanoid⁹⁵. The neuroprotective role of curcumin has been extensively studied in recent years. Curcumin was observed to inhibit the aggregation of A β *in vitro* and *in vivo*. Additionally the administration of curcumin reduced the senile plaques formation in Tg2576 mice brain⁹⁶.

Nardostachys jatamansi or "Jatamansi", is a plant found on higher altitudes in India. The plant belongs to *Caprifoliaceae* family and the rhizome is considered to have the medicinal property. Jatamansinol is an active component of *N.jatamansi*, the treatment of jatamansinol inhibited the GSK-3 β activity and acetylcholine esterase activity, which are known to be involved in AD-related pathogenesis⁹⁷. Similarly, the administration of extract of *N.jatamansi* rescued the rats from the cognitive impaired in streptozotocin (STZ) and selenium stressed rats⁹⁸. The antioxidant enzymes such as glutathione peroxidase, glutathione-S-transferase and catalase were also observed to be elevated after treatment of *N.jatmansii* extract. The extract of *N.jatamansi* was also found to rescue the memory impairments in Parkinson's disease model of rats stressed with Haloperidol and 6-hydroxydopamine⁹⁹.

1.5.3 *Bacopa monnieri*: Nootropic herb in Ayurveda

Bacopa monnieri or "Brahmi" is the well-known neuroprotective herb in Ayurveda. *B.monniieri* is a creeper plant mainly found in marshy and damp area. *B.monniieri* has been recognized as "medhya rasayana" in Ayurveda, which means the medicine for improvement of neuronal health¹⁰⁰. An illustrative characterization of the chemical constituents of *B.monniieri* has been carried out in various studies. The main constituents of *B.monniieri* include alkaloids such as "Brahmine", Nicotine and Herpestine. The dammarane type titerpanoids saponins such as Bacoside A [3-(α -L-arabinopyronosyl)-O- β -D-glucopyronaside, 20-dihydroxy-16-keto-dammar-24-ene] is considered as a major bioactive component of *Bacopa monnieri*. The glycoside component of Brahmi extract contain chemicals such as pseudojubilogenin, which is chemically identified as 3-O-[α -1-arabinofuranosyl (1-2) β -d-glucopyranosyl]. A, phenylethanoid glycoside, 3,4-dihydroxyphenylethyl alcohol (2-O-ferulolyl)- β -D-glucopyronaside and phenylethyl alcohol [5-O-p-hydroxy-benzoyl- β -D-apifuranosyl-(1-2)- β -D-glucopyranoside. The

principle bioactive compounds “Bacoside A” and ‘Bacoside B” have been studied extensively for their neuroprotective property.

1.5.4 The neuroprotective property of *Bacopa monnieri*

The reactive oxygen species are the oxygen radicles having short life span and high reactivity. Accumulation of ROS in cells led to generation of oxidative stress, which ultimately results in several cellular dysfunctions. *B. monnieri* is known to have antioxidant property, which is evidenced by several studies. The administration of *B. monnieri* is known to increase the level of antioxidant enzymes as SOD in the rat brain¹⁰¹. The colchicine is known to induced dementia *via* increasing the oxidative stress in brain, the treatment of *B. monnieri* extract reduced the ROS and NO levels in the rat brain¹⁰². The methanolic extract of *B. monnieri* protected the neuroblastoma cells against H₂O₂-mediated oxidative stress¹⁰³. The oral administration of *B. monnieri* reduced the ROS load in streptozotocin-induced diabetic mouse by modulating the activity of SOD, glutathione peroxidase¹⁰⁴. It was observed the treatment of *B. monnieri* elevated the levels of Nrf2 in okadaic acid treated wistar rats, which assist in reducing the ROS¹⁰⁵. The reactive nitrogen species also result in generation of neurotoxicity. Thus all the studies clearly supported the fact the *B. monnieri* could be considered as antioxidant herb.

The earlier studies have supported the protective role of *B. monnieri* again various aspects of neurodegeneration. Although the potency of *B. monnieri* has not been studies against Tau-mediated toxicity. Thus, we aimed to study the effect of *B. monnieri* extract against Tau aggregation, Tau phosphorylation and Tau mediated toxicity (Fig. 7).

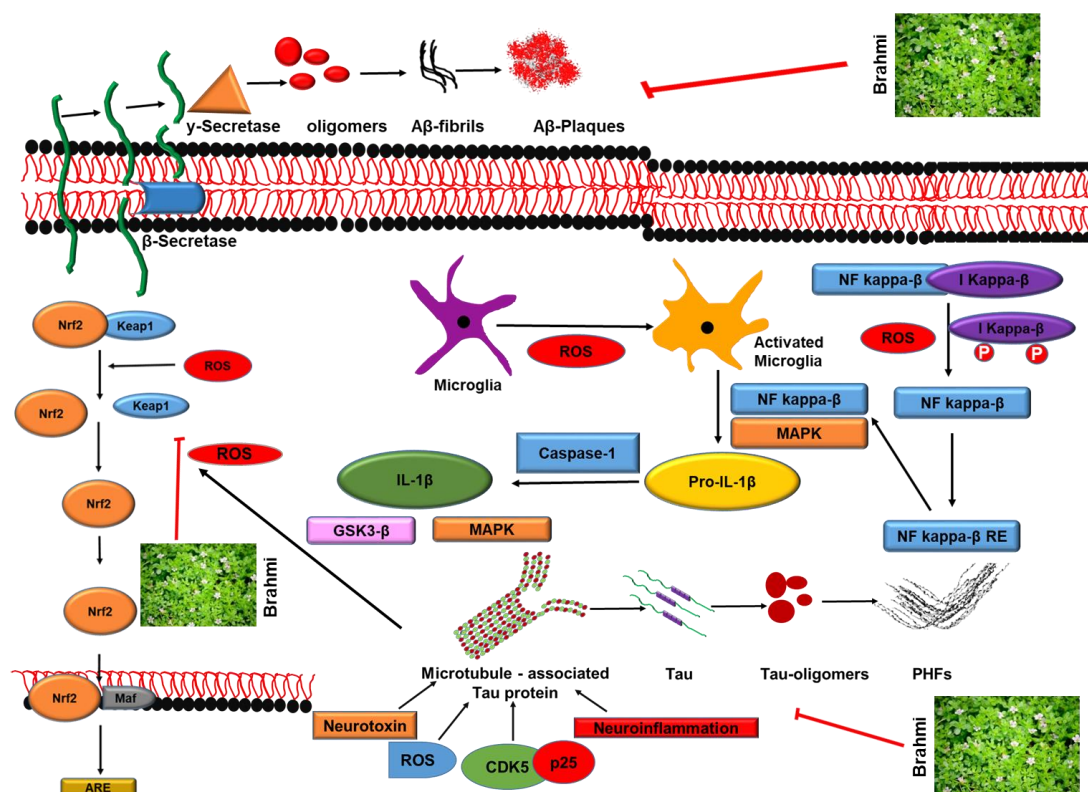


Figure 7. The nootropic property of *Bacopa monnieri*. *Bacopa monnieri* is considered to be a neuroprotective herbs science ancient times. In recent years, studies have proved the neuroprotective property of *Bacopa monnieri*. The treatment of *Bacopa monnieri* reduced the oxidative stress in cells and upregulated the antioxidant machinery of cells. The inflammatory cytokines were also downregulated after the treatment of *Bacopa monnieri*. The A β aggregates led to the generation of AD pathology, *Bacopa monnieri* treatment disintegrated the A β aggregates.

The PD model of flies expressing α -synuclein were fed with various concentrations of *B.monnieri* extract. It was observed the administration of *B. monnieri* improved the locomotor and behavioural deformities in flies¹⁰⁶. Similarly, the treatment of *B. monnieri* extract improved the tyrosine hydroxylase activity in MPTP-induced Swiss albino mice¹⁰⁷. Similarly, the treatment of *B.monnieri* extract reduced the aggregation of α -synuclein in 6-hydroxy dopamine stressed *C.elegans*; a transgenic model expressing “human” alpha synuclein¹⁰⁸. The neuroprotective action of *B.monnieri* was also studied in context of potency to attenuate the aggregation of A β . The studies suggested that *B.monnieri* extract rescued the primary cortical neurons from A β mediated neurotoxicity. Ethylcholine aziridinium ion (AF64A) has high affinity for choline receptors and induces AD like symptoms. The oral administration of *B.monnieri* extract to AF64 stress wistar rats reduced the loss of cholinergic neurons and improved the cognitive function¹⁰⁹. The active component of *B.monnieri* also inhibited the aggregation of A β , Bacoside A inhibited the A β fibril formation and reduced the cytotoxicity¹¹⁰.

Aims of the Study

AD is a progressive type of dementia, the aggregates of microtubule-associated protein Tau are one of the AD's hallmarks. The presence of Tau aggregates led to the generation of various cellular dysfunctions such as ROS production, reduced cell viability, cytoskeletal deformities, impaired nucleocytoplasmic transport *etc.* Phosphorylation is one of the main PTM which is reported to be closely associated with Tau pathology. The kinase such as GSK-3 β phosphorylated Tau at various positions leading to generation Tau pathology. In our work, we focussed on studying the potency of photo-excited dyes (Rose Bengal/Toluidine Blue) against various aspects of Tau aggregation. Another aspect of our study was to check the effect of ethanolic extract of *Bacopa monnieri* against Tau aggregation, Tau phosphorylation, Tau-mediated toxicity and oxidative stress. Our work aims to study the role of photo-excited dyes and Ayurvedic extracts against Tau aggregation. The specific aims are,

1. To study the role of Toluidine blue and photo-excited Toluidine blue against Tau aggregation and preformed fibrils.
2. Studying the role of Rose Bengal and photo-excited Rose Bengal against Tau aggregation.
3. Studying the effect of *Bacopa monnieri* against *invitro* Tau aggregation and mature Tau aggregates. Understanding the role of *Bacopa monnieri* in the modulation of nuclear transport and Tau phosphorylation.

Chapter 2

Materials and methods

2.1.1 List of chemicals and cell growth media

Sr. No	Chemical/Reagent/Media	Company
1.	3-(4, 5-dimethylthiazol-2-yl)-2, 5-diphenyltetrazolium bromide (MTT reagent)	Sigma
2.	4',6-diamidino-2-phenylindole (DAPI reagent)	ThermoFisher Scientific
3.	8-Anilino-naphthalene-1-sulfonic acid (ANS dye)	Sigma
4.	Acrylamide	Invitrogen
5.	Advanced DMEM F12	Invitrogen
6.	Agarose	Invitrogen
7.	Ammonium acetate	MP Biomedicals
8.	Ammonium persulphate (APS)	MP Biomedicals
9.	Ampicillin	MP Biomedicals
10.	BES	Sigma
11.	Bicinchoninic acid	Sigma
12.	Bis-acrylamide	Invitrogen
13.	Bovine Serum Albumin (BSA std)	Sigma
14.	Bradford Reagent	Bio-Rad
15.	Bromophenol blue	MP Biomedicals
16.	Calcium chloride dihydrate	Sigma
17.	Clarity™ Western ECL Substrate	Bio-Rad
18.	Coomassie brilliant blue R-250	MP Biomedicals
19.	Copper sulfate (II)	Sigma
20.	Dimethyl sulfoxide (DMSO)	Life Tech /MP biomedicals
21.	Dithiothreitol	Calbiochem
22.	Dulbecco's Modified Eagle Medium (DMEM)	Invitrogen
23.	EnzChek™ Caspase-3 Assay Kit	Thermo Scientific
24.	Ethanol	MP Biomedicals
25.	Ethylene glycol tetraacetate (EGTA)	MP Biomedicals
26.	Fetal Bovine Serum	Thermo Fisher
27.	Formaldehyde	MP Biomedicals
28.	Gel Loading Dye (6X) (For DNA)	New England Biolabs
29.	Glacial acetic acid	MP Biomedicals
30.	Glycerol	MP Biomedicals
31.	Glycine	Invitrogen
32.	Heparin (MW~17500 Da)	MP Biomedicals
33.	Horse serum	Invitrogen
34.	IPTG	MP Biomedicals
35.	Isopropanol	MP Biomedicals
36.	Lactate dehydrogenase release assay kit	Thermo Scientific
37.	L-glutamine	Invitrogen
38.	LB Broth	Invitrogen/HiMedia
39.	LB Agar	Invitrogen
40.	Magnesium chloride hexahydrate	MP Biomedicals
41.	MES hydrate	Sigma
42.	Methanol	MP Biomedicals
43.	Penicillin-Streptomycin	Invitrogen
44.	Polysorbate 20	MP Biomedicals

45.	Polyvinylidene fluoride membrane	Merck Milipore
46.	Potassium acetate	MP Biomedicals
47.	Potassium chloride	MP Biomedicals
48.	Potassium phosphate dibasic trihydrate	MP Biomedicals
49.	Potassium phosphate dibasic trihydrate	MP Biomedicals
50.	Potassium phosphate monobasic anhydrous	MP Biomedicals
51.	Protease inhibitor Cocktail	Roche
52.	Precision Plus Protein™ Dual Color Standards	Bio-Rad
53.	RIPA buffer	Thermo Scientific
54.	Rose bengal	Sigma
55.	Sodium acetate trihydrate	MP Biomedicals
56.	Sodium azide	MP Biomedicals
57.	Sodium bicarbonate	MP Biomedicals
58.	Sodium carbonate anhydrous	MP Biomedicals
59.	Sodium chloride	MP Biomedicals
60.	Sodium dodecyl sulfate	Sigma
61.	Sodium hydroxide	MP Biomedicals
62.	Sodium phosphate dibasic anhydrous	MP Biomedicals
63.	Sodium phosphate monobasic mono hydrate	Sigma
64.	Sodium thiosulfate pentahydrate	MP Biomedicals
65.	Tetramethylethylenediamine	Invitrogen
66.	Thioflavin S	Sigma
67.	Toluidine Blue	Sigma
68.	Tris base	Biorad
69.	Tris HCl	Invitrogen
70.	Triton X 100	Sigma
71.	Trypan blue	Invitrogen
72.	Trypsin-EDTA	Invitrogen

2.1.2 List of antibodies

Sr. No	Antibodies	Company
1.	GSK3 β monoclonal antibody (MA5-15109)	ThermoFisher Scientific
2.	Phospho-GSK3B (Ser9) monoclonal antibody (MA5—14873)	ThermoFisher Scientific
3.	Nrf2 poly clonal antibody (PA5-68817)	ThermoFisher Scientific
4.	EB1 Monoclonal Antibody (KT51)	ThermoFisher Scientific
5.	Pan Tau (K9JA) (A0024)	Dako
6.	Phospho-Tau (Thr212, Ser214) (MN1060)	ThermoFisher Scientific
7.	Beta-actin loading control (MA515739)	ThermoFisher Scientific
8.	Goat anti-mouse - alexa fluor 555 (A28180)	ThermoFisher Scientific
9.	Goat anti-mouse IgG HRP (32430)	ThermoFisher Scientific
10.	Goat anti-rabbit - alexa fluor 488 (A-11008)	Dako
11.	Goat anti-rabbit IgG HRP (31460)	ThermoFisher Scientific

2.1.3 Laboratory Instruments and Equipment

Sr. No	Instrument/Equipment	Suppliers
1.	AKTA Pure FPLC system	GE Healthcare
2.	AKTA Start FPLC system	GE Healthcare

3.	Amersham Imager 600	GE Healthcare
4.	Amersham Semi Dry blotting apparatus	GE Healthcare
5.	Analytical weighing balances	Mettler Toledo
6.	Autoclave	Spire
7.	Avanti JXN26 High speed Centrifuge	Beckman Coulter
8.	BioSafety cabinet/Clean bench	Thermo Fisher Scientific
9.	CO2 incubator	Thermo Fisher Scientific
10.	Dry bath	Genei
11.	Far-UV CD spectrometer J-815	Jasco
12.	Forma 900 series -80°C	Thermo Scientific
13.	Gel rocker	Benchmark
14.	Heratherm Hot Air Oven	Thermo Scientific
15.	Heraeus Incubator	Thermo Scientific
16.	High Speed Centrifuge 5804R	Eppendorf
17.	Homogenizer	Constant Systems Ltd.
18.	Laminar Air Flow	Microfilt
19.	Magnetic Stirrer	Genei
20.	Microcentrifuge 5418 R	Eppendorf
21.	MiliQ Unit Direct 16	Millipore
22.	Microplate reader Infinite 200 PRO	Tecan
23.	Miniprotean Tetra vertical electrophoresis system	Bio-Rad
24.	MiniSpin Plus Table top centrifuge	Eppendorf
25.	Molecular Imager Gel Doc™ XR+	Bio-Rad
26.	Optima XPN10 Ultracentrifuge	Beckman Coulter
27.	Optima MAX-XP Ultracentrifuge	Beckman Coulter
28.	Avanti JXN-26 centrifuge	Beckman Coulter
29.	pH meter Five Easyplus	Mettler Toledo
30.	Shaker Incubator (H1010-MR)	Benchmark Scientific
31.	Shaker Incubator Multitron Standard	Infors HT
32.	SimpliNano (Nanodrop)	GE Healthcare
33.	T20 Transmission Electron Microscope	Tecnai
34.	UV-Visible spectrophotometer V-530	Jasco
35.	Vacuum Pump	Millipore
36.	Vortexer mixer	Genei
37.	Water bath	Genei
38.	Zeiss Axio observer 7 microscope with Apotome 2.0	Zeiss

2.2 Sodium dodecyl sulphate–polyacrylamide gel electrophoresis

The SDS-PAGE is a technique of separating proteins on the basis of molecular mass. The SDS used in this method acts as a denaturant and masks the protein with a uniform negative charge hence the proteins are separated on basis of molecular weight³¹. The loading dye used in this technique contains bromophenol blue, glycerol, DTT, Tris and SDS. DTT acts as a reducing agent, which helps in denaturing the protein; bromophenol blue is used to trace the mobility of protein. The glycerol helps to impart density to the solution, which facilitates the loading of protein onto the gel. The solutions of 39% acrylamide + 1% bisacrylamide, ammonium persulfate, 10% SDS and TEMED were mixed to prepare the SDS-PAGE of desired percentage. Bisacrylamide cross links to acrylamide, ammonium persulfate generates the free radical which accelerates the polymerization, while TEMED helps to stabilize the free radicals. Various percentages of SDS-PAGE are prepared based on the alternation of acrylamide proportion, the higher percentage of gels are used for proteins of low

molecular weight and vice versa. The SDS-PAGE has two portions one resolving (pH 8.8) and stacking (pH 6.8 and 5% gel). The stacking portion of PAGE helps to align the protein, while the resolving gel helps to resolve the protein based on molecular weight. The gel running buffer is composed of glycine, Tris and SDS. SDS imparts the denaturing condition for protein, tris maintains the buffer conditions while glycine helps in stacking of proteins. As the SDS imparts a negative charge to protein, protein migrates from negative pole to positive pole under the influence of electric field. After the resolution of protein, the gel was stained with the solution containing coomassie brilliant blue R-250, methanol, and glacial acetic acid.

2.3 Protein purification

2.3.1 Expression of protein in bacteria

The bacteria (*BL 21* strain*) from glycerol stock was inoculated in Luria Bertani Broth (LB) supplemented with ampicillin. The primary culture was incubated at 37°C for overnight in a rotatory shaker incubator. The secondary culture supplemented with ampicillin was inoculated from a primary culture and incubated at 37°C in a rotary shaker. Once the culture reaches to exponential phase ($OD_{600} = 0.5$), the culture was induced using 0.5 mM IPTG and further incubated at 37°C. After the incubation, the culture was pelleted by centrifugation at 4,500 rpm for 10 minutes. The bacterial pellets were suspended in lysis buffer and proceeded for protein purification. The bacterial cells were lysed using the mechanical lysis method. Bacterial cells were lysed under high pressure using the constant cell disruption homogenizer pellet was resuspended in the lysis buffer composed of 50 mM MES (pH 6.8), 5 mM DTT, 1 mM EGTA, 1 mM PMSF and protease inhibitor cocktail. The suspension was subjected to homogenization, while passing through the narrow orifice, high-pressure (15,000 psi) was applied on cells, which results in cell lysis. The lysis cycle was repeated 2-3 times and the lysis was collected and kept on ice.

2.3.2 Purification of protein by cation-exchange chromatography

The purification of Tau protein was carried out as per well established procedure in the lab³⁰. The cell lysate was supplemented with 5 mM DTT and 0.5 M NaCl; the lysate was heated for 20 minutes at 90°C. The lysate was centrifuged at 40,000 rpm for 45 minutes at 4°C and kept overnight for dialysis in a buffer composed of 20 mM MES (pH 6.8), 1 mM EGTA, 50 mM NaCl, 2 mM DTT, 1 mM MgCl₂, and 0.1 mM PMSF. The lysate was centrifuged at 40,000 for 45 minutes and with the help of a super-loop loaded on the Sepharose fast-flow column (GE17-0729-01) pre-equilibrated with buffer A. Tau has pI of 8.24, hence cation-exchange chromatography was used for purification of Tau. The cation-exchange column was washed trice with buffer A for removing the unbound protein. The Tau protein was eluted by a linear gradient of NaCl. In first step 6 column wash of 0-60% gradient of 1 M NaCl and in the second step 3 column volume of 60-100% gradient of 1 M NaCl was given for elution. The elution fractions were collected and the quality of protein was checked by SDS-PAGE. The protein fractions were concentrated using vivaspin concentrator 3 kDa (GE healthcare).

2.3.3 Purification of protein by size-exclusion chromatography

Size-exclusion chromatography (SEC) works on the principle of separating the proteins based on their size¹¹¹. The column is packed with matrix whose pore-size is selected based on the size of the proteins needs to be separated. The buffer used in the SEC serves as mobile phase whereas, the matrix acts as the stationary phase. The molecules of higher size elute out first, whereas the smaller molecules enter in the void space of the matrix; hence they have more

retention than large molecules. For the Tau protein purification, Superdex 75pg HiLoad 16/600 was used. The concentrated protein was loaded onto the column with the help of a capillary loop. The protein was eluted by giving the isocratic flow of 1X PBS (pH 7.4). The protein fractions were collected and concentrated using vivaspin concentrator 3 kDa (GE healthcare).

2.3.4 Estimation of protein concentration

The Bicinchoninic Acid assay (BCA) is a reliable method for the estimation of protein concentration¹¹². The BCA works on the principle of reduction of Cu^{2+} to Cu^{1+} by protein in an alkaline medium. The first step of assay involves the chelation of Cu by a protein which forms a light pale blue colour complex in an alkaline environment. In the second step of the BCA reacts with this complex which forms a purple complex having absorbance at 562 nm. The intensity of the purple complex increases with respect to the concentration of protein, which is measured at 562 nm in a spectrophotometer. The protein concentration is estimated by plotting the standard graph of known protein concentration. The BCA assay solution was prepared by mixing 1 part of CuSO_4 and 49 parts of BCA.

2.3.5 Tau aggregation

Tau is a positively charged protein; the pI of full-length Tau is 8.24. In the presence of DTT the intra chain disulphide bonds are not formed properly, which delays the process of aggregation. In our work, polyanionic molecule heparin was used for inducing the aggregation. One molecule of heparin (17,500) was incubated with four molecules of Tau, heparin is considered to interact with the repeat region and insert region of Tau. The charge compensation and conformational changes resulted from initiation of Tau assembly³³. The aggregation of Tau is carried in 20 mM BES buffer supplemented with 25 mM NaCl, 2 mM DTT, 5 μM heparin, 0.01% NaN_3 and protease inhibitor cocktail. The NaCl maintained the ionic strength, NaN_3 was added for avoiding bacterial growth and a protease inhibitor cocktail was added to reduce the degradation of Tau protein. The assembly was kept at 37°C for 72 hours and the aggregation was monitored by SDS-PAGE and ThS assay.

2.3.6 ThS fluorescence assay

The natively unfolded soluble Tau has a random coil structure while the aggregated Tau has a prominent β -sheet structure. The conformational changes in the repeat region, proline-rich region and N-terminal region results in generation of β -sheet in Tau. Thioflavin S is a fluorophore which has excitation at 440 nm and emission at 520 nm. ThS binds to β -sheet-rich region of Tau and generates fluorescence. Hence, the aggregation of Tau could be tracked by monitoring the changes in ThS fluorescence¹¹³. In our work ThS was mixed with Tau in stoichiometric proportion of 4:1 (4 parts ThS and 1 part Tau). 8 μM ThS was prepared from 200 μM sub stock, which was dissolved in 50 mM ammonium acetates (pH 5.5). 8 μM ThS was mixed with 2 μM Tau the mixture was incubated in dark for 10 minutes at room temperature. The fluorescence was measured at excitation of 440 nm and emission wavelength of 521 nm.

2.3.7 Transmission electron microscopy

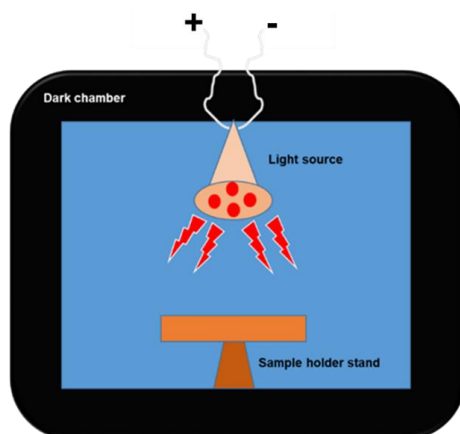
Electron microscopy uses high-energy electrons for the visualization of the specimen. The high-energy electron are focused on the specimen; in transmission electron microscopy, the electrons are passed through the sample. The absorbance and diffraction of electron is based on the chemical nature of sample¹¹⁴. The samples are generally stained with the elements having high electron density, which facilitates producing contrast to images. In our experiments, 2% Uranyl acetate was used for the negative staining. The carbon-coated copper grids were first incubated with protein samples for 60 seconds, after the incubation, the grids were washed twice with Mili Q water (30 seconds each wash). The grids were incubated with 2% Uranyl acetate solution for 5 minutes; the grids were allowed to air dry at room temperature. The imaging was done using Tecnai T20 at 200 kV.

2.3.8 Sedimentation assay

Tau protein aggregates to form heterogeneous population aggregates, oligomer and soluble Tau monomer protein (60-150 kDa). The higher molecular weight Tau aggregates can be separated from the soluble Tau protein with the help of ultracentrifuge. The pellet fraction obtains after ultracentrifuge contains the higher-order Tau aggregates and the supernatant contain the soluble monomer fraction of Tau. The extent of aggregation can be observed by running the supernatant and pellet fractions on SDS-PAGE. Tau aggregates were centrifuged at 60,000 rpm for 60 minutes at 4°C. The supernatant was collected gently and the pellet fraction was suspended in BES buffer. The pellet fraction, supernatant and total aggregates fractions were mixed with gel loading dye and loaded on 10% SDS-PAGE; the samples were allowed to resolve at 90 kV in Bio-Rad.

2.3.9 CD spectroscopy

The secondary structure of the Tau protein is determined by CD spectroscopy. The polarized molecules differentially absorb the left and right circularly polarized light which makes the basis of CD spectroscopy. The natively unfolded Tau has a random coil structure whereas β - sheet structure are observed in aggregated Tau¹⁸. Nitrogen gas was purged in Jasco J-815 CD spectrometer for creating the inert environment. The CD spectra of 50 mM phosphate buffer were acquired and used for further baseline corrections. The samples of soluble Tau and aggregated Tau and Tau treated with various compounds were diluted (1-3 μ M) using phosphate buffer. The CD spectra was acquired in quartz cuvette of 1 mm path length 1 nm band width at 100 nm/min scanning speed. The average of 5-10 acquisitions were recorded by scanning at wavelength 250-190 nm.



Scheme 1. The schematic diagram of photo irradiation apparatus

2.4 Photodynamic treatment assay

For analyzing the effect of photo-excited TB/RB on Tau aggregates, aggregates were incubated for one hour in the dark with varying concentrations of TB/RB (2, 5, 10, 20, 40 μ M). 200 μ L of the reaction mixture was added in 96 black well plate (Eppendorf) and was irradiated in dark using red/green LED. For PDT, three controls were considered; dark control (DC) containing TB/RB treated Tau aggregates, which are not irradiated. The light control (LC) containing light irradiated aggregates, which are not incubated with TB. The untreated, aggregated control (C). The samples were irradiated for different time intervals ranging from 30 to 300 minutes.

2.5 Cytotoxicity assay ,

The cytotoxicity assay was carried out as per standardized protocol in lab. For cell viability assay MTT (Methylthiazolyldiphenyl-tetrazolium bromide) assay was used. 1×10^4 N2a cells were cultured in advanced DMEM-F12 (Dulbecco's modified Eagle's Media) media supplemented with 10% fetal bovine serum and glutamine. After 24 hours of incubation, the cells were treated with various concentration of compounds dissolved in cultured media. Following 24 hours of compound treatment, MTT (Methylthiazolyldiphenyl-tetrazolium bromide) was added to cells at concentration of 0.5 mg/mL and incubated at 37°C for 4 hours. Subsequent to incubation, the media was removed from the wells and the formazan crystals were dissolved in 100 μ L of 100% DMSO (Dimethyl sulfoxide). Cell viability was evaluated by measuring the absorbance at 570 nm.

2.6 ROS Production

The effect on various compounds on ROS production was estimated in N2a cells using DCFDA assay. ROS oxidizes 2,7-dichlorofluorescein diacetate (DCFDA) to 2',7'-dichlorofluorescein (DCF), leading to the generation of fluorescence. For the assay 10,000 cells/well were seeded in 96 well plate and incubated for 24 hours. The cells were treated with various concentrations of compounds. After treatment, the cells were washed subsequently twice with 1X PBS (pH 7.4). The cells were supplemented with 10 μ M DCFDA and incubated for 20 minutes. After incubation, the cells were again washed twice with 1X PBS. In the final step the PBS was replaced with phenol red-free DMEM media and the fluorescence was measured at 535 nm upon exciting at 485 nm.

2.7 Western Blotting

2.7.1 Protein extraction form cells

Neuro2a cells seeded in density of 3×10^6 /well were studied for the effect of formaldehyde stress on various signalling protein and the protective action of BME. The experiment composed of four treatment groups *viz*, untreated cell control, 0.5 mM FA treatment, 5 μ g/mL BME treatment, FA+BME treatment. The cells were exposed to specific treatment for 4 hours, the cells were harvested and pelleted down. The cells were lysed with RIPA buffer and lysate was centrifuged at 12,000 rpm for 20 minute at 4°C.

2.7.2 The western Blotting

The protein concentration was estimated by Bradford assay and 75 µg protein was loaded on SDS-PAGE. After resolution on SDS-PAGE the protein was transferred on activated PVDF membrane. The blot was incubated with 10% skimmed milk for blocking the nonspecific interaction sites. The blot was incubated with the 1° antibody for overnight at 4°C. After three wash of PBST, HRP-tagged secondary antibody was added to blot. After 60 minutes of incubation at room temperature the blot was washed subsequently trice by PBST. The chemiluminescence was developed using Bio-Rad Clarity Western ECL blotting substrates solution and the blots were imaged by Amersham AI600 chemiluminescent imager.

2.7.3 Stripping procedure

The blot was washed with stripping buffer having SDS, twin 20 and pH 2.8. After two consecutive washes of stripping buffer (10 minutes each) the blot was washed twice with PBS (pH 7.4), and blocked with 10% skimmed milk. The probing of next set of antibody and development blot was performed similarly as explained previously.

2.8 Immunofluorescence microscopy

Immunofluorescence microscopy is a technique to study the localization and endogenous expression of protein of interest. The technique involve the fluorescently tagged antibodies against target protein¹¹⁵. In our experiments, 2.5×10^4 cells were seeded on the 12 mm coverslip. After the specific treatment, cells were treated with chilled methanol for 20 minute at -20°C. The permeabilization step involves the treatment of non-ionic detergents such as triton X 100. The permeabilization is followed by step of blocking, blocking involves treatment of cells with solution of 1-5% horse serum. The permeabilization and blocking was performed simultaneously by treating cells with PBS supplemented with 2% horse serum and 0.2% Triton X-100. After 60 minutes of incubation the cells were washed trice with PBS (10 minutes of each wash). The 1° antibody was prepared in PBS supplemented with 2% horse serum, the cells were incubated over night with 1° antibody. After incubation the coverslips were washed trice with PBS. The alexa flour tagged 2° antibody were added on the cells and incubated for 60 minutes at room temperature. After the incubation the coverslips were washed trice with PBS. 4',6-diamidino-2-phenylindole (DAPI) is a fluorescence dye which have strong affinity for adenine- thymine rich region of DNA. The cells were incubated with 300 nM of DAPI for 5 minute. The coverslips were mounted using prolonged diamond anti fade mounting media. The coverslips were scanned by Zeiss Axio Observer 7 with Apotome 2 using 63X oil immersion. The fluorescence images were processed by Zen blue 2.3 software.

2.9 *Drosophila* experiments

2.9.1 Fly Stocks and Genetics

The transgenic *Drosophila* strain used in this study was *UAS-Tau E14. ELAV-Gal4* driver lines were obtained from the National *Drosophila* Stock Centre at the University of Mysore, Mysore, and Karnataka, India. *Drosophila* strains raised on standard medium were crossed at 25°C.

2.9.2 Fly husbandry

Flies were maintained on standard banana-jaggery medium (SM) under standard laboratory conditions of $24 \pm 1^\circ\text{C}$ temperature, $75 \pm 5\%$ relative humidity, and 12:12 L:D cycle (SLC). Flies were maintained in a 2-week discrete generation cycle for 10 generations before being used

in this study. The adult density was regulated at about 100 flies per half-pint bottle with 25 mL of SM. There was total of 10 bottles. Flies from 10 bottles were combined into a single breeding cage, hereafter referred to as parental cage (PC).

2.9.3 Preparation of TB/RB-supplemented diet

A total of 2.5 L of SM was prepared following the procedure and split into 5 batches of 500 mL each. For the control group, SM was poured into the bottles. For the TB/RB-supplemented media, 2.5, 5.0, 10 or 25 μM of TB/RB was added and mixed thoroughly just before pouring into the bottles. All bottles were plugged with non-adsorbent cotton and the media was allowed to set under room temperature. All other laboratory reagents used in this study were purchased from Merck, unless otherwise mentioned.

2.9.4 Larval feeding behaviour assay

The eggs obtained were transferred at a density of 50 eggs/6 mL of SM and allowed to develop till early third instar. The early third instar larvae were removed from the SM vials and used in the feeding behaviour assay. The larvae were individually transferred to an assay petri plate of 5 cm diameter containing 10 mL of either liquid SM (SM without agar) or liquid SM supplemented with different concentrations of TB/RB and allowed for 5 seconds for acclimation. The feeding rate was measured as the mean number of sclerite retractions in 2 consecutive 30-second intervals. The feeding rate of larvae was considered by taking average of the 2 rates. Each treatment group has 20 larvae and the assay was replicated 4 times. Thus, a total of 160 larvae were assayed for feeding rate.

2.9.5 Fecundity assay

Flies from the holding vials were sexed under light CO_2 anaesthesia and single-pair (one male + one female) were transferred to the vial with ~ 3 mL SM. For each treatment group in a population 20 vials were set up. The conscious flies were transferred to fresh SM vials every 24 hours, and the eggs laid during the previous 24 hours were counted under a microscope and recorded. The daily egg counts were carried out till the death of the female fly in each test vial.

2.9.6 Negative geotaxis assay

The physical fitness of flies could be monitored by their ability to climb on the wall of vessels. The vertical climbing ability of male flies that emerged from different treatment bottles was assessed. Twenty male flies per treatment group were collected and transferred to the empty, 0-15 cm graduated vial. The vial was gently tapped and placed in the vertical position. The number of flies that crossed the 15 cm mark in 30 seconds were counted. Three trials were conducted on each set of 20 flies. The data are expressed as the percentage of flies crossed the 15 cm mark.

2.9.7 Viability of fly from egg to adult

The eggs from the media plate were collected and dispensed into a different treatment groups of bottles at a density of ~ 100 eggs/bottle with 45 mL media. Ten bottles were prepared for the five treatment groups of SM, SM+ 2, 5, 10 and 25 μM TB/RB. Bottles were maintained at standard laboratory conditions. The flies emerge from different treatments; SM and SM+2, 5, 10 and 25 μM of TB/RB were designated collected and counted. All the assays were carried out on SM using mated flies. The total number of flies that emerged from each bottle were used to calculate the viability of flies emerging from each treatment group.

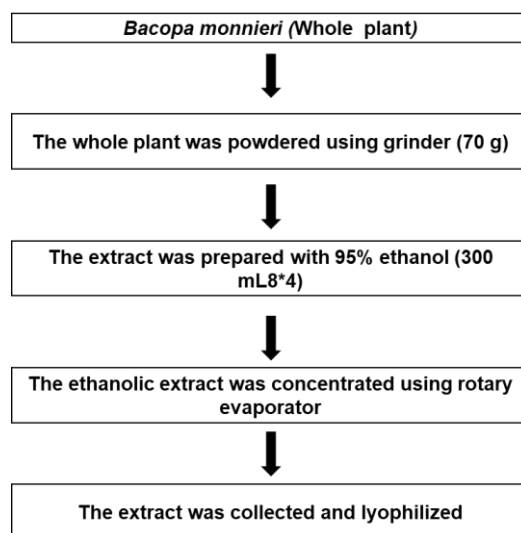
2.9.8 Larval olfactory behaviour

The olfactory test was carried out by employing previous method with minor modifications. 30 larvae were briefly dried on a filter paper before being placed in the centre of petri dish. The petri dish containing 20 μ L of Quinine sulphate dispensed on each of the two 0.5 cm radius filter discs were placed in the diametrically opposite to Quinine zones. After 2 minutes of placing the larvae and covering the petri dish, the numbers of larvae in different zones were counted to calculate the percentage of larvae having ability to avoid the bad odour.

2.10 Preparation of ethanolic extract of *Bacopa monnieri*

Bacopa monnieri whole dried plant was collected from Indore, Madhya Pradesh, India and authenticated by a botanist. The plant material was powdered with the help of a grinder. 70 grams of plant powder was extracted using rectified spirit (300 mL \times 4) at room temperature with constant stirring for 24 hours. The crude ethanol extract was filtered and combined together. Further, it was concentrated under reduced pressure using a rotary evaporator at 40° C. The dark green viscous crude extract was obtained after subjecting to high vacuum, stored at 4° C and used for further investigation.

2.10.1 The preparation of *Bacopa monnieri* extract



Scheme 2. The schematic representation of *Bacopa monnieri* extract formation

2.10.2 HPLC and TLC Conditions

A thin layer chromatogram (TLC) was developed twice on silica gel G pre-coated plates (Merck, 0.25 mm) with 50% ethyl acetate in hexane as the mobile phase. Spots were visualized by dipping the TLC plate in a solution of 3.0% anisaldehyde, 2.8% H₂SO₄, 2% acetic acid in ethanol with subsequent heating. The dried plant extract was dissolved in HPLC-grade methanol and proceeded for HPLC analysis. After filtration, 20 μ L sample was manually injected. The samples were eluted through an X Bridge C-18 reverse phase column of dimension 250 \times 4.6 mm and 5 μ m particle size and monitored by a Diode-Array Detection (DAD) detector at 254 nm. The mobile phase used was milli-Q water containing 0.1% formic acid (solvent A) and methanol (solvent B). The flow rate was 1 mL/min. Gradient elution was employed, commencing at 10% B, increased to 90% B over 8 minutes, and then decreased to 60% B for the next 4 minutes and after the next 7 minutes, it decreased to 10% B, where it

was held for two minutes. The solvent blank readings were considered as reference for subtracting background noise from experimental readings. Data were analyzed through Agilent's Open lab CAD software.

2.10.3 UPLC–ESI (+)-MS condition

Samples were dissolved in LC-MS grade methanol, filtered and 5 μ L of it was injected. The separation was performed with the X bridge C18 column (4.6 mm \times 250 mm, particle-size 5 μ m) using a similar solvent program used for HPLC as described above. The flow rate was set as 0.6 mL/min. MS runs were carried out using the tuning method as follows: sheath gas (nitrogen) flow rate 45 units, auxiliary gas (nitrogen) flow rate 10 units, sweep gas (nitrogen) flow rate 2 units, spray voltage 3.60 kV, spray current 3.70 A, capillary temperature 320 $^{\circ}$ C, s-lens RF level 50, heater temperature 350 $^{\circ}$ C. In positive ion mode, ESI-MS data were recorded within the mass range m/z 100–1500. Data were analyzed through Thermo X calibur software.

2.11 Statistical data analysis

The statistical data for the fluorescence measurement or viability assay was plotted using either duplicate or triplicate reading. We have used student's t-test for finding significance of the values in the aggregation inhibition assay, disaggregation assay, immunofluorescence quantification, MTT assay, DCFDA assay, and caspase-3 assay. * $p < 0.05$, ** $p < 0.001$, *** $p < 0.0001$, correspond to the statistical difference between control and treated groups Raw data were analysed and plotted by Sigma Plot software.

Chapter 3

Photo-excited Toluidine Blue Inhibits Tau Aggregation in Alzheimer's disease

3.1 Background

The application of dyes were restricted to staining and diagnostic purposes, but in recent years research has expanded the application of dyes as therapeutic molecules. After discovery of photodynamic therapy, various dyes of classes such as xanthene, phenothiazine, and porphyrin have gained enormous attention¹¹⁶. The photosensitizers are the dyes or compounds which upon irradiation of specific wavelength of light leads to the generation of singlet oxygen species¹¹⁷. The photosensitive dyes are majorly applied to treat carcinomas such as lung, bladder, skin *etc.* The clinical approval of photosensitive dyes *e.g.* Photofrin, Temoporin, Talaporin, Cholin6, 5-ALA has facilitated the non-invasive treatment of numerous diseases¹¹⁸. These dyes are also emerging as promising treatment molecules in AD; different classes of dyes target various aspects of AD-related pathologies⁷⁹. Methylene blue (MB) is a phenothiazine dye that has been studied extensively for its potency in AD. MB inhibited the Tau aggregation, which is the hallmark of AD pathology. The MB treatment improved mitochondrial respiration by elevating cytochrome C levels in mitochondria¹¹⁹. The derivatives of MB, including Azure A, Azure B and natural red are also observed to be effective against oxidative stress in AD¹²⁰. The photo-excited dyes are recently reported for their therapeutic efficiency in AD. The photo irradiated MB inhibited the aggregation of A β -42 and reduced their toxicity to cells⁸². Apart from MB, several other photo-excited compounds have also showed efficiency against AD. The photosensitizers such as RB/UCNP@ROS and β NaYF₄:Yb/Er@SiO₂@RB are the compounds that have excitation wavelength in the infrared region; these compounds have inhibited the A β fibril formation. Polyoxometalate, Thioflavin T, Tetra (4-sulfonatophenyl) porphyrin (TPPS) were also observed to have potency in inhibiting the A β aggregation and A β -mediated cytotoxicity¹²¹. Similarly xanthene dye Rose Bengal disaggregated the A β aggregates and improved the longevity of the *Drosophila* model of AD⁸⁰. The effect of photo-excited dyes on Tau aggregation has not yet been reported. Toluidine blue (TB) is an acidophilic phenothiazine dye, which has been widely used in histology¹²². TB is known to have photo-excitation properties like its parent compound MB. The exposure of 630 nm red light leads to the photo-excitation of TB¹²³. Although, the therapeutic potency of TB has been reported for the treatment of cancer and bacterial biofilms, but its effect in AD is still unexplored¹²⁴. The four repeat region of Tau plays a crucial role in the aggregation; VQIINK and VQIVYK hexapeptides present in the second and third repeat has majorly contributed to the aggregation propensity in Tau. The repeat region (244Q- 369K) has a basic charge with a pI of 9.6¹¹². The amino acid residues in the repeat region are the targets of several post-translational modifications *e.g.* phosphorylation. Since the repeat region of Tau is necessary for the assembly of Tau and microtubules, various conformational studies have been carried out to study the role of various mutations in repeat Tau residues. The repeat region of Tau forms the core of PHFs; hence the repeat is targeted for studying various aspects of Tau aggregation. The structural analog inhibitors targeting VQIINK and VQIVYK have potency against the Tau aggregation¹¹¹. The anthraquinone such as Daunorubicin, Andriamycin, and Emodin are known to inhibit the aggregation of repeat Tau *in vitro* and *in vivo*³². Another class of compounds based on Rhodanines are found to reduce the Tau oligomer-mediated toxicity in Neuro2a cells¹²⁵. The Tau inhibitors belonging to the phenylthiazolyhydrazide class, interact with the repeat Tau region *via* hydrophobic bonding which is formed by the involvement of nitroaromatic and imidazole amines¹²⁶. Similarly, N-phenylamine-based Tau aggregation

inhibitors such as Meclofenamic acid reduces the toxicity and aggregation of repeat Tau in Neuro2a cells bearing K18 Δ K280 mutation²⁸. In recent screening, Aminothienopyridazines were observed to be potent in inhibiting the aggregation of P301L K18 Tau. Among all these phenothiazine dyes that have been studied extensively against Tau aggregation inhibition, Methylene blue (MB) was reported to inhibit the aggregation of the repeat Tau *via* modulation of cysteine residues. Methylene blue oxidizes the cysteine residue, which restricts the formation of disulphide bonds^{28,68}. MB treatment restores the cognitive defect in the transgenic mice bearing Tau- Δ K280 mutation⁷². The phenothiazine dyes also have the potency of photo-excitation; the effect of photo-excited MB has been illustrated against A β aggregation and A β -mediated neurotoxicity⁸². But the role of photo-excited dyes against Tau aggregation is yet to be explored. Toluidine blue (TB) is the derivative of MB, which is a well-known photosensitizer. Although the potency of PE-TB has been reported in the treatment of various diseases *e.g.* cancer, its role in the neurodegenerative disease is still not addressed. We aim to study the aggregation study of TB against *in vitro* Tau aggregation. We have studied the role of PE-TB against mature Tau fibrils. Actin and tubulin are the major cytoskeletal proteins that are involved in various functions such as maintaining cell integrity, formation of synaptic connections, *etc*¹²⁷. Similarly, cell End-binding protein 1 (EB 1) is plus-end-binding protein, which localizes on the growing end of microtubule. Thus to study cytoskeleton modulation, the role of TB and PE-TB was observed on actin, tubulin and EB 1 protein. The overall aim of this work was to study the potency of TB and PE-TB in various aspects of Tau aggregation.

3.2 Results

3.2.1 Toluidine Blue inhibited the aggregation of full-length Tau *in vitro*

The potency of TB was studied against various aspects of Tau aggregation (Fig. 8A). The *in vitro* aggregation kinetics of Tau was tracked by ThS fluorescence assay. 40 μ M of heparin-induced Tau was incubated with various concentrations of TB (2, 5, 10, 20, 40 μ M) for 72 hours at 37°C. The ThS readings were taken at periodic intervals and the kinetics were plotted. The fluorescence assay suggested that TB potentially inhibited the *in vitro* aggregation of Tau (Fig. 8B). Tau incubated with 40 μ M of TB were observed to have \geq 80% inhibition of aggregation (Fig. 8C). The aggregation of Tau results in generation of conformational changes in its secondary structure. Under native conditions, Tau has random coil structure, whereas the aggregated Tau has prominent β -sheet structure, where we studied the conformational changes in Tau aggregates upon TB treatment. The CD spectroscopy indicates that untreated Tau aggregates has a partial β -sheet structure while the TB treated Tau showed a slight shift towards the random coil (Fig. 8D). The morphological studies of Tau aggregates were performed with the help of electron microscopy. We observed that the untreated aggregates had long thick morphology, whereas TB treated samples had small broken pieces of Tau, which indicated potent disaggregation (Fig. 8E). We carried out UV-visible spectroscopy to calculate the affinity of TB for Tau. Our results showed that Tau has a very weak affinity for TB (Fig. 8F).

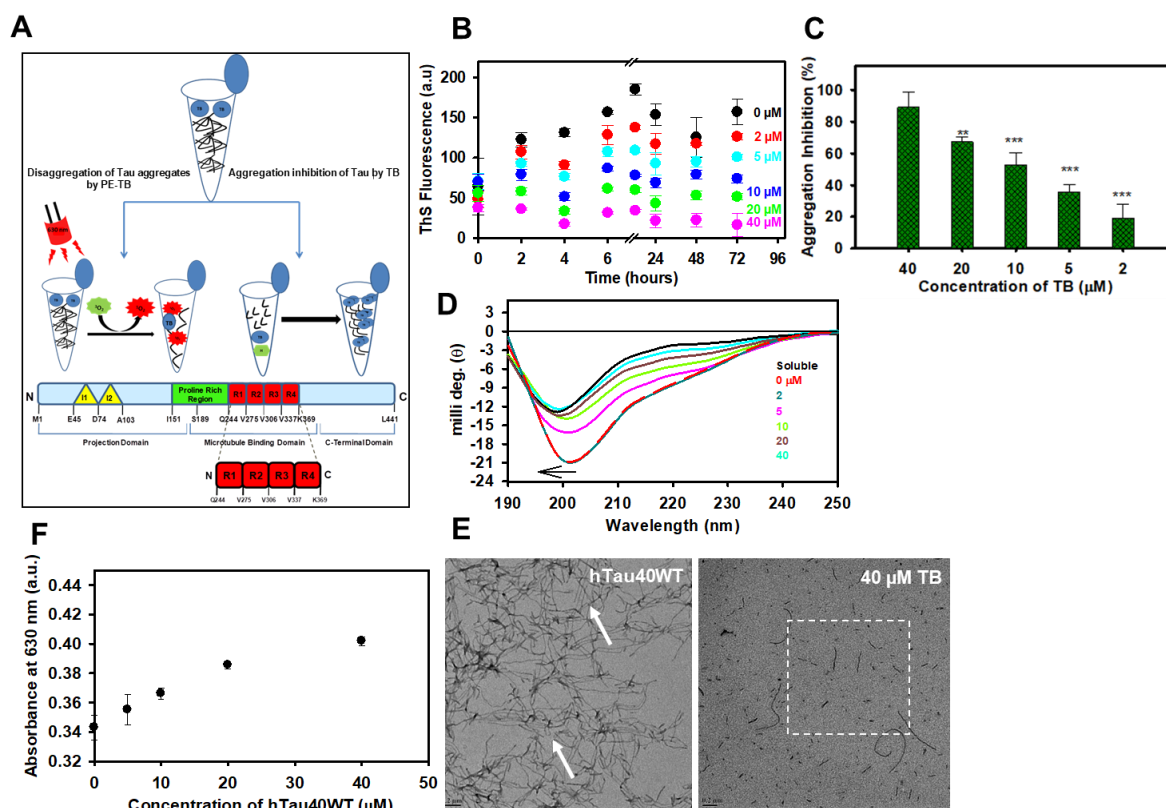


Figure 8. The *in vitro* Tau aggregation inhibition by TB. A) The schematic diagram explains the strategy that is followed in carrying out the experiments. B) ThS fluorescence kinetics shows the effect of various concentrations of TB on heparin-induced Tau aggregation. The kinetics showed that TB potentially inhibited the *in vitro* Tau aggregation. C) The graph shows the percentage of aggregation inhibition at the end of 72 hours. 40 μM of TB showed 80% aggregation inhibition of Tau. D) The changes in the secondary structure of Tau aggregate after TB treatment were monitored by CD spectroscopy. Untreated Tau aggregates showed partial β -sheet structure while TB treated samples that had shifted towards the random coil. E) Electron microscopic images shows the changes in the morphology of TB treated and untreated aggregates. F) UV-visible spectroscopy for studying the interaction between Tau and TB.

3.2.2 Photo-excited Toluidine Blue disaggregates full-length Tau aggregates *in vitro*

TB is a well-known photosensitizer, the exposure of 630 nm red light photo-excites TB. Thus we aimed to study the potency Photo-excited Toluidine Blue (PE-TB) on pre-formed Tau aggregates (Fig. 9A). 40 μM of Tau aggregates were incubated with various concentrations of TB (2, 5, 10, 20, and 40 μM), the samples were irradiated for 180 minutes under 630 nm red light in a dark chamber. After irradiation, the samples were run on 10% SDS-PAGE. We observed that untreated control, dark control and light control had characteristics of higher-order bands, whereas PE-TB treated samples, were lacking the higher order bands, which indicated the potential disaggregation (Fig. 9B). The disaggregation potency of PE-TB was also studied by ThS fluorescence assay. We observed a decrease in fluorescence PE-TB treated samples in concentration-dependent manner; 40 μM PE-TB showed maximum disaggregation in comparison to the untreated samples (Fig. 9C). The changes in Tau aggregate's morphology upon PE-TB treatment were studied by electron microscopy. The untreated aggregates were observed to have long thick fibrils while the PE-TB treated samples had small broken filaments that indicated potential disaggregation (Fig. 9D).

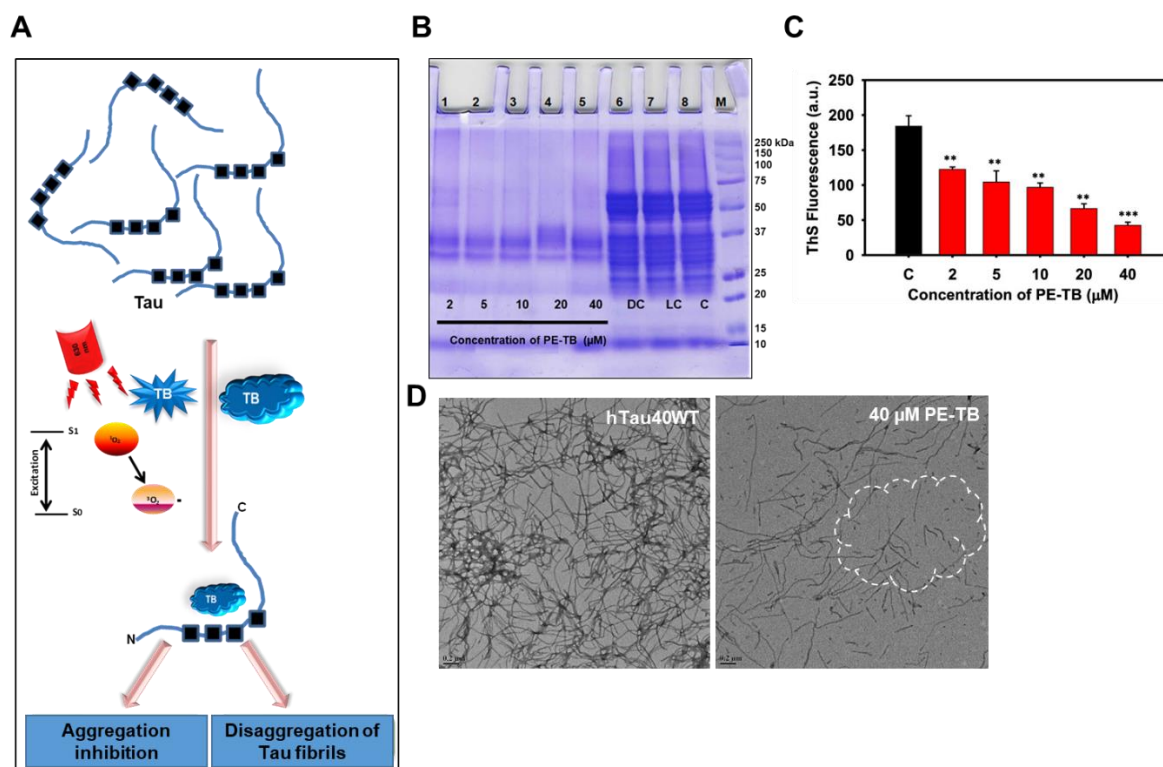


Figure 9. Disaggregation of Pre-formed Tau aggregates by PE-TB. A) The schematic diagram explains the hypothesis designed to carry out the experiments. B) SDS-PAGE shows the effect of PE-TB on Tau aggregates. The untreated control had bands at higher molecular weight, while the PE-TB treated aggregates were not having the higher-order bands. C) The disaggregation of PE-TB treated Tau aggregates was monitored by ThS fluorescence. The ThS assay indicated that PE-TB treated samples lack the aggregates as compared to the untreated samples. D) The electron microscopic images of the untreated aggregates showed long thick fibres, while the PE-TB treated samples had small broken filaments.

3.2.3 TB inhibited the aggregation of repeat Tau *in vitro*

The repeat region of Tau is known to have a high drift of aggregation. As the repeat region is considered to be involved in the generation of Tau pathology, several molecules have been studied for their potency to inhibit repeat Tau aggregation (Fig.10A). The molecules of various origins *e.g.* EGCG, limonoids *etc.* metal-based complexes *etc.*, reported to be potent in inhibiting the aggregation of repeat Tau. In our work, we aim to study the aggregation inhibition potency of TB against repeat Tau. The uniform concentration of repeat Tau (40 μM) was incubated with TB of various concentrations (2- 40 μM). The assay was performed at 37°C and the aggregation kinetics was observed by monitoring the ThS fluorescence periodically. The graph of aggregation kinetics indicated that untreated repeat Tau sample aggregated rapidly than the TB treated repeat Tau. The untreated sample extortionate ThS fluorescence compared to the TB treated samples, which indicated that TB treatment inhibited the repeat Tau aggregation (Fig.10B). The endpoint analysis of assay suggested that 40 μM of TB inhibited ≥80% aggregation of repeat Tau. In lower concentration of TB (10 μM) ≥50% decrease in aggregation was observed after 60 hours of treatment (Fig.10C). Thus from this set of experiments we observed that TB potentially inhibited the aggregation repeat Tau *in vitro*.

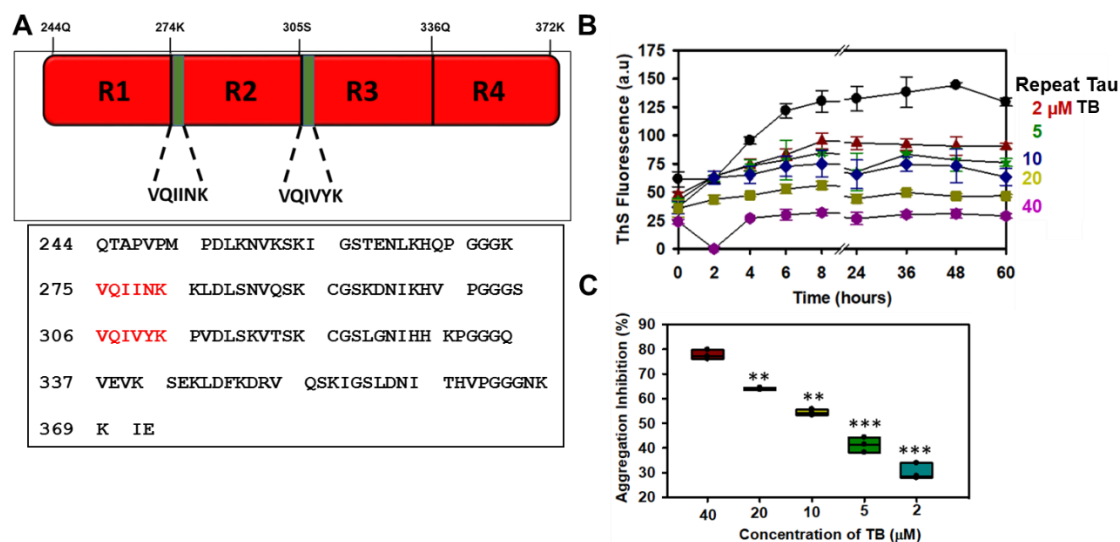


Figure 10. TB inhibited the aggregation of repeat Tau *in vitro*. A) The four repeat region of Tau is prone to aggregation. The mutation and PTMs in the repeat region modulates the aggregation propensity of Tau. B) ThS kinetics shows the effect of TB on repeat Tau aggregation. TB treated aggregates had low fluorescence than the untreated aggregates. C) The graph shows the percentage inhibition at the endpoint of assay. $\geq 80\%$ of aggregation inhibition was observed in the presence of TB.

3.2.4 Photo-excited TB potentially disaggregated the pre-formed repeat Tau aggregates

TB belongs to the phenothiazine class of dyes, which is a well-known class of photosensitive dyes. Phenothiazine dyes are known for their application against cancerous cells, drug-resistant microbial infections, skin lesions *etc*¹²⁸. The role of photo-excited dyes is emerging in the treatment of AD⁸². We studied the effect of photo-excited TB on mature repeat Tau aggregates (Fig.11A). Repeat Tau aggregates (40 μ M) were incubated TB (2-40 μ M), the reaction mixture was exposed to 630 nm red light for 180 minutes. Soluble repeat Tau protein observes as 18 kDa band on SDS-PAGE, but the aggregates of repeat Tau have characteristics of heterogeneous higher-order protein bands. Thus, to study the effect of PE-TB on repeat Tau aggregates, the PE-TB treated samples were run on SDS-PAGE. The untreated repeat Tau aggregates had heterogeneous higher-order protein bands, whereas the PE-TB treated samples were lacking the higher order protein bands, which were an indication of disaggregation (Fig.11B). ThS dye binds to the Tau aggregates and emits the fluorescence thus by quantifying the ThS fluorescence the disaggregation potency of PE-TB could be monitored. The untreated aggregates were having elevated fluorescence than PE-TB treated aggregates. The distinct decrease of fluorescence in concentration-dependent manner of PE-TB suggested that PE-TB potentially disaggregated the mature repeat Tau aggregates (Fig. 11C). The structural changes in Tau aggregates after treatment of PE-TB were studied by electron microscopy. The untreated repeated Tau aggregates were observed to have long thick filamentous morphology, while small broken pieces of Tau filaments were observed in samples exposed to PE-TB (Fig.11D-E). Thus, the cumulative result of these experiments suggested that repeat Tau efficiently disaggregated the pre-formed Tau aggregates.

3.2.5 The biocompatibility of Toluidine Blue in neuronal cells

The effect of molecules on cell viability is one of the crucial aspects for studying its therapeutic potency. The response of molecule in the context of the viability of host cells, determines its compatibility to be applied in biological system.

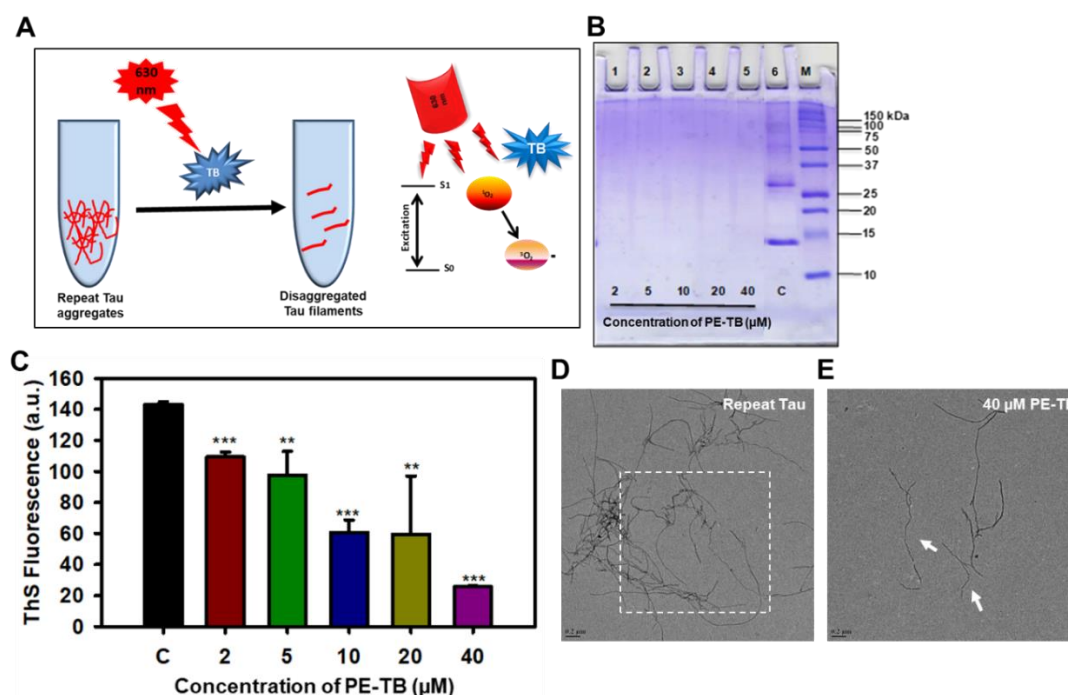


Figure 11. PE-TB disaggregated pre-formed repeat Tau aggregates. A) The schematic diagram shows the hypothesis followed to study the effect of PE-TB on repeat Tau aggregates. B) The effect of PE-TB on repeat Tau aggregates was studied by SDS-PAGE. The untreated control had heterogeneous bands of higher-order aggregates, while PE-TB treated samples lacked the higher-order bands. C) The graph shows the difference in ThS fluorescence reading. The untreated samples had higher fluorescence than the PE-TB treated samples. D) Electron microscopic images of untreated aggregates. E) The electron microscopy images show the morphology of PE-TB treated samples.

The minimal degree of cytotoxicity is one of the major concern to determine the optimal dose of therapeutic molecule. The higher concentrations of organic dyes are known to generate cell toxicity. Thus the effect of various concentrations of TB and PE-TB in neuronal cells was studied by MTT assay. The cytotoxicity studies for TB were performed in Neuro2a cells. The cells were incubated at various concentrations of TB for 24 hours. The viability and metabolic activity of cells was monitored by methylthiazolyldiphenyl-tetrazolium bromide (MTT) assay. The result of the MTT assay suggested that lower concentrations of TB has no adverse effect on cell viability (Fig.12A). Further, the neuro2a cells were incubated with higher concentrations of TB and PE-TB (1-120 μM) and the percentage viability of cells were calculated in comparison to untreated cells. Neuro2a cells incubated with various concentrations of higher TB concentrations were observed to have reduced cell viability. The cells incubated with TB at a concentration of 20-120 μM had viability $\leq 40\%$ (Fig.12B). Similarly, the cells exposed to PE-TB also showed reduced viability. At the same time, PE-TB was observed to induce pronounced toxicity at concentration ranging from 10-120 μM (Fig.12C). The phase-contrast imaging for studying the morphological changes in TB and PE-TB treated cells indicated that at concentrations ≥ 20 μM TB internalized to cells. The cells incubated with a higher concentration of TB (≥ 80 μM) had prominent internalization of TB (Fig.12D). The studies suggested that the higher concentrations of TB induce an adverse effect on the viability of Neuro2a cells. The irradiation of TB generates singlet oxygen species. Thus, we aim to observe

the effect of PE-TB on ROS production in cells. The intracellular ROS was tracked by fluorescence DCFDA assay. The cells were treated with various concentrations of TB (0.025 to 2.5 μM). The DCFDA results indicated that TB-treated cells produced more ROS as compared to untreated cells. However, the cells observed low level of oxidative stress in lower concentration of TB treatment (Fig. 12E). Thus we stated that in lower concentrations, TB could be considered as a biocompatible molecule.

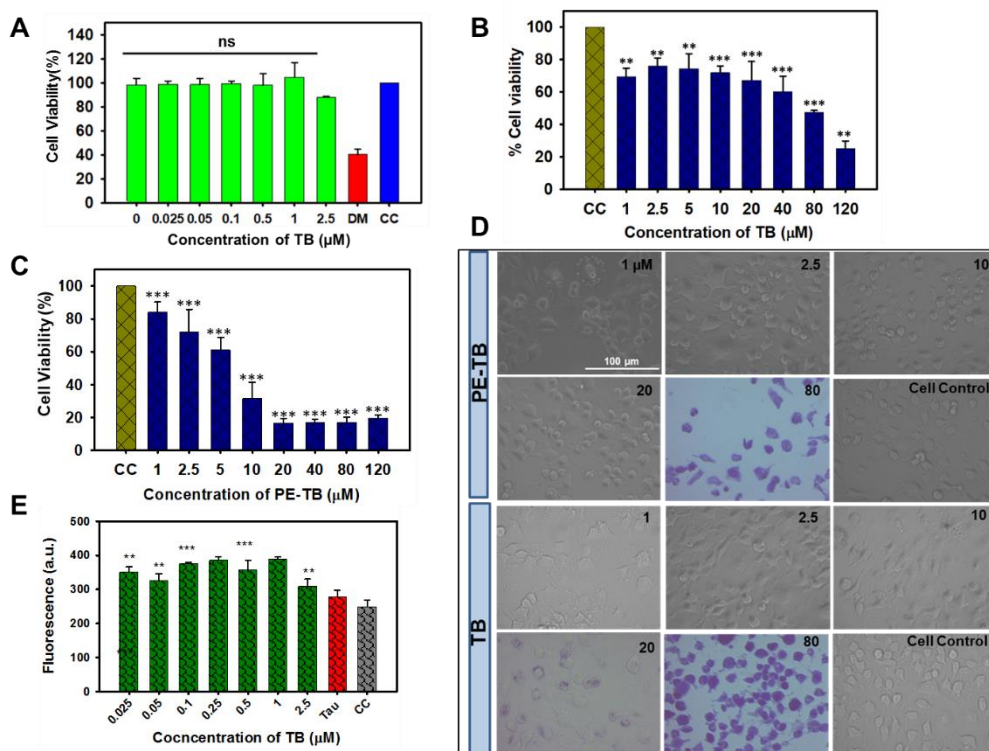


Figure 12. The biocompatibility of TB. A) The effect of various concentrations of TB on neuro2a cells was studied by MTT. The lower concentration of TB did not show any adverse effects on cell viability. B) The graph of MTT assay, shows the effect of a higher concentration of TB on cell viability. The concentration above 10 μM and above was found to be toxic to cells. C) The graph of the MTT assay indicates the effect of higher concentrations of PE-TB on cells. D) The phase-contrast images of TB and PE-TB treated cells. At higher concentrations, TB gets accumulated in cells leading to the generation of toxicity. E) The effect of TB on intracellular ROS production was studied by DCFDA assay. TB was observed to produce a low level of oxidative stress in cells.

3.2.6 Toluidine Blue and photo-excited Toluidine Blue modulate the cytoskeleton of neuronal cells

The neurodegenerative diseases result in generation of various cytoskeleton deformities¹³⁰. Earlier studies have suggested that several potent PSs such as 3,3'-dihexyloxycarbocyanine iodide, Tetra-cationic platinum (II) porphyrins, 5-aminolevulinic acid target the cytoskeleton⁷⁹. The role of PSs on neuronal cytoskeleton needs to be explored extensively. Thus we are focused on studying the effect of TB and PE-TB on cytoskeleton modulation. Tubulin protein polymerizes and forms microtubules that play an essential role in maintaining the integrity of neurons, formation of synaptic connection, cell division, and early neuronal development¹³¹. The photosensitizers like meta-tetrahydroxyphenyl chlorin (mTHPC), TMPyP–Porphyrine etc causes, disassembly of microtubules¹³². We studied the effect of TB and PE-TB on tubulin expression was observed by immunofluorescence. The results showed that the cells exposed to 0.5 μM TB and PE-TB had increased tubulin intensity and neuritic extension as compared

to unexposed cells. The increase in tubulin intensity after the exposure of TB supported the modulation of tubulin network (Fig.13).

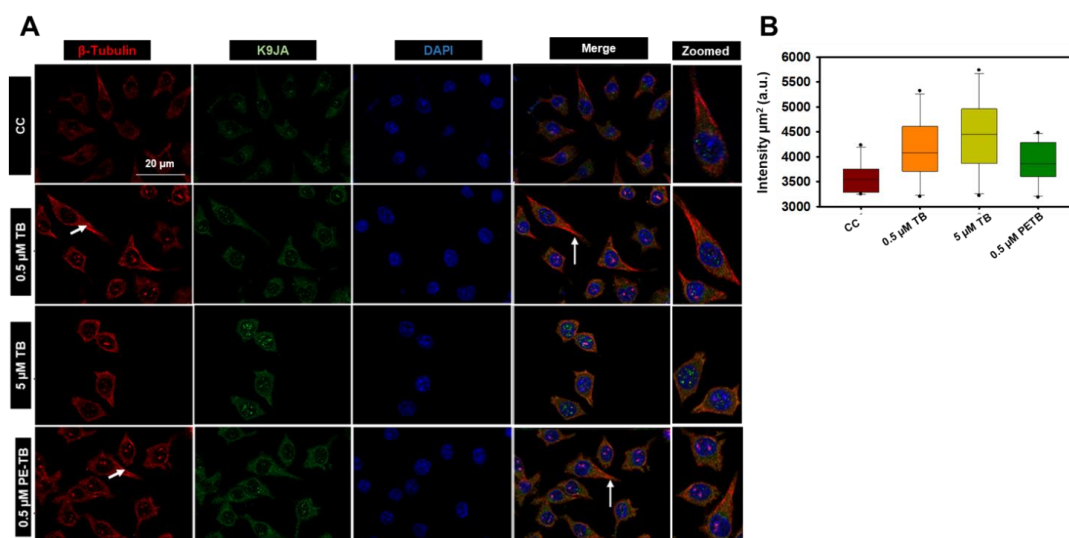


Figure 13. TB modulated tubulin cytoskeleton of neurons. Tubulin plays a crucial role in maintaining the integrity of cells. Immunofluorescence images of TB and PE-TB treated cells were observed to have elevated tubulin intensity compared to untreated cells.

Similarly, actin is another important protein of the cytoskeleton. The F-actin are formed by polymerization of globular G-actin¹³³. These F-actin crosslinks and forms actin-rich structures e.g. filopodia and lamellipodia. The filopodia are thin hair-like structures mainly involved in making cell- to-cell contact and synapse formation, while lamellipodia are fan-like structures involving cell adhesion (Fig.14A)¹³⁴. Various photosensitizers target the actin cytoskeleton. Sinoporphyrin, 5-ALA, hypericin are examples of photosensitizers, which inhibit the polymerization of F-actin¹³⁵. We observed that exposure to TB and PE-TB increases the actin-rich filopodia and lamellipodia structure in the neuron as compared to untreated cells. These results indicate that TB and PE-TB have the potency to modulate actin cytoskeleton (Fig.14B, C).

3.2.7 TB modulates the EB1 levels in neuronal cells

Microtubules have a critical role in regulating of cell dynamics and maintaining of cell integrity. The polymerization of tubulin on growing end of microtubule is facilitated by EB1. Thus, by tracking the levels of EB1 and Tau, the rate of microtubule polymerization could be understood¹³⁶. We studied the effect of TB and PE-TB on the EB1 and Tau level in neuronal cells. The result of IF studies suggested that the cells exposed to TB have an increased intensity of EB1 as compared to untreated cells. Whereas, no differential changes were observed for PE-TB treated cells. The observation of these studies supported that the TB treatment modulated the EB1 level in cells, which ultimately indicated the polymerization of microtubules. However, no difference in total Tau intensity was observed after treatment of TB and PE-TB (Fig. 15 A, B). The result of the experiment indicated that TB could have potency to modulate microtubule polymerization.

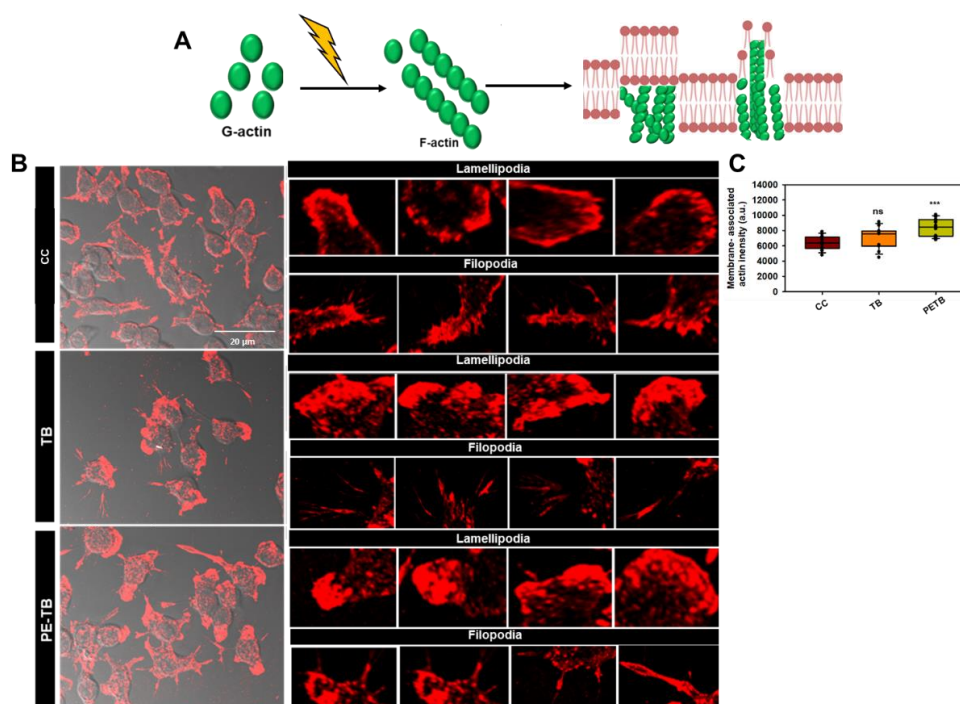


Figure 14. Modulation of the actin cytoskeleton by TB and PE-TB. Actin is another essential cytoskeleton protein in cells. A) The schematic diagram shows the actin modulation hypothesis by PE-TB treatment. B) Immunofluorescence images of PE-TB and TB treated neurons showing increase in the number of filopodia and lamellipodia. C) The quantification of IF images suggested that TB and PE-TB modulated the actin cytoskeleton.

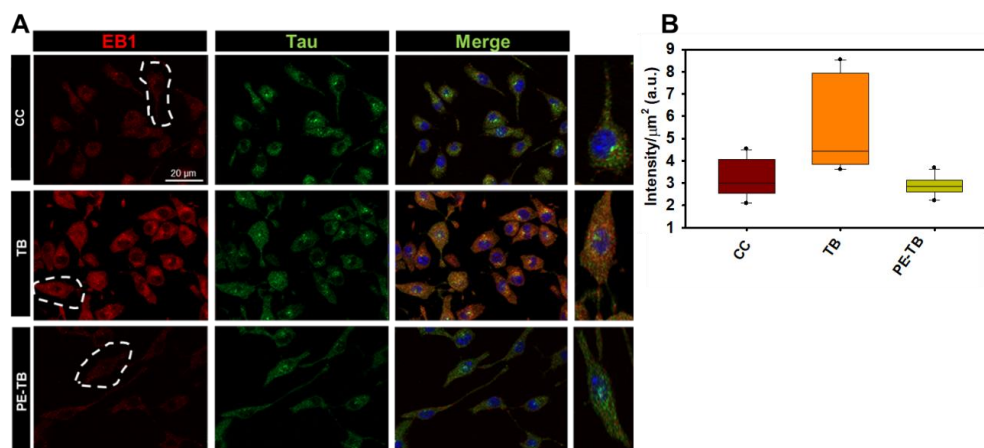


Figure 15. TB and PE-TB modulated EB1 levels in cells. A) Immunofluorescence images showing the effect of TB and PE-TB on EB1 level in Neuro2a cells. The intensity of EB1 was higher in TB treated cells than in untreated cells. B) The quantification of IF images indicated the difference in EB1 intensity in TB treated and untreated cells. The increased intensity of EB1 supported the modulation of the cytoskeleton.

3.2.8 Toluidine Blue and photo-excited Toluidine Blue modulate the longevity and learning in UAS E-14 Tau mutant of *Drosophila*

Drosophila is one of the model system for studying neurodegenerative diseases, as it has advantages such as annotated genome, short life cycle and flexible culturing conditions. Several molecules have been tested for their neuroprotective potency in *Drosophila* system¹³⁷. We studied the effect of TB and PE-TB on the viability and learning of *Drosophila* (Fig. 16A). The Tau mutant of *Drosophila* was fed on food supplemented with various concentrations of TB (2-25 μ M). The results suggested that the treatment of TB and PE-TB improved the life

span of *Drosophila*. We observed a bell-shaped pattern in our results that suggested that 5 μM of TB was the optimum concentration of TB (Fig.16B). The exposure to PE-TB and TB improved the egg-laying in flies, which indicated the improved longevity of flies (Fig.16C). Similarly, we carried out the assay for avoidance of bad odour of quinine to study the learning behaviour. The result showed that the TB and PE-TB-fed flies were able to avoid the bad odour more efficiently than the untreated flies (Fig.16D). The negative geotaxis assay suggested that the exposure of TB and PE-TB improved the locomotor activity of flies as the number of flies escaped were more in the TB and PE-TB treated flies than untreated flies (Fig. 16E). Thus the results of *in vivo* studies supported the potency of TB and PE-TB against Tau-mediated deformities.

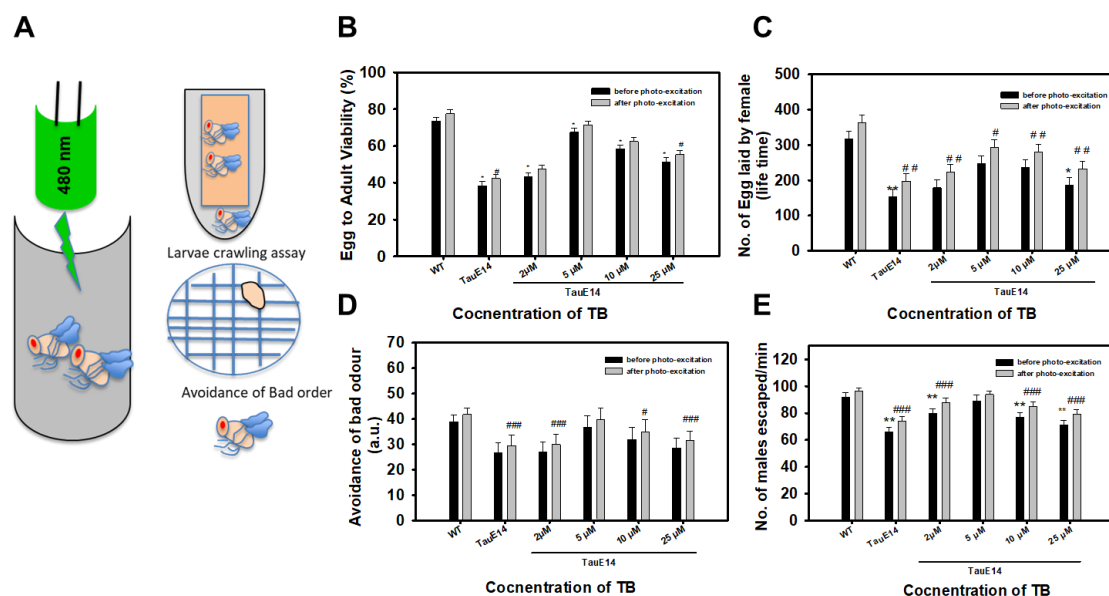


Figure 16. TB and PE-TB improved the longevity and learning behaviour of the UAS E-14 Tau mutant of *Drosophila*. A) The schematic diagram explains the strategy followed to study the effect of TB and PE-TB on *Drosophila*. B) Graph showing the effect of TB and PE-TB on survival rate of flies. The result clearly indicates that TB and PE-TB treatment improved the survival rate of flies. C) The egg laying assay was performed to observe the longevity of flies. The treatment of TB and PE-TB improved the egg laying of female flies. D) The learning behaviour of flies was monitored by their ability to avoid quinine. PE-TB and TB-treated flies efficiently avoided the bad odour of quinine as compared to untreated flies. E) The result of negative geotaxis assay indicating the improved locomotor behaviour of flies after treatment of TB and PE-TB.

3.3 Summary

The intracellular neurofibrillary tangles composed of Tau are one of the major hallmarks of Alzheimer's disease. In recent years, the potency of photo-excited molecules against AD-related amyloid protein has been reported in recent studies. Our study is focused on observing the efficiency of photo-excited Toluidine Blue on Tau aggregation. TB potentially inhibited the aggregation and disaggregated pre-formed matured Tau fibrils. The cell-based studies suggested that TB and PE-TB generate low level of cytotoxicity and ROS production in neuronal cells. TB and PE-TB treated cells had increased neuritic extension and increased lamellipodia and filopodia in cells. The immunofluorescence images showed that TB treated cells were having elevated level of EB1 protein. The *in vivo* studies carried on UAS Tau E14 transgenic *Drosophila* model suggested that photo-excited Toluidine Blue was potent enough to improve the longevity and learning behaviour of *Drosophila*. Thus, this part of work, suggests that Toluidine Blue is a potent molecule in inhibiting the Tau aggregation.

Chapter 4

Photodynamic exposure of Rose-Bengal inhibits Tau aggregation and modulates cytoskeletal network in neuronal cells

4.1 Background

The involvement of intracellular aggregates of Tau protein in the generation of AD pathology has gained the interest to target these aggregates for treatment of AD pathology¹³⁸. The novel strategies involving the various chemical formulations of natural and synthetic origin have been studied for inhibition of Tau aggregation¹³⁹. Photodynamic therapy (PDT) is a strategy involving application of photo-excited molecules as therapeutic agents¹⁴⁰. Methylene blue, cyanine dyes, Rose Bengal are examples of photosensitizers showed promising results against protein aggregates^{73,82,121}. Rose Bengal (RB) is a xanthene dyes. The photo-excited RB has been studied for the treatment of cancers like colon cancer, melanoma and microbial infections¹⁴¹. RB attenuated the formation of A β aggregates, the PE-RB disaggregated the mature A β aggregates *in vitro* and reduced the brain vacuole formation¹²¹. In our study we aim to check the potency of RB and PE-RB for aggregation inhibition of Tau and disaggregation of mature Tau aggregates. We studied the effect of RB and PE-RB on neuronal cytoskeleton modulation. We have carried out assays on *UAS E-14* Tau mutant of *Drosophila* for studying the effect of RB and PE-RB on learning, memory and locomotor behaviour. The overall objective of our study was to observe the neuroprotective potency of RB and PE-RB in various aspects of Tau aggregation.

4.2 Results

4.2.1 Attenuation of *in vitro* Tau aggregation by RB

The potency of xanthene dye Rose Bengal was studied against *in vitro* Tau aggregation. (Fig. 17A). In our experiments Tau protein (40 μ M) was incubated with RB (2-40 μ M) and the aggregation of Tau was traced using ThS fluorescence assay. The ThS kinetics showed that RB has potency to inhibit the aggregation of Tau (Fig.17B). We observed a significant decrease in ThS fluorescence for RB treated samples as compared to untreated samples. The endpoint analysis of the assay suggested a $\geq 85\%$ aggregation inhibition for the RB treated samples (Fig.17C). The secondary structure of Tau aggregates has a prominent β -sheet-rich structure thus we studied the changes in Tau protein's secondary structure upon treatment of RB. The CD spectroscopy indicated that untreated Tau aggregates had a partial β -sheet structure, whereas RB treated sample showed a shift towards random coil structure (Fig.17D). Tau aggregates have characteristic long thick entangle fibrillar morphology. We observe that the untreated samples had long thick filamentous Tau aggregates, while the RB treated samples had small broken pieces of Tau. This morphological differences supported the aggregation inhibition potency of RB (Fig.17E). The overall results suggested that RB efficiently attenuated the Tau aggregation.

4.2.2 Photo-excited RB disaggregates the pre-formed Tau aggregates

The disaggregation of mature Tau aggregates is another strategy for the treatment of AD. RB is a recognized photo-sensitizer, the exposure of 480 nm green light leads to excitation of RB. PE-RB has been used as a therapeutic agent in various carcinomas and other diseases¹⁴². Earlier studies have reported, the inhibitory effect of RB and PE-RB on A β aggregation, in the context of Tau aggregation, the studies have not yet been reported¹²¹.

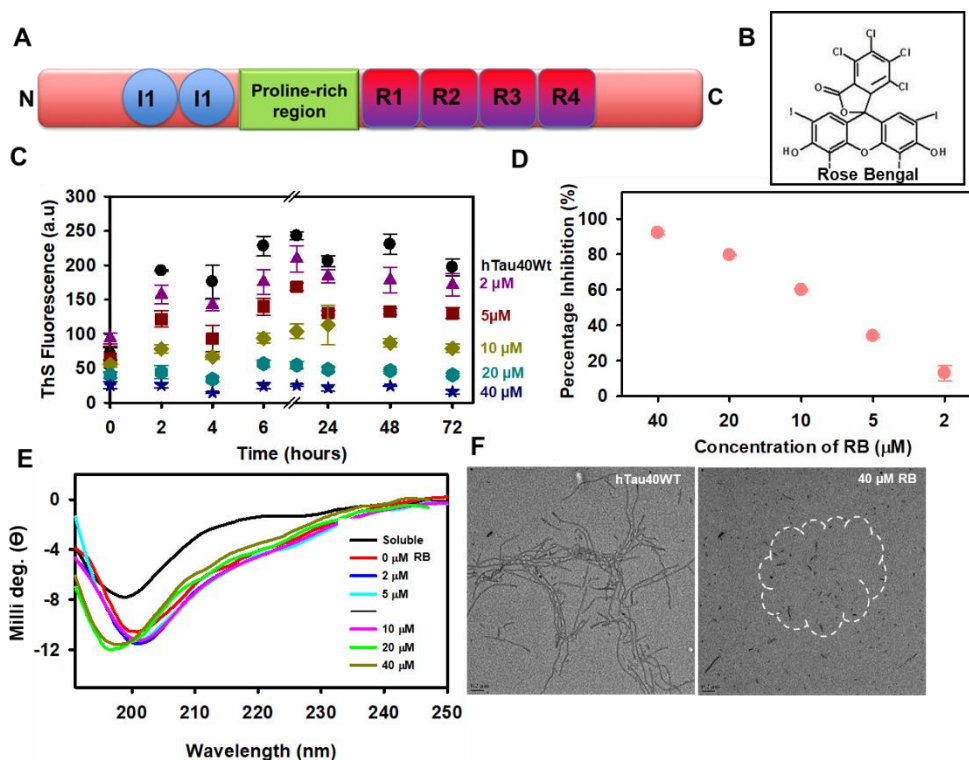


Figure 17. RB inhibits the aggregation of Tau *in vitro*. A-B) The inhibitory potency of RB against heparin-induced Tau aggregation was monitored under *in vitro* conditions. C) ThS fluorescence monitored the aggregation of Tau. ThS fluorescence kinetics showed RB potentially inhibited Tau aggregation. D) The endpoint analysis showed the presence of RB $\geq 85\%$ of aggregation inhibition. E) The changes in the secondary structure of Tau after RB treatment was monitored by CD spectroscopy. The untreated sample had absorbance in β -sheet region, while RB treated sample had a shift towards random coil. F) The untreated aggregates had characteristic long tangled morphology, while RB treatment generated small broken pieces of Tau.

We studied the effect of photo-excited RB (PE-RB) on pre-formed Tau aggregates *in vitro* (Fig.18A). To avoid the exposure of PSs from surrounding light, the reaction was carried out in a dark chamber. Heparin-induced mature Tau aggregates (40 μ M) were incubated with various concentrations of RB (2-40 μ M). After 180 minutes of irradiation, the samples were run on SDS-PAGE. The untreated control was observed to have band of higher-order aggregates, whereas the higher order bands were absent in PE-RB treated samples indicating the disaggregation potency of PE-RB (Fig.18B). The disaggregation potency of PE-RB was monitored by ThS assay. The untreated aggregates were observed to have high ThS fluorescence, while in PE-RB treated samples had reduced fluorescence in a concentration-dependent suggesting the disaggregation of Tau (Fig.18C). The untreated aggregates and PE-RB treated samples were scanned under the electron microscope for studying the morphological changes. The untreated aggregates had long thick fibres of Tau; on the contrary the exposure of PE-RB disaggregated the fibrils into small broken pieces (Fig.18D). Thus, the overall results suggested that PE-RB potentially disaggregates the pre-formed Tau aggregates.

4.2.3 RB induces no adverse effect of neuronal viability

The effect of the therapeutic molecules on the viability of cells is a crucial point of consideration. To carry out various assays on the cellular systems, preliminary the effect of various concentrations of molecules on cell viability has to be studied.

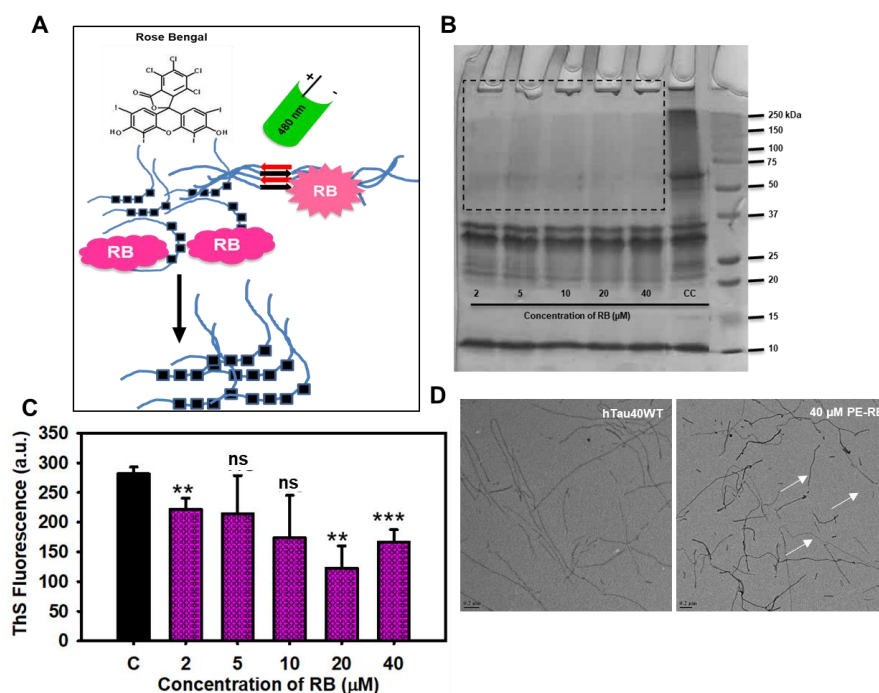


Figure 18. PE-RB disaggregates mature Tau fibrils. A) Schematic diagram showing the hypothesis of work. The effect of PE-RB was studied on pre-formed Tau aggregates. B) The SDS-PAGE for the aggregates after PE-RB treatment. Untreated samples had protein bands at higher order, while PE-RB treated samples lacked higher-order bands. C) The ThS reading shows the difference in PE-RB treated samples and untreated control. The PE-RB treated samples showed a decrease in ThS fluorescence in a concentration-dependent manner. D) The electron microscopic images show the morphological difference between PE-RB treated and untreated samples. The untreated sample had fibrils of elongated morphology, while PE-RB treated sample had broken filaments.

RB is a synthetic xanthene dye; upon photo-excitation, it generates the singlet oxygen species, and thus we studied the effect of RB and PE-RB on cell viability. The cell viability and metabolic activity were monitored by classical MTT assay. Neuro2a cells were incubated with various concentrations of RB (25-500 nM), the cells were exposed to 10 minutes of irradiation. The results of MTT showed that RB and PE-RB-induced had no adverse effect on cell viability (Fig. 19A, B).

4.2.4 RB and PE-RB modulate the tubulin cytoskeleton

The cytoskeleton plays a crucial roles in neuron which includes transport, axon elongation, maintenance of cellular integrity *etc.* Several studies have targeted the microtubule cytoskeleton for understanding the pathology outcome of AD. We aim to study the effect of RB and PE-RB on the tubulin network of neurons Neuro2a cells incubated 100 nM RB and PE-RB were observed for cytoskeleton modulation (Fig. 20A). The results of IF microscopy suggested that the neuron exposed to PE-RB had distinctively extended neurites, whereas the untreated cells had comparatively shorter neurites (Fig. 20B, C). However, no difference in total intracellular Tau intensity was observed. This observation of IF microscopy supported that RB and PE-RB could have the potency to modulate tubulin cytoskeleton.

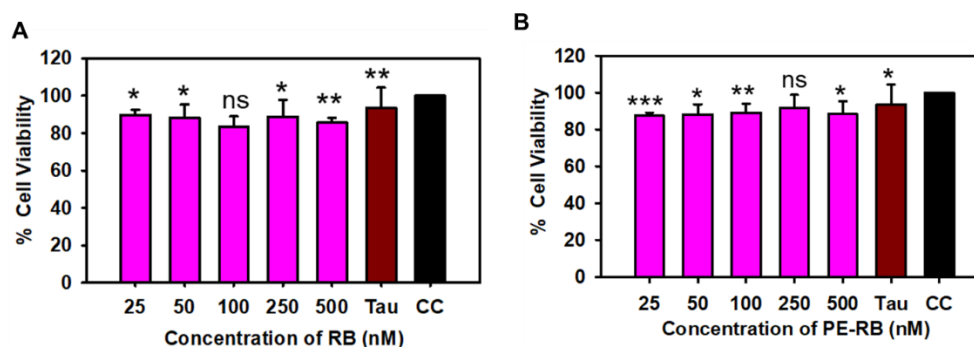


Figure 19. RB and PE-RB have no adverse effect on cell viability. A) The MTT graph showing the effect of various RB concentrations on Neuro2a cell viability. B) MTT graph shows the effect of PE-RB on Neuro2a cells viability. PE-RB has no adverse effect on the Neuro2a cell viability.

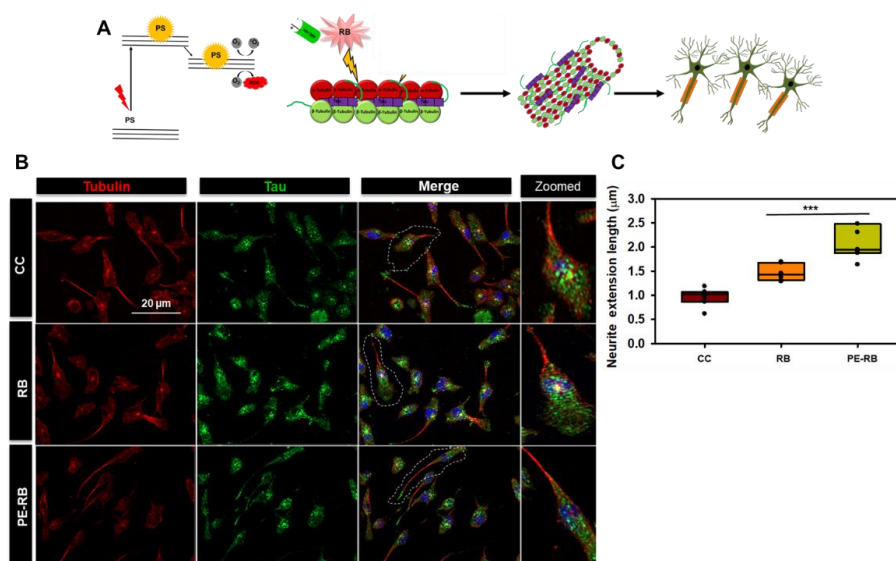


Figure 20. RB and PE-RB modulate the Tubulin cytoskeleton. A) The schematic diagram shows the effect RB and PE-RB on tubulin cytoskeleton. B) The immunofluorescence images show the effect of RB and PE-RB on tubulin network. PE-RB treated cells showed elongated neurites. C) The graph shows the quantification of neurite length. The PE-RB treated cells have elongated neurites as compared to untreated cells.

4.2.5 RB and PE-RB modulate actin cytoskeleton

The actin cytoskeleton plays an important role in structural modification of adult neurons and neuronal development. The actin cytoskeleton is a crucial aspect to be considered while studying neurodegeneration. Several studies suggested that PDT efficiently targets the actin cytoskeleton. 5-ALA-mediated PDT caused the alteration of cellular morphology indicating, the modulation of actin cytoskeleton¹⁴³. D54Mg glioma cells exposed to 5-ALA PDT showed reduced growth cone and surface blabbing. The SW480 cells treated with photo excited Ce6 cause the downregulation of F-actin formation¹⁴⁴. We aim to study the effect of RB and PE-RB on the actin cytoskeleton (Fig.21A). The modulation of actin cytoskeleton was studied after incubating cells with 100 nM RB and PE-RB. We observed an increased number of hair-like structure filopodia in RB and PE-RB treated cells (Fig.21B-D). Podosomes are three-dimensional actin-rich structures. We observed that exposure to RB increased the number of podosome-like structures in neurons. The RB and PE-RB treated cells had more podosome-like structures than the untreated cells (Fig.22 A,B). These results indicated that the treatment

of RB and PE-RB could have the potency to modulate the actin cytoskeleton and to for the maintenance of cell synapse and integrity.

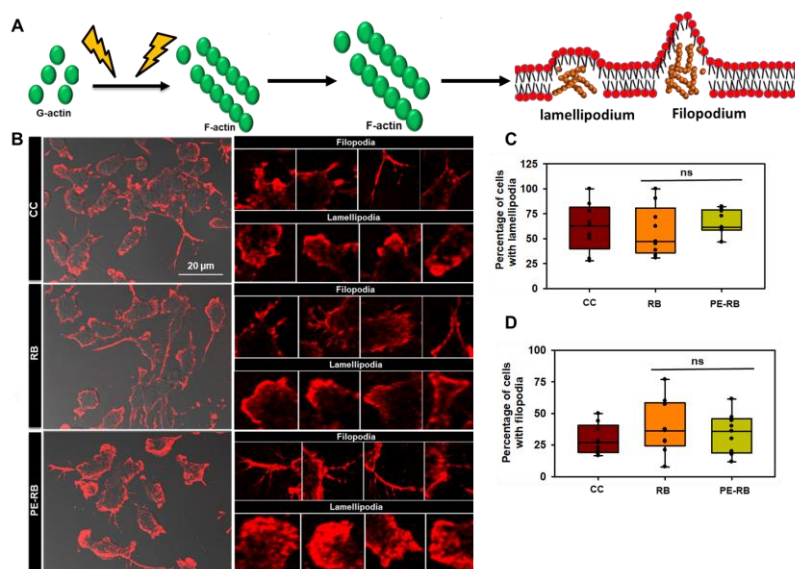


Figure 21. RB and PE-RB modulate the actin cytoskeleton. A) The schematic diagram shows the hypothesis that RB and PE-RB' modulate cytoskeleton. B) The immunofluorescence images show RB and PE-RB's effect on actin cytoskeleton. The RB and PE-RB treatment showed modulation of actin-rich filopodia and lamellipodia. C) The graph showing percentage of cells bearing lamellipodia. The number of cells bearing lamellipodia were increased after RB and PE-RB treated. D) The graph showing percentage of cells bearing filopodia. The percentage of cells bearing filopodia was more in RB and PE-RB treatment group.

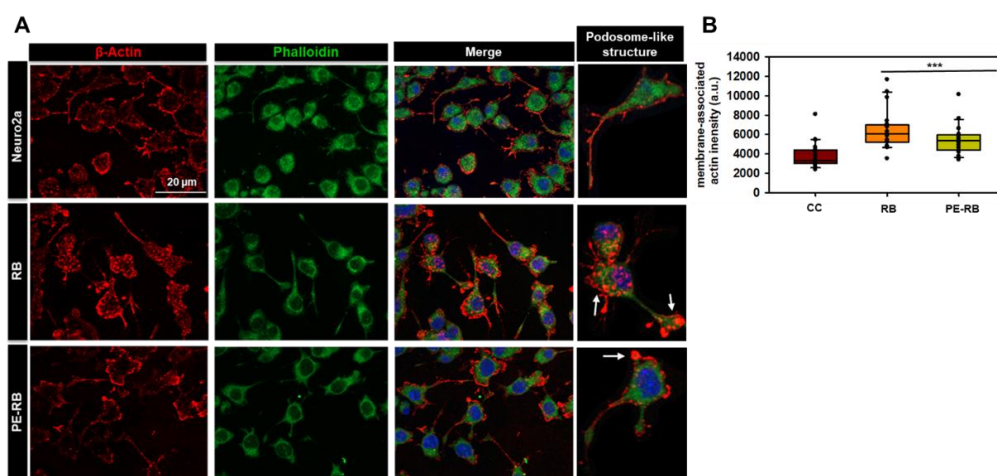


Figure 22. RB and PE-RB induces Podosome-like structures. A) The immunofluorescence images showed the modulation of the actin cytoskeleton. The cells exposed to RB and PE-RB showed an increased number of actin-rich podosome-like structures. B) The graph showing quantification of membrane-bound actin intensity.

4.2.6 RB and PE-RB ameliorate the longevity and memory in UAS E-14 Tau mutant of *Drosophila*

The neuroprotective effect of molecule is evaluated based on efficiency in improving the memory, learning and longevity. *Drosophila* model is considered as one of the reliable model systems for studying neurodegeneration. Several molecules e.g. curcumin have been studied for their neuroprotective efficiency¹⁴⁵. We have studied the neuroprotective property of RB and PE-RB the experiments were carried on UAS E-14 Tau mutant of *Drosophila*. The potency of RB and PE-RB on learning and viability was assessed by larvae crawling assay, survival

assay, negative geotaxis assay (Fig. 23A). The negative geotaxis assay suggested that flies treated with RB and PE-RB efficiently climbed over in comparison on to untreated mutant flies (Fig. 23B). The learning behaviour of flies were studied by their ability to avoid bad odour of quinine (Fig. 23C). Similarly, the larvae fed on food supplemented with RB were able to cross more grids in comparison to untreated larvae (Fig. 23D). Our assay suggested that RB and PE-RB treated flies were more potent to avoid the bad odour than the untreated flies. We observed a bell-shaped pattern, which indicated that 20 μ M RB was the optimum concentration for *Drosophila*. The overall result of *in vivo* studies indicated that RB and PE-RB showed neuroprotective properties against Tau-mediated toxicity, memory dysfunction and locomotor impairment.

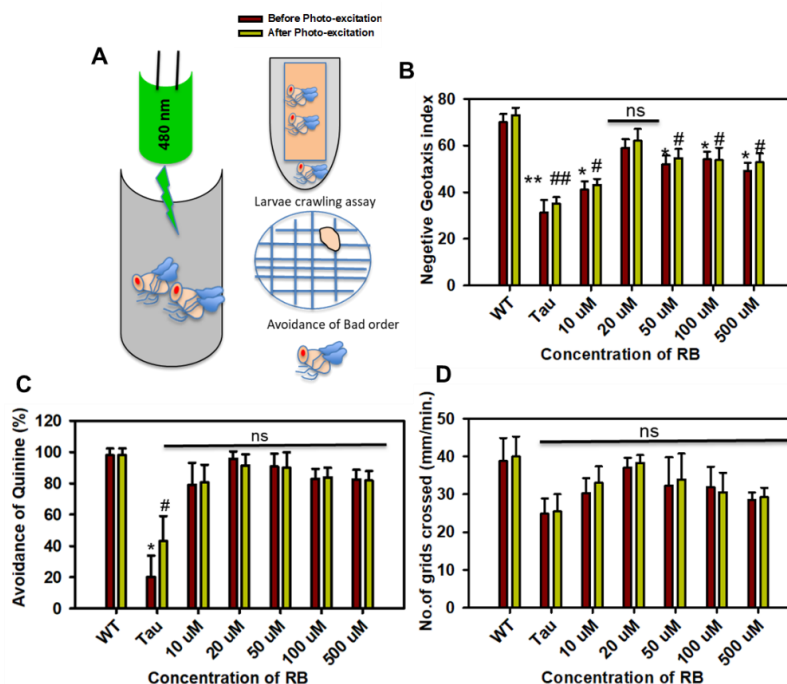


Figure 23. RB and PE-RB show neuroprotection in the UAS E-14 Tau mutant of *Drosophila*. A) The schematic diagram shows the strategy followed to study the effect of RB and PE-RB *in vivo*. B) The graph showing negative geotaxis assay. PE-RB and RB treated flies efficiently climb over as compared to untreated mutants. C) The graph shows flies learning behavior after RB and PE-RB treatment. RB and PE-RB treated flies were more potent in avoiding the bad order of quinine. D) The larvae crawling assay was performed for studying the locomotor behaviour. The graph showed RB and PE-RB treated larvae crossed more grids than untreated larvae.

4.3 Summary

The accumulation of Tau aggregates results in generation of AD pathology. RB is a known photosensitizer, which was observed to be effective in inhibiting A β aggregation and improving the longevity of A β model of *Drosophila*. We have shown the inhibitory effect of RB against Tau aggregation. The results suggests that RB potentially attenuated the aggregation of Tau. The photo-excited RB potentially disaggregated the mature Tau fibrils. The viability assay suggested that RB and PE-RB have no adverse effect on cell viability. AD leads to the generation of cytoskeleton deformities, the Neu2a cells exposed to RB and PE-RB were had extended neurites and increased number of actin-rich structures. The *in vivo* studies on UAS E-14 Tau mutant of *Drosophila* indicated that RB and PE-RB improve flies longevity, memory and locomotor function of flies. Thus, based these results, we stated that RB and PE-RB could be considered a potential molecule against AD.

Chapter 4

Photodynamic exposure of Rose-Bengal inhibits Tau aggregation and modulates cytoskeletal network in neuronal cells

4.1 Background

The involvement of intracellular aggregates of Tau protein in the generation of AD pathology has gained the interest to target these aggregates for treatment of AD pathology¹³⁸. The novel strategies involving the various chemical formulations of natural and synthetic origin have been studied for inhibition of Tau aggregation¹³⁹. Photodynamic therapy (PDT) is a strategy involving application of photo-excited molecules as therapeutic agents¹⁴⁰. Methylene blue, cyanine dyes, Rose Bengal are examples of photosensitizers showed promising results against protein aggregates^{73,82,121}. Rose Bengal (RB) is a xanthene dyes. The photo-excited RB has been studied for the treatment of cancers like colon cancer, melanoma and microbial infections¹⁴¹. RB attenuated the formation of A β aggregates, the PE-RB disaggregated the mature A β aggregates *in vitro* and reduced the brain vacuole formation¹²¹. In our study we aim to check the potency of RB and PE-RB for aggregation inhibition of Tau and disaggregation of mature Tau aggregates. We studied the effect of RB and PE-RB on neuronal cytoskeleton modulation. We have carried out assays on *UAS E-14* Tau mutant of *Drosophila* for studying the effect of RB and PE-RB on learning, memory and locomotor behaviour. The overall objective of our study was to observe the neuroprotective potency of RB and PE-RB in various aspects of Tau aggregation.

4.2 Results

4.2.1 Attenuation of *in vitro* Tau aggregation by RB

The potency of xanthene dye Rose Bengal was studied against *in vitro* Tau aggregation. (Fig. 17A). In our experiments Tau protein (40 μ M) was incubated with RB (2-40 μ M) and the aggregation of Tau was traced using ThS fluorescence assay. The ThS kinetics showed that RB has potency to inhibit the aggregation of Tau (Fig.17B). We observed a significant decrease in ThS fluorescence for RB treated samples as compared to untreated samples. The endpoint analysis of the assay suggested a $\geq 85\%$ aggregation inhibition for the RB treated samples (Fig.17C). The secondary structure of Tau aggregates has a prominent β -sheet-rich structure thus we studied the changes in Tau protein's secondary structure upon treatment of RB. The CD spectroscopy indicated that untreated Tau aggregates had a partial β -sheet structure, whereas RB treated sample showed a shift towards random coil structure (Fig.17D). Tau aggregates have characteristic long thick entangle fibrillar morphology. We observe that the untreated samples had long thick filamentous Tau aggregates, while the RB treated samples had small broken pieces of Tau. This morphological differences supported the aggregation inhibition potency of RB (Fig.17E). The overall results suggested that RB efficiently attenuated the Tau aggregation.

4.2.2 Photo-excited RB disaggregates the pre-formed Tau aggregates

The disaggregation of mature Tau aggregates is another strategy for the treatment of AD. RB is a recognized photo-sensitizer, the exposure of 480 nm green light leads to excitation of RB. PE-RB has been used as a therapeutic agent in various carcinomas and other diseases¹⁴². Earlier studies have reported, the inhibitory effect of RB and PE-RB on A β aggregation, in the context of Tau aggregation, the studies have not yet been reported¹²¹.

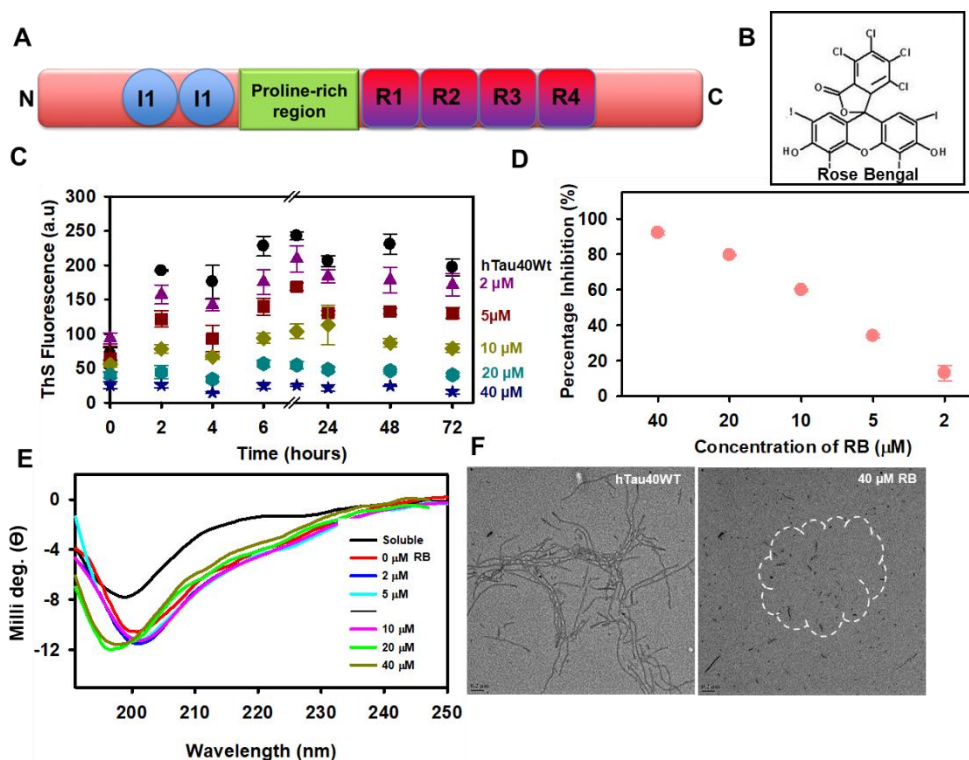


Figure 17. RB inhibits the aggregation of Tau *in vitro*. A-B) The inhibitory potency of RB against heparin-induced Tau aggregation was monitored under *in vitro* conditions. C) ThS fluorescence monitored the aggregation of Tau. ThS fluorescence kinetics showed RB potentially inhibited Tau aggregation. D) The endpoint analysis showed the presence of RB $\geq 85\%$ of aggregation inhibition. E) The changes in the secondary structure of Tau after RB treatment was monitored by CD spectroscopy. The untreated sample had absorbance in β -sheet region, while RB treated sample had a shift towards random coil. F) The untreated aggregates had characteristic long tangled morphology, while RB treatment generated small broken pieces of Tau.

We studied the effect of photo-excited RB (PE-RB) on pre-formed Tau aggregates *in vitro* (Fig.18A). To avoid the exposure of PSs from surrounding light, the reaction was carried out in a dark chamber. Heparin-induced mature Tau aggregates ($40 \mu\text{M}$) were incubated with various concentrations of RB ($2\text{--}40 \mu\text{M}$). After 180 minutes of irradiation, the samples were run on SDS-PAGE. The untreated control was observed to have band of higher-order aggregates, whereas the higher order bands were absent in PE-RB treated samples indicating the disaggregation potency of PE-RB (Fig.18B). The disaggregation potency of PE-RB was monitored by ThS assay. The untreated aggregates were observed to have high ThS fluorescence, while in PE-RB treated samples had reduced fluorescence in a concentration-dependent suggesting the disaggregation of Tau (Fig.18C). The untreated aggregates and PE-RB treated samples were scanned under the electron microscope for studying the morphological changes. The untreated aggregates had long thick fibres of Tau; on the contrary the exposure of PE-RB disaggregated the fibrils into small broken pieces (Fig.18D). Thus, the overall results suggested that PE-RB potentially disaggregates the pre-formed Tau aggregates.

4.2.3 RB induces no adverse effect of neuronal viability

The effect of the therapeutic molecules on the viability of cells is a crucial point of consideration. To carry out various assays on the cellular systems, preliminary the effect of various concentrations of molecules on cell viability has to be studied.

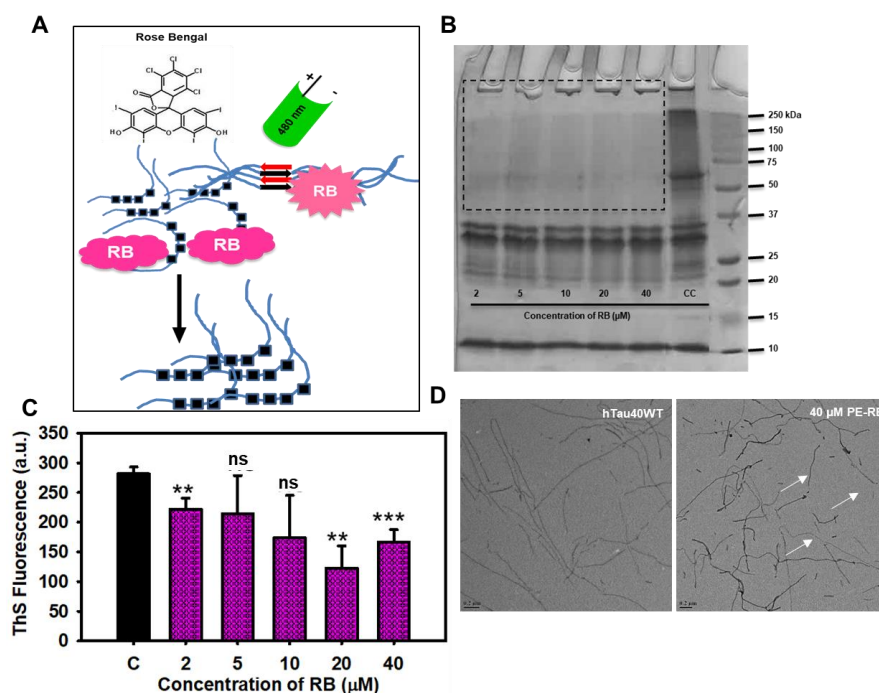


Figure 18. PE-RB disaggregates mature Tau fibrils. A) Schematic diagram showing the hypothesis of work. The effect of PE-RB was studied on pre-formed Tau aggregates. B) The SDS-PAGE for the aggregates after PE-RB treatment. Untreated samples had protein bands at higher order, while PE-RB treated samples lacked higher-order bands. C) The ThS reading shows the difference in PE-RB treated samples and untreated control. The PE-RB treated samples showed a decrease in ThS fluorescence in a concentration-dependent manner. D) The electron microscopic images show the morphological difference between PE-RB treated and untreated samples. The untreated sample had fibrils of elongated morphology, while PE-RB treated sample had broken filaments.

RB is a synthetic xanthene dye; upon photo-excitation, it generates the singlet oxygen species, and thus we studied the effect of RB and PE-RB on cell viability. The cell viability and metabolic activity were monitored by classical MTT assay. Neuro2a cells were incubated with various concentrations of RB (25-500 nM), the cells were exposed to 10 minutes of irradiation. The results of MTT showed that RB and PE-RB-induced had no adverse effect on cell viability (Fig. 19A, B).

4.2.4 RB and PE-RB modulate the tubulin cytoskeleton

The cytoskeleton plays a crucial roles in neuron which includes transport, axon elongation, maintenance of cellular integrity *etc.* Several studies have targeted the microtubule cytoskeleton for understanding the pathology outcome of AD. We aim to study the effect of RB and PE-RB on the tubulin network of neurons Neuro2a cells incubated 100 nM RB and PE-RB were observed for cytoskeleton modulation (Fig. 20A). The results of IF microscopy suggested that the neuron exposed to PE-RB had distinctively extended neurites, whereas the untreated cells had comparatively shorter neurites (Fig. 20B, C). However, no difference in total intracellular Tau intensity was observed. This observation of IF microscopy supported that RB and PE-RB could have the potency to modulate tubulin cytoskeleton.

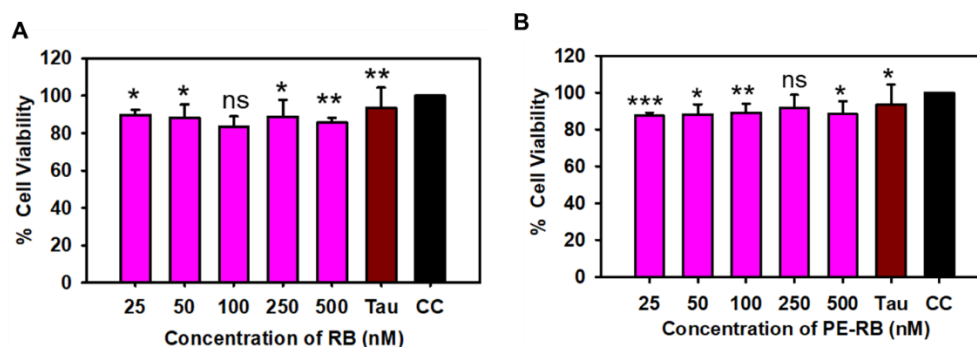


Figure 19. RB and PE-RB have no adverse effect on cell viability. A) The MTT graph showing the effect of various RB concentrations on Neuro2a cell viability. B) MTT graph shows the effect of PE-RB on Neuro2a cells viability. PE-RB has no adverse effect on the Neuro2a cell viability.

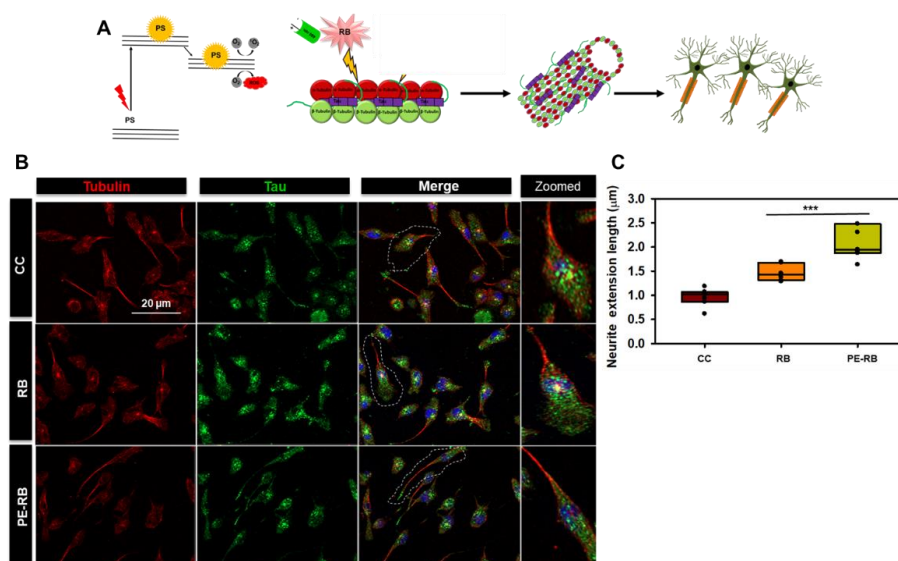


Figure 20. RB and PE-RB modulate the Tubulin cytoskeleton. A) The schematic diagram shows the effect RB and PE-RB on tubulin cytoskeleton. B) The immunofluorescence images show the effect of RB and PE-RB on tubulin network. PE-RB treated cells showed elongated neurites. C) The graph shows the quantification of neurite length. The PE-RB treated cells have elongated neurites as compared to untreated cells.

4.2.5 RB and PE-RB modulate actin cytoskeleton

The actin cytoskeleton plays an important role in structural modification of adult neurons and neuronal development. The actin cytoskeleton is a crucial aspect to be considered while studying neurodegeneration. Several studies suggested that PDT efficiently targets the actin cytoskeleton. 5-ALA-mediated PDT caused the alteration of cellular morphology indicating, the modulation of actin cytoskeleton¹⁴³. D54Mg glioma cells exposed to 5-ALA PDT showed reduced growth cone and surface blabbing. The SW480 cells treated with photo excited Ce6 cause the downregulation of F-actin formation¹⁴⁴. We aim to study the effect of RB and PE-RB on the actin cytoskeleton (Fig.21A). The modulation of actin cytoskeleton was studied after incubating cells with 100 nM RB and PE-RB. We observed an increased number of hair-like structure filopodia in RB and PE-RB treated cells (Fig.21B-D). Podosomes are three-dimensional actin-rich structures. We observed that exposure to RB increased the number of podosome-like structures in neurons. The RB and PE-RB treated cells had more podosome-like structures than the untreated cells (Fig.22 A,B). These results indicated that the treatment

of RB and PE-RB could have the potency to modulate the actin cytoskeleton and to for the maintenance of cell synapse and integrity.

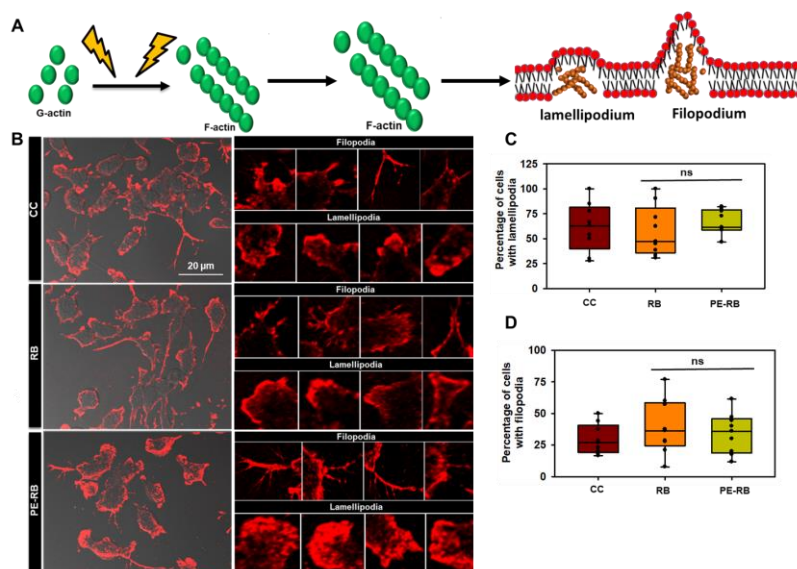


Figure 21. RB and PE-RB modulate the actin cytoskeleton. A) The schematic diagram shows the hypothesis that RB and PE-RB' modulate cytoskeleton. B) The immunofluorescence images show RB and PE-RB's effect on actin cytoskeleton. The RB and PE-RB treatment showed modulation of actin-rich filopodia and lamellipodia. C) The graph showing percentage of cells bearing lamellipodia. The number of cells bearing lamellipodia were increased after RB and PE-RB treated. D) The graph showing percentage of cells bearing filopodia. The percentage of cells bearing filopodia was more in RB and PE-RB treatment group.

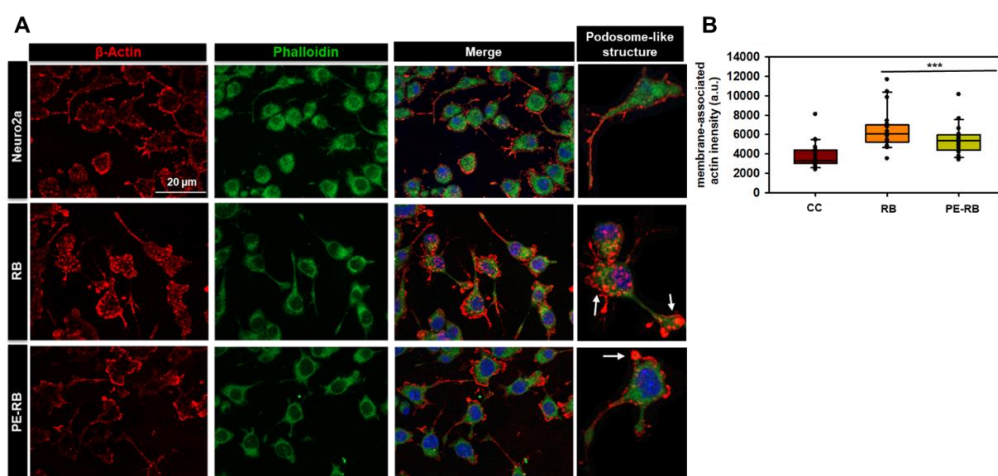


Figure 22. RB and PE-RB induces Podosome-like structures. A) The immunofluorescence images showed the modulation of the actin cytoskeleton. The cells exposed to RB and PE-RB showed an increased number of actin-rich podosome-like structures. B) The graph showing quantification of membrane-bound actin intensity.

4.2.6 RB and PE-RB ameliorate the longevity and memory in UAS E-14 Tau mutant of *Drosophila*

The neuroprotective effect of molecule is evaluated based on efficiency in improving the memory, learning and longevity. *Drosophila* model is considered as one of the reliable model systems for studying neurodegeneration. Several molecules e.g. curcumin have been studied for their neuroprotective efficiency¹⁴⁵. We have studied the neuroprotective property of RB and PE-RB the experiments were carried on UAS E-14 Tau mutant of *Drosophila*. The potency of RB and PE-RB on learning and viability was assessed by larvae crawling assay, survival

assay, negative geotaxis assay (Fig. 23A). The negative geotaxis assay suggested that flies treated with RB and PE-RB efficiently climbed over in comparison on to untreated mutant flies (Fig. 23B). The learning behaviour of flies were studied by their ability to avoid bad odour of quinine (Fig. 23C). Similarly, the larvae fed on food supplemented with RB were able to cross more grids in comparison to untreated larvae (Fig. 23D). Our assay suggested that RB and PE-RB treated flies were more potent to avoid the bad odour than the untreated flies. We observed a bell-shaped pattern, which indicated that 20 μ M RB was the optimum concentration for *Drosophila*. The overall result of *in vivo* studies indicated that RB and PE-RB showed neuroprotective properties against Tau-mediated toxicity, memory dysfunction and locomotor impairment.

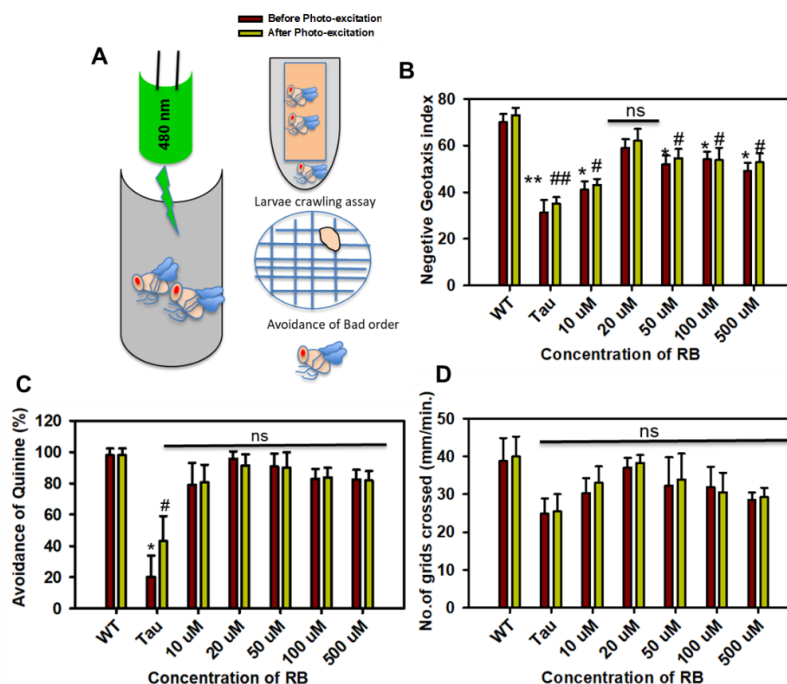


Figure 23. RB and PE-RB show neuroprotection in the UAS E-14 Tau mutant of *Drosophila*. A) The schematic diagram shows the strategy followed to study the effect of RB and PE-RB *in vivo*. B) The graph showing negative geotaxis assay. PE-RB and RB treated flies efficiently climb over as compared to untreated mutants. C) The graph shows flies learning behavior after RB and PE-RB treatment. RB and PE-RB treated flies were more potent in avoiding the bad order of quinine. D) The larvae crawling assay was performed for studying the locomotor behaviour. The graph showed RB and PE-RB treated larvae crossed more grids than untreated larvae.

4.3 Summary

The accumulation of Tau aggregates results in generation of AD pathology. RB is a known photosensitizer, which was observed to be effective in inhibiting A β aggregation and improving the longevity of A β model of *Drosophila*. We have shown the inhibitory effect of RB against Tau aggregation. The results suggests that RB potentially attenuated the aggregation of Tau. The photo-excited RB potentially disaggregated the mature Tau fibrils. The viability assay suggested that RB and PE-RB have no adverse effect on cell viability. AD leads to the generation of cytoskeleton deformities, the Neu2a cells exposed to RB and PE-RB were had extended neurites and increased number of actin-rich structures. The *in vivo* studies on UAS E-14 Tau mutant of *Drosophila* indicated that RB and PE-RB improve flies longevity, memory and locomotor function of flies. Thus, based these results, we stated that RB and PE-RB could be considered a potential molecule against AD.

Chapter 5

Ethanollic extract of *Bacopa monnieri* attenuates the *in-vitro* Tau aggregation, Tau phosphorylation, and Tau-mediated toxicity

5.1 Background

Ayurveda is the science of studying human health, which is based on treating diseases by either applying herbal formulations, diet modulation or basic yoga exercises¹⁴⁶. Alzheimer's disease (AD) is the most severe and prevalent type of dementia characterized by accelerative loss in memory and locomotory functions¹⁴⁷. The phosphorylation of Tau is one of the main PTMs-related to AD pathology. GSK-3 β is the proline-directed Ser/Thr kinase, which is considered to be involved in AD. The hyperactivity of GSK-3 β has been observed in various models of AD. GSK-3 β phosphorylates Tau at different sites leading to the generation of Tau-mediated toxicity¹⁴⁸. The hyper-phosphorylated Tau impairs diverse signalling cascades in neurons¹⁴⁹. Hence GSK-3 β and phospho-Tau are emerging as important targets for studying the potency of molecules in AD¹⁵⁰. Several GSK-3 β inhibitors e.g. lithium, valproate, tideglusib etc. were studied for the treatment of AD¹⁵¹. Tau mediated intracellular oxidative stress is another factor, widely studied in the context of AD. Tau is reported to induce oxidative stress in neurons *via* modulating various trafficking and signalling cascades¹⁵². Thus, the chelators of ROS e.g. melatonin, serotonin (5-hydroxytryptamine), tacrine, lipoic acid, Carotene, lycopene, retinol etc. showed protective action against Tau mediated stress in AD. *Bacopa Monnieri* has been known reported as herb having memory-enhancing, anti-inflammatory, analgesic, antipyretic, sedative, anti-depressant, anti-anxiety, anti-oxidant and anti-epileptic properties¹⁵³. Bacoside A is considered the major chemical moiety known to be responsible for neuropharmacological effects and the nootropic action of *Bacopa Monnieri*¹⁵⁴. *Bacopa Monnieri* is also known to upregulate the expression of antioxidant enzymes SOD and catalase¹⁰⁰. The treatment of BME has improved the cognitive function in AD models. The treatment of BME rescued primary neuronal cells from A β -mediated oxidative stress and toxicity. Although the role of BME in the context of Tau phosphorylation and Tau toxicity is still yet to be addressed. In our work we aim to study the role of BME in downregulation the Tau phosphorylation, reducing the oxidative stress in neuroblastoma cells and improving the nuclear transport. The objective of the present study was to analyze the therapeutic potency of BME against Tau toxicity and AD.

5.2 Results

5.2.1 Phytochemical extraction and characterization of *Bacopa monnieri*

Bacopa monnieri (BM) is known for its neuroprotective property; in traditional therapy, various herbal formulations of BM have been prescribed for treatment of neurological disorders (Fig. 24A). We aim to study the effect of ethanollic extract of BM (BME) on various aspects of Tau aggregation. The crude extract of BM was prepared by extracting powdered dried BM with rectified spirit. The crude extract was characterized by subjecting to Thin-layer chromatography (TLC), High-pressure liquid chromatography (HPLC) and Liquid chromatography high-resolution mass spectrometry (LC-HRMS) analysis. The TLC analysis indicated the presence of various compounds in the BME, which HPLC and LC-HRMS were further identified. The 21 peaks in the HPLC chromatogram suggested the presence of a mixture of compounds in the extract (Fig. 24B-D). The phytochemical present in the crude

extract were identified on the basis of molecular weight and molecular formulae, comparing ESI (+)-MS data with the earlier reports the probable compounds were identified (Table 2).

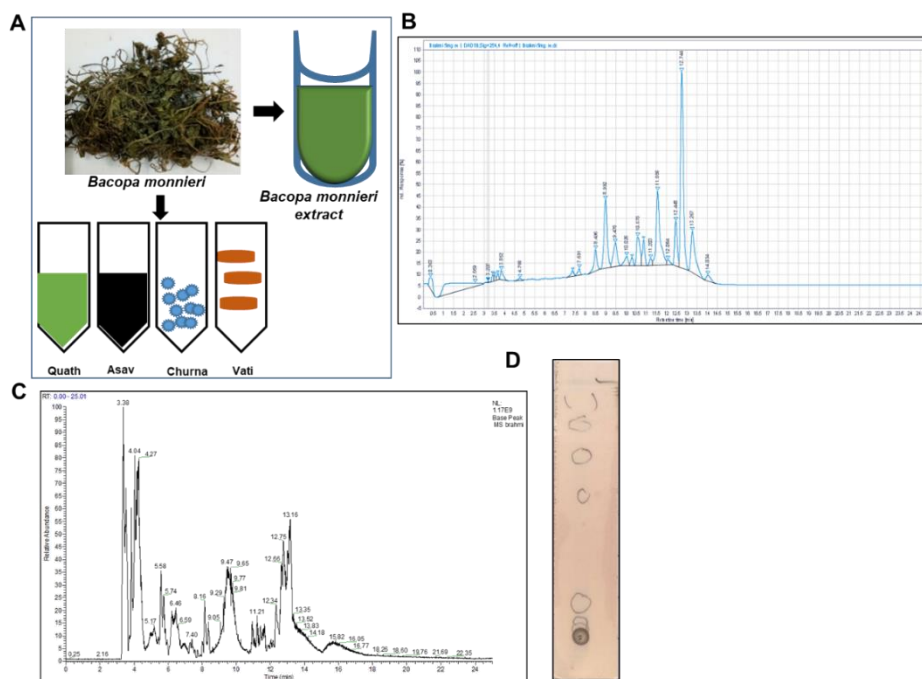


Figure 24. The phytochemical extraction of *Bacopa Monnieri*. A) *Bacopa Monnieri* is a herb found in marshy areas and considered to have a neuroprotective effect. Various formulations of *Bacopa Monnieri* such as kwath, asav, churna, vati have been prescribed to patients of neurological disorders. B) HPLC chromatogram of BME showing the presence of a mixture of compounds in the extract. C) The LC-MS analysis of BME indicated the presence of 21 peaks, corresponding to various compounds in the extract. D) The dried powder of *Bacopa Monnieri* was extracted rectified spirit, and the crude extract was subjected to TLC.

5.2.2 BME potentially modulated the aggregation of full-length Tau

The role of BM in the aspect of Tau aggregation was still unexplored, the effect of BME on *in vitro* Tau aggregation was studied (Fig. 25A). In the present study, heparin-induced Tau was incubated with various concentrations of BME (10, 25, 50, and 100 $\mu\text{g/ml}$), the aggregation kinetics was studied by the ThS fluorescence assay. At a concentration of 25 $\mu\text{g/ml}$ and above, an explicit reduction in ThS fluorescence was observed, which attested to the aggregation inhibition (Fig. 25B). We studied the untreated Tau aggregates that were observed to have a partial β -sheet structure, at the same time BME treated Tau aggregates had shifted towards the random coil, which suggested the aggregation inhibition (Fig. 25C). Tau aggregates have long filamentous morphology, the electron microscopic images of untreated samples showed extended inter tangled thick Tau fibrils. While the BME treated samples had broken filaments, thus the morphological differences in Tau fibrils suggested that BME inhibited aggregation of Tau (Fig. 25D). The overall results supported that BME could be considered as a potent compound against Tau aggregation.

5.2.3 The disaggregation of pre-formed Tau fibrils by BME

The efficiency of a compound to disaggregate the mature Tau fibrils aids to its therapeutic potency. We studied the disaggregating potency of BME against mature Tau aggregates.

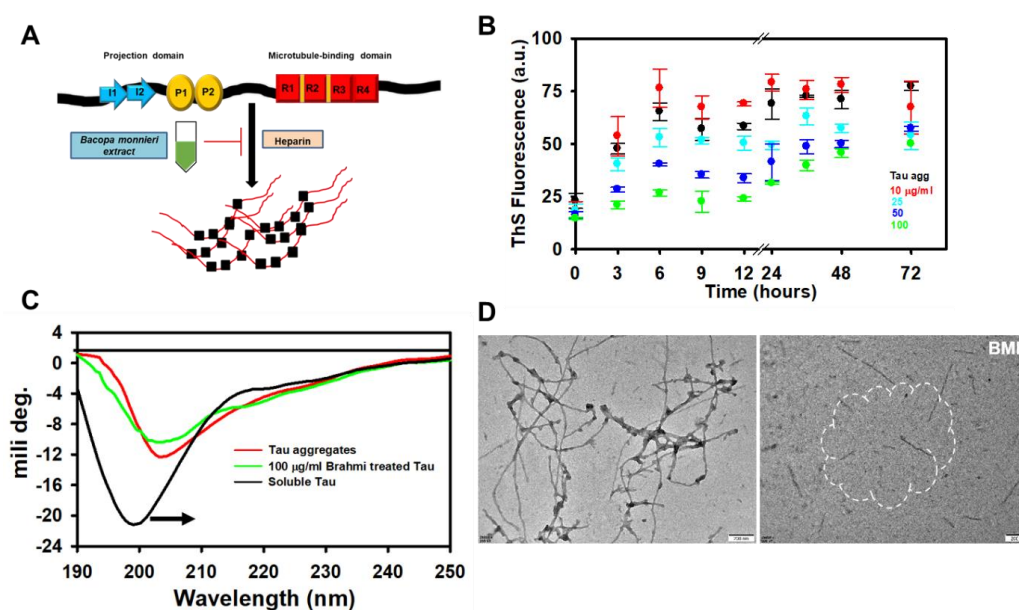


Figure 25. BME attenuated the aggregation of soluble Tau *in vitro*. A) The schematic diagram shows the hypothesis that BME attenuates the aggregation of *in vitro* Tau aggregation. B) The ThS kinetics show the potency of BME against Tau aggregation. The untreated sample had higher fluorescence than the BME treated samples indicating the inhibition of aggregation. C) CD spectroscopy graph indicating the changes in the secondary structure of Tau after the treatment of BME. The untreated Tau aggregates had a partial β -sheet-rich structure, whereas BME treated samples showed a shift towards the random coil. D) The electron microscopic images of BME treated and untreated aggregates. The untreated aggregates had long thick filamentous morphology; the BME treated aggregates had small broken pieces.

The ThS assay suggested that at higher concentrations of BME (100 $\mu\text{g/ml}$), moderately disaggregated Tau fibrils (Fig. 26A). Subsequently, the assay samples were subjected to sedimentation assay. In the untreated sample, prominent bands of the higher molecular weight were visible on SDS-PAGE, whereas in samples treated with a higher concentration of BME, the higher-order bands were absent indicating the disaggregation potency of BME (Fig. 26B). The electron microscopic images revealed that the untreated aggregates were having fibrillary, long morphology (Fig. 26C). Whereas the BME treated aggregated were observed to have small broken pieces which indicated potent disaggregation (Fig. 26D). The overall results suggests that BME could have a potency of disaggregation at higher concentrations.

5.2.4 The rejuvenating property of BME in neuronal cells

The compounds which improves the viability of neuronal cells are considered as neuroprotective. Crude extract of the herb contains a mixture of compounds belonging to different classes. Hence, the effect of crude extract on cell viability has to be considered for addressing its neuroprotective effect (Fig. 27A). Caspase-3 are important executional caspases that could be traced for monitoring apoptosis¹⁵⁶. In the present study, effect of BME on cell viability and metabolism were studied by MTT assay. Tau aggregate exposed cells were observed to have reduced cell viability; on contrary, the BME treatment improved the viability of cells (Fig. 27B).

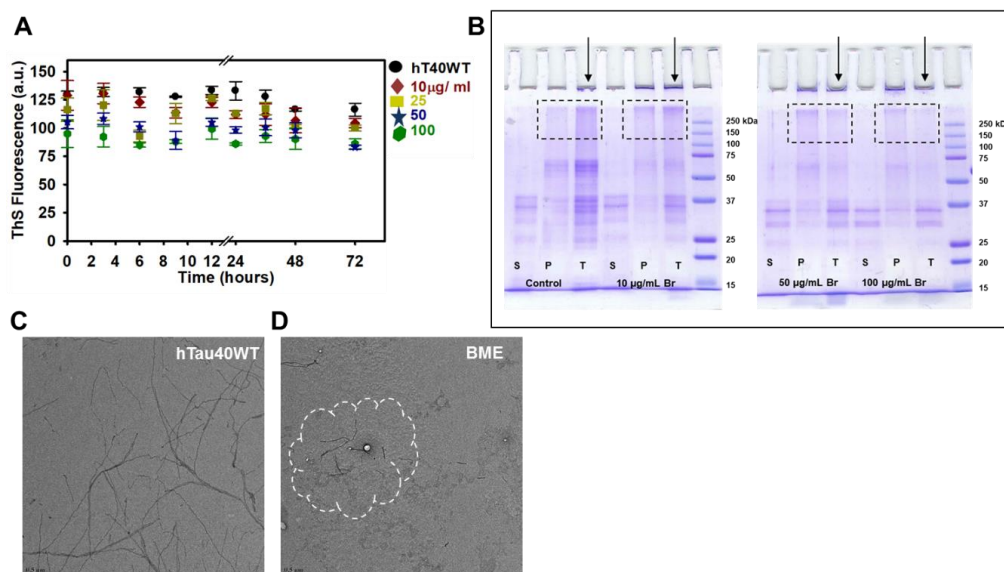


Figure 26. BME disaggregated the mature pre-formed aggregates. A) The graph for the ThS fluorescence kinetics of BME treated aggregates. At higher concentration, BME showed moderate disaggregation potency. At the lower concentration no significant disaggregation was observed. B) The SDS-PAGE for the sedimentation assay. BME treated and untreated aggregates were differentiated for supernatant and pellet fractions. The higher order bands were absent in the pellet fraction after BME treatment. C) The electron microscopic images of mature Tau aggregates. The untreated Tau aggregates were observed to have a long thick fibrils. D) The electron microscopic images of BME treated aggregates. The BME treated aggregates had broken morphology indicating the potent disaggregation.

Tau aggregates are known to initiate the process of apoptosis in neurons. In this study, Neuro2a exposed to Tau aggregates had elevated Caspase-3 activity than the cells exposed to BME, which indicated that BME potentially reduced the apoptosis (Fig 27C). The presence of Tau aggregates induces oxidative stress in cells. The result of the 2',7'-Dichlorofluorescein (DCFDA) assay suggested that BME potentially quenched the intracellular ROS in Tau stressed cells. A significant reduction ($\geq 40\%$) of intracellular ROS was observed in cells treated with 100 $\mu\text{g}/\text{ml}$ BME (Fig. 27D). Hence the results of these assays supported the rejuvenating and antioxidant potency of BME.

5.2.5 BME modulated the Nrf2 levels in neurons

The Nrf2 signalling cascade is involved in the cellular antioxidant machinery (Fig. 28A). We aim to study the antioxidant property of BME by modulation of Nrf2 levels. The formaldehyde-stressed Neuro2a cells (0.5 mM formaldehyde) were treated with BME (5 $\mu\text{g}/\text{ml}$ BME). The western blot suggested that FA downregulated the Nrf2 levels, while BME treated cells were having elevated levels of Nrf2 (Fig. 28B-C). Additionally, in immunofluorescence studies, the BME-treated cells were observed to have an elevated intensity of Nrf2, than FA-treated cells. The modulation of Nrf2 level in cells after BME treatment indicated that BME supported the cells in overcoming the FA-mediated oxidative stress (Fig. 28D-E). Hence, from results of this experiment supported the antioxidant property of BME.

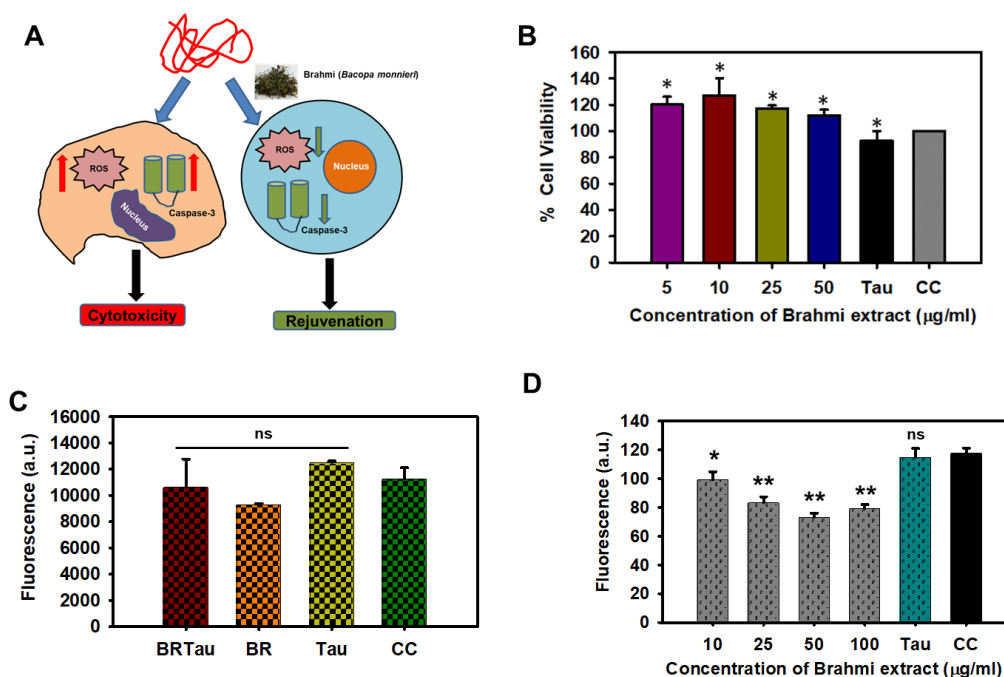


Figure 27. BME rescues the neuron from Tau-mediated toxicity. A) Tau induces toxicity in neurons by the generation of oxidative stress. The neurons undergo apoptosis in the presence of Tau aggregates. BME treatment rescue the Tau mediated toxicity in neurons. B) The graph showing the result of MTT assay stressed cells had reduced viability, BME treatment improved the viability of Tau stressed cells. C) Tau treated neurons had elevated Caspase-3 activity. BME treated downregulated the Caspase-3 activity. D) BME act as an antioxidant, The DCFDA assay showed the potency of BME to quench the intracellular ROS levels in Tai stressed neurons.

5.2.6 BME restores the nuclear transport in neuronal cells

Nucleoporins (Nups) are the nuclear pore complex (NPC) forming proteins, which act as a passage through the nuclear membrane which facilitates the nucleocytoplasmic transport of macromolecules (Fig. 29A)¹⁵⁷. Neurodegenerative diseases are associated with dysfunction in nucleocytoplasmic transport and distorted morphology of nuclear envelop¹⁵⁸. AD has been reported to be associated with disorganization of Nup98¹⁵⁹. The most significant protein of the Nup complex is Nup358 which localizes on the cytoplasmic side of NPC and acts as a clamp of NPC. In our study, the effect of BME on Nup358 arrangement in FA-stressed Neuro2a cells were observed. The FA stressed cells had a distorted arrangement of Nup358 around the nucleus; on contrary, the BME treatment restored the arrangement of Nup358 suggesting the constructive role of BME on Nups358 (Fig. 29B-C). These indicated that BME potentially rescues the nucleocytoplasmic transport from FA-mediated stress.

5.2.7 BME modulates GSK-3 β phosphorylation in neurons

GSK-3 β plays a central role in Tau phosphorylation and generation of AD pathology. Several studies have targeted GSK-3 β for evaluating the potency of therapeutic molecules in AD. In our study, the effect of BME was observed in formaldehyde stressed cells. The western blot showed that FA treatment elevated the GSK-3 β phosphorylation. The FA-treated cells and cells treated with BME had distinguished difference in pGSK-3 β band intensity.

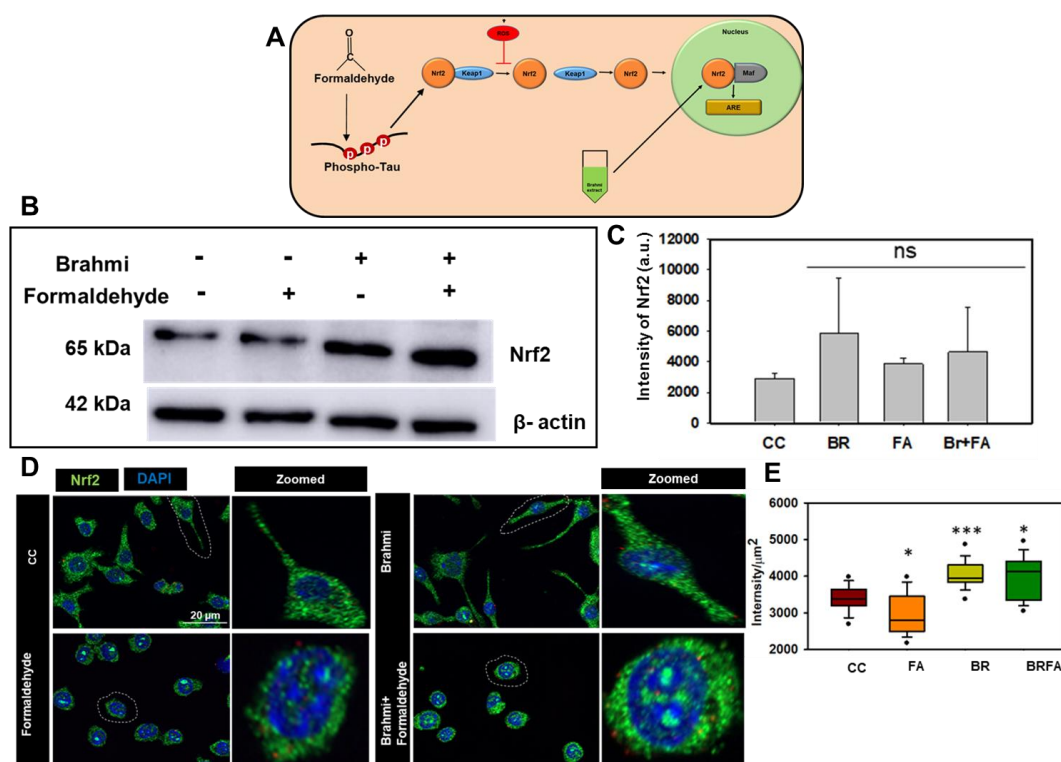


Figure 28. BME modulated the Nrf2 level in cells. A) Nrf2 signalling acts as the antioxidant machinery in cells. The oxidative stress activates the Nrf2, which binds to ARE in cells leading to the expression of antioxidant enzymes. B) The western blot showed the effect of BME in FA stressed cells. BME was observed to elevate the expression of Nrf2. C) The quantification of Nrf2 blot indicates a clear difference in expression of Nrf2 in FA stressed cells and BME treated cells. D) Immunofluorescence images showing the effect of BME in FA-stressed cells. The BME-treated cells were having high intensity of Nrf2 than the FA stressed cells. E) The quantification of IF images, indicates the difference in Nrf2 intensity in various treatment groups.

Similarly, in the cells treated with both BME and FA a low level of pGSK-3 β was observed. Interestingly, no significant difference was observed in the GSK-3 β levels for all four groups (Fig. 30A-C). The immunofluorescence studies indicated that FA-treated cells were having elevated levels of pGSK-3 β as compared to cell control and BME-treated cells. Which supported that FA led to phosphorylation of GSK-3 β . Whereas BME attenuated the FA-mediated phosphorylation of GSK-3 β (Fig. 30D-F).

5.2.8 BME reduced the formaldehyde-mediated Tau phosphorylation

Tau phosphorylation is one of the crucial events related to Tau aggregation generation (Fig. 31A). The studies have targeted the phosphorylated Tau for analysing the therapeutic potency of molecules. In our study, the effect of BME was observed on FA-mediated Tau phosphorylation. The dot blot assay indicated that FA treatment induced the Tau phosphorylation in cells. Whereas, BME-treated cells had a reduced level of phospho-Tau (Thr212/Ser 214) as compared to FA treated cells (Fig 31B). The immunofluorescence studies suggested that FA stressed cells had increased intensity of phospho-Tau, while BME treated cells had significantly reduced intensity of phospho-Tau (Fig. 31C,D). The overall results of these experiments suggested that BME has a protective role against Tau phosphorylation, which aids in its therapeutic potency in AD.

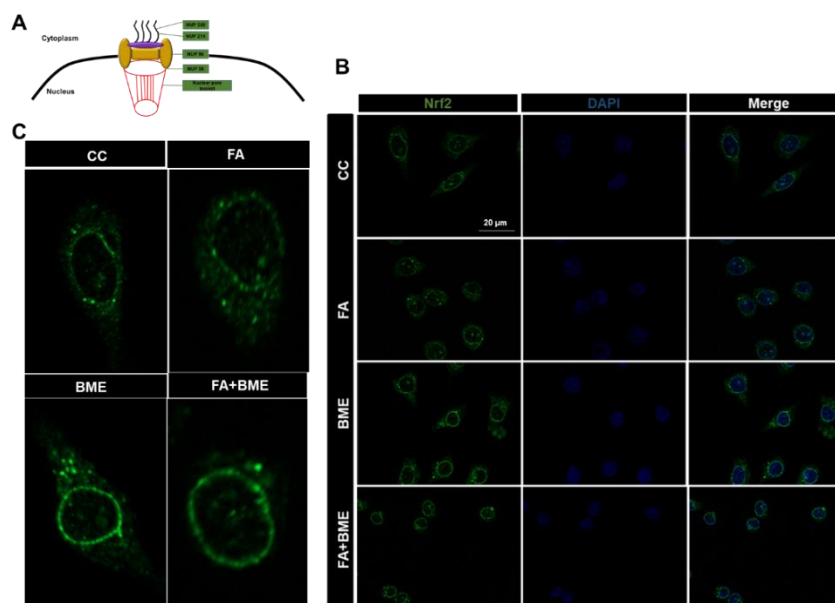


Figure 29. BME restored the Nup358 arrangement. A) The Nup proteins from the nuclear pore complex (NPC), which facilitates the nuclear transport of macromolecules. Nup358 acts as the clamp of NPC. B-C) The FA treatment disrupted the arrangement of Nup 358 around the nucleus. BME treatment restored the Nup358 arrangement assisting in proper nuclear transport.

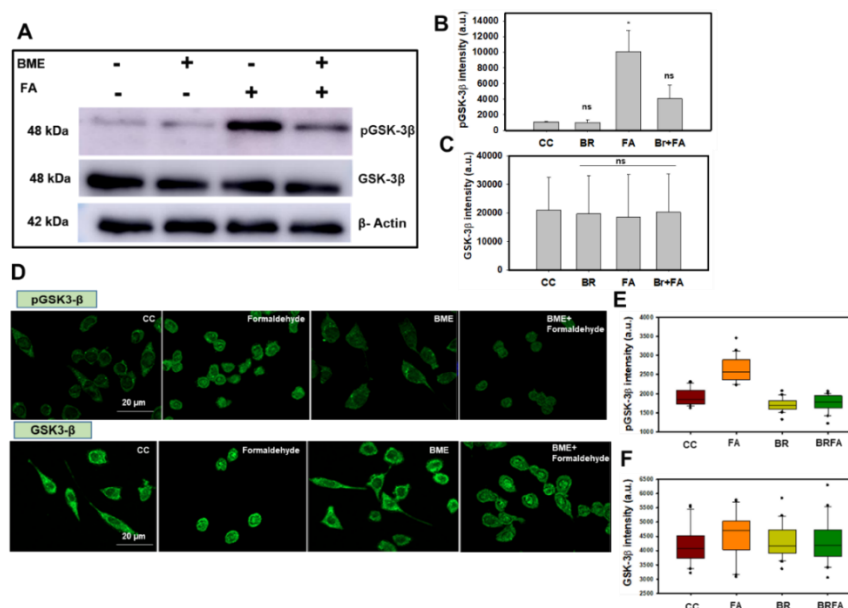


Figure 30. BME modulated the GSK-3 β phosphorylation. A) The western blot designated for the effect of BME on GSK-3 β phosphorylation in FA stressed cells. The FA-induced phosphorylation of GSK-3 β , whereas BME treatment downregulated the GSK-3 β phosphorylation. B) The quantification of western blot indicating the difference in band intensity of pGSK-3 β in various treatment groups. C) The quantification graph of western blot for GSK-3 β . There was no difference in GSK-3 β were observed in various treatment groups. D) The immunofluorescence images of various treatment groups having difference in intensity of pGSK-3 β and GSK-3 β levels. D-F) The quantification of IF images, the difference in pGSK-3 β levels in FA treated cells and BME treated cells, suggested the modulation of GSK-3 β phosphorylation. There were no significant changes in GSK-3 β level was observed.

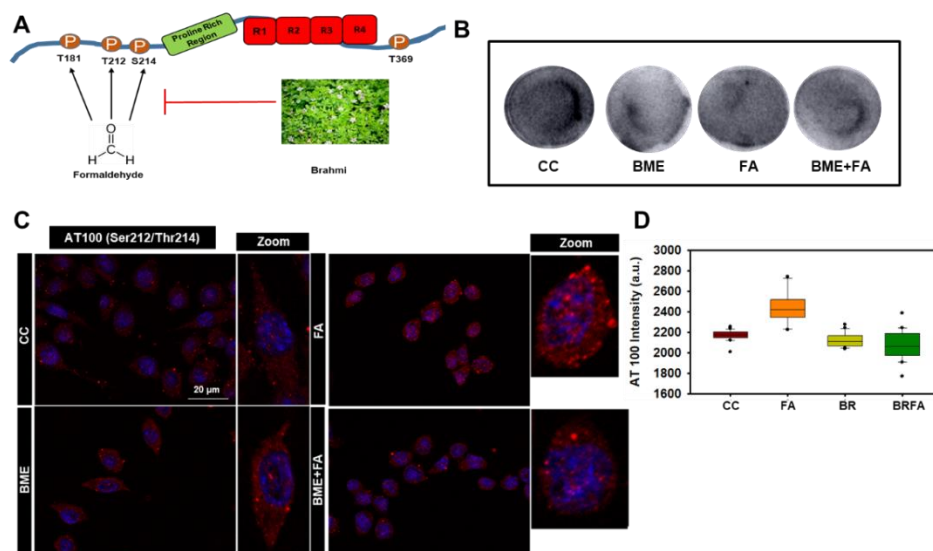


Figure 31. BME reduced the Tau phosphorylation. A) Formaldehyde (FA) treatment led to phosphorylation of Tau. B) The dot blot showing difference in phospho-Tau (Thr212/Ser214) levels between FA treated and BME treated cells. C) The immunofluorescence images indicating the significant difference between phospho-Tau intensity in BME treated and FA treated cells. D) The quantification of IF images, the graph suggested a significant reduction in phospho-Tau intensity after BME treatment in FA stressed cells.

Table .2

S. No.	Retention Time	*Chemical formula	M+H	M+Na	error (ppm)	Frag ments	Name of probable phytochemicals
1.	7.95	C ₂₄ H ₂₈ O ₁₁	493.169 3		-2.3462		Monnieraside II
2.	8.38	C ₂₇ H ₃₀ O ₁₅	595.166 3	617.1484	0.7598		Luteolin-7-rutinoside
3.	8.52	C ₂₃ H ₂₆ O ₁₁	479.154 7		-0.197		Plantioside B
4.	8.77	C ₃₃ H ₄₀ O ₂₀	757.218 3	779.1994	-0.3263		Luteolin-7-rutinoside-3'-glucoside
5.	8.80	C ₃₃ H ₄₀ O ₂₀	757.218 3	779.1994	-0.3263		Luteolin-7-rutinoside-4'-glucoside
6.	9.14	C ₂₁ H ₂₄ O ₁₀	437.143		-2.856		Monnieraside III
7.	9.78	C ₄₀ H ₆₄ O ₁₇		839.4	-4.2256		Deprenyl-ara-glc-ara
8.	9.85	C ₅₄ H ₈₀ O ₂₄		1135.493	-0.1163	579	Bacobitacin C
9.	9.98	C ₂₁ H ₁₉ O ₁₂	463.087 2	485.0693	0.2542		Luteolin-7-glucuronide
10.	10.18	C ₂₁ H ₂₀ O ₁₁	449.108 1	471.09	0.5008		Luteolin-7-glucoside
11.	10.39	C ₂₁ H ₁₉ O ₁₂	463.087 2	485.0693	0.2542		Luteolin-7-glucuronide
12.	10.62	C ₄₆ H ₇₄ O ₁₈		937.4777	0.9865		Oxy-p-glc-ara
13.	10.64	C ₃₅ H ₅₆ O ₈	605.403 8		-1.6295	473,4 55	Bacopasaponin H
14.	10.69	C ₃₂ H ₄₆ O ₈	559.328 5		3.4799		Cucurbitacin B
15.	10.77	C ₄₇ H ₇₆ O ₁₈	951.493 1		-1.7747	617, 455	Bacoside A3 isomer
16.	10.84	C ₄₆ H ₇₄ O ₁₇		921.4828	1.0487	477, 455	Bacoside A2
17.	10.94	C ₄₂ H ₆₆ O ₁₅	811.447 4		-0.0738	487	Methyl-p-2glc
18.	11.21	C ₄₂ H ₆₈ O ₁₄	797.468 0		-0.2075	779, 635	Bacopasaponin N ₁ / Bacopasaponin N ₂
19.	11.36	C ₄₆ H ₇₄ O ₁₇		921.4828	1.0487	587, 455	Bacoside X

20.	11.42	C ₁₅ H ₁₀ O ₆	287.052 2				Luteolin
21.	11.43	C ₄₂ H ₆₈ O ₁₄	797.467 3		-1.1260	779	Bacopasaponin N ₁ /Bacopasaponin N ₂
22.	11.54	C ₁₅ H ₁₀ O ₅	271.060 0				Apigenin
23.	11.69	C ₄₇ H ₇₆ O ₁₉		967.488	0.7609		Oxy-p-2glc-ara
24.	11.76	C ₄₁ H ₆₆ O ₁₃	767.457 1		-0.6855		Bacoside V /Bacoside IV/ Bacopasaponin D
25.	11.83	C ₄₀ H ₆₄ O ₁₂	737.444 2		-4.8442	605, 437	Bacoside A1/ Bacopasaponin A/ Bacopasaponin G/ Bacopasaponin B
26.	11.89	C ₄₀ H ₆₄ O ₁₂	737.447 2		-3.5199		Bacoside A1/ Bacopasaponin A/ Bacopasaponin G/ Bacopasaponin B
27.	11.92	C ₄₁ H ₆₆ O ₁₃	767.458 8		1.5413	473	Bacoside V /Bacoside IV/ Bacopasaponin D
28.	12.2	C ₃₂ H ₄₆ O ₉	575.320 5		-1.6752		Cucurbitacin A
29.	12.35	C ₁₆ H ₃₅ NO 3	290.269		0.1446		Imino diethanol
30.	12.79	C ₄₀ H ₆₄ O ₁₂	737.449 3		3.0186		Bacoside A1/ Bacopasaponin A/ Bacopasaponin G/ Bacopasaponin B
31.	13.19	C ₄₁ H ₆₆ O ₁₃	767.459 3		2.1775	605	Bacoside V /Bacoside IV/ Bacopasaponin D
32.	13.38	C ₄₀ H ₆₄ O ₁₂	737.446 5		-0.7886		Bacoside A1/ Bacopasaponin A/ Bacopasaponin G/ Bacopasaponin B
33.	17.29	C ₅₈ H ₈₆ O ₂₄	1167.55 91		0.7729		Deoxy-p-2glc-ara- phenylglucoside

Table 2. LC-HRMS analysis shows the molecular formula list, retention time and the respective phytochemicals identified based on protonated, Na adduct and m/z fragments.

5.3 Summary

In our study, the potency of ethanolic extract of *Bacopa monnieri* was studied against Tau aggregation, Tau-mediated oxidative stress, cytotoxicity, and Tau phosphorylation. The BME potentially inhibited the *invitro* aggregation of Tau. The treatment of BME improved the vitality of Tau stressed cells, and downregulated the apoptosis *via* modulating the Caspas-3 activity. The BME was also found to have efficiency of quenching intracellular ROS. Additionally BME upregulated the Nrf2 level in cells, which indicated the antioxidant property of BME. The Neuro2a cells incubated with BME had low level of phospho-Tau and phospho-GSK-3 β , which indicated the potency of BME against Tau phosphorylation. It was observed that BME restored the Nup358 arrangement in FA-stressed cells, which facilitated the nucleocytoplasmic transport. These results advocated that BME could be considered as a potent herb in attenuation of Tau aggregation and Tau toxicity.

Chapter 6

Discussion

6.1 The diverse role of Tau in neuron

Alzheimer's disease (AD) is a neurodegenerative disease characterized by progressive loss of memory, cognitive function and behavioural impairments. The accumulation of extracellular A β plaques and intracellular Tau aggregates are causes of AD¹⁶⁰. The Tau protein is known to be closely involved with the AD-related pathology. Physiologically, Tau is a microtubule-binding protein, which provides stability to microtubules¹³⁸. Under-pathological conditions such as AD, the dissociation of Tau from microtubules led to microtubule disintegration, while Tau monomers self-aggregates resulting in neurotoxic Tau aggregates¹⁶¹. The aggregates of Tau are known to interfere with various vital signalling cascades of neurons. The accumulation of Tau is reported to impair the protein quality check machinery in the endoplasmic reticulum¹⁶². Similarly Tau aggregates and oligomers are reported to induce mitochondrial dysfunction¹⁶³. Tau protein is localized in the cytosol, but the studies evidenced the presence of nuclear Tau. Tau found to be associated with dysfunction of nucleocytoplasmic transport²⁰. The missorted Nup98 interacts with Tau protein resulting in impairment of nucleocytoplasmic transport¹⁶⁴. Since Tau is associated to the microtubule, the presence of Tau aggregates modulates the cytoskeleton of the neuron. The neuron having Tau aggregates stress had reduced neuritic extensions, similarly Tau aggregates led to modulation of actin cytoskeleton network¹⁶⁵. Additionally, the generation of oxidative stress and autophagy are the common symptoms generated in presence of Tau aggregates. The molecules having potency against Tau aggregates were targeted to evaluate the neuroprotective potency in AD. The compounds of natural origin e.g. curcumin, cinnamaldehyde, anthraquinones, daunorubicin, baicalein, epigallocatechin-3-gallate (EGCG), limonoids etc; have shown a remarkable potency against Tau aggregation¹⁴⁶. At the same time, the synthetic Tau aggregation inhibitors such as Methylene blue and Tideglusib successfully cleared the phase II clinical trial but failed in the subsequent clinical trials³⁶. Henceforth, it could be stated that the presence of Tau aggregates imparts the toxicity to neurons by interfering with cellular components of neuron.

6.2 Tau phosphorylation and Neurotoxicity

Several post-translational modifications *viz*, glycation, glycosylation, ubiquitination, nitration, phosphorylation have been associated with Tau aggregation and pathology¹⁶. Tau phosphorylation is one of the extensively studied PTM, *in vitro* and *in vivo* studies have evidenced the neurotoxicity of hyper-phosphorylated Tau¹⁶⁶. Tau is a phospho protein, one mole of Tau is known to have two-three moles of phosphate. A total of 85 phosphorylation-prone sites, including serine (S), threonine (T), and tyrosine (Y) are present on Tau^{167,168}. These sites are phosphorylated by various kinase e.g. proline-directed glycogen synthase kinase-3 (GSK-3, cyclin-dependent kinase 5 (cdk5), and 5' adenosine monophosphate-activated protein kinase (AMPK), non- proline-directed kinase kinases (MARKs), cyclic AMP-dependent protein kinase A (PKA)^{169,170}. The hyper-phosphorylated Tau detaches from the microtubule and aggregates at an accelerated rate¹⁷¹. The accumulation of A β accelerated the phosphorylation of Tau caused toxicity in Tg2576 mice¹⁷². Chronic oxidative stress increased the phosphorylation of Tau, which generated toxicity in neuroblastoma cells¹⁷³. Similarly, the presence of hyper-phosphorylated Tau imparts adverse effects on nucleocytoplasmic transport¹⁷⁴. Additionally, the deficiency of vitamin B upregulated the Tau phosphorylation *via* modulating GSK-3 β ¹⁷⁵. Hence, several molecules and compounds have been screened for

their efficiency to downregulate Tau phosphorylation. Methylene blue was observed to reduce MARK4/PAR1-mediated Tau phosphorylation resulting in attenuation of synaptic toxicity⁶⁹. The treatment of Harmine, a β -carboline alkaloid, inhibited the Tau phosphorylation at multiple sites¹⁷⁶. Lithium is a well-known GSK-3 β inhibitor; treatment of lithium reduced the Tau phosphorylation *via* downregulation of GSK-3 β in aged 3xTg-AD mice¹⁷⁷. Caffeic acid is a plant-derived neuroprotective phenolic compound. The treatment of caffeic acid reduced the Tau phosphorylation in A β stressed PC12 cells¹⁷⁸. The mice exposed to high doses of iron were observed to have elevated level of phospho-Tau in the brain. The treatment of iron chelators e.g. Deferoxamine, reduced the Tau phosphorylation¹⁷⁹. The natural compounds e.g. curcumin, ginsenoside Rd, Peloruside A *etc*; are also reported to downregulate the Tau phosphorylation in neuronal cells^{180,181}. The treatment of chemical stress e.g. 0.5 mM formaldehyde, led to phosphorylation of Tau at multiple sites. The formaldehyde treatment also elevated the activity of Tau specific kinase GSK-3 β in neuro2a cells¹⁸². In the presence of resveratrol the level of phospho-Tau were reduced to an appreciable extent¹⁸³. Hence the previous studies conclude that downregulation of Tau phosphorylation is a reliable therapeutic strategy against AD.

6.3 The effect of photo-excited molecules on protein aggregates

Photodynamic therapy is a non-conventional therapeutic strategy that implies photo-excited dyes against the target tissues. In recent years, PDT has evolved as a therapy for the treatment of neuronal tissues^{184,185}. Various photosensitizers have potency to effect the brain tissues. The application of PDT for treatment of neuronal tissues has always been a challenging approach in treatment of neurological disorders, PDT has several challenges to be answered (Table 3). Although, the recent advancement and research in field of PDT have indicated potency of photosensitizers for the treatment of neuronal disorders. The 5-aminolevulinic acid (5-ALA) is a well-researched and reviewed photosensitizer for treatment of neuronal tissues including brain tumours¹⁸⁶. In recent years numerous photosensitizers (PS) have been reported for their potency to disaggregate the A β fibrils. Polyoxometalates (POMs) are fullerene-like inorganic molecules; in recent studies, it was observed that photo-excited POMs efficiently inhibited the aggregation of A β and disaggregated the mature A β aggregates *in vitro*¹⁸⁷. Similarly, another photo-catalytic compound, Bismuth vanadate (BiVO₄) was also observed to photo-oxidize the A β aggregates resulting in irreversible degradation of A β aggregates¹⁸⁸. The photo-sensitive porphyrin-peptide (KLVFF) hybrid molecules were studied to attenuate the A β ¹⁸⁹. *meso*-tetra(4-sulfonatophenyl)porphyrin (TPPS) is the photosensitizer which has excitation in blue light; *in vitro* studies showed that photo-excited TPPS inhibited the aggregation of A β . In another study, A β has treated riboflavin in the presence of white light irradiation. The result of these studies showed that riboflavin treated A β peptides had lower potency for aggregation and cytotoxicity¹⁹⁰. In a study, the photo-sensitive ruthenium (II) {[Ru(bpy)₃]²⁺} complex was tested against A β aggregates. The *in vitro* studies such as CD spectroscopy, ThT fluorescence assay, Fourier transform infrared spectroscopy suggested that treatment of white light irradiated ruthenium (II) complex inhibited the aggregation of *in vitro* aggregation of A β and cytotoxicity in PC12 cells¹⁹¹.

Rose Bengal (RB) belongs to xanthene dyes, RB is known to have photosensitivity when irradiated with green light. In recent studies, the role of photo-excited RB has been reported against A β aggregation. The photo-excited RB attenuated the aggregation of A β under *in-vitro* conditions. Moreover, the treatment of photo-excited RB also observed to rescue the PC12 cells from A β mediated toxicity⁸⁰. Similarly, the phenothiazine dye Methylene blue inhibited

the A β aggregation and toxicity. The treatment of photo-excited Methylene blue (MB) disaggregated the mature A β fibrils. Whereas, under *in vivo* studies, the photo-excited MB improved the crawling behaviour of UAS-A β 42 *Drosophila* larvae and reduced the brain vacuole formation in adult flies⁸². β NaYF4:Yb/Er@SiO2@RB and RB/UCNP@ROS are examples of photo-sensitive compounds which have excitation at 980 nm. The preliminary studies have demonstrated the effectiveness of these compounds in attenuation of A β aggregation¹²¹. Although the effect of photo-excited dyes against Tau fibrilization and Tau-mediated toxicity was not studied exclusively. Our work, observed that the treatment of phenothiazine dye Toluidine blue (TB) appreciably inhibited the aggregation of heparin-induced Tau. Additionally, treatment of photo-excited TB resulted in potent disaggregation of pre-mature Tau aggregates. Similarly, the xanthene dye Rose Bengal (RB) was also studied for its potency against Tau aggregation. The *in vitro* studies clearly suggested that the treatment of RB attenuated the aggregation of heparin-treated Tau. The photo-excited RB treatment led to disaggregation of mature Tau filaments, which was confirmed by biochemical and biophysical techniques such as ThS assay, SDS-PAGE and electron microscopy. The behavioral studies were performed in *Drosophila* model suggested that the treatment of both the dyes *viz*; photo-excited RB and photo-excited TB improved the memory, longevity, and locomotor function of UAS-A14 Tau *Drosophila*. Hence, the photo-excited dyes RB and TB were observed to have potency against against Tau aggregation and Tau toxicity (Fig. 32).

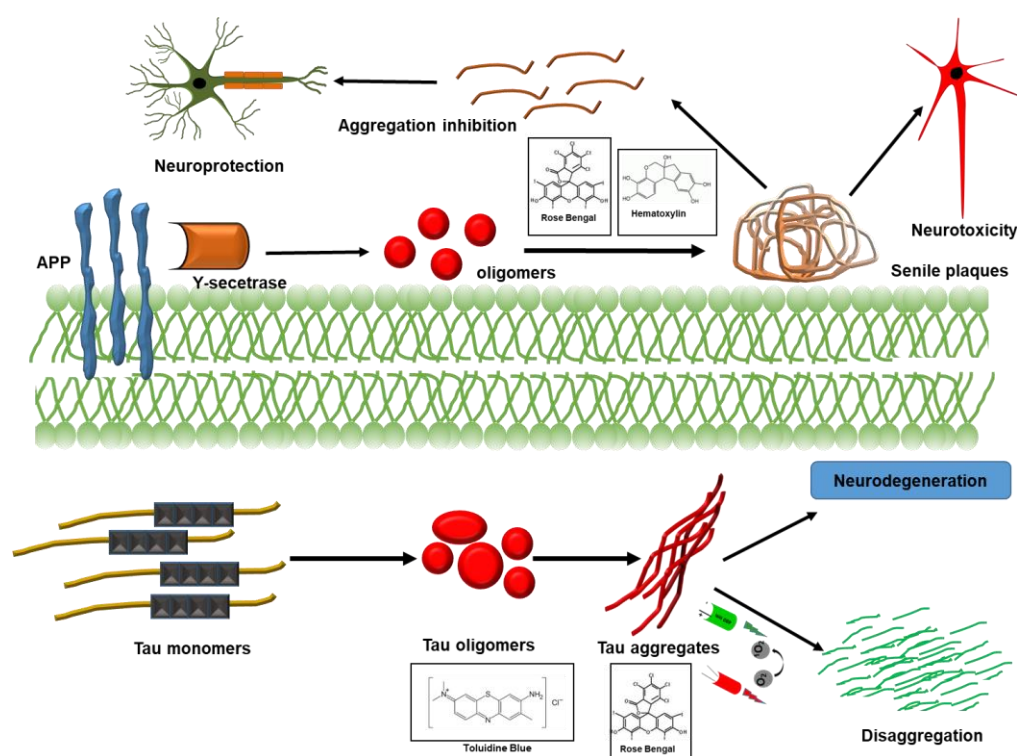


Figure 32. The photo-excited dyes disaggregate the protein aggregates. Amyloid- β aggregates are formed by the activity of γ -secretase on APP. The mature aggregates of amyloid- β are neurotoxic. . The treatment of photo-excited dyes e.g Rose Bengal, methylene blue etc., inhibits the aggregation of amyloid- β , which reduces the amyloid- β -mediated toxicity. Tau aggregates are toxic to neurons, which modulate several cellular signalling ultimately resulting in toxicity. The treatment of photo-excited dyes e.g. Rose Bengal and Toluidine blue, disaggregates the Tau aggregates.

6.4 Cytoskeleton deformities and PDT

The cytoskeleton plays a crucial role in the maintenance of the neuronal integrity, neurite extension, synapse formation, axonal elongation *etc.* The modulation in the microtubule network led to various changes in neurons. The studies showed that cholesterol treatment attenuated the dendritic outgrowth by the microtubule network¹⁹². Similarly, overexpression of microtubule destabilizing factor SCG 10 resulted in reduced neuronal outgrowth¹⁹³. The treatment of lysophosphatidic acid (LPA) led to tubulin modulation and Tau hyper phosphorylation. The neurons exposed to LPA treatment were observed to have retracted neurite outgrowth¹⁹⁴. Lipid peroxidation results in formation of various stress molecules such as 4-hydroxy-2(E)-nonenal (HNE). HNE interfered with the microtubule stability which caused the reduction in neurites length¹⁹⁵. Similarly, the modulation of another cytoskeleton protein actin also results in various neuronal defects. The recent studies suggest that accumulation and bundling of F-actin result in Tau-mediated neurodegeneration in *Drosophila*¹⁹⁶. Huntington's disease is another neurodegenerative disease known to be caused from Huntingtin protein. It was observed that mutation in the huntingtin protein led to modulation in actin cytoskeleton¹⁹⁷. The accumulation of actin/cofilin rods are among the common processes observed in several neurodegenerative diseases such as AD, PD, HD¹⁹⁸. The localization of A β causes the oxidation of F-actin, while the treatment of Glutaredoxin1 inhibited the F-actin oxidation resulting in restoration of cognitive function¹⁹⁹.

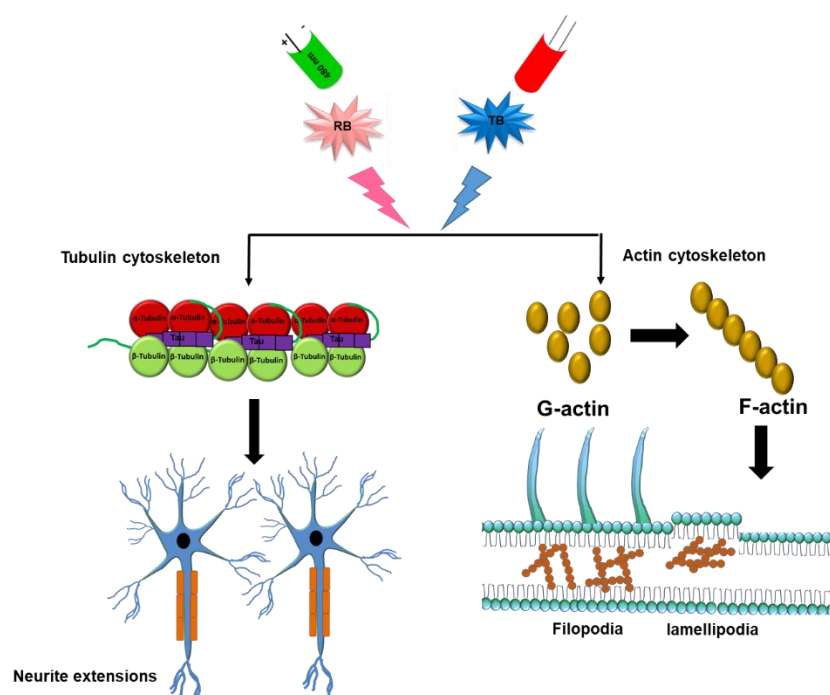


Figure 33. Cytoskeleton modulation by photo-excited dyes. The cytoskeleton plays various crucial roles in neurons. The processes such as synaptic connection formation, neuronal development, and axonal guidance have the role in the cytoskeleton. Neurodegenerative diseases are known to be associated with cytoskeleton deformities the treatment of photo-excited Rose Bengal and Toluidine blue up regulated the polymerization of tubulin resulting in neurite extension. The actin cytoskeleton is also modulated by photo-excited dyes. The filopodia are hair-like actin-rich structures, whereas the lamellipodia are the fan-like structures involved in cell addition and cell-cell communication. The cells exposed to photo-excited Rose Bengal and Toluidine blue had increased actin rich structures in membrane indicating the modulation of actin cytoskeleton.

Thus, the deformities in the neuronal cytoskeleton are closely associated with neurodegenerative diseases. Photodynamic therapy is known to target the cytoskeleton. The PDT using aminolevulinic acid showed the alternation of glioma cell morphology *via* actin

cytoskeleton²⁰⁰. The Photofrin-mediated PDT resulted in microtubule depolymerisation²⁰¹. Similarly, the application of photo-excited 3,3'-dihexyloxycarbocyanine iodide and TMPyP–Porphyrine resulted in depolymerisation of microtubules^{79,202}. Thus, we studied the effect of photo excited dyes Rose Bengal and Toluidine blue on neuronal cytoskeleton modulation. We observed that the exposure of photo-excited RB, and TB potentially modulated the actin cytoskeleton. Elevated number of actin-rich hair like structures filopodia and fan-like lamellipodia were observed in cells exposed to photo-excited RB and TB. The photo-excited RB treated cells were having podosome-like structures actin rich structures, which suggested the modulation of actin cytoskeleton. Tubulin are another important cytoskeleton protein. In our studies we observed that treatment of photo-excited RB and TB resulted in modulation of tubulin network which was evidenced by presence of long neurite extensions having elevated intensity of tubulin. Hence, the overall result of these studies suggested that treatment of photo-excited dyes may have potency to modulate neuronal cytoskeleton (Fig. 33).

6.5 Ayurveda and neurodegeneration

Ayurveda includes the approach that deals with prevention, diagnosis, and therapeutic strategies for diseases. Ayurveda counsels about the diet and nutrition for an individual based on analysis of body components or "Prakriti". Charaka Samhita and Sushruta Samhita (400 BC–200 AD) are ancient literature, which include various formulations of Ayurveda²⁰³. According to Ayurveda, the neuronal system of the human body is dominated by the Vata component (dosha). There are medicinal plants that are believed to have potency against Alzheimer's disease²⁰⁴. The application of various formulations of these herbs were found to improve the memory deficits (Table 4). *Withania somnifera*, *Convolvulus prostrates*, *Nardostachys jatamans* and *Bacopa monnieri* are acknowledged to have nootropic potency²⁰⁵.

Table. 4

S.No.	Name of Herb	Medicinal part of plant	Bioactive component	Function	Reference
1.	Ashwagandha (<i>Withania somnifera</i>)	Roots	withanine, withananine, somniferine, sominone, somnine	Reduction of neuroinflammation, Depression, Memory deficit	Kaur <i>et al.</i> , 2001
2.	Jatamansi (<i>Nardostachys jatamansi</i>)	Roots	sesquiterpenoids, valeriananoids	Memory deficit, Insomnia	Rather A <i>et al.</i> , 2012
3.	Sarpagandha (<i>Rauvolfia serpentina</i>)	Roots	Reserpine	Hypertension, Insomnia, Depression	Lobay <i>et al.</i> , 2015
4.	Turmeric (<i>Curcuma longa</i>)	Roots	Curcumin	Reduction of Neuroinflammation, neurodegeneration, memory deficit	Monroy <i>et al.</i> , 2013
5.	Shankpushpi (<i>Convolvulus pluricaulis</i>)	Leaves	Shankpushpin e, convolamine, convoline,	improvement of memory and learning ability	Agarwa <i>et al.</i> , 2013
6.	Brahmi (<i>Bacopa monnieri</i>)	Leaves	Bacoside A, Betulinic acid, Bacoposide	Improvement in memory and cognitive function	Augiar <i>et al.</i> , 2013
7.	Gotu kola (<i>Centella asiatica</i>)	Leaves	Asiaticoside A, Asiaticoside B, Asiatic acid	Improvement of memory and learning	Dey <i>et al.</i> , 2015

					Xu Y <i>et al.</i> , 2008
8.	Jyotishmati (<i>Celastrus paniculatus</i>)	Seed/Seed oil	Pristimerin	Antioxidant Memory enhancer	Summers <i>et al.</i> , 2004
9.	Giloy (<i>Tinospora cordifolia</i>)	Leaves	Tinocordioside Cordiosides	Anti-depressant	Saha <i>et al.</i> , 2012
10.	Tulsi (<i>Ocimum santum</i>)	Leaves	Eugenol	Acetyl choline booster	Pattanayak <i>et al.</i> , 2010
11.	Neem (<i>Azadirachta indica</i>)	Leaves	Limonoids	Improvement of cognition	Raghvendra <i>et al.</i> , 2013
12.	Bringraj (<i>Eclipta alba</i>)	Leaves	Wedelolactone	Antioxidant Improves learning	Vidhya shree <i>et al.</i> , 2018
13.	Vacha (<i>Acorus calamus</i>)	Rizome	Asarone, Asareldehyde	Improves the learning	Kumar A 2013
14.	Shatavar (<i>Asparagus racemosus</i>)	Rizome	Shatavarin IV	Antioxidant Anti-Parkinson's herb	Smita S <i>et al.</i> ; 2017
15.	Vldari Kanda (<i>Pueraria tuberosa</i>)	Rizome	Tuberosin	Antioxidant Nootropic	Rao <i>et al.</i> ;2008
16.	Kesar (<i>Crocus sativus</i>)	Stigma, styl of flower	Crocins	Antioxidant	Shaterzadeh H <i>et al.</i> ; 2018
17.	Almond (<i>Prunus amygdalus</i>)	Seed	Morin	Destabilises the Amyloid- β Firbils	Lamkul JA <i>et al.</i> ; 2010
18.	Garlic (<i>Allium sativum</i>)	Cloves	Crude extract	Downregulation of Amyloid- β induced apoptosis in PC12 cells.	Guo JP <i>et al.</i> ; 2010
19.	Ginger (<i>Zingier officials</i>)	Rizome	Crude extract	Inhibition of Amyloid- β aggregation	Guo JP <i>et al.</i> ;2010

Table 3. The Ayurveda applies various formulations of herbs for the treatment of neurodegenerative diseases. The table showing list of plant considered to have neuroprotective property.

The protein aggregates is considered as one of the reason for AD. Numerous plants contain mildly toxic non-mutagenic flavone “Apigenin”. The apigenin treatment reduces the copper-mediated A β aggregation and oxidative stress in neurons. The apigenin treatment reduced the A β burden in the APP/PS1 mice model of AD²⁰⁶. It was also observed that oligomers of A β -induced toxicity to the astrocyte and neurons obtained from the cortex of newborn and embryonic wistar rats, whereas apigenin rescued the neuronal and astrocyte from A β mediated toxicity²⁰⁷. Baicalein is another naturally occurring flavone isolated from the roots of *Scutellaria baicalensis*. The recent studies suggested the neuroprotective property of Baicalein against A β and Tau-mediated toxicity. Baicalein (10–50 mg/kg, i.p.) reduced the A β mediated amentia in mice²⁰⁸. The treatment of Baicalein reduced the A β -mediated toxicity, cell apoptosis and oxidative stress in PC12 cells²⁰⁹. *Curcuma longa* is an acknowledged herb in Ayurveda; curcumin is the polyphenolic bioactive component isolated from blubs of *Curcuma longa*²¹⁰. The injection of curcumin in aged Tg2576 mice reduced the formation of senile plaques⁹⁶. The inhibition of Tau aggregation is another important therapeutic strategy against AD. Curcumin treatment inhibited the β -sheet formation and aggregation of Tau *in vitro*²¹¹. The conjugate of Ruthenium(II) and curcumin efficiently inhibited the aggregation of peptide corresponding to R3 repeat of Tau²¹². Another derivative of curcumin PE859 was observed to inhibit the aggregation of both A β and Tau *in vitro* furthermore, the treatment of PE859 reduced the load of Tau aggregates and improved the cognitive behavior in senescence-accelerated

mouse prone 8 (SAMP8)²¹³. *Withania somnifera* is another nootropic herb in Ayurveda, withanamide is one of the active components of *Withania somnifera*, the treatment of withanamide rescued the viability of A β stressed PC12 cells²¹⁴. The crude root extract of *Withania somnifera* reduced the H₂O₂ and A β mediated toxicity in differentiated PC12 cells²¹⁵. *Crocus sativus* or saffron is known for its antihypertensive, anticonvulsant, antitussive, antigenotoxic and cytotoxic effects²¹⁶. In recent studies *Crocus sativus* was observed to have neuroprotective efficiency against AD, the extract prepared from the stigma of *Crocus sativus* inhibited the fibrillogenesis of A β ²¹⁷. Crocin is a carotenoid isolated from stigma of *Crocus sativus*, the treatment of crocin efficiently inhibited the aggregation of A β peptides *in vitro*²¹⁸. The administration of crocin improved the A β mediated memory deficits and long-term potentiation in rats²¹⁹. The aggregates of α -Synuclein are considered to be associated with Parkinson's disease²²⁰. Epigallocatechin gallate (EGCG) is an active component of green tea, which is known to have potency in inhibiting the aggregation of A β and A β mediated toxicity. EGCG was found to be effective in attenuation of Tau aggregation^{34,221}. *Bacopa monnieri* is a nootropic herb that has been studied in various aspects of neurodegeneration. The extract of *Bacopa monnieri* protected the primary cortical neurons from A β -mediated toxicity and oxidative stress. Extract of *Bacopa monnieri* also showed the improvement of cognitive behavior and memory dysfunction in AD model¹⁰⁹. Bacoside-A is an active compound isolated from *Bacopa monnieri*, was found have significant inhibitory effect on A β aggregation¹⁵⁵. In our studies we have also observed that the crude extract of *Bacopa monnieri* inhibited (BME) the aggregation of Tau *in vitro*. The results of ThS assay, electron microscopic analysis, CD spectroscopy supported the aggregation inhibition potency of BME.

6.6 The rejuvenating effect of BME

Accumulation of Tau aggregates results in impairments of various signalling cascades that direct the cells for apoptosis or necrosis²²². Several key Tau aggregation modulators have been observed to improve the vitality of cells. Heptelidic acid is one of the Tau aggregation inhibitors, the treatment of heptelidic acid improved the viability of cells²²³. The Caspase-3 activity was also reduced by heptelidic acid treatment indicating the reduction in cell death. *Azadirachta indica* is known for its exceptional medicinal property, nimbin and salanine are two limonoids isolated from *Azadirachta indica* fruits. Nimbin and Salanine were found to inhibit the aggregation of Tau *in vitro*. Additionally, these limonoids demonstrated a protective effect in cells and rescued them from Tau-mediated toxicity³⁰. Baicalein is another naturally occurring flavonoid that can attenuate Tau aggregation and Tau-mediated toxicity^{33,111}. Our study also observed that BME rescues the cells from Tau-mediated toxicity. Additionally, we observed that the cells had improved viability after BME treatment. The BME was also found to downregulate the apoptosis by modulating the activity of Caspase-3. Thus, we stated that BME has a rejuvenating effect in Tau stressed cells.

6.7 The antioxidant property of BME

The oxidative stress is one of the principle reason for generation of neurodegeneration. The Ayurvedic herbs and their active components are known to have antioxidant properties. *Withania somnifera* reduced the Bisphenol A (BPA) induced oxidative stress in mice model²²⁴. Similarly, the root extract of *Withania somnifera* demonstrated neuroprotective action by reducing the oxidative stress in maneb (MB) and paraquat (PQ) mice models²²⁵. The treatment of curcumin defended the neurons from A β induced oxidative stress. Rotenone treatment induces Parkinson's disease like pathology *via* generation of oxidative stress. The

administration of resveratrol reduced the 1-methyl-4-phenylpyridinium ion (MPP⁺) mediated oxidative stress in neurons²²⁶. *Bacopa monnieri* is widely acknowledged for its antioxidant properties. The treatment of BME upregulated the Nrf2 level, which protected the rat against oxidative stress¹⁰⁵. Similarly, the administration of BME upregulated the expression of antioxidant enzymes e.g. superoxide dismutase (SOD), catalase (CAT), and glutathione peroxidase (GPx) in brain of wistar rats¹⁰¹. Similarly, in primary cortical cultured neurons BME treatment reduced the A β -mediated oxidative stress and glutamate-induced toxicity²²⁷. In our experiments, the cells treated with BME were having low level of intracellular ROS and elevated levels of Nrf2 which suggested the antioxidant property of BME.

6.8 BME recued Tau phosphorylation

The hyper-phosphorylation of Tau is considered to be one of the crucial factors in the generation of Tau aggregation and Tau pathology²²⁸. Proline-directed kinase e.g. GSK-3 β , CDK5, JNK and non proline-directed kinase e.g. PKA, PKC, CaMKII, MARK or CKII *etc*²²⁹. The accumulation of hyper-phosphorylated Tau induces oxidative stress, neurotoxicity and impairment in signalling cascades^{230,231}. The compounds of natural origin have potency to downregulate Tau phosphorylation. The natural plant derivative “Isobavachalcon”, was

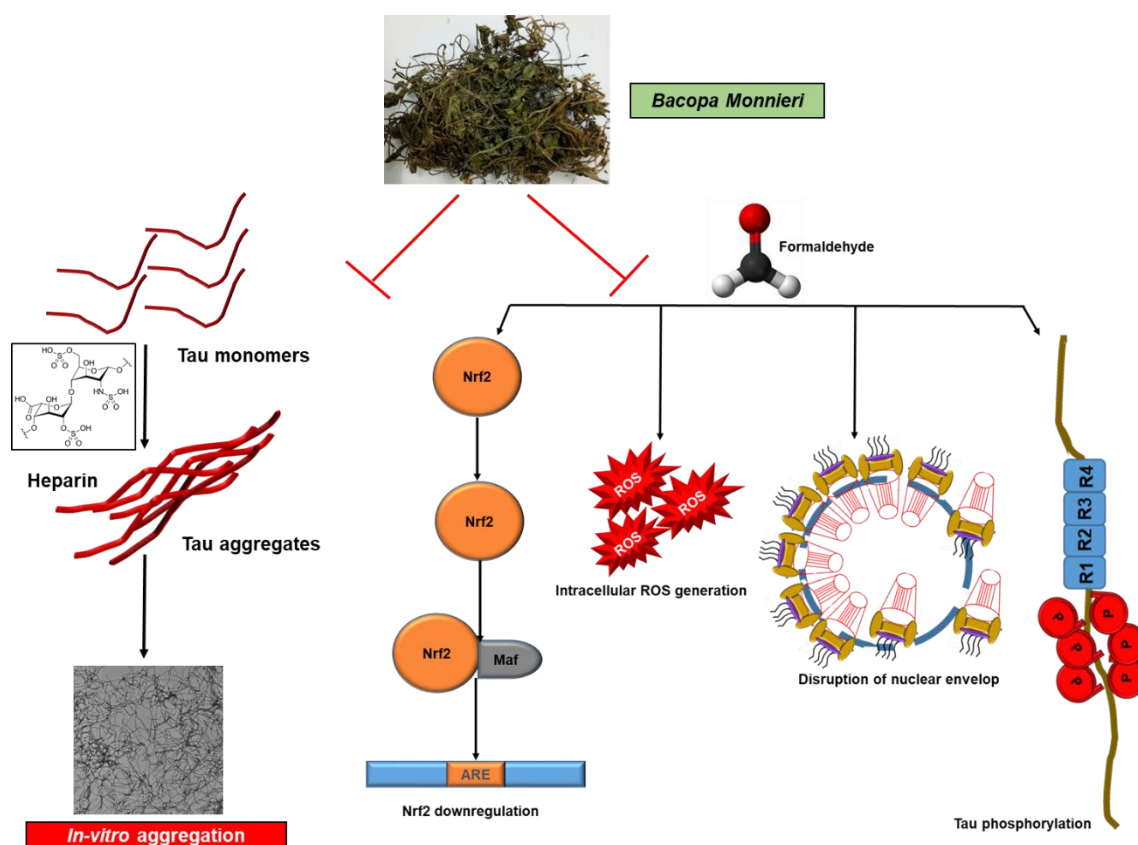


Figure 34. The *Bacopa monnieri* extract (BME) have neuroprotective property against Tau toxicity. The Tau aggregation is one of the hallmarks of AD; under *in vitro* conditions, the Tau aggregation is mimicked by incubation with polyanionic compounds such as heparin. The BME potentially attenuated the aggregation of Tau *in vitro*. In the presence of BME the viability of neurons improved, which aids to its neuroprotective property. The phosphorylation of Tau led to the generation of its pathology. Formaldehyde treatment results in Tau phosphorylation and neurotoxicity. The treatment of FA increased the intracellular ROS and disrupted the nuclear envelope. BME treatment reduced the intracellular ROS and upregulated the Nrf2 pathways, which supports its antioxidant property. The BME treatment assists in the reorganization of Nup358 around the nucleus, which aids in its neuroprotective property.

studied to have a neuroprotective effect as it reduced the Tau phosphorylation by modulating the activity of GSK-3 β and PP2A¹⁴⁹. Similarly the natural compound “wogonin”, tested to be effective in reducing the Tau phosphorylation *via* inhibiting the GSK-3 β activity²³². The naturally occurring polyphenol “curcumin”, was observed to have neuroprotective potency *via* modulating the level of phospho-Tau. Curcumin treatment effect the GSK-3 β activity in SH-SY5Y cells, and thus, it reduces the level of phospho-Tau²³³. Epigallocatechin-3-gallate (EGCG) s another polyphenol found in green tea, recent studies suggested that EGCG reduced the formaldehyde-mediated phosphorylation of Tau in neuro2a cells³⁴. Trans-Crocin 4 and trans-Crocetin are the bioactive components of *Crocus sativus*, which are known to have neuroprotective potency. In the presence of trans-Crocin 4 and trans-Crocetin the activity of GSK-3 β and ERK1/2 were downregulated resulting in reduced phospho-Tau levels in SH-SY5Y cells²³⁴. The plant-derived stilbenoid resveratrol reduced the formaldehyde-mediated Tau phosphorylation¹⁸³. In our work, we observed that the formaldehyde treated Neuro2a cells had a significantly elevated level of phospho-Tau, whereas BME treatment reduced the phospho-Tau. Interestingly the BME was also observed to modulate the phosphorylation of GSK-3 β . We observed that in formaldehyde treated cells, pGSK-3 β level were more as compared to untreated cells. On the contrary the BME treatment decreased the level of pGSK-3 β . Thus, we stated that BME has the potency to modulate the Tau phosphorylation in neurons (Fig. 34).

References

- 1 Barnham, K. J., Masters, C. L. & Bush, A. I. Neurodegenerative diseases and oxidative stress. *Nature reviews Drug discovery* 3, 205-214 (2004).
- 2 Agorogiannis, E., Agorogiannis, G., Papadimitriou, A. & Hadjigeorgiou, G. Protein misfolding in neurodegenerative diseases. *Neuropathology and applied neurobiology* 30, 215-224 (2004).
- 3 Hartl, F. U. Protein misfolding diseases. *Annual review of biochemistry* 86, 21-26 (2017).
- 4 Lücking, C. & Brice, A. Alpha-synuclein and Parkinson's disease. *Cellular and Molecular Life Sciences CMLS* 57, 1894-1908 (2000).
- 5 Iwasaki, Y. Creutzfeldt-Jakob disease. *Neuropathology* 37, 174-188 (2017).
- 6 Bates, G. P. *et al.* Huntington disease. *Nature reviews Disease primers* 1, 1-21 (2015).
- 7 Cruts, M., Hendriks, L. & Van Broeckhoven, C. The presenilin genes: a new gene family involved in Alzheimer disease pathology. *Human molecular genetics* 5, 1449-1455 (1996).
- 8 Williamson, J., Goldman, J. & Marder, K. S. Genetic aspects of Alzheimer disease. *The neurologist* 15, 80 (2009).
- 9 Du, X., Wang, X. & Geng, M. Alzheimer's disease hypothesis and related therapies. *Translational neurodegeneration* 7, 1-7 (2018).
- 10 Makin, S. The amyloid hypothesis on trial. *Nature* 559, S4-S4 (2018).
- 11 Gorantla, N. V. & Chinnathambi, S. Tau protein squired by molecular chaperones during Alzheimer's disease. *Journal of Molecular Neuroscience* 66, 356-368 (2018).
- 12 Kirkitadze, M. D. & Kowalska, A. Molecular mechanisms initiating amyloid beta-fibril formation in Alzheimer's disease. *Acta Biochimica Polonica* 52, 417-423 (2005).
- 13 Sadigh-Eteghad, S. *et al.* Amyloid-beta: a crucial factor in Alzheimer's disease. *Medical principles and practice* 24, 1-10 (2015).
- 14 Mandelkow, E.-M. & Mandelkow, E. Tau in Alzheimer's disease. *Trends in cell biology* 8, 425-427 (1998).
- 15 Mandelkow, E.-M. & Mandelkow, E. Biochemistry and cell biology of tau protein in neurofibrillary degeneration. *Cold Spring Harbor perspectives in medicine* 2, a006247 (2012).
- 16 Martin, L., Latypova, X. & Terro, F. Post-translational modifications of tau protein: implications for Alzheimer's disease. *Neurochemistry international* 58, 458-471 (2011).
- 17 Run, X. *et al.* Anesthesia induces phosphorylation of tau. *Journal of Alzheimer's Disease* 16, 619-626 (2009).
- 18 Gorantla, N. V., Khandelwal, P., Poddar, P. & Chinnathambi, S. in *Tau Protein* 21-31 (Springer, 2017).
- 19 Bukar Maina, M., Al-Hilaly, Y. K. & Serpell, L. C. Nuclear tau and its potential role in Alzheimer's disease. *Biomolecules* 6, 9 (2016).
- 20 Sultan, A. *et al.* Nuclear tau, a key player in neuronal DNA protection. *Journal of Biological Chemistry* 286, 4566-4575 (2011).
- 21 Balmik, A. A., Chidambaram, H., Dangji, A., Marelli, U. K. & Chinnathambi, S. HDAC6 ZnF UBP as the modifier of Tau structure and function. *Biochemistry* 59, 4546-4562 (2020).
- 22 Hernández, F. I. & Avila, J. Tauopathies. *Cellular and Molecular Life Sciences* 64, 2219-2233 (2007).
- 23 Avila, J. Tau phosphorylation and aggregation in Alzheimer's disease pathology. *FEBS letters* 580, 2922-2927 (2006).
- 24 Martin, L. *et al.* Tau protein kinases: involvement in Alzheimer's disease. *Ageing research reviews* 12, 289-309 (2013).
- 25 Dias-Santagata, D., Fulga, T. A., Duttaroy, A. & Feany, M. B. Oxidative stress mediates tau-induced neurodegeneration in *Drosophila*. *The Journal of clinical investigation* 117, 236-245 (2007).

- 26 Laurent, C., Buée, L. & Blum, D. Tau and neuroinflammation: What impact for Alzheimer's Disease and Tauopathies? *Biomedical journal* 41, 21-33 (2018).
- 27 Diez, L. & Wegmann, S. Nuclear Transport Deficits in Tau-Related Neurodegenerative Diseases. *Frontiers in Neurology* 11 (2020).
- 28 Bulic, B., Pickhardt, M., Mandelkow, E.-M. & Mandelkow, E. Tau protein and tau aggregation inhibitors. *Neuropharmacology* 59, 276-289 (2010).
- 29 George, R. C., Lew, J. & Graves, D. J. Interaction of cinnamaldehyde and epicatechin with tau: implications of beneficial effects in modulating Alzheimer's disease pathogenesis. *Journal of Alzheimer's Disease* 36, 21-40 (2013).
- 30 Gorantla, N. V., Das, R., Mulani, F. A., Thulasiram, H. V. & Chinnathambi, S. Neem derivatives inhibits tau aggregation. *Journal of Alzheimer's disease reports* 3, 169-178 (2019).
- 31 Gorantla, N. V. *et al.* Basic limonoid modulates chaperone-mediated proteostasis and dissolve Tau fibrils. *Scientific reports* 10, 1-19 (2020).
- 32 Pickhardt, M. *et al.* Anthraquinones inhibit tau aggregation and dissolve Alzheimer's paired helical filaments in vitro and in cells. *Journal of Biological Chemistry* 280, 3628-3635 (2005).
- 33 Sonawane, S. K., Uversky, V. N. & Chinnathambi, S. Baicalein inhibits heparin-induced Tau aggregation by initializing non-toxic Tau oligomer formation. *Cell Communication and Signaling* 19, 1-16 (2021).
- 34 Sonawane, S. K. *et al.* EGCG impedes human Tau aggregation and interacts with Tau. *Scientific reports* 10, 1-17 (2020).
- 35 Gorantla, N. V. *et al.* Molecular cobalt (II) complexes for tau polymerization in Alzheimer's disease. *ACS omega* 4, 16702-16714 (2019).
- 36 Schirmer, R. H., Adler, H., Pickhardt, M. & Mandelkow, E. Lest we forget you—methylene blue.... *Neurobiology of aging* 32, 2325. e2327-2325. e2316 (2011).
- 37 Himmelstein, D. S., Ward, S. M., Lancia, J. K., Patterson, K. R. & Binder, L. I. Tau as a therapeutic target in neurodegenerative disease. *Pharmacology & therapeutics* 136, 8-22 (2012).
- 38 Luksiene, Z. Photodynamic therapy: mechanism of action and ways to improve the efficiency of treatment. *Medicina (Kaunas, Lithuania)* 39, 1137-1150 (2003).
- 39 Castano, A. P., Demidova, T. N. & Hamblin, M. R. Mechanisms in photodynamic therapy: part one—photosensitizers, photochemistry and cellular localization. *Photodiagnosis and photodynamic therapy* 1, 279-293 (2004).
- 40 Daniell, M. & Hill, J. A history of photodynamic therapy. *Australian and New Zealand Journal of Surgery* 61, 340-348 (1991).
- 41 Kessel, D. Photodynamic therapy: a brief history. *Journal of clinical medicine* 8, 1581 (2019).
- 42 Kessel, D. Photodynamic therapy: from the beginning. *Photodiagnosis and Photodynamic Therapy* 1, 3-7 (2004).
- 43 Moan, J. & Peng, Q. An outline of the hundred-year history of PDT. *Anticancer research* 23, 3591-3600 (2003).
- 44 Pushpan, S. *et al.* Porphyrins in photodynamic therapy—a search for ideal photosensitizers. *Current Medicinal Chemistry-Anti-Cancer Agents* 2, 187-207 (2002).
- 45 O'Connor, A. E., Gallagher, W. M. & Byrne, A. T. Porphyrin and nonporphyrin photosensitizers in oncology: preclinical and clinical advances in photodynamic therapy. *Photochemistry and photobiology* 85, 1053-1074 (2009).
- 46 Ormond, A. B. & Freeman, H. S. Dye sensitizers for photodynamic therapy. *Materials* 6, 817-840 (2013).
- 47 Senge, M. O. & Brandt, J. C. Temoporfin (Foscan®), 5, 10, 15, 20-tetra (m-hydroxyphenyl) chlorin—a second-generation photosensitizer. *Photochemistry and photobiology* 87, 1240-1296 (2011).
- 48 D'Alessandro, S. & Priefer, R. Non-porphyrin dyes used as photosensitizers in photodynamic therapy. *Journal of Drug Delivery Science and Technology*, 101979 (2020).

- 49 Ghnenis, A. B., Czaikowski, R. E., Zhang, Z. J. & Bushman, J. S. Toluidine blue staining of resin-embedded sections for evaluation of peripheral nerve morphology. *Journal of visualized experiments: JoVE* (2018).
- 50 Sharma, M. *et al.* Toluidine blue-mediated photodynamic effects on staphylococcal biofilms. *Antimicrobial agents and chemotherapy* 52, 299-305 (2008).
- 51 Wiench, R., Skaba, D., Matys, J. & Grzech-Leśniak, K. Efficacy of Toluidine Blue—Mediated Antimicrobial Photodynamic Therapy on *Candida* spp. A Systematic Review. *Antibiotics* 10, 349 (2021).
- 52 da Fonseca, A. d. S., Mencialha, A. L. & de Paoli, F. Antimicrobial photodynamic therapy against *Acinetobacter baumannii*. *Photodiagnosis and Photodynamic Therapy* 35, 102430 (2021).
- 53 Li, C. *et al.* Self-assembled rose bengal-exopolysaccharide nanoparticles for improved photodynamic inactivation of bacteria by enhancing singlet oxygen generation directly in the solution. *ACS applied materials & interfaces* 10, 16715-16722 (2018).
- 54 Wang, B. *et al.* Rose-bengal-conjugated gold nanorods for in vivo photodynamic and photothermal oral cancer therapies. *Biomaterials* 35, 1954-1966 (2014).
- 55 Durkee, H. *et al.* Rose bengal photodynamic antimicrobial therapy to inhibit *Pseudomonas aeruginosa* keratitis isolates. *Lasers in medical science* 35, 861-866 (2020).
- 56 Gravier, J. *et al.* Improvement of meta-tetra (hydroxyphenyl) chlorin-like photosensitizer selectivity with folate-based targeted delivery. Synthesis and in vivo delivery studies. *Journal of medicinal chemistry* 51, 3867-3877 (2008).
- 57 Triesscheijn, M. *et al.* The pharmacokinetic behavior of the photosensitizer meso-tetra-hydroxyphenyl-chlorin in mice and men. *Cancer chemotherapy and pharmacology* 60, 113-122 (2007).
- 58 Xiao, Q. *et al.* Discovery and development of natural products and their derivatives as photosensitizers for photodynamic therapy. *Current medicinal chemistry* 25, 839-860 (2018).
- 59 Wong, N. C., Scherz, A., Coleman, J. A. & Murray, K. S. in *Interventional Urology* 249-255 (Springer, 2021).
- 60 Bharathiraja, S. *et al.* Chlorin e6 conjugated silica nanoparticles for targeted and effective photodynamic therapy. *Photodiagnosis and photodynamic therapy* 19, 212-220 (2017).
- 61 Kim, J.-Y., Choi, W. I., Kim, M. & Tae, G. Tumor-targeting nanogel that can function independently for both photodynamic and photothermal therapy and its synergy from the procedure of PDT followed by PTT. *Journal of Controlled Release* 171, 113-121 (2013).
- 62 Guo, D. *et al.* Platinum (IV) complex-based two-in-one prodrug for a combinatorial chemo-photodynamic therapy. *Biomaterials* 177, 67-77 (2018).
- 63 Sun, J.-H. *et al.* Multifunctional mesoporous silica nanoparticles as efficient transporters of doxorubicin and chlorin e6 for chemo-photodynamic combinatorial cancer therapy. *Journal of biomaterials applications* 32, 1253-1264 (2018).
- 64 Park, K.-s. *et al.* A curcumin-based molecular probe for near-infrared fluorescence imaging of tau fibrils in Alzheimer's disease. *Organic & biomolecular chemistry* 13, 11194-11199 (2015).
- 65 Li, H. *et al.* Functional bioprobe for responsive imaging and inhibition of Amyloid- β oligomer based on curcuminoid scaffold. *Journal of Luminescence*, 118218 (2021).
- 66 Mani, V., Krishnakumar, V. G., Gupta, S., Mori, S. & Gupta, I. Synthesis and characterization of styryl-BODIPY derivatives for monitoring in vitro Tau aggregation. *Sensors and Actuators B: Chemical* 244, 673-683 (2017).
- 67 Yan, J.-w. *et al.* Neutral merocyanine dyes: for in vivo NIR fluorescence imaging of amyloid- β plaques. *Chemical Communications* 53, 9910-9913 (2017).
- 68 Crowe, A. *et al.* Aminothienopyridazines and methylene blue affect Tau fibrillization via cysteine oxidation. *Journal of Biological Chemistry* 288, 11024-11037 (2013).

- 69 Sun, W. *et al.* Attenuation of synaptic toxicity and MARK4/PAR1-mediated Tau phosphorylation by methylene blue for Alzheimer's disease treatment. *Scientific reports* 6, 1-10 (2016).
- 70 Akoury, E. *et al.* Mechanistic basis of phenothiazine-driven inhibition of Tau aggregation. *Angewandte Chemie International Edition* 52, 3511-3515 (2013).
- 71 Soeda, Y. *et al.* Methylene blue inhibits formation of tau fibrils but not of granular tau oligomers: A plausible key to understanding failure of a clinical trial for Alzheimer's disease. *Journal of Alzheimer's Disease* 68, 1677-1686 (2019).
- 72 Hochgräfe, K. *et al.* Preventive methylene blue treatment preserves cognition in mice expressing full-length pro-aggregant human Tau. *Acta neuropathologica communications* 3, 1-22 (2015).
- 73 Necula, M., Chirita, C. N. & Kuret, J. Cyanine dye N744 inhibits tau fibrillization by blocking filament extension: implications for the treatment of tauopathic neurodegenerative diseases. *Biochemistry* 44, 10227-10237 (2005).
- 74 Congdon, E. E. *et al.* Inhibition of tau polymerization with a cyanine dye in two distinct model systems. *Journal of Biological Chemistry* 284, 20830-20839 (2009).
- 75 Wong, H. E. & Kwon, I. Xanthene food dye, as a modulator of Alzheimer's disease amyloid-beta peptide aggregation and the associated impaired neuronal cell function. *PLoS One* 6, e25752 (2011).
- 76 Liu, F., Ma, Z., Sang, J. & Lu, F. Edaravone inhibits the conformational transition of amyloid- β 42: Insights from molecular dynamics simulations. *Journal of Biomolecular Structure and Dynamics* (2019).
- 77 Mishra, S. & Palanivelu, K. The effect of curcumin (turmeric) on Alzheimer's disease: An overview. *Annals of Indian Academy of Neurology* 11, 13 (2008).
- 78 Park, S.-Y. *et al.* Curcumin protected PC12 cells against beta-amyloid-induced toxicity through the inhibition of oxidative damage and tau hyperphosphorylation. *Food and Chemical Toxicology* 46, 2881-2887 (2008).
- 79 Dubey, T. & Chinnathambi, S. Photodynamic sensitizers modulate cytoskeleton structural dynamics in neuronal cells. *Cytoskeleton* (2021).
- 80 Lee, J. S., Lee, B. I. & Park, C. B. Photo-induced inhibition of Alzheimer's β -amyloid aggregation in vitro by rose bengal. *Biomaterials* 38, 43-49 (2015).
- 81 Zhang, J. *et al.* Photodynamic micelles for amyloid β degradation and aggregation inhibition. *Chemical Communications* 52, 12044-12047 (2016).
- 82 Lee, B. I., Suh, Y. S., Chung, Y. J., Yu, K. & Park, C. B. Shedding light on Alzheimer's β -amyloidosis: photosensitized methylene blue inhibits self-assembly of β -amyloid peptides and disintegrates their aggregates. *Scientific reports* 7, 1-10 (2017).
- 83 Dahanukar, S. A. & Thatte, U. M. *Ayurveda revisited*. (Popular Prakashan, 2000).
- 84 Malik, J., Choudhary, S. & Kumar, P. Protective effect of Convolvulus pluricaulis standardized extract and its fractions against 3-nitropropionic acid-induced neurotoxicity in rats. *Pharmaceutical biology* 53, 1448-1457 (2015).
- 85 Verma, S. *et al.* Study of Convolvulus pluricaulis for antioxidant and anticonvulsant activity. *Central Nervous System Agents in Medicinal Chemistry (Formerly Current Medicinal Chemistry-Central Nervous System Agents)* 12, 55-59 (2012).
- 86 Malik, J., Karan, M. & Vasisht, K. Attenuating effect of bioactive coumarins from Convolvulus pluricaulis on scopolamine-induced amnesia in mice. *Natural product research* 30, 578-582 (2016).
- 87 Das, R., Sengupta, T., Roy, S., Chattarji, S. & Ray, J. Convolvulus pluricaulis extract can modulate synaptic plasticity in rat brain hippocampus. *NeuroReport* 31, 597-604 (2020).
- 88 Nile, S. H. *et al.* Chemical composition, cytotoxic and pro-inflammatory enzyme inhibitory properties of Withania somnifera (L.) Dunal root extracts. *South African Journal of Botany* (2021).
- 89 Ahmad, M. *et al.* Neuroprotective effects of Withania somnifera on 6-hydroxydopamine induced Parkinsonism in rats. *Human & experimental toxicology* 24, 137-147 (2005).

- 90 Gohil, K. J., Patel, J. A. & Gajjar, A. K. Pharmacological review on *Centella asiatica*: a potential herbal cure-all. *Indian journal of pharmaceutical sciences* 72, 546 (2010).
- 91 Kumar, A., Dogra, S. & Prakash, A. Neuroprotective effects of *Centella asiatica* against intracerebroventricular colchicine-induced cognitive impairment and oxidative stress. *International Journal of Alzheimer's disease* 2009 (2009).
- 92 Dhanasekaran, M. *et al.* *Centella asiatica* extract selectively decreases amyloid β levels in hippocampus of Alzheimer's disease animal model. *Phytotherapy Research: An International Journal Devoted to Pharmacological and Toxicological Evaluation of Natural Product Derivatives* 23, 14-19 (2009).
- 93 Chen, C.-L., Tsai, W.-H., Chen, C.-J. & Pan, T.-M. *Centella asiatica* extract protects against amyloid β 1–40-induced neurotoxicity in neuronal cells by activating the antioxidative defence system. *Journal of Traditional and Complementary Medicine* 6, 362-369 (2016).
- 94 Kumar, N. & Sakhya, S. K. Ethnopharmacological properties of *Curcuma longa*: a review. *International Journal of Pharmaceutical Sciences and Research* 4, 103 (2013).
- 95 Lestari, M. L. & Indrayanto, G. Curcumin. *Profiles of drug substances, excipients and related methodology* 39, 113-204 (2014).
- 96 Yang, F. *et al.* Curcumin inhibits formation of amyloid β oligomers and fibrils, binds plaques, and reduces amyloid in vivo. *Journal of Biological Chemistry* 280, 5892-5901 (2005).
- 97 Anupama, K. P., Shilpa, O., Antony, A. & Gurushankara, H. P. Jatamansinol from *Nardostachys jatamansi*: a multi-targeted neuroprotective agent for Alzheimer's disease. *Journal of Biomolecular Structure and Dynamics*, 1-21 (2021).
- 98 Khan, M. B. *et al.* Neuroprotective efficacy of *Nardostachys jatamansi* and crocetin in conjunction with selenium in cognitive impairment. *Neurological Sciences* 33, 1011-1020 (2012).
- 99 Ahmad, M. *et al.* Attenuation by *Nardostachys jatamansi* of 6-hydroxydopamine-induced parkinsonism in rats: behavioral, neurochemical, and immunohistochemical studies. *Pharmacology Biochemistry and Behavior* 83, 150-160 (2006).
- 100 Aguiar, S. & Borowski, T. Neuropharmacological review of the nootropic herb *Bacopa monnieri*. *Rejuvenation research* 16, 313-326 (2013).
- 101 Simpson, T., Pase, M. & Stough, C. *Bacopa monnieri* as an antioxidant therapy to reduce oxidative stress in the aging brain. *Evidence-based complementary and alternative medicine* 2015 (2015).
- 102 Saini, N., Singh, D. & Sandhir, R. *Bacopa monnieri* prevents colchicine-induced dementia by anti-inflammatory action. *Metabolic brain disease* 34, 505-518 (2019).
- 103 Bhatia, G., Dhuna, V., Dhuna, K., Kaur, M. & Singh, J. *Bacopa monnieri* extracts prevent hydrogen peroxide-induced oxidative damage in a cellular model of neuroblastoma IMR32 cells. *Chinese journal of natural medicines* 15, 834-846 (2017).
- 104 Pandey, S. P. & Prasad, S. in *Topics in Biomedical Gerontology* 335-355 (Springer, 2017).
- 105 Dwivedi, S. *et al.* Standardized extract of *Bacopa monnieri* attenuates okadaic acid induced memory dysfunction in rats: effect on Nrf2 pathway. *Evidence-based complementary and alternative medicine* 2013 (2013).
- 106 Siddique, Y. H., Mujtaba, S. F., Faisal, M., Jyoti, S. & Naz, F. The effect of *Bacopa monnieri* leaf extract on dietary supplementation in transgenic *Drosophila* model of Parkinson's disease. *European Journal of Integrative Medicine* 6, 571-580 (2014).
- 107 Singh, B., Pandey, S., Verma, R., Ansari, J. A. & Mahdi, A. A. Comparative evaluation of extract of *Bacopa monnieri* and *Mucuna pruriens* as neuroprotectant in MPTP model of Parkinson's disease. (2016).
- 108 Anjaneyulu, J., Vidyashankar, R. & Godbole, A. Differential effect of Ayurvedic nootropics on *C. elegans* models of Parkinson's disease. *Journal of Ayurveda and Integrative Medicine* 11, 440-447 (2020).

- 109 Uabundit, N., Wattanathorn, J., Mucimapura, S. & Ingkaninan, K. Cognitive enhancement and neuroprotective effects of *Bacopa monnieri* in Alzheimer's disease model. *Journal of ethnopharmacology* 127, 26-31 (2010).
- 110 Malishev, R. *et al.* Bacoside-A, an Indian traditional-medicine substance, inhibits β -amyloid cytotoxicity, fibrillation, and membrane interactions. *ACS chemical neuroscience* 8, 884-891 (2017).
- 111 Sonawane, S. K., Balmik, A. A., Boral, D., Ramasamy, S. & Chinnathambi, S. Baicalein suppresses Repeat Tau fibrillization by sequestering oligomers. *Archives of biochemistry and biophysics* 675, 108119 (2019).
- 112 Balmik, A. A. *et al.* Melatonin interacts with repeat domain of Tau to mediate disaggregation of paired helical filaments. *Biochimica et Biophysica Acta (BBA)-General Subjects* 1864, 129467 (2020).
- 113 Desale, S. E. & Chinnathambi, S. α -Linolenic acid induces clearance of Tau seeds via Actin-remodeling in Microglia. *Molecular Biomedicine* 2, 1-14 (2021).
- 114 Dubey, T., Gorantla, N. V., Chandrashekhara, K. T. & Chinnathambi, S. Photoexcited Toluidine Blue Inhibits Tau Aggregation in Alzheimer's Disease. *ACS Omega* 4, 18793-18802, doi:10.1021/acsomega.9b02792 (2019).
- 115 Das, R. & Chinnathambi, S. Microglial priming of antigen presentation and adaptive stimulation in Alzheimer's disease. *Cellular and Molecular Life Sciences* 76, 3681-3694 (2019).
- 116 Marcus, S. L. in *Photodynamic therapy* 219-268 (CRC Press, 2020).
- 117 Baron, E. D. & Suggs, A. K. Introduction to photobiology. *Dermatologic clinics* 32, 255-266 (2014).
- 118 Allison, R. R. *et al.* Photosensitizers in clinical PDT. *Photodiagnosis and photodynamic therapy* 1, 27-42 (2004).
- 119 Atamna, H. & Kumar, R. Protective role of methylene blue in Alzheimer's disease via mitochondria and cytochrome c oxidase. *Journal of Alzheimer's Disease* 20, S439-S452 (2010).
- 120 Lo Cascio, F. & Kaye, R. Azure C targets and modulates toxic tau oligomers. *ACS chemical neuroscience* 9, 1317-1326 (2018).
- 121 Lee, B. I., Chung, Y. J. & Park, C. B. Photosensitizing materials and platforms for light-triggered modulation of Alzheimer's β -amyloid self-assembly. *Biomaterials* 190, 121-132 (2019).
- 122 Sridharan, G. & Shankar, A. A. Toluidine blue: A review of its chemistry and clinical utility. *Journal of oral and maxillofacial pathology: JOMFP* 16, 251 (2012).
- 123 Nuernberg, M. A. A. *et al.* Effects of butyl toluidine blue photosensitizer on antimicrobial photodynamic therapy for experimental periodontitis treatment in rats. *Photodiagnosis and Photodynamic Therapy* 31, 101868 (2020).
- 124 Parasuraman, P. *et al.* Antimicrobial photodynamic activity of toluidine blue encapsulated in mesoporous silica nanoparticles against *Pseudomonas aeruginosa* and *Staphylococcus aureus*. *Biofouling* 35, 89-103 (2019).
- 125 Bulic, B. *et al.* Rhodanine-based tau aggregation inhibitors in cell models of tauopathy. *Angewandte Chemie International Edition* 46, 9215-9219 (2007).
- 126 Bulic, B., Pickhardt, M. & Mandelkow, E. Progress and developments in tau aggregation inhibitors for Alzheimer disease. *Journal of medicinal chemistry* 56, 4135-4155 (2013).
- 127 Gordon-Weeks, P. R. & Fournier, A. E. Neuronal cytoskeleton in synaptic plasticity and regeneration. *Journal of neurochemistry* 129, 206-212 (2014).
- 128 Qin, Y. *et al.* Comparison of toluidine blue-mediated photodynamic therapy and conventional scaling treatment for periodontitis in rats. *Journal of periodontal research* 43, 162-167 (2008).
- 129 Williams, D. Revisiting the definition of biocompatibility. *Medical device technology* 14, 10-13 (2003).
- 130 McMurray, C. Neurodegeneration: diseases of the cytoskeleton? *Cell Death & Differentiation* 7, 861-865 (2000).

- 131 Janke, C. & Kneussel, M. Tubulin post-translational modifications: encoding functions on the neuronal microtubule cytoskeleton. *Trends in neurosciences* 33, 362-372 (2010).
- 132 Wright, K. E., MacRobert, A. J. & Phillips, J. B. Inhibition of Specific Cellular Antioxidant Pathways Increases the Sensitivity of Neurons to Meta-tetrahydroxyphenyl Chlorin-Mediated Photodynamic Therapy in a 3D Co-culture Model. *Photochemistry and photobiology* 88, 1539-1545 (2012).
- 133 Stricker, J., Falzone, T. & Gardel, M. L. Mechanics of the F-actin cytoskeleton. *Journal of biomechanics* 43, 9-14 (2010).
- 134 Nemethova, M., Auinger, S. & Small, J. V. Building the actin cytoskeleton: filopodia contribute to the construction of contractile bundles in the lamella. *The Journal of cell biology* 180, 1233-1244 (2008).
- 135 Wang, X. *et al.* Analysis of the in vivo and in vitro effects of photodynamic therapy on breast cancer by using a sensitizer, sinoporphyrin sodium. *Theranostics* 5, 772 (2015).
- 136 Nehlig, A., Molina, A., Rodrigues-Ferreira, S., Honoré, S. & Nahmias, C. Regulation of end-binding protein EB1 in the control of microtubule dynamics. *Cellular and Molecular Life Sciences* 74, 2381-2393 (2017).
- 137 Sang, T.-K. & Jackson, G. R. Drosophila models of neurodegenerative disease. *NeuroRx* 2, 438-446 (2005).
- 138 Gorantla, N. V., Das, R., Balaraman, E. & Chinnathambi, S. Transition metal nickel prevents Tau aggregation in Alzheimer's disease. *International journal of biological macromolecules* 156, 1359-1365 (2020).
- 139 Wischik, C. M. *et al.* Tau aggregation inhibitor therapy: an exploratory phase 2 study in mild or moderate Alzheimer's disease. *Journal of Alzheimer's Disease* 44, 705-720 (2015).
- 140 Pham, T. C., Nguyen, V.-N., Choi, Y., Lee, S. & Yoon, J. Recent strategies to develop innovative photosensitizers for enhanced photodynamic therapy. *Chemical Reviews* 121, 13454-13619 (2021).
- 141 Hirose, M., Yoshida, Y., Horii, K., Hasegawa, Y. & Shibuya, Y. Efficacy of antimicrobial photodynamic therapy with Rose Bengal and blue light against cariogenic bacteria. *Archives of Oral Biology* 122, 105024 (2021).
- 142 Dabrzalska, M. *et al.* Cationic phosphorus dendrimer enhances photodynamic activity of rose bengal against basal cell carcinoma cell lines. *Molecular pharmaceuticals* 14, 1821-1830 (2017).
- 143 Ma, H. *et al.* Photodynamic effect of chlorin e6 on cytoskeleton protein of human colon cancer SW480 cells. *Photodiagnosis and Photodynamic Therapy* 33, 102201 (2021).
- 144 Cogno, I. S. *et al.* Natural photosensitizers in photodynamic therapy: In vitro activity against monolayers and spheroids of human colorectal adenocarcinoma SW480 cells. *Photodiagnosis and Photodynamic Therapy* 31, 101852 (2020).
- 145 Senthilkumar, S. *et al.* Developmental and behavioural toxicity induced by acrylamide exposure and amelioration using phytochemicals in Drosophila melanogaster. *Journal of hazardous materials* 394, 122533 (2020).
- 146 Dubey, T. & Chinnathambi, S. Brahmi (Bacopa monnieri): An ayurvedic herb against the Alzheimer's disease. *Archives of biochemistry and biophysics* 676, 108153 (2019).
- 147 Guo, T. *et al.* Molecular and cellular mechanisms underlying the pathogenesis of Alzheimer's disease. *Molecular neurodegeneration* 15, 1-37 (2020).
- 148 Hu, S. *et al.* Phosphorylation of tau and α -synuclein induced neurodegeneration in MPTP mouse model of Parkinson's disease. *Neuropsychiatric disease and treatment* 16, 651 (2020).
- 149 Xiao, S. *et al.* Inhibitory Effects of Isobavachalcone on Tau Protein Aggregation, Tau Phosphorylation, and Oligomeric Tau-Induced Apoptosis. *ACS Chemical Neuroscience* 12, 123-132 (2020).
- 150 Avila, J. *et al.* Tau phosphorylation by GSK3 in different conditions. *International Journal of Alzheimer's Disease* 2012 (2012).

- 151 Avila, J. & Hernández, F. GSK-3 inhibitors for Alzheimer's disease. *Expert review of neurotherapeutics* 7, 1527-1533 (2007).
- 152 Ezekiel, I. *et al.* Comparative Effects of Taurine and Vitamin E in Acetaminophen-Induced Oxidative Stress on Learning and Memory in Male Wistar Rats. (2018).
- 153 Devendra, P. *et al.* Brahmi (*Bacopa monnieri*) as functional food ingredient in food processing industry. *Journal of Pharmacognosy and Phytochemistry* 7, 189-194 (2018).
- 154 Chowdhuri, D. K. *et al.* Antistress effects of bacosides of *Bacopa monnieri*: modulation of Hsp70 expression, superoxide dismutase and cytochrome P450 activity in rat brain. *Phytotherapy Research: An International Journal Devoted to Pharmacological and Toxicological Evaluation of Natural Product Derivatives* 16, 639-645 (2002).
- 155 Limpeanchob, N., Jaipan, S., Rattanakaruna, S., Phrompittayarat, W. & Ingkaninan, K. Neuroprotective effect of *Bacopa monnieri* on beta-amyloid-induced cell death in primary cortical culture. *Journal of Ethnopharmacology* 120, 112-117 (2008).
- 156 Brentnall, M., Rodriguez-Menocal, L., De Guevara, R. L., Cepero, E. & Boise, L. H. Caspase-9, caspase-3 and caspase-7 have distinct roles during intrinsic apoptosis. *BMC cell biology* 14, 1-9 (2013).
- 157 Alber, F. *et al.* The molecular architecture of the nuclear pore complex. *Nature* 450, 695-701 (2007).
- 158 Sheffield, L. G., Miskiewicz, H. B., Tannenbaum, L. B. & Mirra, S. S. Nuclear pore complex proteins in Alzheimer disease. *Journal of Neuropathology & Experimental Neurology* 65, 45-54 (2006).
- 159 Tripathi, T., Prakash, J. & Shav-Tal, Y. Phospho-tau impairs nuclear-cytoplasmic transport. *ACS chemical neuroscience* 10, 36-38 (2018).
- 160 Chidambaram, H., Das, R. & Chinnathambi, S. Interaction of Tau with the chemokine receptor, CX3CR1 and its effect on microglial activation, migration and proliferation. *Cell & bioscience* 10, 1-9 (2020).
- 161 Das, R., Balmik, A. A. & Chinnathambi, S. Phagocytosis of full-length Tau oligomers by Actin-remodeling of activated microglia. *Journal of neuroinflammation* 17, 1-15 (2020).
- 162 Gorantla, N. V. & Chinnathambi, S. Autophagic pathways to clear the tau aggregates in Alzheimer's disease. *Cellular and Molecular Neurobiology* 41, 1175-1181 (2021).
- 163 Cheng, Y. & Bai, F. The association of tau with mitochondrial dysfunction in Alzheimer's disease. *Frontiers in neuroscience* 12, 163 (2018).
- 164 Lester, E. & Parker, R. The tau of nuclear-cytoplasmic transport. *Neuron* 99, 869-871 (2018).
- 165 He, Z. *et al.* Amyloid- β plaques enhance Alzheimer's brain tau-seeded pathologies by facilitating neuritic plaque tau aggregation. *Nature medicine* 24, 29-38 (2018).
- 166 Steinhilb, M. L. *et al.* S/P and T/P phosphorylation is critical for tau neurotoxicity in *Drosophila*. *Journal of neuroscience research* 85, 1271-1278 (2007).
- 167 Hanger, D. P., Anderton, B. H. & Noble, W. Tau phosphorylation: the therapeutic challenge for neurodegenerative disease. *Trends in molecular medicine* 15, 112-119 (2009).
- 168 Hanger, D. P. *et al.* Novel phosphorylation sites in tau from Alzheimer brain support a role for casein kinase 1 in disease pathogenesis. *Journal of Biological Chemistry* 282, 23645-23654 (2007).
- 169 Thakur, M., Virk, R., Sangha, P. S. & Saxena, V. The Effects of turmeric on Alzheimer's patients. *Journal of Food Science and Nutrition Research* 2, 347-353 (2019).
- 170 Saito, T. *et al.* Cdk5 increases MARK4 activity and augments pathological tau accumulation and toxicity through tau phosphorylation at Ser262. *Human molecular genetics* 28, 3062-3071 (2019).
- 171 Hernández, F., García-García, E. & Avila, J. Microtubule depolymerization and tau phosphorylation. *Journal of Alzheimer's Disease* 37, 507-513 (2013).

- 172 Ali, T., Yoon, G. H., Shah, S. A., Lee, H. Y. & Kim, M. O. Osmotin attenuates amyloid beta-induced memory impairment, tau phosphorylation and neurodegeneration in the mouse hippocampus. *Scientific reports* 5, 1-17 (2015).
- 173 Su, B. *et al.* Chronic oxidative stress causes increased tau phosphorylation in M17 neuroblastoma cells. *Neuroscience letters* 468, 267-271 (2010).
- 174 Eftekharzadeh, B. *et al.* Tau protein disrupts nucleocytoplasmic transport in Alzheimer's disease. *Neuron* 99, 925-940. e927 (2018).
- 175 Rafiee, S., Asadollahi, K., Riazi, G., Ahmadian, S. & Saboury, A. A. Vitamin B12 inhibits tau fibrillization via binding to cysteine residues of tau. *ACS chemical neuroscience* 8, 2676-2682 (2017).
- 176 Frost, D. *et al.* β -carboline compounds, including harmine, inhibit DYRK1A and tau phosphorylation at multiple Alzheimer's disease-related sites. *Plos one* 6, e19264 (2011).
- 177 Caccamo, A., Oddo, S., Tran, L. X. & LaFerla, F. M. Lithium reduces tau phosphorylation but not A β or working memory deficits in a transgenic model with both plaques and tangles. *The American journal of pathology* 170, 1669-1675 (2007).
- 178 Sul, D. *et al.* Protective effect of caffeic acid against beta-amyloid-induced neurotoxicity by the inhibition of calcium influx and tau phosphorylation. *Life sciences* 84, 257-262 (2009).
- 179 Guo, C. *et al.* Deferoxamine inhibits iron induced hippocampal tau phosphorylation in the Alzheimer transgenic mouse brain. *Neurochemistry international* 62, 165-172 (2013).
- 180 Li, L. *et al.* Ginsenoside Rd attenuates beta-amyloid-induced tau phosphorylation by altering the functional balance of glycogen synthase kinase 3beta and protein phosphatase 2A. *Neurobiology of disease* 54, 320-328 (2013).
- 181 Das, V. & Miller, J. H. Microtubule stabilization by peloruside A and paclitaxel rescues degenerating neurons from okadaic acid-induced tau phosphorylation. *European Journal of Neuroscience* 35, 1705-1717 (2012).
- 182 Lu, J., Miao, J., Su, T., Liu, Y. & He, R. Formaldehyde induces hyperphosphorylation and polymerization of Tau protein both in vitro and in vivo. *Biochimica et Biophysica Acta (BBA)-General Subjects* 1830, 4102-4116 (2013).
- 183 He, X. *et al.* Resveratrol attenuates formaldehyde induced hyperphosphorylation of tau protein and cytotoxicity in N2a cells. *Frontiers in neuroscience* 10, 598 (2017).
- 184 Fisher, C. J. *et al.* ALA-PpIX mediated photodynamic therapy of malignant gliomas augmented by hypothermia. *PLoS One* 12, e0181654 (2017).
- 185 Du, E. *et al.* Taurine-modified Ru (II)-complex targets cancerous brain cells for photodynamic therapy. *Chemical Communications* 53, 6033-6036 (2017).
- 186 Mahmoudi, K. *et al.* 5-aminolevulinic acid photodynamic therapy for the treatment of high-grade gliomas. *Journal of neuro-oncology* 141, 595-607 (2019).
- 187 Du, Z., Li, M., Ren, J. & Qu, X. Current Strategies for Modulating A β Aggregation with Multifunctional Agents. *Accounts of Chemical Research* 54, 2172-2184 (2021).
- 188 Kim, K., Lee, S. H., Choi, D. S. & Park, C. B. Photoactive Bismuth Vanadate Structure for Light-Triggered Dissociation of Alzheimer's β -Amyloid Aggregates. *Advanced Functional Materials* 28, 1802813 (2018).
- 189 Hirabayashi, A., Shindo, Y., Oka, K., Takahashi, D. & Toshima, K. Photodegradation of amyloid β and reduction of its cytotoxicity to PC12 cells using porphyrin derivatives. *Chemical Communications* 50, 9543-9546 (2014).
- 190 Ni, J. *et al.* Near-infrared photoactivatable oxygenation catalysts of amyloid peptide. *Chem* 4, 807-820 (2018).
- 191 Cook, N. P., Torres, V., Jain, D. & Martí, A. A. Sensing amyloid- β aggregation using luminescent dipyrrophenazine ruthenium (II) complexes. *Journal of the American Chemical Society* 133, 11121-11123 (2011).
- 192 Fan, Q. W. *et al.* Cholesterol-dependent modulation of dendrite outgrowth and microtubule stability in cultured neurons. *Journal of neurochemistry* 80, 178-190 (2002).

- 193 Morii, H., Shiraishi-Yamaguchi, Y. & Mori, N. SCG10, a microtubule destabilizing factor, stimulates the neurite outgrowth by modulating microtubule dynamics in rat hippocampal primary cultured neurons. *Journal of neurobiology* 66, 1101-1114 (2006).
- 194 TC, E. S., Dezone, R. S., Rehen, S. K. & Gomes, F. Astrocytes treated by lysophosphatidic acid induce axonal outgrowth of cortical progenitors through extracellular matrix protein and epidermal growth factor signaling pathway. *Journal of neurochemistry* 119, 113-123 (2011).
- 195 Akude, E., Zherebitskaya, E., Chowdhury, S. K. R., Girling, K. & Fernyhough, P. 4-Hydroxy-2-nonenal induces mitochondrial dysfunction and aberrant axonal outgrowth in adult sensory neurons that mimics features of diabetic neuropathy. *Neurotoxicity research* 17, 28-38 (2010).
- 196 Fulga, T. A. *et al.* Abnormal bundling and accumulation of F-actin mediates tau-induced neuronal degeneration in vivo. *Nature cell biology* 9, 139-148 (2007).
- 197 Tousley, A. *et al.* Rac1 activity is modulated by Huntingtin and dysregulated in models of Huntington's disease. *Journal of Huntington's disease* 8, 53-69 (2019).
- 198 Bamburg, J. *et al.* ADF/Cofilin-actin rods in neurodegenerative diseases. *Current Alzheimer Research* 7, 241-250 (2010).
- 199 Kommaddi, R. P. *et al.* Glutaredoxin1 diminishes amyloid beta-mediated oxidation of F-actin and reverses cognitive deficits in an Alzheimer's disease mouse model. *Antioxidants & redox signaling* 31, 1321-1338 (2019).
- 200 Etminan, N. *et al.* Modulation of migratory activity and invasiveness of human glioma spheroids following 5-aminolevulinic acid-based photodynamic treatment. *Journal of neurosurgery* 115, 281-288 (2011).
- 201 Di Venosa, G., Perotti, C., Batlle, A. & Casas, A. The role of cytoskeleton and adhesion proteins in the resistance to photodynamic therapy. Possible therapeutic interventions. *Photochemical & Photobiological Sciences* 14, 1451-1464 (2015).
- 202 Lee, C., Wu, S. S. & Chen, L. B. Photosensitization by 3, 3'-dihexyloxycarbocyanine iodide: specific disruption of microtubules and inactivation of organelle motility. *Cancer research* 55, 2063-2069 (1995).
- 203 Jain, R., Kosta, S. & Tiwari, A. Ayurveda and cancer. *Pharmacognosy research* 2 (2010).
- 204 Sharma, R., Kabra, A., Rao, M. & Prajapati, P. Herbal and Holistic solutions for Neurodegenerative and Depressive disorders: Leads from Ayurveda. *Current pharmaceutical design* 24, 2597-2608 (2018).
- 205 Rao, R. V. Ayurveda and the science of aging. *Journal of Ayurveda and integrative medicine* 9, 225-232 (2018).
- 206 Zhao, L. *et al.* Neuroprotective, anti-amyloidogenic and neurotrophic effects of apigenin in an Alzheimer's disease mouse model. *Molecules* 18, 9949-9965 (2013).
- 207 Zhao, L., Wang, J.-l., Wang, Y.-r. & Fa, X.-z. Apigenin attenuates copper-mediated β -amyloid neurotoxicity through antioxidation, mitochondrion protection and MAPK signal inactivation in an AD cell model. *Brain research* 1492, 33-45 (2013).
- 208 Zhang, S. Q. *et al.* Baicalein reduces β -amyloid and promotes nonamyloidogenic amyloid precursor protein processing in an Alzheimer's disease transgenic mouse model. *Journal of neuroscience research* 91, 1239-1246 (2013).
- 209 Gao, L. *et al.* Baicalein protects PC12 cells from A β 25–35-induced cytotoxicity via inhibition of apoptosis and metabolic disorders. *Life sciences* 248, 117471 (2020).
- 210 Caesar, I., Jonson, M., Nilsson, K. P. R., Thor, S. & Hammarström, P. Curcumin promotes A-beta fibrillation and reduces neurotoxicity in transgenic Drosophila. *PLoS one* 7, e31424 (2012).
- 211 Rane, J. S., Bhaumik, P. & Panda, D. Curcumin inhibits tau aggregation and disintegrates preformed tau filaments in vitro. *Journal of Alzheimer's Disease* 60, 999-1014 (2017).
- 212 Liu, W. *et al.* Orientation-inspired perspective on molecular inhibitor of tau aggregation by curcumin conjugated with ruthenium (II) complex scaffold. *The Journal of Physical Chemistry B* 124, 2343-2353 (2020).

- 213 Okuda, M. *et al.* PE859, a novel curcumin derivative, inhibits amyloid- β and tau aggregation, and ameliorates cognitive dysfunction in senescence-accelerated mouse prone 8. *Journal of Alzheimer's Disease* 59, 313-328 (2017).
- 214 Jayaprakasam, B., Padmanabhan, K. & Nair, M. G. Withanamides in *Withania somnifera* fruit protect PC-12 cells from β -amyloid responsible for Alzheimer's disease. *Phytotherapy Research* 24, 859-863 (2010).
- 215 Kumar, S., Seal, C. J., Howes, M., Kite, G. C. & Okello, E. J. In vitro protective effects of *Withania somnifera* (L.) dunal root extract against hydrogen peroxide and β -amyloid (1–42)-induced cytotoxicity in differentiated PC12 cells. *Phytotherapy Research* 24, 1567-1574 (2010).
- 216 Bhargava, V. Medicinal uses and pharmacological properties of *Crocus sativus* Linn (Saffron). *Int. J. Pharm. Pharm. Sci* 3 (2011).
- 217 Papandreou, M. A. *et al.* Inhibitory activity on amyloid- β aggregation and antioxidant properties of *Crocus sativus* stigmas extract and its crocin constituents. *Journal of agricultural and food chemistry* 54, 8762-8768 (2006).
- 218 Ghahghaei, A., Bathaie, S. Z., Kheirkhah, H. & Bahraminejad, E. The protective effect of crocin on the amyloid fibril formation of A β 42 peptide in vitro. *Cellular & molecular biology letters* 18, 328-339 (2013).
- 219 Hadipour, M. *et al.* Crocin improved amyloid beta induced long-term potentiation and memory deficits in the hippocampal CA1 neurons in freely moving rats. *Synapse* 72, e22026 (2018).
- 220 Inoue, E. *et al.* Effects of saffron and its constituents, crocin-1, crocin-2, and crocetin on α -synuclein fibrils. *Journal of natural medicines* 72, 274-279 (2018).
- 221 Ngo, S. T., Truong, D. T., Tam, N. M. & Nguyen, M. T. EGCG inhibits the oligomerization of amyloid beta (16-22) hexamer: Theoretical studies. *Journal of Molecular Graphics and Modelling* 76, 1-10 (2017).
- 222 Oshima, E. *et al.* Accelerated tau aggregation, apoptosis and neurological dysfunction caused by chronic oral administration of aluminum in a mouse model of tauopathies. *Brain Pathology* 23, 633-644 (2013).
- 223 Zhang, L., Wang, Z., Yuan, X., Sui, R. & Falahati, M. Evaluation of heptelidic acid as a potential inhibitor for tau aggregation-induced Alzheimer's disease and associated neurotoxicity. *International Journal of Biological Macromolecules* 183, 1155-1161 (2021).
- 224 Birla, H. *et al.* Neuroprotective effects of *Withania somnifera* in BPA induced-cognitive dysfunction and oxidative stress in mice. *Behavioral and Brain Functions* 15, 9 (2019).
- 225 Prakash, J., Yadav, S. K., Chouhan, S. & Singh, S. P. Neuroprotective role of *Withania somnifera* root extract in Maneb–Paraquat induced mouse model of parkinsonism. *Neurochemical research* 38, 972-980 (2013).
- 226 Bournival, J., Quessy, P. & Martinoli, M.-G. Protective effects of resveratrol and quercetin against MPP $^{+}$ -induced oxidative stress act by modulating markers of apoptotic death in dopaminergic neurons. *Cellular and molecular neurobiology* 29, 1169-1180 (2009).
- 227 Saini, N., Singh, D. & Sandhir, R. Neuroprotective effects of *Bacopa monnieri* in experimental model of dementia. *Neurochemical research* 37, 1928-1937 (2012).
- 228 Stoothoff, W. H. & Johnson, G. V. Tau phosphorylation: physiological and pathological consequences. *Biochimica et Biophysica Acta (BBA)-Molecular Basis of Disease* 1739, 280-297 (2005).
- 229 Yu, Y. *et al.* Developmental regulation of tau phosphorylation, tau kinases, and tau phosphatases. *Journal of neurochemistry* 108, 1480-1494 (2009).
- 230 De Felice, F. G. *et al.* Alzheimer's disease-type neuronal tau hyperphosphorylation induced by A β oligomers. *Neurobiology of aging* 29, 1334-1347 (2008).
- 231 Rankin, C. A., Sun, Q. & Gamblin, T. C. Tau phosphorylation by GSK-3 β promotes tangle-like filament morphology. *Molecular neurodegeneration* 2, 1-14 (2007).

- 232 Zhu, Y. & Wang, J. Wogonin increases β -amyloid clearance and inhibits tau phosphorylation via inhibition of mammalian target of rapamycin: potential drug to treat Alzheimer's disease. *Neurological Sciences* 36, 1181-1188 (2015).
- 233 Huang, H.-C., Tang, D., Xu, K. & Jiang, Z.-F. Curcumin attenuates amyloid- β -induced tau hyperphosphorylation in human neuroblastoma SH-SY5Y cells involving PTEN/Akt/GSK-3 β signaling pathway. *Journal of Receptors and Signal Transduction* 34, 26-37 (2014).
- 234 Chalatsa, I. *et al.* The Crocus sativus compounds trans-crocin 4 and trans-crocetin modulate the amyloidogenic pathway and tau misprocessing in Alzheimer disease neuronal cell culture models. *Frontiers in neuroscience* 13, 249 (2019).

Abstract

Name of the Student: Tushar Dubey	Registration No. : 10BB15A26043
Faculty of Study: Biological Sciences	Year of Submission : 2022
CSIR Lab: CSIR-National Chemical laboratory	Name of the Supervisor: Dr. Subashchandrabose Chinnathambi

Title of the thesis: Photosensitizers and natural compounds attenuate the Tau aggregation and restore the signalling cascades of Tau

Abstract

The intracellular Tau aggregates are known to be associated with Alzheimer's disease. The inhibition of Tau aggregation is an important strategy for screening of therapeutic molecules in Alzheimer's disease. Various compounds of natural and synthetic origins have been screened for the potency against Tau aggregation. The photo-excited dyes showed inhibitory effect on amyloid protein aggregation and toxicity. In the present work, we studied the effect of two acknowledged photosensitizers Toluidine Blue (TB) and Rose Bengal (RB) against Tau aggregation. The aim of this work was to study the protective role of these dyes against Tau aggregation and cytoskeleton modulations. The studies carried out with help of ThS fluorescence, circular dichroism, and electron microscopy suggested that TB and RB attenuated the *in vitro* Tau aggregation. Whereas, the PE-TB and PE-RB disaggregated the mature Tau fibrils. In our studies, we observed that PE-RB and PE-TB Bengal modulated the cytoskeleton network. The Neuro2a cells exposed to PE-RB and PE-TB were having extended neurite, which indicated the modulation of tubulin network. Similarly, the treatment of photo-excited dyes modulated actin structures in cells. Neuro2a cells exposed to PE-RB and PE-TB had increased actin-rich filopodia and lamellipodia. The behavioural studies on *Drosophila* transgenic models suggested that exposure to these dyes improved the longevity and egg laying capacity of flies. Similarly the negative geotaxis assay suggested that flies exposed to PE-RB and PE-TB were having improved locomotor function. The treatment of PE-RB and PE-TB improved memory and learning of UAS E-14 Tau mutant of *Drosophila*.

Bacopa monnieri is a nootropic herb described in Ayurveda. In our work the ethanolic extract of *Bacopa monnieri* was studied for its potency to inhibit Tau aggregation and rescue of viability of Tau stressed cells. *Bacopa monnieri* was observed to inhibit the Tau aggregation *in vitro*. The cells exposed to *Bacopa monnieri* were also observed to have low level of ROS and caspase-3 activity. The western blot and immunofluorescence analysis showed that the *Bacopa monnieri* elevated the Nrf2 levels and downregulated phospho-Tau level in cells. NUP358 are the key proteins involved in nuclear transport. It was observed that *Bacopa monnieri* treatment restored NUP358 arrangement in formaldehyde stressed cells.

The overall results of our studies suggested that PE-TB and PE-RB have potency against Tau aggregation and Tau-mediated toxicity. Whereas, *Bacopa monnieri* showed potency against Tau phosphorylation and Tau aggregation. Hence these compounds could be considered for further studies in treatment of Alzheimer's disease.

List of publications in SCI Journals

1. **Dubey, T.**, Gorantla, N. V., Chandrashekara, K. T. & **Chinnathambi, S***. Photoexcited toluidine blue inhibits Tau aggregation in Alzheimer's disease. ACS omega 4, 18793-18802 (2019). (Cover page).
2. **Dubey, T.**, Gorantla, N. V., Chandrashekara, K. T. & **Chinnathambi, S***. Photodynamic exposure of Rose-Bengal inhibits Tau aggregation and modulates cytoskeletal network in neuronal cells. Scientific Reports 10, 1-16 (2020).
3. **Dubey, T.** & **Chinnathambi, S***. Photodynamic sensitizers modulate cytoskeleton structural dynamics in neuronal cells. Cytoskeleton (2021). (Review article)
4. **Dubey, T.** & **Chinnathambi, S***. Photodynamic treatment modulates various GTPase and cellular signalling pathways in Tauopathy. Small GTPases, 1-13 (2021). (Review article)
5. **Dubey, T.** & **Chinnathambi, S.** Brahmi (*Bacopa monnieri*)*: An ayurvedic herb against the Alzheimer's disease. Archives of biochemistry and biophysics, 676, 108153 (2019). (Review article)

List of poster presentation in various conferences

1. **Tushar Dubey**, Priti Kushwah, H. V. Thulasiram and **Subashchandrabose Chinnathambi***. Brahmi attenuates the Tau-mediated Alzheimer's pathology, 2019-National Science day, CSIR-National Chemical Laboratory. (Best poster award)

Abstract

Alzheimer's disease (AD) is the dominant type of dementia emerging worldwide as a leading health concern. Tau under pathological conditions leads to formation of neurotoxic aggregates, which leads to AD. Thus considering Tau as hallmark of AD, various molecules have been studied for their potency against Tau aggregation. "Ayurveda", is an ancient science, which implies the application of natural compounds for restoring the disease related symptoms. Ayurveda include several neuroprotective herbs, and brahmi is the commanding herb among them. The objective of present study was to reveal the effect of ethanolic extract of brahmi in various aspect of Tau-mediated neurotoxicity. The biochemical, cell biology and microscopic studies suggested that brahmi owns rejuvenating properties against Tau stressed neuronal cells. Brahmi reduces ROS, Tau hypophosphorylation and accelerates cell viability, nuclear transport and cell proliferation. The overall study indicated that brahmi is a potent herb against Tau pathology in Alzheimer's disease.

2. **Tushar Dubey**, and **Subashchandrabose Chinnathambi***. Understanding Role of Tau in Nuclear Transport, 2017-XXXV Annual Conference of Indian Academy of Neuroscience.

Abstract

Alzheimer's disease is a neurodegenerative disorder characterized by progressive decline in cognitive functions and memory. The two hallmarks of Alzheimer's disease are the extracellular senile plaques and intracellular neurofibrillary tangles. Neurofibrillary tangles are formed by aggregation of microtubule-associated protein Tau. Its main function is to stabilize the microtubule, thus maintaining the axonal integrity in neurons. In our current work the studies are being carried out to understand the novel role of Tau in nuclear transport. Objective of our work is to identify the novel interaction of Tau and the hydrotrope (GTP/ATP) in nuclear transport system. Following our hypothesis we are targeting the RAN GTPase which is the key protein in nuclear transport. The preliminary experiments evidenced the cysteine directed GTPase activity of human Tau. Additionally, Pull-down assays signifies role of Tau in nuclear transport.

3. **Tushar Dubey** and **Subashchandrabose Chinnathambi***. Photodynamic exposure of Rose-Bengal inhibits Tau aggregation and modulates cytoskeletal network, 2021-National Science day, CSIR-National Chemical Laboratory.

Abstract

The intracellular Tau aggregates are known to be associated with Alzheimer's disease. The inhibition of Tau aggregation is an important strategy for screening of therapeutic molecules in Alzheimer's disease. Rose Bengal is a Xanthene dye, which has been widely used as a photosensitizer in photodynamic therapy. The aim of this work was to study the protective role of Rose Bengal against Tau aggregation and cytoskeleton modulations in neuronal cells. The aggregation inhibition and disaggregation potency of Rose Bengal and photo-excited Rose Bengal were

observed by *in vitro* fluorescence, circular dichroism, and electron microscopy. In our studies, we observed that Rose Bengal and photo-excited Rose Bengal modulate the cytoskeleton network of actin and tubulin. The immunofluorescence studies showed the increased filopodia structures after photo-excited Rose Bengal treatment. Furthermore, Rose Bengal treatment increases the connections between the cells and actin-rich podosome-like structures. Thus, the overall results suggest that Rose Bengal could have a therapeutic potency against Tau aggregation.

4. **Tushar Dubey**, Abhishek Ankur Balmik, and **Subashchandrabose Chinnathambi***. Signalling Cascades and Post-translational modifications of Tau, 2015-EMBO-Meeting, Indo-French Conference.

Abstract

Tauopathy is one of the most widely accepted pathological symptom of Alzheimer's disease. Tauopathy or generation of neurofibrillary tangles are associated with aggregation of Tau protein. Posttranslational modifications (PTMs) and deregulation of Tau Signaling cascade are the main culprits for pathological condition of Tau. Many kinases are involved in signaling cascades, among all those molecules CDK is drawing attention of researchers because it is known to be involved in early neuronal development. In normal condition, activity of CDK5 is regulated by p35 protein, but under stress condition the calpain-mediated proteolytic cleavage of p35 leads to generation of p25 and p10. The CDK5/p25 complex hyperphosphorylates Tau and facilitates its aggregation whereas, p10 is known to provide survival signals to cells. In our lab we will emphasize on demonstrating the effect of p10 peptide on Tau hyperphosphorylation.



Photoexcited Toluidine Blue Inhibits Tau Aggregation in Alzheimer's Disease

Tushar Dubey,^{†,‡} Nalini Vijay Gorantla,^{†,‡} Kagepura Thammaiah Chandrashekar,[§] and Subashchandrabose Chinnathambi^{*,†,‡,§}

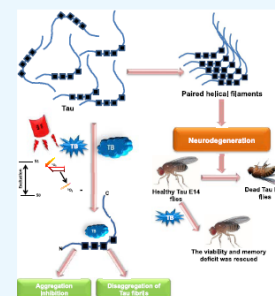
[†]Neurobiology Group, Division of Biochemical Sciences, CSIR-National Chemical Laboratory, Dr. Homi Bhabha Road, 411008 Pune, India

[‡]Academy of Scientific and Innovative Research (AcSIR), 411008 Pune, India

[§]Institution of Excellence, Vijnana Bhavan, University of Mysore, Manasagangotri, 570006 Mysore, India

Supporting Information

ABSTRACT: The aggregates of microtubule-associated protein Tau are considered as a major hallmark of Alzheimer's disease. Tau aggregates accumulate intracellularly leading to neuronal toxicity. Numerous approaches have been targeted against Tau protein aggregation, which include application of synthetic and natural compounds. Toluidine blue is a basic dye of phenothiazine family, which on irradiation with a 630 nm light gets converted into a photoexcited form, leading to generation of singlet oxygen species. Methylene blue is the parent compound of toluidine blue, which has been reported to be potent against tauopathy. In the present work, we studied the potency of toluidine blue and photoexcited toluidine blue against Tau aggregation. Biochemical and biophysical analyses using sodium dodecyl sulfate-polyacrylamide gel electrophoresis, ThS fluorescence, circular dichroism spectroscopy, and electron microscopy suggested that toluidine blue inhibited the aggregation of Tau in vitro. The photoexcited toluidine blue potentially dissolved the matured Tau fibrils, which indicated the disaggregation property of toluidine blue. The cell biology studies including the cytotoxicity assay and reactive oxygen species (ROS) production assay suggested toluidine blue to be a biocompatible dye as it reduced ROS levels and cell death. The photoexcited toluidine blue modulates the cytoskeleton network in cells, which was supported by immunofluorescence studies of neuronal cells. The studies in a UAS Tau E14 transgenic *Drosophila* model suggested that photoexcited toluidine blue was potent to restore the survival and memory deficits of *Drosophila*. The overall finding of our studies suggested toluidine blue to be a potent molecule in rescuing the Tau-mediated pathology by inhibiting its aggregation, reducing the cell death, and modulating the tubulin levels and behavioral characteristics of *Drosophila*. Thus, toluidine blue can be addressed as a potent molecule against Alzheimer's disease.



INTRODUCTION

Alzheimer's disease (AD) is a progressive neurodegenerative disorder characterized by decline in the cognitive function, inefficacy to perform regular work, social withdrawal, and poor judgment. AD is associated with short-term memory loss, which predominantly affects CA1, CA3, and dentate gyrus regions of hippocampus. Extracellular senile plaques composed of amyloid- β ($A\beta$) and intracellular neurofibrillary tangles (NFTs) are the hallmarks of AD.^{1–4} In physiological conditions, Tau is found to be associated with microtubules and functions to stabilize the microtubules. In pathological conditions, Tau undergoes various post-translational modifications, oxidative stress, and truncation, resulting in its aggregation.^{5–9} The molecules that are potent in inhibiting the aggregation of Tau fibrils are now being considered as a therapeutic for AD.^{5,10} Small molecules of natural and synthetic origin were being studied extensively for their medicinal potency against AD pathology.^{3,6,7,11} Dyes have been reported for their medicinal potency in AD, and different classes of dyes including porphyrins, phenothiazine, xanthine,

etc. showed therapeutic potency in AD. Certain dyes have the property of photoexcitation and are applied in the treatment of several dermatological, microbial, and cancerous disorders. Photodynamic therapy (PDT) or the application of photoexcited (PE) dyes is widely used for the treatment of carcinomas, biofilms, dental plaques, dermatological problems, etc. Photoexcited toluidine blue (TB) is widely used as bactericide, but its effect on neuronal degeneration is yet to be addressed. Principally, the therapy is based on targeting the disaggregation potency of photoexcited dyes against pathological protein aggregates. PDT was found to be effective in inhibiting amyloid- β aggregation and increasing its disaggregation by employing xanthene and porphyrin dyes. TB has been reported for its inhibitory properties against proteins like prion, amyloid- β , Tau, etc.^{12–14} Methylene blue (MB) and its derivatives were found to be more potent against AD.¹⁵

Received: August 29, 2019

Accepted: September 19, 2019

Published: October 29, 2019

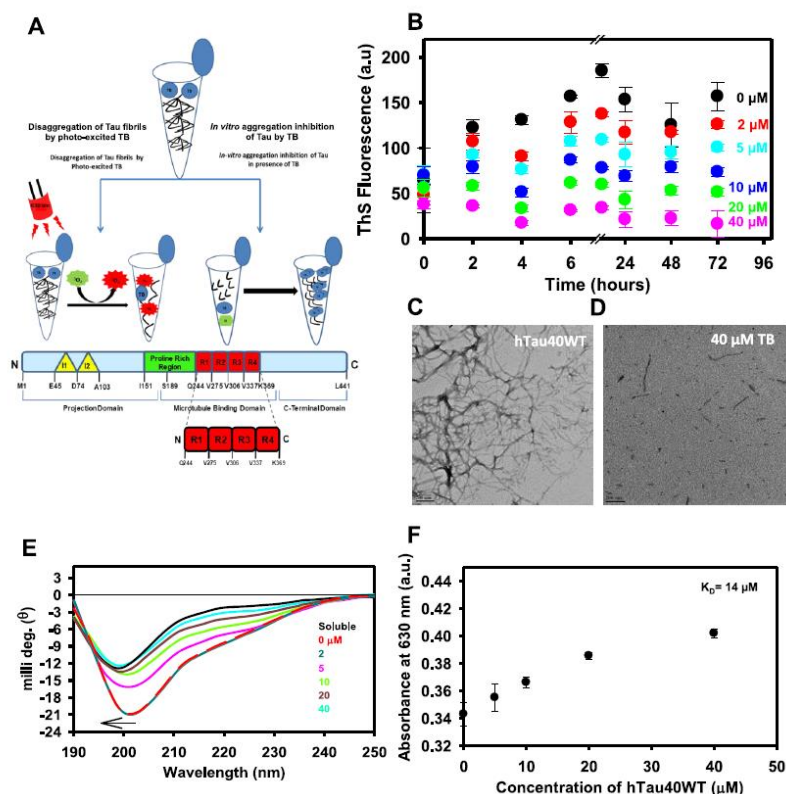


Figure 1. Tau inhibition by toluidine blue. (A) Schematic hypothesis of Tau aggregation inhibition by TB. The bar diagram demonstrates the domain organization of 441 amino acid long full-length Tau. Structurally, Tau can be divided into two domains, viz., the projection domain and the microtubule-binding domain. The four-repeat regions contribute majorly in aggregation of Tau, and the proline-rich region is a target for many post-translation modifications. (B) Effect of TB on inhibiting Tau aggregation was monitored by the ThS fluorescence assay. (C, D) Electron micrograph of Tau aggregates revealed long fibrillar morphology of Tau aggregates, whereas in the presence of TB, small broken fibrils were observed. Tau aggregates after incubating with TB exhibited the population of small, broken filaments after PDT treatment. This indicated the potency of TB in disintegrating Tau aggregates. (E) Native Tau has a random coil conformation, but as it aggregates, it attains a β -sheet conformation. Treatment with TB inhibited the conformational change in Tau, in concentration-dependent manner. (F) The absorbance maximum curve of TB in the presence of Tau at a fixed wavelength of 630 nm was measured, and the hyperbolic curve with a K_D value of 14 μM was observed.

Moreover, MB inhibits oligomer formation in amyloid- β , which is more toxic and accelerates the less toxic fibril formation. HT-22 cells were used to study the role of oxidized and reduced forms of MB in neurodegenerative disorders.¹⁶ Additionally, photoexcited MB was also found to inhibit the aggregation of A β . *Drosophila* has a similar organization of brain to that of humans, where Tau plays a critical role in maintaining the integrity of the cytoskeleton of neurons. The mutation of Tau protein in *Drosophila* brain leads to formation of NFTs, which mimic the tauopathy condition of human brain.¹⁷ The earlier works have demonstrated the potency of photoexcited xanthene dyes and porphyrin dyes against A β aggregation. The potency of photoexcited dyes with respect to Tau aggregation has not been reported. The aim of the present work was to study the potency of TB and PE-TB against Tau aggregation and its biocompatibility. The hypothesis was evaluated using the biochemical and biophysical assays such as the ThS fluorescence assay, sodium dodecyl sulfate-polyacrylamide gel electrophoresis (SDS-PAGE), transmission electron microscopy (TEM), and circular dichroism (CD) spectroscopy. The biocompatibility of TB and PE-TB was tested in Neuro2a cells and the transgenic *Drosophila* model.

The aim of the present study was to evaluate the potency of TB and PE-TB in tauopathy. The in vitro and in vivo studies suggested the potency of TB against Alzheimer's-related pathology.

RESULTS

Toluidine Blue Inhibits Tau Aggregation in Vitro. Tau protein domain organization comprises a projection domain and a microtubule-binding domain. The schematic hypothesis depicts the domain organization of full-length Tau and its interaction with TB (Figure 1A). The four-repeat region of Tau, R1 to R4, is the aggregation-prone region. The potency of TB for inhibiting in vitro Tau aggregation was studied. For the assay, the heparin-treated Tau was incubated with various concentrations of TB ranging from 0 to 40 μM . The aggregation was measured by observing ThS fluorescence at different time intervals, and the fluorescence kinetics suggested that TB showed potent Tau aggregation inhibition. The 40 μM concentration of TB was found to show appreciable inhibition of Tau assembly (Figure 1B). Moreover, the morphological changes in TB-treated Tau were studied by electron microscopy. The electron micrographs suggested long

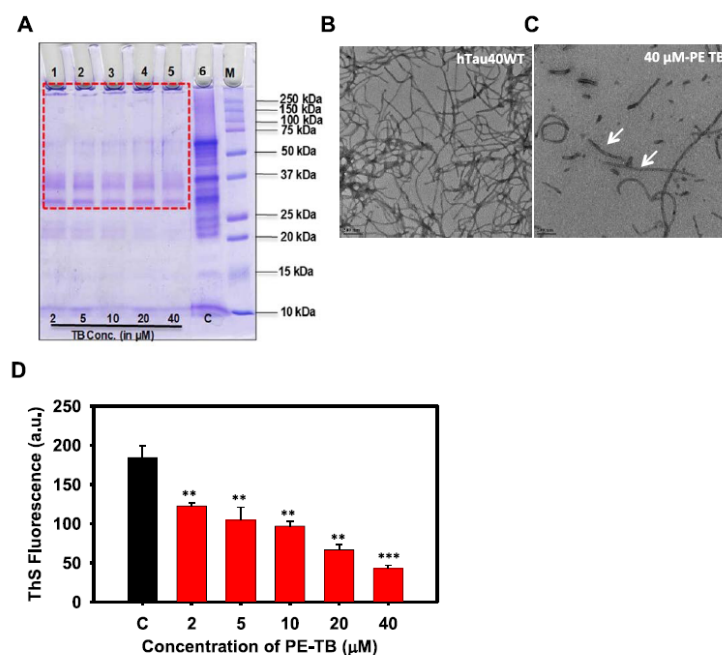


Figure 2. PE-TB disaggregates the mature Tau fibrils. (A) SDS-PAGE analysis of Tau aggregates treated with varying concentrations of PE-TB ranging from 2 to 40 μM demonstrates a clear decrease in higher-order aggregates. These results indicate the effective role of PDT against higher-order aggregates. The red box indicates the disappearance of higher-order aggregates on SDS-PAGE, which was apparent in the control group. (B, C) Electron microscopy shows long, thick, matured fibrils of Tau, whereas after incubating with PE-TB, Tau exhibits the population of small, broken filaments. This indicated the potency of TB in disintegrating Tau aggregates. (D) ThS fluorescence analysis of PE-TB-treated Tau aggregates. In PDT-treated samples, the fluorescence intensity decreased drastically. Here, 40 μM TB showed the maximum effect in disaggregating the mature aggregates.

extended filamentous Tau aggregates in the control sample, whereas incubation with TB resulted in small broken pieces of Tau, which indicated the inefficacy of Tau to aggregate (Figure 1C,D). The conformation of Tau plays an important role in pathophysiology of AD. In physiological conditions, Tau has a typical random coil conformation, but during aggregation, Tau attains a β -sheet conformation that absorbs at 220 nm. In our work, the effect of TB treatment on the secondary structure of Tau was studied. The untreated Tau aggregates showed CD spectrum of a β -sheet structure, whereas the TB-treated protein was found to be random coil (Figure 1E). TB has an absorption maximum at 630 nm (Figure S1A,B). Furthermore, the binding constant of TB for Tau was measured by UV spectroscopy. The binding constant (K_D) for TB and Tau was calculated by measuring the long-range spectrum of TB on incubating with various concentrations of full-length Tau. As Tau and TB both have basic charge, TB showed low affinity for Tau. A high K_D value of 14 μM suggested a weak interaction between the dye and protein (Figure 1F).

Photoexcited Toluidine Blue Disaggregates Tau Filaments. The potency of PE-TB in dissolving the preformed Tau aggregates was studied by incubating mature Tau fibrils with varying concentrations of PE-TB. In present experiments, TB was irradiated with red light (630 ± 10 nm), which led to photoexcitation of TB. The effect of PE-TB on Tau disaggregation was characterized by different biochemical and biophysical methods. SDS-PAGE showed the characteristic signature of higher-order aggregates in control samples (Figure 2A), while the treated samples showed no higher-order aggregates on SDS-PAGE. These results firmly indicated the

effective role of photoexcited TB in destabilizing preformed Tau aggregates in vitro. Moreover, TEM studies indicated the disaggregation potency of PE-TB for Tau, as Tau aggregates were disassembled into short and fragile aggregates (Figure 2B,C). The ThS fluorescence assay suggested that PE-TB potentially reduces the Tau fibrils as a decrease in fluorescence intensity was observed in a concentration-dependent manner (Figure 2D). Here, we speculate that the disaggregation potency of PE-TB could be a cumulative effect of TB and the singlet oxygen species produced after photoexcitation.

Biocompatibility and Toxicity of TB. TB is a photosensitizer; thus, the efficiency of TB to produce singlet oxygen species in cells was estimated by the fluorometric 2',7'-dichlorofluoresceindiacetate (DCFDA) assay. In our work, neuronal cells were treated with various concentrations of PE-TB and TB (Figures 3A and S2A) ranging from 0.025 to 2.5 μM . The results indicated the neuroprotective property of TB, as it generated low reactive oxygen species (ROS) levels. The effect of TB and PE-TB was studied for cellular toxicity. The methylthiazolyldiphenyl-tetrazolium bromide (MTT) assay suggested that in the presence of TB the viability of cells was rescued in the Tau-stressed group (Figures 3B and S2B). TB-treated cells were exposed to 10 min of irradiation so as to observe the cytotoxicity of PE-TB. The results suggested that PE-TB was not toxic to cells up to 500 nM, but the high concentration of PE-TB was found to be toxic. The results suggested that viability of Tau-assaulted Neuro2a cells was rescued in the presence of PE-TB. Morphologically, no distinguished change was observed after the TB treatment, but the PE-TB treatment at lower concentration (500 nM) led

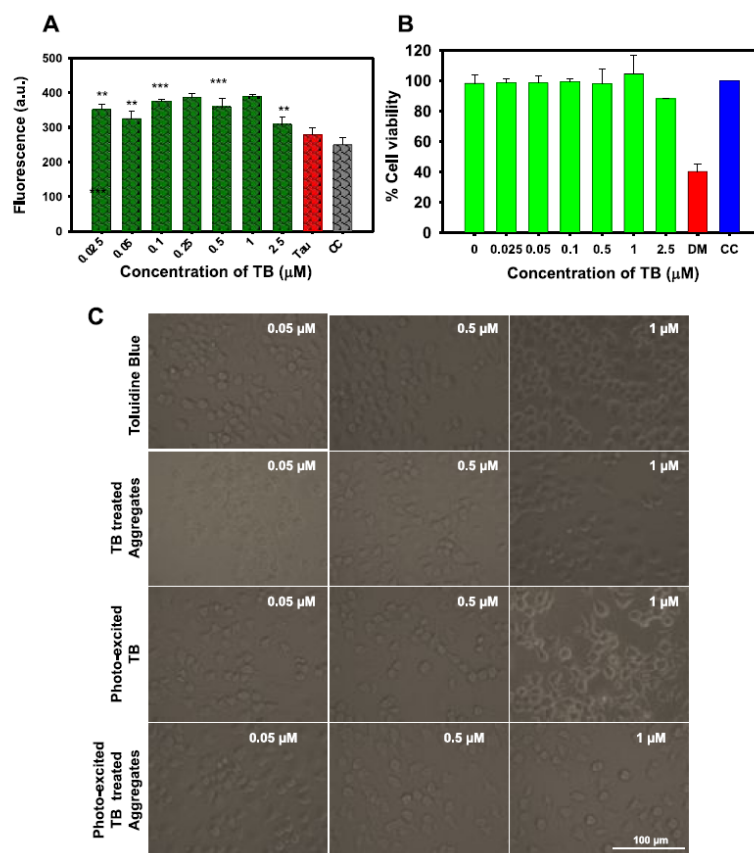


Figure 3. Biocompatibility of PE-TB. (A) The DCFDA assay indicated the extent of ROS production by PE-TB in Neuro2a cells treated with 2.5 μM Tau aggregates. These data suggest that in the presence of TB low levels of ROS were produced. (B) MTT analysis showed that the presence of TB rescued cell viability after exposing to Tau aggregates. PE-TB exhibited a protective role on cell viability in Tau-stressed cells. (C) Cell morphology did not alter after exposure to TB and PE-TB, which indicated healthy cells.

to the formation of neuronal outgrowths in Neuro2a cells, which was indicative of cytoskeleton modulation (Figure 3C).

Toluidine Blue Modulates the Cytoskeleton. Microtubules are the key component of the cytoskeleton network. The effect of TB on the cell cytoskeleton was studied by immunofluorescence assays. The effect of TB and PE-TB on cytoskeleton modulation was studied by targeting tubulin levels in cells. The cells treated with lower concentration of TB (0.5 μM) found to have healthy morphology with long neurite outgrowth and high tubulin expression as compared to untreated cells. On the contrary, a higher concentration of 5 μM of TB and PE-TB generates toxicity to the cells, leading to change in cell morphology. Additionally, the cells were also tagged with the pan-Tau K9JA antibody to observe the levels of Tau expression. The treatment showed increased Tau expression, which supports the fact that PE-TB modulates the cytoskeleton network. The fluorescence images of single neuronal cells clearly indicated that distribution of tubulin and Tau was increased after the PDT treatment. The distribution of Tau and tubulin in neurons was clearly observed in the fluorescent microscopic images of single neuronal cells (Figure 4).

Effect of TB and PE-TB on Transgenic *Drosophila* Model. The overexpression of Tau in the nervous system of *Drosophila* mimics tauopathy, i.e., the neuronal accumulation

of Tau aggregates leading to abnormal behavior. The effect of TB and PE-TB on various behavioral aspects of UAS-E14 Tau mutant *Drosophila* was studied. *Drosophila* behavioral studies were carried out in two sets: the first set was with TB and the other was with PE-TB. The parameters chosen for the studies were feeding behavior, locomotory dysfunction, and loss of memory and potency to reproduce. The current data suggest that PE-TB has a rescuing effect on transgenic flies (Figure 5A). The flies treated with PE-TB showed increased food uptake when compared to the group exposed to TB. There was no concentration-dependent change in either set of TB exposure (Figure 5B). The next set of experiments were carried out to analyze the effect of TB and PE-TB on olfactory sensation of *Drosophila* larvae, that is, basically, the ability to avoid bad odor. The objective behind the experiment was to check the memory deficit in UAS Tau E14 transgenic *Drosophila* larvae after treatment with dye. The transgenic UAS Tau E14 larvae were unable to avoid the odor efficiently as compared to wild-type flies. The TB treatment restored olfactory sensation, indicating the potency of TB to affect the nervous system of E14 Tau *Drosophila*. Here, the photoexcited dye showed more potency over non-photoexcited TB. In the case of concentration-dependent treatment, a bell-shaped pattern was observed, which indicates that 5 μM PE-TB has maximum activity in restoring olfactory sensation of flies

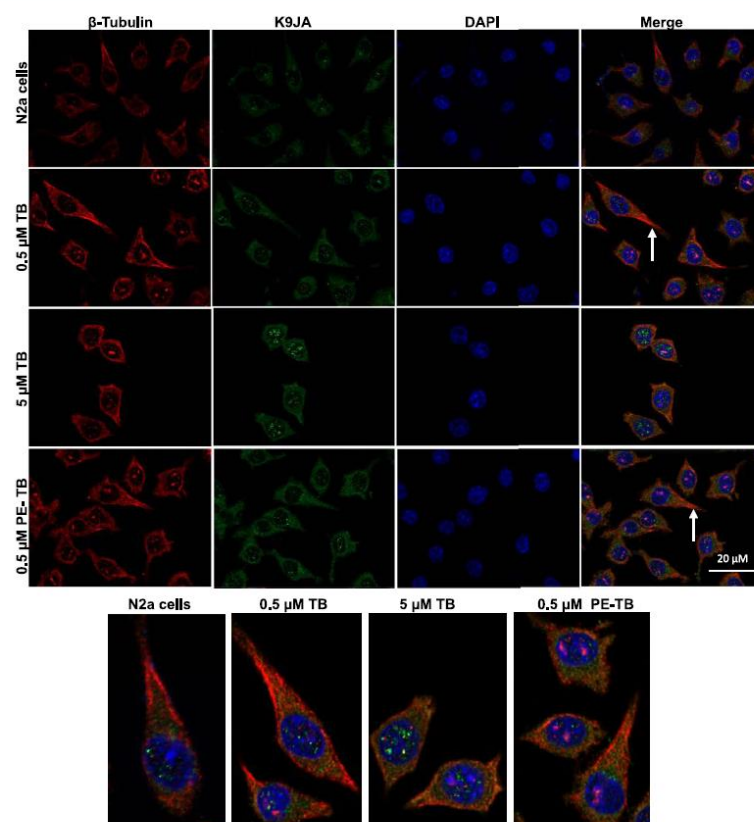


Figure 4. Modulation of the cytoskeleton network by PE-TB. The cells were treated with various concentrations of TB. At lower concentration, TB ($0.5 \mu\text{M}$) showed high expression of tubulin with increased neurite outgrowth, whereas high TB concentration ($5 \mu\text{M}$) was found to be toxic to cells. PE-TB also showed extended neurite outgrowth at lower concentration, whereas $5 \mu\text{M}$ PE-TB was cytotoxic. The fluorescent image of a tubulin-stained single neuronal cell suggested that distribution of tubulin was prominently in neurite outgrowths and Tau was distributed in the cell soma.

(Figure 5C). Succeeding experiments were performed to examine the effect of TB and PE-TB on the locomotor system in Tau flies. The negative geotaxis assay was performed, and the numbers of flies escaped were plotted against the time to interpret results in terms of percentage. The results showed a similar bell-shaped pattern as in the earlier experiment. The $5 \mu\text{M}$ concentration of PE-TB was estimated to be potent for rehabilitating the locomotor activity of flies (Figure 5D). Furthermore, the effect of TB and PE-TB was observed on the longevity of flies. For this objective, two assays, viz., the viability assay and fecundity assay, were carried out. It was observed that PE-TB increases the longevity of flies more efficiently than TB. After the treatment of dye, survival and egg laying ability of flies increased and a bell-shaped pattern was observed, indicating the efficiency of $5 \mu\text{M}$ dye to increase survival of tauopathy *Drosophila* mutant UAS Tau E14 flies (Figures 5E and S3). The overall experimental data concluded that TB was effective in restoring the adverse effect of tauopathy in Tau E14 flies. Additionally, PE-TB was more effective than non-photo-excited TB. Of all concentrations, $5 \mu\text{M}$ concentration of TB and PE-TB was found to be optimal and most effective in treating *Drosophila* tauopathy.

DISCUSSION

Pathological Tau leads to generation of paired helical filaments (PHFs), which are characteristic features of AD.⁸ The importance of small molecules has been reported, which include synthetic and naturally originated compounds.^{18,19} Dyes were tested thoroughly for their medicinal property because of being inexpensive, highly specific, and more potent. Their photoexcitation property was explored against various protein aggregates including $A\beta$, Tau, Prion, etc.^{12,20,21} Toluidine blue is a phenothiazine dye, which was known to decrease the AD pathology. TB was reported to decrease the secretion of pathological $A\beta$ -40 and $A\beta$ -42.²² Furthermore, TB was found to modulate the amyloid-protein-mediated pathology in hippocampus; on the contrary, TB was unable to rescue the Tau phosphorylation in transgenic $3 \times \text{Tg}$ mice.²² Moreover, in the present study, we investigated the effects of TB and PE-TB against Tau aggregation. MB, the parent compound of TB, has been reported in the literature as a potent Tau aggregation inhibitor. In our experiments, the K_D value of $14 \mu\text{M}$ indicated weak binding affinity of TB for Tau, which could be due to the basic charge of TB. However, in this contemporary study, the potency of PE-TB in dissolving the preformed Tau aggregates has also been analyzed by various biochemical and biophysical methods such as ThS fluorescence, SDS-PAGE, CD spectroscopy, and electron micros-

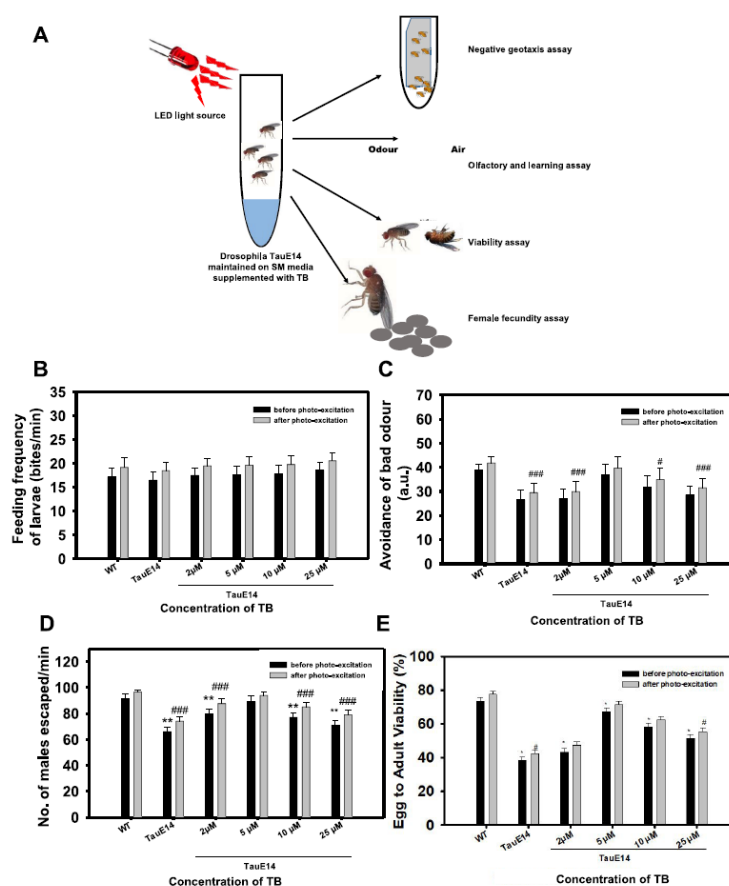


Figure 5. Effect of TB and PE-TB on behavior of transgenic *Drosophila*. (A) Transgenic flies were exposed to TB and PE-TB for various time points at different stages of life cycle to study their effect in restoring memory deficit, locomotory dysfunction, and viability. (B) Results suggest the effect of various concentrations of TB and PE-TB on feeding behavior of flies. PE-TB was found to be more potent than non-photo-excited TB. (C) E14 Tau flies were exposed to various concentrations of TB to analyze changes in olfactory sensation by avoiding the bad odor of quinine. The 5 μM concentration of PE-TB demonstrated appreciable potency in restoring the olfaction. (D) Negative geotaxis assay was performed to examine the effect of TB on locomotion of flies. The bell-shaped graph indicated 5 μM PE-TB to be effective in rescuing the locomotory system of E14 Tau *Drosophila*. (E) Data indicates 5 μM TB to have appreciable effect on the survival rate of transgenic flies. The significance was calculated using Student's *t*-test in SigmaPlot 10.0, where * $p < 0.05$, ** $p < 0.001$, and *** $p < 0.0001$, the statistical difference between control and treated groups before photoexcitation, and # $p < 0.05$, ## $p < 0.001$, and ### $p < 0.0001$, the statistical difference between control and treated groups after photoexcitation.

copy. Additionally, TB possesses the tendency of photoexcitation like its parent compound MB and exposure at 630 nm leads to generation of singlet oxygen species.²³ The ThS binding revealed the role of TB in inhibiting the aggregation of Tau. The aggregates formed were analyzed qualitatively using TEM, which details the effect of small molecules on the aggregate morphology. The phenothiazine dye MB effectively inhibited Tau aggregate formation.²⁴ However, other dyes such as methyl yellow, azo dye, and ponceau, a sulfonated dye, had no effect on Tau aggregation.²⁵ The morphology of Tau in the presence of TB evidenced the potential in preventing aggregate formation, resulting in fragmented filaments. The protein loses its native conformation during aggregation, and this was shown by change in absorbance in the far-UV region. Studies showed that photoexcited MB prevented the conformational changes in A β from a random coil to a β -sheet-rich structure.²⁶ Similarly, TB also prevented conformational changes in Tau and maintained its random coil conformation. Generation of

singlet oxygen species is a characteristic of a photosensitizer, and being a potent photosensitizer, TB generates singlet oxygen.^{27,28} TB is a reported photosensitizer; thus, the levels of ROS produced by PE-TB have been studied. The minimal generation of ROS by PE-TB projects it as a biocompatible photosensitizer, which can be further implied in vivo to check its efficiency. Protein aggregates are known to induce oxidative stress in cells.^{29–31} Thus, we studied the effect of TB in the context of ROS production, and the result suggested that in Tau-stressed cells low levels of ROS generated in the presence of TB. A dye is considered as biocompatible if it generates low levels of toxicity in cells.³² Our findings suggested that TB has moderate cytotoxic potency at lower concentrations. Additionally, it protects cells from oxidative stress and other toxic insults.³³ Similar results were observed in the present experiments, which evidenced TB to be nontoxic in Neuro2a cells up to a sub-micro-molar level. There are studies suggesting the fact that treatment with natural compounds

such as curcumin and resveratrol increases the neurite outgrowths and helps in proliferation of cells.³⁴ Similarly, the high throughput screening of cerivastatin identified it as a neurite growth accelerator.³⁵ Likewise in our experiments, TB and PE-TB were found to increase the neurite outgrowth in Neuro2a cells. *Drosophila* has been proven to be an ideal model for neurodegenerative diseases. Several mutants of *Drosophila* have been reported in the context to tauopathy.³⁶ Recently, the studies stated that photoexcited MB decreased the vacuole formation in *Drosophila* brain, indicating the rescue from neurodegeneration.³⁷ Human Tau pathology has been effectively modeled in *Drosophila*, which was based on overexpression of mutant Tau in fly brain. PE-TB rescued the tauopathy in *Drosophila*. We found that PE-TB reversed tauopathy-induced neurodegenerative phenotypic disorders like olfactory disability, reproductive potentiality, loss of memory, and locomotory disability in UAS Tau E14 *Drosophila* mutants. The behavioral deficits were targeted for studying the effect of Tau expression in *Drosophila* neurons. These results indicate that PE-TB could suppress behavioral defects by reducing the formation of Tau aggregates in *Drosophila* brain. Collectively, behavioral analysis in *Drosophila* indicates that tauopathy-induced behavioral defects were rescued after TB treatment. Neurons are essential for olfactory learning, which is elicited by memory retrieval or stability. This underlies the cognitive deficits observed early in many tauopathies. The overall studies on TB in various in vitro and in vivo systems strongly support its efficiency against AD-related tauopathy.

CONCLUSIONS

The Tau aggregates are considered to be one of the leading causes of AD. Thus, for studying a new therapeutic molecule for AD, Tau aggregates are being targeted. We investigated the potency of TB against Tau aggregation, and the results of all of the studies suggested that TB possesses a dual property of aggregation inhibition and disaggregation. In this study, we addressed, for the first time, the role of PE-TB against mature Tau aggregates. The in vitro assays supported that PE-TB has potency to dissolve the pathological Tau fibrils. Additionally, the low levels of singlet oxygen species generation by PE-TB make the dye more appropriate for administration in a biological system. The in vivo studies on the *Drosophila* model of tauopathy also supported TB as well as PE-TB to be a biocompatible molecule. The overall results of our study provide evidence to support the efficiency of TB as well as PE-TB as a novel molecule against tauopathy.

MATERIALS AND METHODS

Chemicals and Reagents. MES, heparin, BES, bicinechonic acid (BCA), CuSO₄, thioflavin S (ThS), ANS, toluidine blue, MTT, and dimethyl sulfoxide (DMSO) were purchased from Sigma. IPTG and dithiothreitol (DTT) were purchased from Calbiochem. Other chemicals such as ampicillin, NaCl, KCl, Na₂HPO₄, KH₂PO₄, ethylene glycol tetraacetic acid (EGTA), MgCl₂, phenylmethylsulfonyl fluoride (PMSF), ammonium acetate, and bovine serum albumin (BSA) were obtained from MP and protease inhibitor cocktail was obtained from Roche. Copper-coated carbon grids were purchased from Ted Pella, Inc. Advanced DMEM/F-12 media, fetal bovine serum (FBS), penstrep cocktail, and anti-anti were purchased

from Gibco. All laboratory reagents used for *Drosophila* studies were purchased from Merck.

Recombinant Preparation of Tau. The recombinant full-length Tau was purified as per the published protocol.¹¹ Briefly, the recombinant full-length Tau was expressed in the *Escherichia coli* BL21* strain. The cells were grown at 37 °C till the OD₆₀₀ reached 0.5 to 0.6. They were then induced with 0.5 mM IPTG and were further incubated for 4 h and harvested by centrifugation at 4000 rpm for 10 min. The protein isolation and purification were done as described previously.³⁸ The lysing of cells was done using homogenizer constant cell disruption systems. The cells were resuspended in buffer A composed of 50 mM MES, 1 mM EGTA, 2 mM MgCl₂, 5 mM DTT, 1 mM PMSF, and 50 mM NaCl and were subjected to homogenization at 15 000 psi pressure. The obtained lysate was heated at 90 °C for 20 min in the presence of 0.5 M NaCl and 5 mM DTT. This was cooled and centrifuged at 40 000 rpm for 45 min. The supernatant was collected and dialyzed overnight against buffer A before loading to a cation exchange column. Increasing the ionic gradient of NaCl to 1 M, the Tau protein was eluted. The protein quality was analyzed by SDS-PAGE, and the protein was further passed through size exclusion chromatography columns. The obtained protein was analyzed, pooled, and concentrated. The concentration was estimated by the BCA assay, and the protein was stored at -80 °C till further use. Tau aggregation was induced at 37 °C with heparin as previously described.³⁹ Tau in the presence of an anionic inducer such as heparin, RNA, arachidonic acid, etc. undergoes aggregation. Among all of these molecules, the heparin-induced Tau aggregation is a widely accepted model for in vitro tauopathy studies. Earlier studies suggested the heparin-mediated Tau aggregation model to demonstrate the transition of Tau from random coil to β -sheets upon aggregation.⁴⁰ Taniguchi et al. demonstrate the inhibition of heparin-induced Tau filaments by phenothiazine, polyphenols, and porphyrins.²⁵ In the present work, Tau aggregation was induced by heparin where the soluble full-length Tau was mixed with heparin (17 500 Da) at a ratio of 4:1. The reaction was carried out in 20 mM BES buffer supplemented with 25 mM NaCl, 1 mM DTT, and 0.01% NaN₃ and protease inhibitor cocktail mixtures.

Thioflavin S Fluorescence Assay. The effect of TB on the aggregation property of Tau was measured by the thioflavin S (ThS) fluorescence assay.¹⁰ ThS is a mixture of methylated dehydrothiolumidine and sulfonic acid and has the property to fluoresce on binding to β -sheet structures. The fluorescence measurement was carried out by incubating 2 μ M Tau with ThS in a 1:4 ratio for 15 min in the dark. All of the reaction mixtures were measured in triplicate, in a TECAN Infinite M200 PRO spectrophotometer, at an excitation of 440 nm and emission of 521 nm. Further, the data was analyzed using SigmaPlot 10.0.

Circular Dichroism Spectroscopy. The conformational changes in Tau were analyzed using CD spectroscopy in the far-UV region. In native conditions, Tau has a typical random coil conformation, but the aggregation causes a conformational change to β -sheet, which absorbs at around 220 nm. The effect of TB on conformational changes in Tau was studied as described previously.⁴¹ All of the spectra were measured in a Jasco J-815 spectrometer by diluting full-length Tau to 3 μ M in 50 mM phosphate buffer at pH 6.8.

Binding Constant. The binding constant of TB with Tau was estimated by UV-visible spectroscopy. The experiment

was performed using a 96-well clear bottom plate (Eppendorf), and measurements were recorded in a Tecan Infinite M200 PRO spectrophotometer. TB (20 μM) was incubated with varying concentrations of Tau (0, 10, 20, 30, 40, and 50 μM). The binding constant (K_D) value was calculated after recording the spectrum ranging from 230 to 800 nm. The absorption maximum of Tau was observed at 314 nm. All of the samples were diluted in phosphate buffer, at pH 6.8.

$$[\text{PL}] = \frac{[\text{P}_0] \times [\text{L}]}{K_D + [\text{L}]}$$

Here, $[\text{P}_0]$ is the initial protein concentration, $[\text{L}]$ is the free ligand concentration, $[\text{PL}]$ is the concentration of the protein–ligand complex, and K_D is the dissociation constant.

Light-Induced Inhibition of Tau Assembly. For analyzing the effect of photoexcited TB on Tau aggregates, aggregates were incubated for 1 h in the dark with varying concentrations of TB (2, 5, 10, 20, and 40 μM). Then, 200 μL of the reaction mixture was added in a 96-well black plate (Eppendorf) and was irradiated in the dark using red LED. After 1 h of incubation, the samples were analyzed by ThS fluorescence and SDS-PAGE for the presence of disintegrated Tau.

Light-Induced Inhibition of Tau Aggregates Analyzed by SDS-PAGE. The inhibitory effect of TB on Tau aggregation was observed by SDS-PAGE. Various TB-treated reaction mixtures were analyzed. Aggregates have a characteristic pattern of higher molecular weights around 250 kDa; thus, the effect of TB on aggregation propensity of Tau can be easily observed by SDS-PAGE. The experiments were performed using a GE miniVE electrophoresis unit and a BIORAD Mini-PROTEAN electrophoresis unit.

Transmission Electron Microscopy. The morphological analysis of Tau fibrils was done by electron microscopy, and the samples were prepared according to the published protocol.¹¹ For electron microscopic analysis, 2 μM Tau was incubated on carbon-coated copper grids. Following this, the samples were negatively stained with 2% uranyl acetate. The images were captured by TECNAI T20 at 120 kV.

ROS Production in Neuro2a Cells. The effect of photoexcited TB on ROS production was estimated in Neuro2a cells using the 2',7'-dichlorofluoresceindiacetate (DCFDA) assay.^{42,43} ROS oxidizes 2,7-dichlorofluoresceindiacetate to 2',7'-dichlorofluorescein (DCF), leading to the generation of fluorescence. For the assay, 10 000 cells/well were seeded in a 96-well plate and incubated for 24 h. The cells were treated with various concentrations of TB following 10 min of irradiation in the dark. After treatment, the cells were washed twice with 1 \times PBS (pH 7.4), supplemented with 10 μM DCFDA, and incubated for 20 min. After incubation, the cells were again washed twice with 1 \times PBS. Finally, 100 μL of phenol red-free Dulbecco's modified Eagle medium (DMEM) was added in each well and fluorescence was measured at 535 nm upon exciting at 485 nm.

Cytotoxicity Assay. The cell viability was analyzed by the methylthiazolylidiphenyl-tetrazolium bromide (MTT) assay.^{10,44,45} Neuro2a cells were cultured in advanced DMEM/F-12 media supplemented with 10% FBS and glutamine. The cells were trypsinized with a 0.25% trypsin-EDTA solution. A total of 10 000 cells/well were seeded in 96-well plates for the assays. After 24 h, the cells were treated with various concentrations of TB for 24 h, followed by addition of

MTT at a concentration of 0.5 mg/mL and incubation at 37 $^\circ\text{C}$ for 4 h. The formazan crystals formed were dissolved in 100 μL of 100% DMSO. Cell viability was evaluated by measuring the absorbance at 570 nm. Similarly, cells were incubated with 2.5 μM aggregates to observe the cytotoxicity of Tau aggregates; additionally, TB was also added to cells along with aggregates for analyzing the effect of TB in the presence of aggregates. TB-treated cells were subjected to 10 min of irradiation for the cytotoxicity analysis of PE-TB.

Immunofluorescence Analysis of Tubulin Expression in Neuro2a Cells. Neuro2a cells were seeded at a density of 50 000 cells on glass cover slips. The cells were treated with various concentrations of TB (0.5, 5, and 50 μM) and incubated overnight at 37 $^\circ\text{C}$. Similarly, another set of cells treated with various concentrations of TB were irradiated with red light for 10 min and incubated at 37 $^\circ\text{C}$. The cells were fixed with absolute methanol for 20 min at -20 $^\circ\text{C}$. After fixation, cells were permeabilized by 0.2% Triton X-100. After 3 subsequent washes of PBS, the cells were incubated with 5% horse serum for 1 h. The cells were incubated with the anti-tubulin (Thermo PA1-41331) and K9JA (Dako A0024) antibody. After overnight incubation, the cells were incubated with Alexa Fluor 488 (A11034)- and Alexa Fluor 555 (A32727)-tagged secondary antibodies. The nucleus was stained with DAPI. The cells were scanned by a Zeiss Axio observer 7.0, apotome 2.0 inverted microscope using 63 \times magnifications in oil immersion and at 40% light intensity.

Fly Stocks and Genetics. The transgenic *Drosophila* strain used in this study was UAS Tau E14. The ELAV-Gal4 driver line was obtained from the National *Drosophila* Stock Center at the University of Mysore, Mysore, Karnataka, India. *Drosophila* strains were raised on standard medium. Fly cultures and crosses were carried out at 25 $^\circ\text{C}$.

Fly Husbandry. Flies were maintained on standard banana-jaggery medium (SM) under standard laboratory conditions of 24 \pm 1 $^\circ\text{C}$ temperature, 75 \pm 5% relative humidity, and 12:12 light and dark cycle (SLC).⁴⁶ Flies were maintained in a 2 week discrete generation cycle for 10 generations before being used in this study. The adult density was regulated at about 100 flies per half-pint bottle with 25 mL of SM in 10 bottles. Flies from 10 bottles were combined into a single breeding cage, hereafter referred to as parental cage.

Preparation of TB-Supplemented Diet. A total of 2.5 L of SM was prepared and split into five batches of 500 mL each as described previously.⁴⁶ For the control group, SM was poured into the bottles. For the TB-supplemented media, 2.5, 5.0, 10, and 25 μM TB was added and mixed thoroughly just before pouring into the bottles. All bottles were plugged with nonadsorbent cotton, and the media were allowed to set under room temperature.

Larval Feeding Behavior Assay. The eggs obtained were transferred at a density of 50 eggs/6 mL of SM and allowed to develop till early third instar. The early third instar larvae were removed from the SM vials and used in the feeding behavior assay. Larvae were individually transferred to an assay Petri plate of 5 cm diameter containing 10 mL of either liquid SM (SM without agar) or liquid SM supplemented with different concentrations of TB and allowed to acclimate for 5 s. The feeding rate was measured as the mean number of sclerite retractions in two consecutive 30 s intervals. The average of the two rates was taken as the feeding rate of that larva. Then, 20 larvae were assayed for each of the two treatment groups. The

feeding rate assays were replicated four times. A total of 160 larvae were assayed for the feeding rate.

Fecundity Assay. Flies from the holding vials were sexed under low CO₂ anesthesia, and a single pair (one male + one female) was transferred to a vial with ~3 mL of SM. Then, 20 such vials were set up per treatment, per population. Flies were transferred without anesthesia to fresh SM vials every 24 h, and the eggs laid during the previous 24 h were counted under a microscope and recorded. The daily egg counts were carried out till the death of female fly in each test vial.

Negative Geotaxis Assay. The ability to move against gravity and climb indicated the level of physical fitness of test animals. Vertical climbing ability of male flies that emerged from different treatment bottles was assessed. Twenty male flies per treatment group were collected and transferred to the empty, 0–15 cm graduated vial. The vial was gently tapped and placed in a vertical position. The number of flies that crossed the 15 cm mark in 30 s was counted. Three trials were conducted on each set of 20 flies. The data was expressed as percentage of flies that crossed the 15 cm mark.

Viability of Fly from Egg to Adult. The eggs from medium plates were collected and dispensed into different treatment groups of bottles at a density of ~100 eggs/bottle with 45 mL of media. Ten bottles each for five treatment groups of SM and SM with 2, 5, 10, and 25 μ M TB were prepared. Bottles were maintained at standard laboratory conditions. The flies emerged from different treatments, SM and SM with 2, 5, 10, and 25 μ M TB, were designated, collected, and counted. All of the assays were carried out on SM using mated flies. The total number of flies that emerged from each bottle were used to calculate the viability of flies emerging from each treatment group.

Larval Olfactory Behavior. The olfactory test was carried out by employing the previous method with minor modifications.⁴⁷ A total of 30 larvae were briefly dried on a filter paper before being placed in the center of the Petri dish. The Petri dish containing 20 μ L of quinine sulfad odate dispensed on each of the two 0.5 cm radius filter disks were placed in a diametrically opposite position to quinine zones. After 2 min of placing the larvae and covering the Petri dish, numbers of larvae in different zones were counted to calculate the percentage of larvae avoiding the bad odor after training.

Statistical Analysis. Using either duplicate or triplicate reading, the statistical data were plotted. Untransformed (raw) data were analyzed and plotted by SigmaPlot 10.0 software. The data were analyzed for significance by Student's *t*-test, where **p* < 0.05, ***p* < 0.001, and ****p* < 0.0001.

■ ASSOCIATED CONTENT

📄 Supporting Information

The Supporting Information is available free of charge on the ACS Publications website at DOI: 10.1021/acsomega.9b02792.

UV absorption spectrum of TB, TB absorption in the presence of Tau, ROS production after TB exposure, effect of TB on drosophila (PDF)

■ AUTHOR INFORMATION

Corresponding Author

*E-mail: s.chinnathambi@ncl.res.in. Tel: +91-20-25902232. Fax: +91-20-25902648.

ORCID

Subashchandrabose Chinnathambi: 0000-0002-5468-2129

Author Contributions

T.D, N.V.G., and S.C. designed the experiments. T.D. and N.V.G. carried out the experiments. T.D., N.V.G., and S.C. analyzed the data and wrote the article. *Drosophila* studies were carried out by K.T.C., S.C. conceived the idea of the project. All authors contributed to the discussions and manuscript review.

Notes

The authors declare no competing financial interest.

■ ACKNOWLEDGMENTS

This project is supported in part by grants from the in-house, National Chemical Laboratory, Council of Scientific Industrial Research (CSIR-NCL) grant MLP029526. Tau constructs were kindly gifted by Prof. Roland Brandt from the University of Osnabruck, Germany. Tushar Dubey and Nalini Vijay Gorantla acknowledge the fellowship from the University Grants Commission (UGC), India.

■ ABBREVIATIONS

AD, Alzheimer's disease; PHFs, Paired Helical Filaments; NFTs, neurofibrillary tangles; TB, toluidine blue; MB, methylene blue; PDT, photodynamic therapy; ThS, thioflavin S; MTT, methylthiazolyldiphenyl-tetrazolium bromide; SEC, size exclusion chromatography; BCA, bicinchoninic acid; DMSO, dimethyl sulfoxide; DNPH, dinitrophenylhydrazine; ROS, reactive oxygen species; SDS-PAGE, sodium dodecyl sulfate-polyacrylamide gel electrophoresis; TEM, transmission electron microscopy; BSA, bovine serum albumin

■ REFERENCES

- Arriagada, P. V.; Growdon, J. H.; Hedley-Whyte, E. T.; Hyman, B. T. Neurofibrillary tangles but not senile plaques parallel duration and severity of Alzheimer's disease. *Neurology* 1992, 42, 631.
- Selkoe, D. J. The molecular pathology of Alzheimer's disease. *Neuron* 1991, 6, 487–498.
- Forman, M. S.; Trojanowski, J. Q.; Lee, V. M. Y. Neurodegenerative diseases: a decade of discoveries paves the way for therapeutic breakthroughs. *Nat. Med.* 2004, 10, 1055–1063.
- Morris, M.; Maeda, S.; Vossel, K.; Mucke, L. The many faces of tau. *Neuron* 2011, 70, 410–426.
- Giacobini, E.; Gold, G. Alzheimer disease therapy moving from amyloid- β to tau. *Nat. Rev. Neurol.* 2013, 9, 677–686.
- Mandelkow, E.-M.; Mandelkow, E. Biochemistry and cell biology of tau protein in neurofibrillary degeneration. *Cold Spring Harbor Perspect. Med.* 2012, 2, No. a006247.
- Obulesu, M.; Venu, R.; Somashekhar, R. Tau mediated neurodegeneration: an insight into Alzheimer's disease pathology. *Neurochem. Res.* 36 1329–1335. DOI: 10.1007/s11064-011-0475-5.
- Wang, Y.; Mandelkow, E. Tau in physiology and pathology. *Nat. Rev. Neurosci.* 2016, 17, 22–35.
- Sonawane, S. K.; Chinnathambi, S. Prion-Like Propagation of Post-Translationally Modified Tau in Alzheimer's Disease: A Hypothesis. *J. Mol. Neurosci.* 2018, 65, 480–490.
- Sonawane, S. K.; Ahmad, A.; Chinnathambi, S. Protein-Capped Metal Nanoparticles Inhibit Tau Aggregation in Alzheimer's Disease. *ACS Omega* 2019, 4, 12833–12840.
- Gorantla, N. V.; Das, R.; Mulani, F. A.; Thulasiram, H. V.; Chinnathambi, S. Neem Derivatives Inhibits Tau Aggregation. *J. Alzheimer's Dis. Rep.* 2019, 3, 169–178.
- Janouskova, O.; Rakusan, J.; Karaskova, M.; Holada, K. Photodynamic inactivation of prions by disulfonated hydroxylaluminum phthalocyanine. *J. Gen. Virol.* 2012, 93, 2512–2517.

- (13) Lee, B. I.; Lee, S.; Suh, Y. S.; Lee, J. S.; Kim, A.; Kwon, O. Y.; Yu, K.; Park, C. B. Photoexcited Porphyrins as a Strong Suppressor of Amyloid Aggregation and Synaptic Toxicity. *Angew. Chem.* **2015**, *127*, 11634–11638.
- (14) Wischik, C. M.; Harrington, C. R.; Storey, J. M. D. Tau-aggregation inhibitor therapy for Alzheimer's disease. *Biochem. Pharmacol.* **2014**, *88*, 529–539.
- (15) Oz, M.; Lorke, D. E.; Petroianu, G. A. Methylene blue and Alzheimer's disease. *Biochem. Pharmacol.* **2009**, *78*, 927–932.
- (16) Atamna, H.; Kumar, R. Protective role of methylene blue in Alzheimer's disease via mitochondria and cytochrome c oxidase. *J. Alzheimer's Dis.* **2010**, *20*, S439–S452.
- (17) Bolkan, B. J.; Kretschmar, D. Loss of Tau results in defects in photoreceptor development and progressive neuronal degeneration in *Drosophila*. *Develop. Neurobiol.* **2014**, *74*, 1210–1225.
- (18) Calcul, L.; Zhang, B.; Jinwal, U. K.; Dickey, C. A.; Baker, B. J. Natural products as a rich source of tau-targeting drugs for Alzheimer's disease. *Future Med. Chem.* **2012**, *4*, 1751–1761.
- (19) Pickhardt, M.; Neumann, T.; Schwizer, D.; Callaway, K.; Vendruscolo, M.; Schenk, D.; George-Hyslop, S. P.; Mandelkow, E.; Dobson, C.; McConlogue, L. Identification of small molecule inhibitors of tau aggregation by targeting monomeric tau as a potential therapeutic approach for tauopathies. *Curr. Alzheimer Res.* **2015**, *12*, 814–828.
- (20) Lee, B. I.; Suh, Y. S.; Chung, Y. J.; Yu, K.; Park, C. B. Shedding Light on Alzheimer's Amyloidosis: Photosensitized Methylene Blue Inhibits Self-Assembly of β -Amyloid Peptides and Disintegrates Their Aggregates. *Sci. Rep.* **2017**, *7*, No. 7523.
- (21) Gorantla, N. V.; Chinnathambi, S. Tau Protein Squired by Molecular Chaperones During Alzheimer's Disease. *J. Mol. Neurosci.* **2018**, *66*, 356–368.
- (22) Yuksel, M.; Biberoglu, K.; Onder, S.; Akbulut, K. G.; Tacal, O. Effects of phenothiazine-structured compounds on APP processing in Alzheimer's disease cellular model. *Biochimie* **2017**, *138*, 82–89.
- (23) Page, K.; Wilson, M.; Parkin, I. P. Antimicrobial surfaces and their potential in reducing the role of the inanimate environment in the incidence of hospital-acquired infections. *J. Mater. Chem.* **2009**, *19*, 3819–3831.
- (24) Wischik, C. M.; Edwards, P. C.; Lai, R. Y.; Roth, M.; Harrington, C. R. Selective inhibition of Alzheimer disease-like tau aggregation by phenothiazines. *Proc. Natl. Acad. Sci. U.S.A.* **1996**, *93*, 11213–11218.
- (25) Taniguchi, S.; Suzuki, N.; Masuda, M.; Hisanaga, S.-i.; Iwatsubo, T.; Goedert, M.; Hasegawa, M. Inhibition of heparin-induced tau filament formation by phenothiazines, polyphenols, and porphyrins. *J. Biol. Chem.* **2005**, *280*, 7614–7623.
- (26) Akoury, E.; Pickhardt, M.; Gajda, M.; Biernat, J.; Mandelkow, E.; Zweckstetter, M. Mechanistic basis of phenothiazinedriven inhibition of Tau aggregation. *Angew. Chem., Int. Ed.* **2013**, *52*, 3511–3515.
- (27) Komerik, N.; Nakanishi, H.; MacRobert, A. J.; Henderson, B.; Speight, P.; Wilson, M. In vivo killing of *Porphyromonas gingivalis* by toluidine blue-mediated photosensitization in an animal model. *Antimicrob. Agents Chemother.* **2003**, *47*, 932–940.
- (28) Bouillaguet, S.; Wataha, J. C.; Zapata, O.; Campo, M.; Lange, N.; Schrenzel, J. Production of reactive oxygen species from photosensitizers activated with visible light sources available in dental offices. *Photomed. Laser Surg.* **2010**, *28*, 519–525.
- (29) Zhang, W.; Wang, T.; Pei, Z.; Miller, D. S.; Wu, X.; Block, M. L.; Wilson, B.; Zhang, W.; Zhou, Y.; Hong, J.-S.; et al. Aggregated α -synuclein activates microglia: a process leading to disease progression in Parkinson's disease. *FASEB J.* **2005**, *19*, 533–542.
- (30) Schilling, T.; Eder, C. Amyloid β induced reactive oxygen species production and priming are differentially regulated by ion channels in microglia. *J. Cell. Physiol.* **2011**, *226*, 3295–3302.
- (31) Zraika, S.; Hull, R. L.; Udayasankar, J.; Aston-Mourney, K.; Subramanian, S. L.; Kisilevsky, R.; Szarek, W. A.; Kahn, S. E. Oxidative stress is induced by islet amyloid formation and time-dependently mediates amyloid-induced beta cell apoptosis. *Diabetologia* **2009**, *52*, 626–635.
- (32) Tremblay, J.-F. O.; Dussault, S.; Viau, G.; Gad, F.; Boushira, M.; Bissonnette, R. Photodynamic therapy with toluidine blue in Jurkat cells: cytotoxicity, subcellular localization and apoptosis induction. *Photochem. Photobiol. Sci.* **2002**, *1*, 852–856.
- (33) Harrington, C. R.; Storey, J. M. D.; Clunas, S.; Harrington, K. A.; Horsley, D.; Ishaq, A.; Kemp, S. J.; Larch, C. P.; Marshall, C.; Nicoll, S. L. Cellular models of aggregation-dependent template-directed proteolysis to characterize tau aggregation inhibitors for treatment of Alzheimer disease. *J. Biol. Chem.* **2015**, *290*, 10862–10875.
- (34) Bora-Tatar, G.; Erdem-Yurter, H. Investigations of curcumin and resveratrol on neurite outgrowth: perspectives on spinal muscular atrophy. *BioMed Res. Int.* **2014**, No. 709108.
- (35) Sherman, S. P.; Bang, A. G. High-throughput screen for compounds that modulate neurite growth of human induced pluripotent stem cell derived neurons. *Dis. Models Mech.* **2018**, No. 031906.
- (36) Iijima-Ando, K.; Iijima, K. Transgenic *Drosophila* models of Alzheimer's disease and tauopathies. *Brain Struct. Funct.* **2010**, *214*, 245–262.
- (37) Lee, B. I.; Suh, Y. S.; Chung, Y. J.; Yu, K.; Park, C. B. Shedding Light on Alzheimer's β -Amyloidosis: Photosensitized Methylene Blue Inhibits Self-Assembly of β -Amyloid Peptides and Disintegrates Their Aggregates. *Sci. Rep.* **2017**, *7*, No. 7523.
- (38) Gorantla, N. V.; Khandelwal, P.; Poddar, P.; Chinnathambi, S. Global Conformation of Tau Protein Mapped by Raman Spectroscopy. In *Tau Protein: Methods and Protocols*; Humana Press: NY, pp 21–31.
- (39) Barghorn, S.; Biernat, J.; Mandelkow, E. Purification of Recombinant Tau Protein and Preparation of Alzheimer-Paired Helical Filaments in Vitro. In *Amyloid Proteins: Methods and Protocols*; Humana Press: NY, 2005; pp 35–51.
- (40) Barghorn, S.; Biernat, J.; Mandelkow, E. Purification of Recombinant Tau Protein and Preparation of Alzheimer-Paired Helical Filaments in Vitro. In *Amyloid Proteins*; Springer, 2005; pp 35–51.
- (41) Gorantla, N. V.; Shkumatov, A. V.; Chinnathambi, S. Conformational Dynamics of Intracellular Tau Protein Revealed by CD and SAXS. In *Tau Protein: Methods and Protocols*; Humana Press: NY, pp 3–20.
- (42) Alexandre, J.; Batteux, F.; Nicco, C.; Chreau, C.; Laurent, A.; Guillemin, L.; Weill, B.; Goldwasser, F. Accumulation of hydrogen peroxide is an early and crucial step for paclitaxel induced cancer cell death both in vitro and in vivo. *Int. J. Cancer* **2006**, *119*, 41–48.
- (43) Degli Esposti, M. Measuring mitochondrial reactive oxygen species. *Methods* **2002**, *26*, 335–340.
- (44) Pasinelli, P.; Borchelt, D. R.; Houseweart, M. K.; Cleveland, D. W.; Brown, R. H. Caspase-1 is activated in neural cells and tissue with amyotrophic lateral sclerosis-associated mutations in copper-zinc superoxide dismutase. *Proc. Natl. Acad. Sci. U.S.A.* **1998**, *95*, 15763–15768.
- (45) Fioriti, L.; Dossena, S.; Stewart, L. R.; Stewart, R. S.; Harris, D. A.; Forloni, G.; Chiesa, R. Cytosolic prion protein (PrP) is not toxic in N2a cells and primary neurons expressing pathogenic PrP mutations. *J. Biol. Chem.* **2005**, *280*, 11320–11328.
- (46) Chandrashekar, K. T.; Shakarad, M. N. Aloe vera or resveratrol supplementation in larval diet delays adult aging in the fruit fly, *Drosophila melanogaster*. *J. Gerontol., Ser. A* **2011**, *66*, 965–971.
- (47) Heisenberg, M.; Borst, A.; Wagner, S.; Byers, D. *Drosophila* mushroom body mutants are deficient in olfactory learning. *J. Neurogenet.* **1985**, *2*, 1–30.



OPEN

Photodynamic exposure of Rose-Bengal inhibits Tau aggregation and modulates cytoskeletal network in neuronal cells

Tushar Dubey^{1,2}, Nalini Vijay Gorantla^{1,2}, Kagepura Thammaiah Chandrashekar³ & Subashchandraboese Chinnathambi^{1,2}✉

The intracellular Tau aggregates are known to be associated with Alzheimer's disease. The inhibition of Tau aggregation is an important strategy for screening of therapeutic molecules in Alzheimer's disease. Several classes of dyes possess a unique property of photo-excitation, which is applied as a therapeutic measure against numerous neurological dysfunctions. Rose Bengal is a Xanthene dye, which has been widely used as a photosensitizer in photodynamic therapy. The aim of this work was to study the protective role of Rose Bengal against Tau aggregation and cytoskeleton modulations. The aggregation inhibition and disaggregation potency of Rose Bengal and photo-excited Rose Bengal were observed by in-vitro fluorescence, circular dichroism, and electron microscopy. Rose Bengal and photo-excited Rose Bengal induce minimal cytotoxicity in neuronal cells. In our studies, we observed that Rose Bengal and photo-excited Rose Bengal modulate the cytoskeleton network of actin and tubulin. The immunofluorescence studies showed the increased filopodia structures after photo-excited Rose Bengal treatment. Furthermore, Rose Bengal treatment increases the connections between the cells. Rose Bengal and photo-excited Rose Bengal treatment-induced actin-rich podosome-like structures associated with cell membranes. The in-vivo studies on *UAS E-14* Tau mutant *Drosophila* suggested that exposure to Rose Bengal and photo-excited Rose Bengal efficiency rescues the behavioural and memory deficit in flies. Thus, the overall results suggest that Rose Bengal could have a therapeutic potency against Tau aggregation.

Abbreviations

AD	Alzheimer's disease
BCA	Bicinchoninic acid
BSA	Bovine serum albumin
DMSO	Dimethyl sulfoxide
MB	Methylene blue
MTT	Methylthiazolyl-diphenyl-tetrazolium bromide
NFTs	Neurofibrillary tangles
PDT	Photodynamic treatment
PHFs	Paired helical filaments
RB	Rose Bengal
SDS-PAGE	Sodium dodecyl sulphate-polyacrylamide gel electrophoresis
SEC	Size-exclusion chromatography

¹Neurobiology Group, Division of Biochemical Sciences, CSIR-National Chemical Laboratory (CSIR-NCL), Dr. Homi Bhabha Road, Pune 411008, India. ²Academy of Scientific and Innovative Research (AcSIR), New Delhi 110025, India. ³Institution of Excellence, Vijnana Bhavan, University of Mysore, Manasagangotri, Mysore 570006, India. ✉email: s.chinnathambi@ncl.res.in

ThS Thioflavin S
TEM Transmission electron microscopy

Alzheimer's disease (AD), is the severely emerging neurological disorder, which is considered as a principal cause of dementia^{1,2}. The aggregates of Tau are being considered as the hallmarks of AD. Tau protein belongs to type II microtubule-associated protein, which are associated with the stabilization of microtubules³. Under physiological conditions, Tau assists in maintaining the microtubule integrity while under pathological conditions, Tau detaches from microtubules leading to the formation of intracellular aggregates of Tau⁴. The interference of Tau aggregates in various cellular metabolism processes leads to the generation of toxicity ultimately resulting in the generation of the disease state. Several factors including post-translational modifications (PTMs), reactive oxygen species (ROS), neurotoxin stress, hypertension, physical trauma, diabetes, etc., have been reported to induce modulation in Tau structures, which triggers the aggregation of Tau^{5,6}. The modulation in cytoskeleton is considered as one of the major cause for neuronal death⁷. In order to investigate molecules against AD, Tau aggregation inhibition has been considered as an important target of these studies. An array of natural and synthetic molecules have been screened for the potency to inhibit Tau aggregation⁸. Natural molecules-like Oleocanthal, Anthraquinones, Nimbin, Salannin, Curcumin and Cinnamaldehyde have been reported to possess the potency of aggregation inhibition^{8–11}. Additionally, synthetic molecules as cyanine dyes, methylene blue, congo red, phenyl amines were studied for inhibition of Tau aggregation^{12–15}. Moreover, metal complexes and metal nanoparticles are also reported to have potency against Tau aggregation^{16,17}. Several model systems have been studied for screening therapeutic molecules, the in-vitro heparin-induced Tau aggregation and transgenic E14 *Drosophila* is widely examined as a model system for Tauopathy^{18–20}. Rose Bengal (RB) is a xanthene dye, which is known to possess the property of photo-excitation and hence it has been widely used as a photo-sensitizer²¹. RB is reported to be effective against various bacterial infections and cancerous cells^{22,23}. The potency of RB in inhibiting the Amyloid- β aggregation-induced toxicity was reported earlier²⁴. Several factors have been reported for microtubule disassembly; the post-translational modification of Tau is one of the major cause resulting in microtubule destabilization. In present work, we focused on studying the efficiency of RB and photo-excited RB (PE-RB) against Tau aggregation. Our studies were based on the in-vitro biochemical and biophysical methods including SDS-PAGE, Thioflavin S (ThS) fluorescence assay, circular dichroism (CD) spectroscopy, and electron microscopy, which were performed to observe the potency of RB against Tau aggregation. Furthermore, the biocompatibility of RB and PE-RB was studied by monitoring the cell viability assays, which include MTT assay. Moreover, the effect of RB on cytoskeleton modulation was studied by immunofluorescence assay. *Drosophila melanogaster* is an ideal system for studying the neurodegeneration. The transgenic *Drosophila* overexpresses Tau in the nervous system which mimics the human Tauopathy. In our work, the in-vivo studies on *UAS E-14 Drosophila* model were conducted for confirming the protective property of RB against Tau-mediated memory and locomotor dysfunction. Several dyes have been reported to be effective as a therapeutic molecule, the aim of the present study was to analyze the potency of RB and PE-RB against Tauopathy.

Results

Rose Bengal inhibits in-vitro Tau assembly. Tau is natively unfolded, randomly coiled protein with 441 amino acid in its longest isoform of Tau. The domain organisation of Tau comprises of projection domain, proline-rich domain and microtubule-binding domain. Tau has four repeats in the microtubule-binding domain, which are prone to aggregation^{25,26}. Tau protein aggregates and forms paired helical filaments that are considered to be the cause of AD pathology^{27,28}. RB is an anionic Xanthene dye, which is applied in various clinical diagnosis purposes (Fig. 1A). The potency of RB in restraining in-vitro Tau aggregation was studied by various biochemical and biophysical methods. For studying the aggregation inhibition potency of RB, recombinant Tau was incubated with heparin and various concentrations of RB (2–40 μ M). The results suggested that reduced Thioflavin S (ThS) fluorescence in RB treated Tau, indicating aggregation inhibition (Fig. 1B–C). Tau has a random coil structure in native state whereas, aggregated Tau has characteristic β -sheet. Circular dichroism spectra (CD) of RB treated Tau were analyzed to study the effect of RB on Tau aggregation. The CD spectra analysis suggested that RB induces conformational changes in Tau at concentrations of 20 and 40 μ M (Fig. 1D). Furthermore, the electron microscopic analysis was performed to observe the change in aggregates morphology after incubation with RB. These results suggested that RB treatment inhibited the Tau aggregation as small broken filaments were prevalent in the sample. On the contrary, the untreated sample has long, thick filaments (Fig. 1E). The overall studies suggested that RB efficiently inhibits in-vitro Tau aggregation.

Mature Tau fibrils dissolved by photo-excited Rose Bengal. RB is one of the well-studied photosensitizers reported to be applied as a therapeutic molecule. The potency of photo-excited RB (PE-RB) was tested against mature Tau filaments. The pre-formed mature Tau aggregates incubated with various concentrations of RB (2–40 μ M) were irradiated with green light for 180 min at an irradiance of 9.9×10^6 W/m². The disaggregation potency of PE-RB was addressed by various biochemical and biophysical assays (Fig. 2A). The heterogeneous Tau aggregates could be observed as the higher-order species on SDS-PAGE. Thus, the PE-RB treated aggregates were analyzed by SDS-PAGE for the presence of higher-order species. The SDS-PAGE suggested the dissolution of higher-order aggregates in PE-RB treated samples as a comparison to untreated aggregates where higher-order species were visible (Fig. 2B). Furthermore, the extent of disaggregation was analyzed by ThS fluorescence assay. The reduced fluorescence in PE-RB treated samples in comparison to untreated aggregates suggested a potent disaggregation of Tau fibrils by PE-RB treatment (Fig. 2C). Furthermore, the PE-RB treated aggregates observed to have modulation in secondary structure. The PE-RB treated samples observed to have minimal spectral dip in the random coil region whereas, changes as compared to untreated aggregates

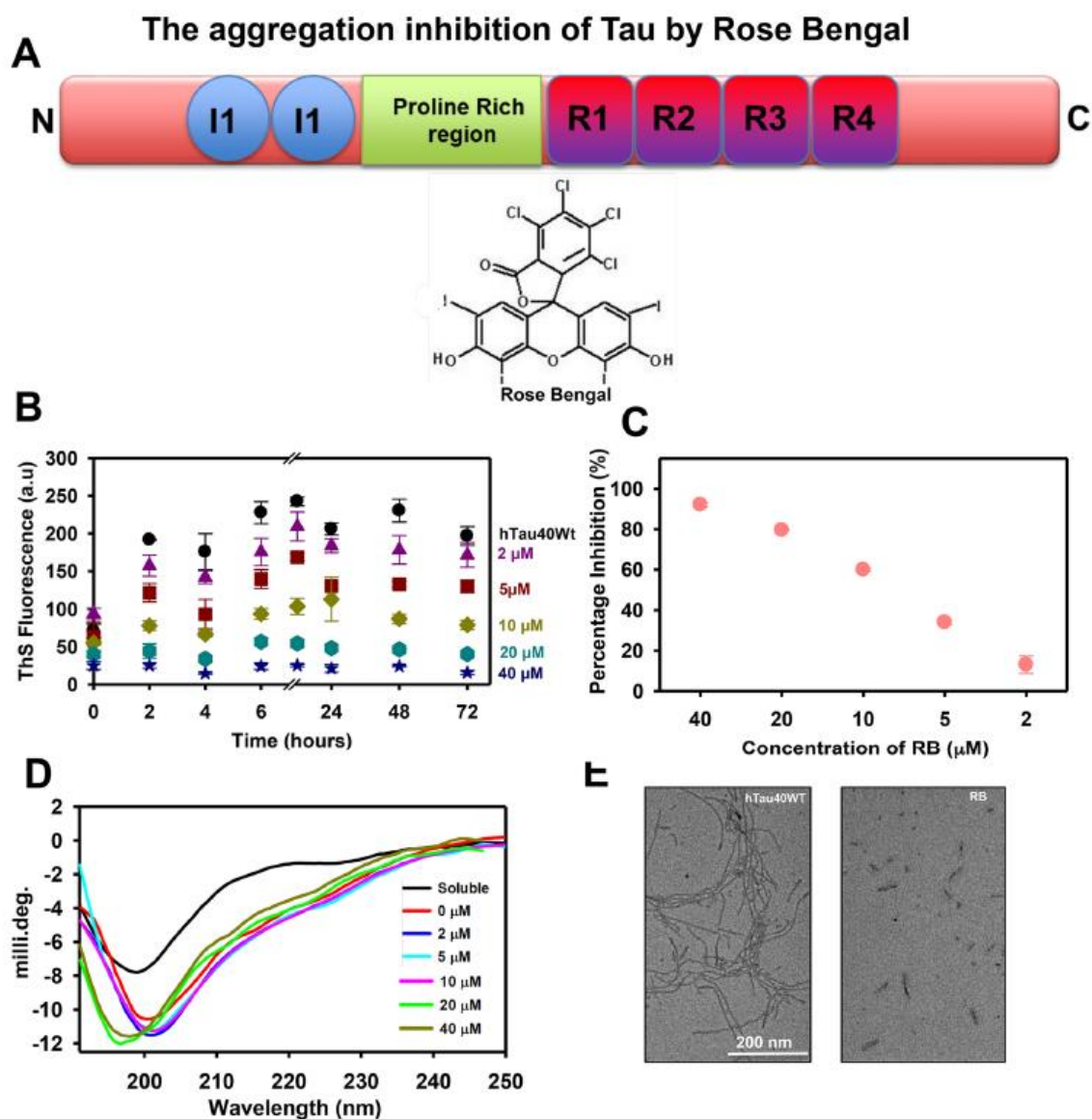


Figure 1. RB inhibits the Tau aggregation in vitro. (A) The domain organization of Tau. Tau is a natively unfolded protein having two domains, projection domain and a microtubule-binding domain. Rose Bengal is an anionic Xanthene dye widely used in clinical diagnosis. (B) The aggregation kinetics demonstrating a reduction in ThS fluorescence in samples incubated with various concentrations of RB. 40 μM RB showed maximum inhibition of Tau aggregation. (C) The graph showing the percentage of aggregation inhibition at the end of 72 h. (D) CD spectroscopy of RB treated samples, 40 μM RB and 20 μM RB observed to induce conformational changes in Tau aggregates. (E) The electron microscopy images of the RB treated sample have small broken fragments of Tau while the untreated sample has long tangled filaments.

(Fig. 2D). Thus, the CD results suggested that PE-RB treatment could break the β -sheet rich aggregates of Tau. The morphological studies including electron microscopy images showed that the untreated Tau aggregated were having long filamentous structure whereas, PE-RB treated samples have broken filament, which evidenced a potent disaggregation (Fig. 2E). Thus, the above-results divulge the disaggregation potency of PE-RB against mature Tau aggregates.

PE-Rose Bengal Disaggregates Tau filaments

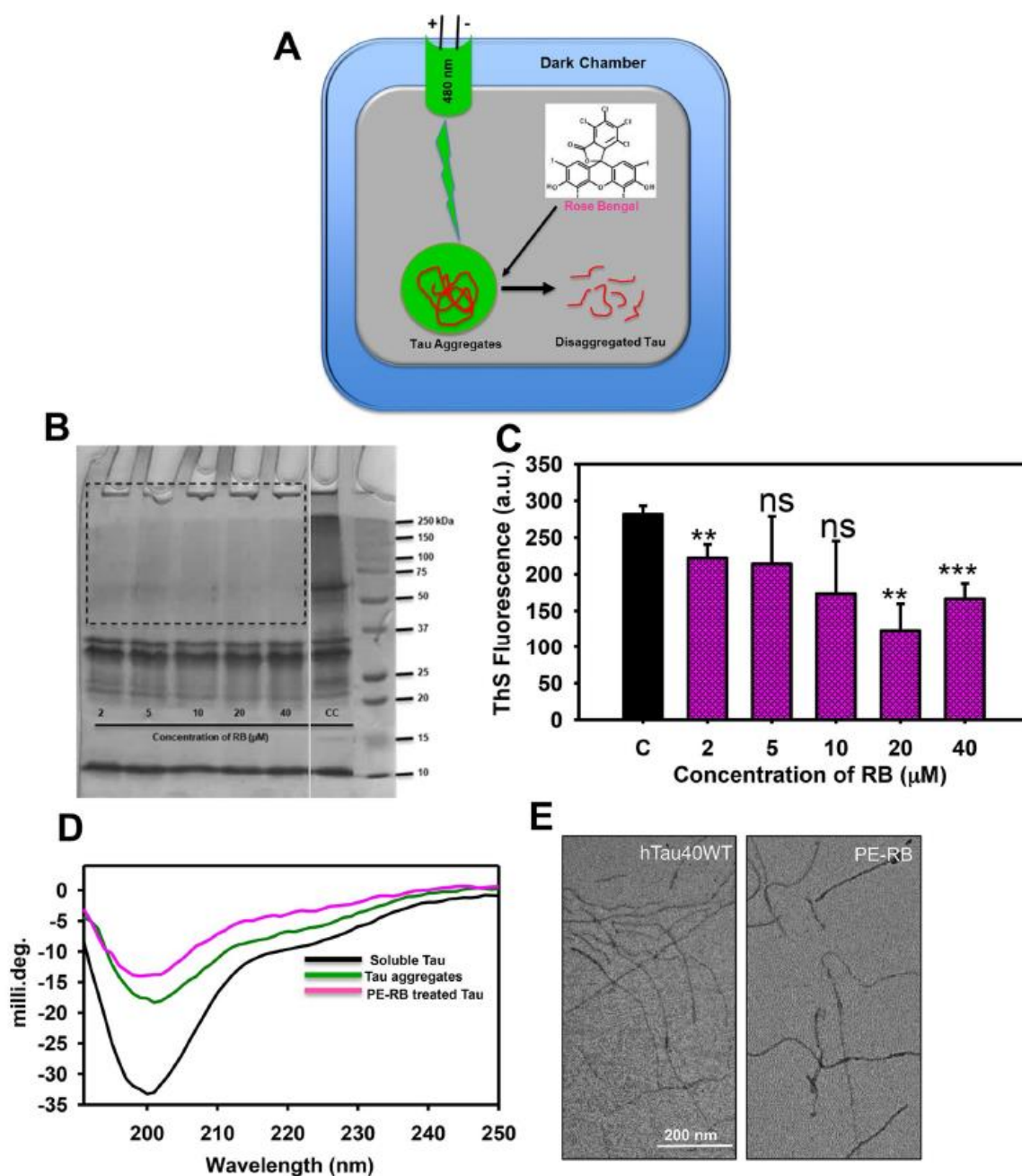


Figure 2. PE-RB disaggregated the mature Tau filaments. (A) The schematic diagram demonstrating the irradiation assembly. A dark chamber was designed for irradiating the RB treated Tau aggregates where the green LED was used as a light source. (B) The SDS-PAGE analysis of Tau aggregates treated with various concentrations of RB. PE-RB was found to dissolve the aggregates as no higher-order bands were visible in the treated sample compared to untreated control (CC). The gel has been cropped for better representation of results. Raw SDS-PAGE is available with supplementary information. (C) The bar graph showing the decrease in ThS fluorescence in PE-RB treated samples indicating an efficient disaggregation of Tau filaments. (D) CD spectroscopic analysis of PE-RB treated Tau aggregates showed a shift in random coil region whereas the untreated aggregates have a dip near β -sheet structure. (E) The electron microscopy images of PE-RB treated samples showed broken Tau filaments; unlikely, the untreated samples have intact long filaments. $p < 0.05$, $**p < 0.001$, $***p < 0.0001$ represents the statistical difference between control and treated groups.

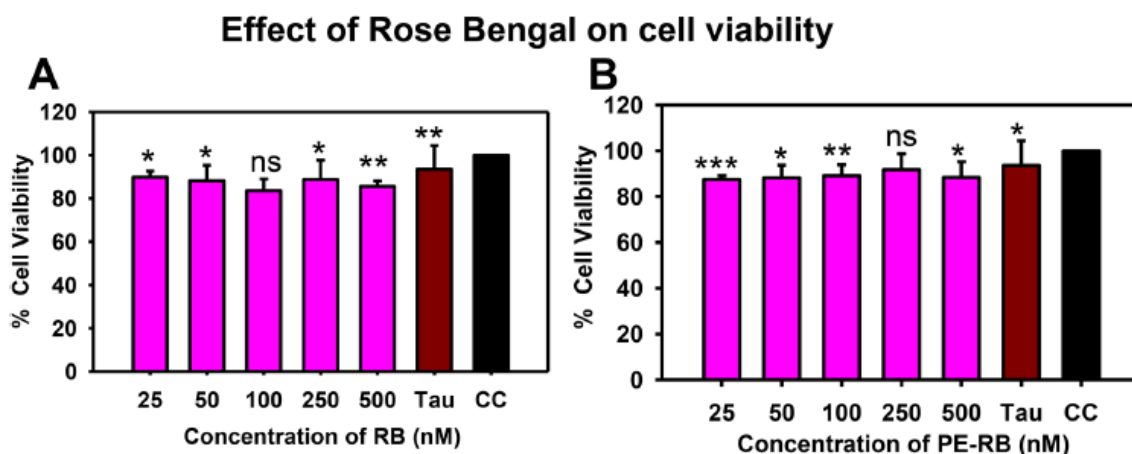


Figure 3. The effect of RB on cell viability. (A) The MTT assay performed for observing the effect of various concentrations of RB on cell viability. RB showed minimal cytotoxicity up to 500 irradiation. (B) The PE-RB showed negligible cytotoxicity at a concentration of 500 nM. Whereas, the cells treated with 2.5 μ M Tau aggregates also showed very minimal reduction in cell viability. $p < 0.05$, $**p < 0.001$, $***p < 0.0001$ represents the statistical difference between control and treated groups.

The biocompatibility of Rose Bengal. The preliminary test to check the biocompatibility of molecule has been investigated based on their effect on cell viability. Thus, to address the therapeutic potency of dye, we aimed to test the effect of various concentrations of RB and PE-RB in Neuro2a cells. The effect of RB and PE-RB on cell viability was observed by MTT assay. Neuro2a cells were incubated with various concentrations of RB. The RB treated cells were irradiated for 10 min at room temperature for photo-excitation. The MTT results indicated that RB and PE-RB showed a minimal detrimental effect on cell viability. An 80% rescue of cell viability was observed even at higher concentrations of RB (Fig. 3A,B). There was minimal cytotoxicity observed after the exposure of Tau aggregates. Hence, due to the generation of low cytotoxicity, RB and PE-RB could be advocated as biocompatible molecule.

RB and PE-RB modulate the cytoskeleton. AD has been reported to be associated with various cytoskeletal deformities²⁹. Thus, we studied the cytoskeleton modulation in context of RB treatment. Tubulin and actin are the basic cytoskeleton network, which are involved in cell integrity and cell migration³⁰. Tubulin has an important role in microtubule stability, cell integrity, cellular trafficking and cell division³¹. The globular actin (G-actin) polymerizes to form filamentous actin (F-actin), which has been reported to be involved in several cellular functions such as cell motility, organelle movement and cell signalling etc.^{32–34}. Actin-rich structures e.g. filopodia and lamellipodia are associated with the cell membrane that assist in cell motility, synapse formation and cell adhesion^{35,36}. In our work, we aimed to study the effect of RB and PE-RB on the cytoskeleton network (Fig. 4A). Based on the results of cell viability assay, we observe 100 nM of RB as the optimal concentration for cell culture studies, thus further studies were done considering 100 nM of RB. These results suggested that cells exposed to PE-RB treatment were having long neurite extensions in comparison to untreated cells. Although, the modulation in tubulin network was not observed after the treatment (Fig. 4B). Furthermore, we have quantified the length of neurite extensions from the fluorescence images. Here, tubulin was used as a marker of neurite extension. The quantitative data generated using Image J software suggested a significant increase in the length of neurites after the treatment of RB and PE-RB, which indicated the modulation of cytoskeleton by RB and PE-RB (Fig. 4C).

RB and PE-RB modulates actin network. Actin is a class of cytoskeletal protein that assists in cell motility and migration³³. Thus, we studied the effect of RB and PE-RB on the actin cytoskeleton. The effect of PE-RB and RB on the modulation of actin modulation was observed by immunofluorescence (Fig. 5A). The cell treated with 100 nM RB showed an increased number of filopodia whereas; lamellipodia structure was not altered as compared to untreated control. Moreover, the increased number of connections were observed in RB treated cells, which was not prominent in untreated cells. PE-RB treated cells were observed to have modulated actin networks, as the cells have prominent growth cone and differentially increased number of filopodia (Fig. 5B). The elevated presence of filopodia structure in RB and PE-RB treatment group suggested that RB has a potency to target the cytoskeleton (Fig. 5C,D). Podosomes are the actin-rich structure, which assists in cell migration. Cell motility and cell adhesion are considered to be the main functions of podosomes. In our work, the cells were treated with 100 nM RB observed to have an increased podosome-like structure in the membrane (Fig. 6A). The quantification of fluorescence images suggested that in PE-RB and RB treatment increased the membrane-associated actin localization, which supported the fact that RB and PE-RB could modulate the cytoskeleton by targeting actin dynamics (Fig. 6B).

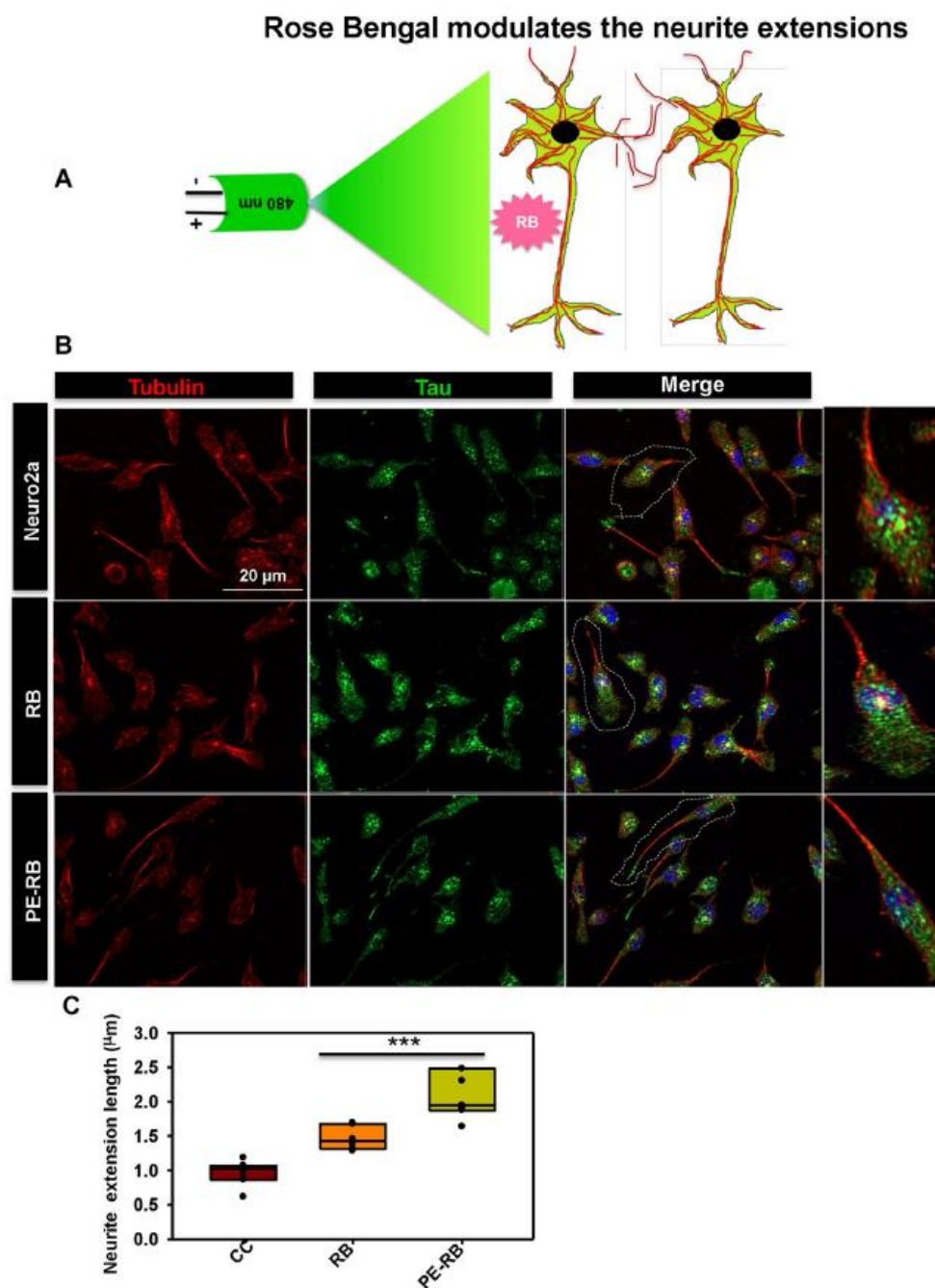


Figure 4. Modulation of the cytoskeleton by RB. (A) The effect of RB and PE-RB was monitored on the cytoskeleton network in neuro2a cells. (B) The RB and PE-RB treated cells had extended axonal outgrowth with high tubulin intensity. (C) The quantification of neurite extension suggested that RB and PE-RB could modulate the tubulin cytoskeleton.

Irradiation time influences cytoskeleton modulation. Time-dependent irradiation is one of the factors for deciding the irradiance dose on target. Several studies suggest that irradiance have a role in deciding the potency of photosensitizer³⁷. In present work, the effect of varying times of irradiation on actin dynamics

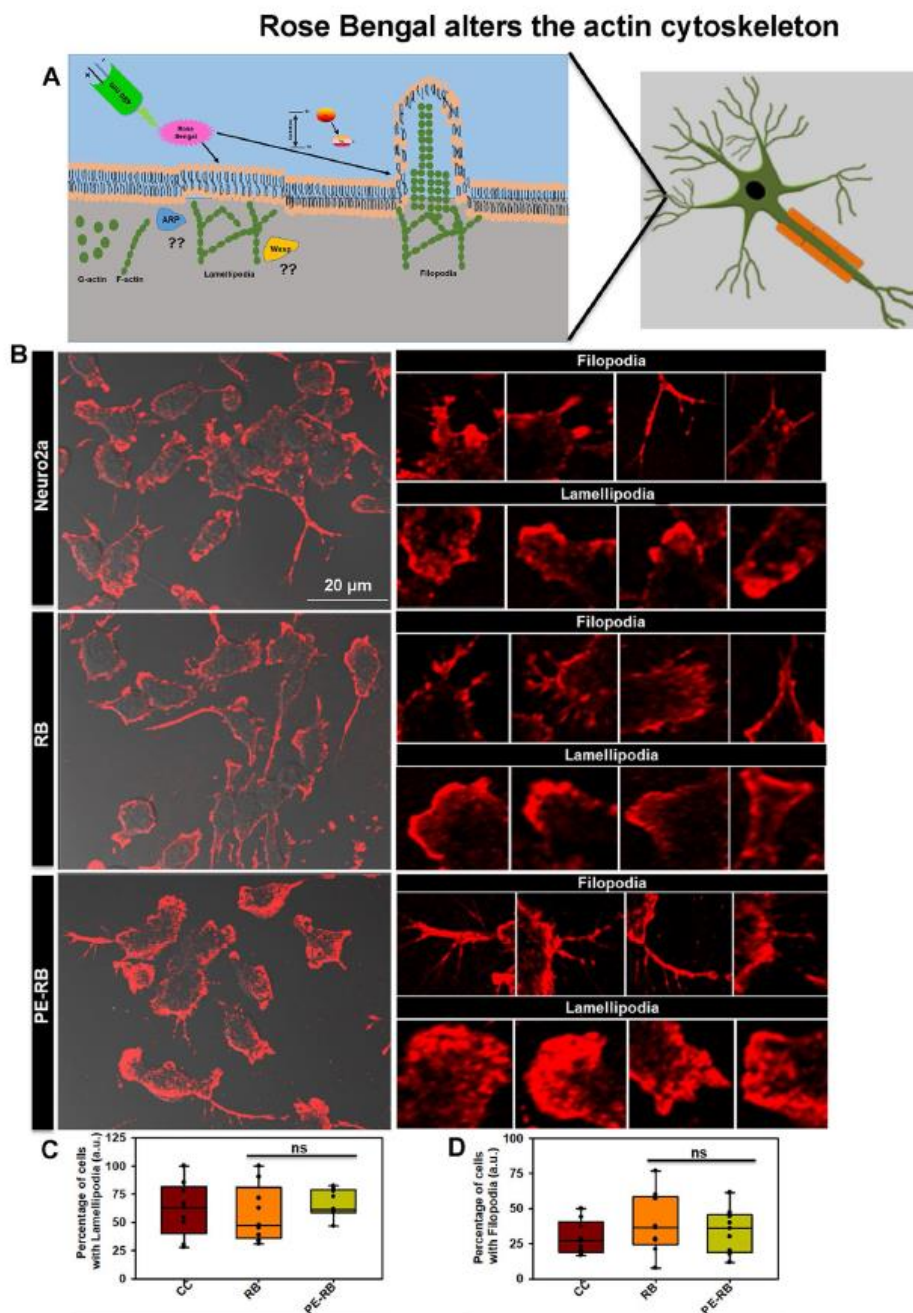


Figure 5. Modulation of the actin cytoskeleton by RB. (A) The effect of RB and PE-RB treatment on the actin cytoskeleton was monitored by immunofluorescence. (B) The immunofluorescence studies suggested that RB and PE-RB treatment generates various changes in actin cytoskeleton. (C) The quantification of images depicting the percentage of cells bearing lamellipodia in each experiment group. (D) The cells were quantified for the presence of filopodia using Image J software. The increased number of filopodia were observed in PE-RB treated cells.

Rose Bengal induces Podosome-like structure

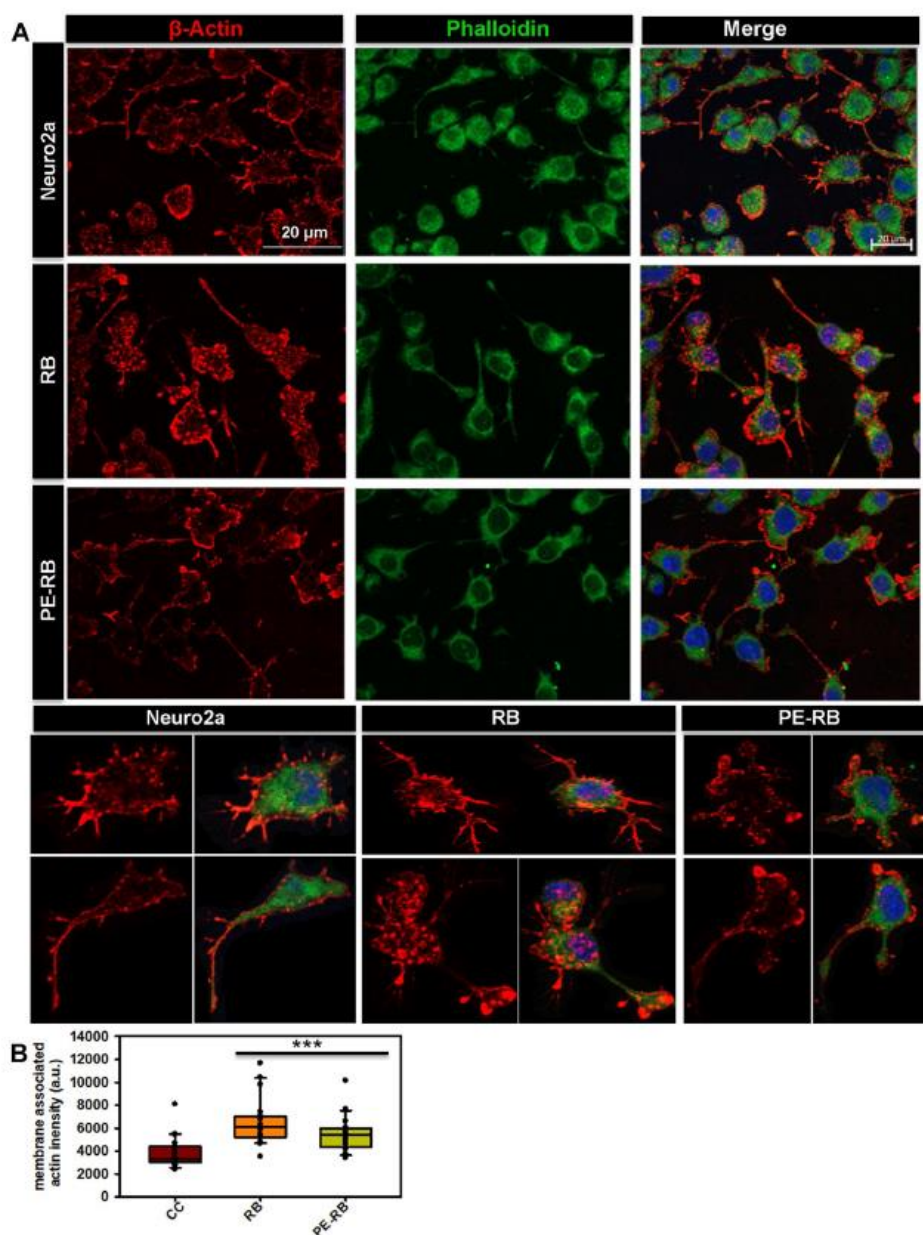


Figure 6. RB and PE-RB increase podosome-like structure in cells. (A) The immunofluorescence studies for actin cytoskeleton modulation in presence of RB and PE-RB. The podosome-like structure in the cell membrane were observed after RB and PE-RB treatment. (B) The quantification of membrane-associated actin suggesting the increased localization of actin in the membrane after RB and PE-RB treatment.

was also studied. In our work, 10 and 30 min irradiated cells were observed to possess an increased number of filopodia extensions. On the contrary cells exposed to 60 min of irradiation observed to have reduced filopodia numbers in comparison to cells with shorter irradiation time. The reduced potency of RB upon longer expo-

sure to irradiation could be a result of the photo-bleaching of dye (Fig. 7A,B). Thus, we speculate that RB and PE-RB treatment might accelerate the cell-migration as distinguished filopodial and growth cone modulation was observed after the treatment. Hence, the time-dependent studies suggested that understood that PE-RB and RB potentially modulated the cytoskeleton.

Protective effect of PE-RB in transgenic *Drosophila*. Tau mutant of *Drosophila* mimics the condition of human Tauopathy by overexpressing the Tau in the central nervous system of *Drosophila*. UAS E14 Tau lines carry 14 disease-associated mutations in Ser-Thr-Pro sites. Many studies have been carried on the *Drosophila* model for screening the molecules against AD³⁸. *Drosophila* UAS-E14 flies overexpressing Tau mimics the behavioural aspects of Tauopathy. RB and PE-RB were studied for their potency to rescue the memory and locomotor impairment in mutant *Drosophila* (Fig. 8A). Based on results of in-vitro assay on recombinant Tau, we have studied RB in concentration ranging from 10 to 500 μ M. The aim to use the higher concentration of RB was to observe the extent of RB toxicity in the in-vivo model. Negative geotaxis assay allows a rapid, high throughput screening of molecules on a large population of flies. A negative geotaxis assay was performed to study the effect of RB and PE-RB on the locomotory dysfunctions of UAS E-14 *Drosophila*. The flies treated with RB and PE-RB observed to have restored locomotory function. 20 μ M of RB and PE-RB observed to be maximum effective whereas, compared to RB, PE-RB found to more efficiency in rescuing the locomotory impairment (Fig. 8B). Succeeding larval crawling experiments were performed for studying locomotory behaviour. In our studies, we noticed that bell-shaped curve in the context of the number of grids crossed by larvae per minute. The larval crawling assay provides precise information for the early locomotor disabilities in *Drosophila*, thus the assay is being performed for screening of various therapeutic molecules. In our studies, 20 μ M of PE-RB efficiently restored the locomotory activity of larvae (Fig. 8C). Furthermore, the flies were tested for olfactory dysfunctions in order to study the protective effect of RB and PE-RB on the memory dysfunction. The flies exposed to RB and PE-RB were observed to be efficient in avoiding the bad odour of quinine as compared to untreated mutants. 20 μ M of RB showed a remarkable rescue of memory deficit in the flies (Fig. 8D). Thus, RB was found to be effective in rescuing Tau-mediated locomotory and memory deficit in flies. Overall results of in-vivo studies suggested that RB and PE-RB have the potency to rescue the Tau-mediated memory and locomotor impairment thus it could be considered as a therapeutic molecule against Tau.

Discussion

AD is prevailing at an exponential rate worldwide, which has emerged as a major cause of dementia³⁹. Various aspects of AD have been studied for screening of therapeutics. Intracellular aggregates of microtubule-associated protein Tau is considered to be a leading cause of neurodegeneration in AD⁴⁰. In physiological conditions, Tau is abundantly distributed in axons, which functions to stabilize the microtubules. Furthermore, Tau is being reported to be localized in the nucleus and dendrites, which might function in maintaining the synaptic plasticity and DNA integrity⁴¹. Accumulation of Tau aggregates alters the viability of neuron in numerous ways as they interfere with signalling cascades, induce ROS and downregulates the cytoskeleton machinery⁴². Different classes of dyes have been investigated as therapeutic molecules in AD. The diazo dye Congo red was reported to attenuate the amyloid- β -related toxicity. Similarly, a cyanine dye N744 was reported to efficiently inhibit the aggregation of Tau⁴³. Methylene blue and its derivatives have been studied as Tau aggregation inhibitors⁴³. Rose Bengal (RB) is a xanthene dye, which has been widely applied as a photosensitizer in photodynamic treatments²³. In our studies, RB was investigated for its efficiency against Tau aggregation. RB has been reported to inhibit the fibrilization of another AD-related protein A β -42⁴⁴. In present work, RB was observed to be efficient in attenuating the Tau aggregation even at the lower concentrations. In the present study, dual property of RB was observed, as RB inhibited the aggregation of soluble Tau and additionally, the PE-RB dissolved the mature Tau filaments. The biocompatibility of a molecule is among the necessary criteria to be evaluated for a therapeutic molecule. Thus, the toxicity of molecule in neuronal cells have to be considered⁴⁴. In our studies, RB and PE-RB showed low levels of cytotoxicity even at higher concentrations. Microtubules are the basic cytoskeleton elements that assist in maintaining the integrity and structure of cells. Microtubules can be addressed as "polymers" of Tubulin protein as α and β -tubulin polymerizes to generate the microtubules⁴⁵. Cytoskeleton network is a one of the potential for the screening of drugs against various diseases⁴⁶. Several cytoskeleton defects as microtubule destabilization, disturbed actin dynamics and axonal transport are being reported to be related to neurodegeneration⁴⁷. Thus, as a strategy for studying drugs for neurodegeneration, therapeutic molecules have been screened for their potency to revert the cytoskeleton defects⁴⁸. Molecules having the mode of action against the cytoskeleton integrity have been screened as a therapeutics for various diseases⁴⁹. Colchicine, rhizoxin, maytansine, centauriedin, combretastatin, etc.; are the therapeutic molecule, which targets tubulin⁵⁰⁻⁵³. Photodynamic therapy modulates cytoskeleton assembly in various aspects. The photo-excited porphyrin dye reported to inhibit the tubulin assembly, whereas the xanthene dye RB was observed to disrupt the actin network in cells^{54,55}. In our studies also, we observed that RB and PE-RB treatment modulates the cytoskeleton networks of cells. The growth cone and filopodia structure assist the cells in migration, cytokinesis etc⁵⁶. Our results suggests that RB and PE-RB can regulate the filopodia length, which suggested that the treatment might induce accelerated cell motility. Another function of filopodia is to facilitate the synapse formation⁵⁷. Here, we stated that RB and PE-RB treatment assists in the development of connections between the cells, increased filopodia, and actin-rich podosome structures suggested that the RB and PE-RB may induce the modulation in cell migration. Filopodia are actin-rich protrusions that assist the cell in migration and cell motility⁵⁸. AG1478 and cetuximab results in reduced cell migration by inhibiting actin dynamics⁵⁹. Calumenin-15 has been reported to increase filopodia formation by targeting member of TGF- β superfamily⁶⁰. Similarly, jasplakinolide (Jasp) also induces F-actin polymerization by activating ERK and AKT pathways⁶¹. Here based on present study we hypothesized that

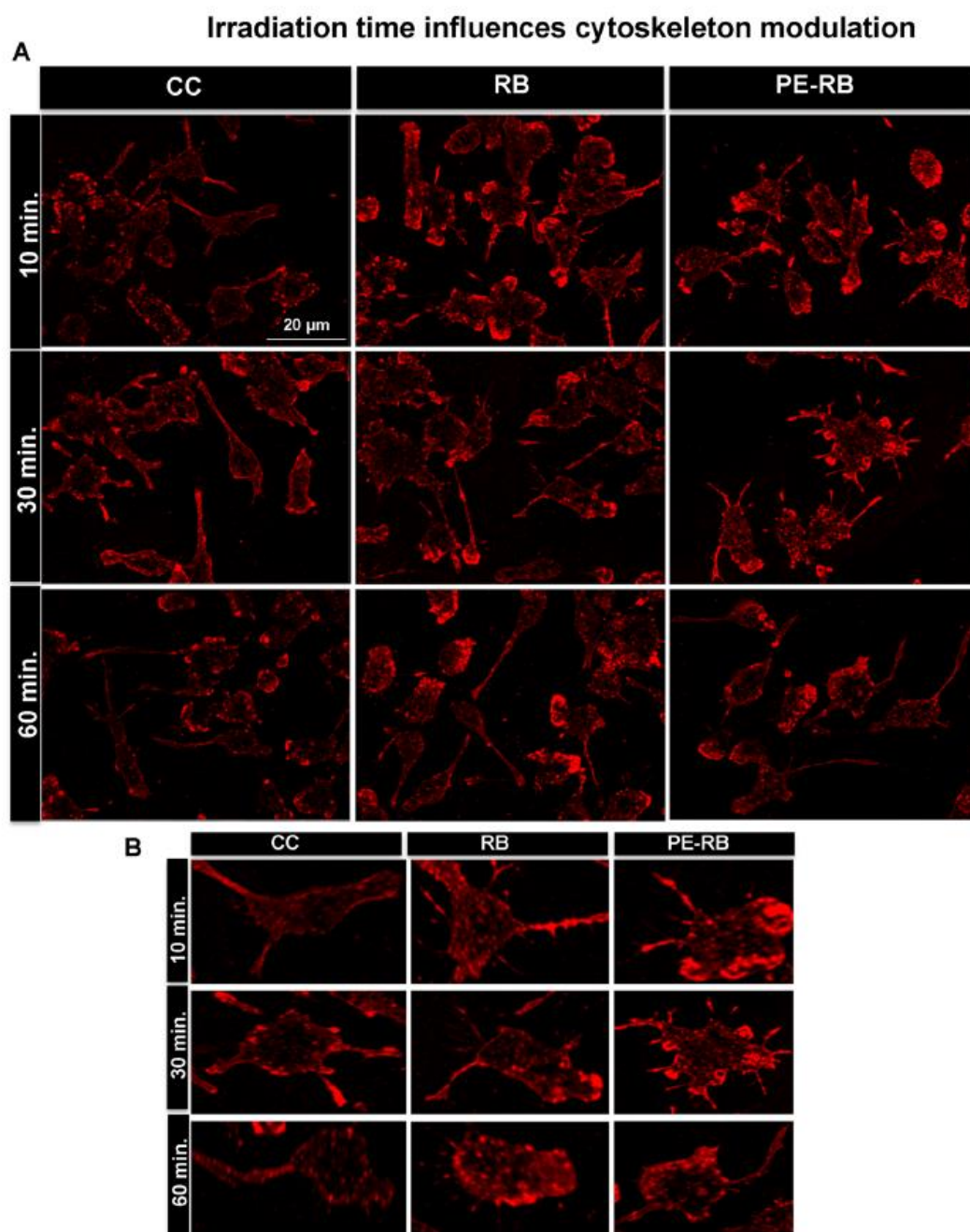


Figure 7. Time of irradiation influences the cytoskeleton. (A,B) The cells were irradiated for different time points (10, 30 and 60 min). The 10 min and 30 min experimental set showed increased number of filopodia in treated cells. Cells subjected to an irradiation for 60 min showed decreased number of filopodia.

RB and PE-RB may have potency to modulate various signalling cascades, which are involved in cytoskeleton dynamics. Tubulin is known to play role in neuronal differentiation⁶². The result of our present studies suggested that the PE-RB modulated the tubulin network of cell, thus it could be stated that PE-RB might have potency to induce the neuronal differentiation. *Drosophila* has a small, completely annotated and simple genotype. *Drosophila* has a 69% homology with human genotype, thus for several in-vivo studies, *Drosophila* has been chosen as a model organism⁶³. UAS E14 Tau is a transgenic flies, which mimics the condition of AD as it overexpresses

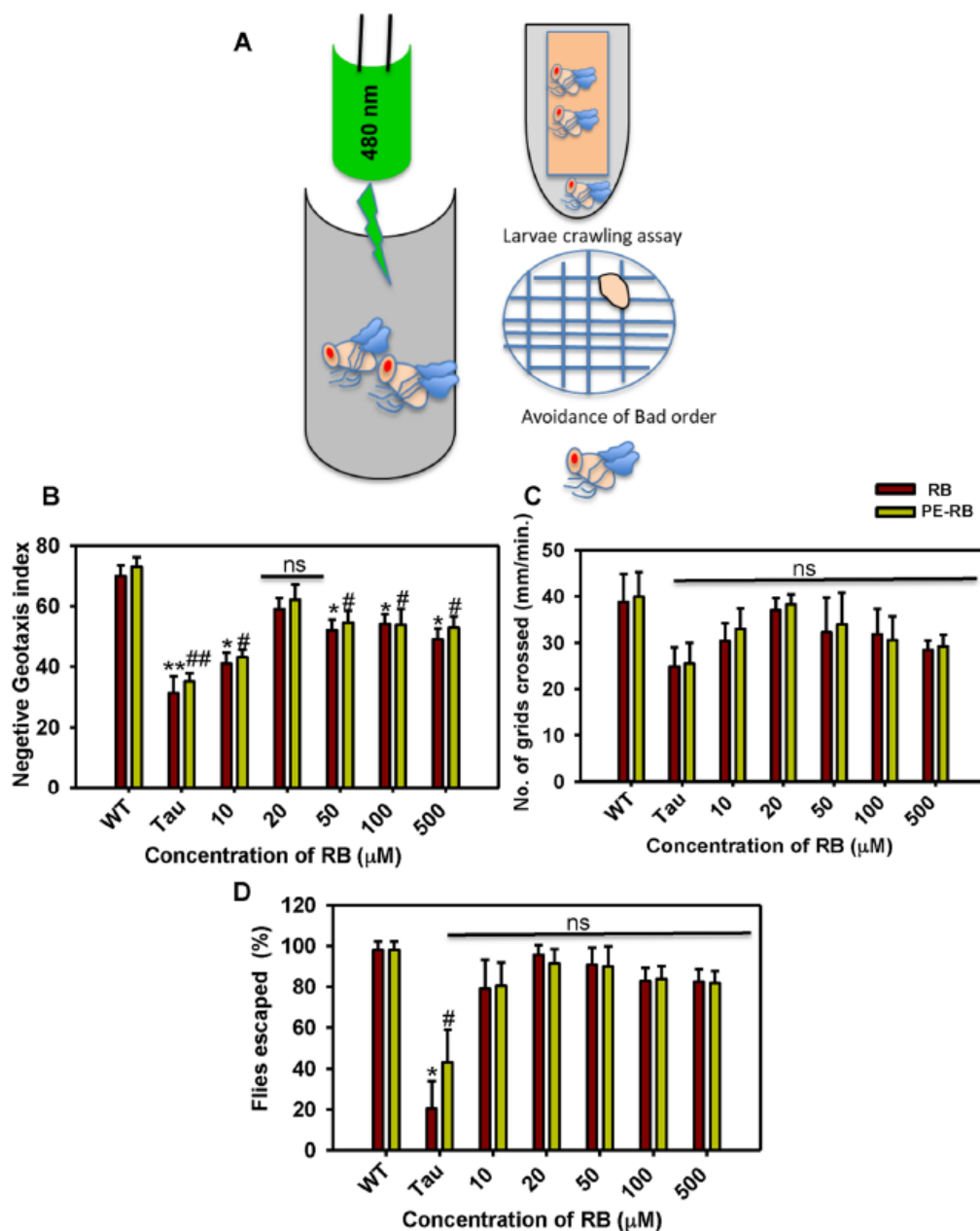
Effect of Rose Bengal on *Drosophila* longevity

Figure 8. RB and PE-RB rescue the Memory and locomotor deficits. (A) UAS E-14 *Drosophila* flies treated with RB and PE-RB, various locomotor and olfactory assay was carried for observing the potency of RB against Tau toxicity. (B) A rescue in locomotor function after RB and PE-RB treatment was observed in negative geotaxis assay. (C) The larval crawling assay suggesting the positive regulation of locomotor activity by RB and PE-RB treatment. (D) Olfactory learning assay suggested that the cognitive function in Tau mutant flies were restored after RB and PE-RB treatment. (* $p < 0.05$, ** $p < 0.001$, *** $p < 0.0001$, assigned for the difference between control and treated groups before photo-excitation. # $p < 0.05$, ## $p < 0.001$, ### $p < 0.0001$ represents the statistical difference between control and treated groups after photo-excitation.).

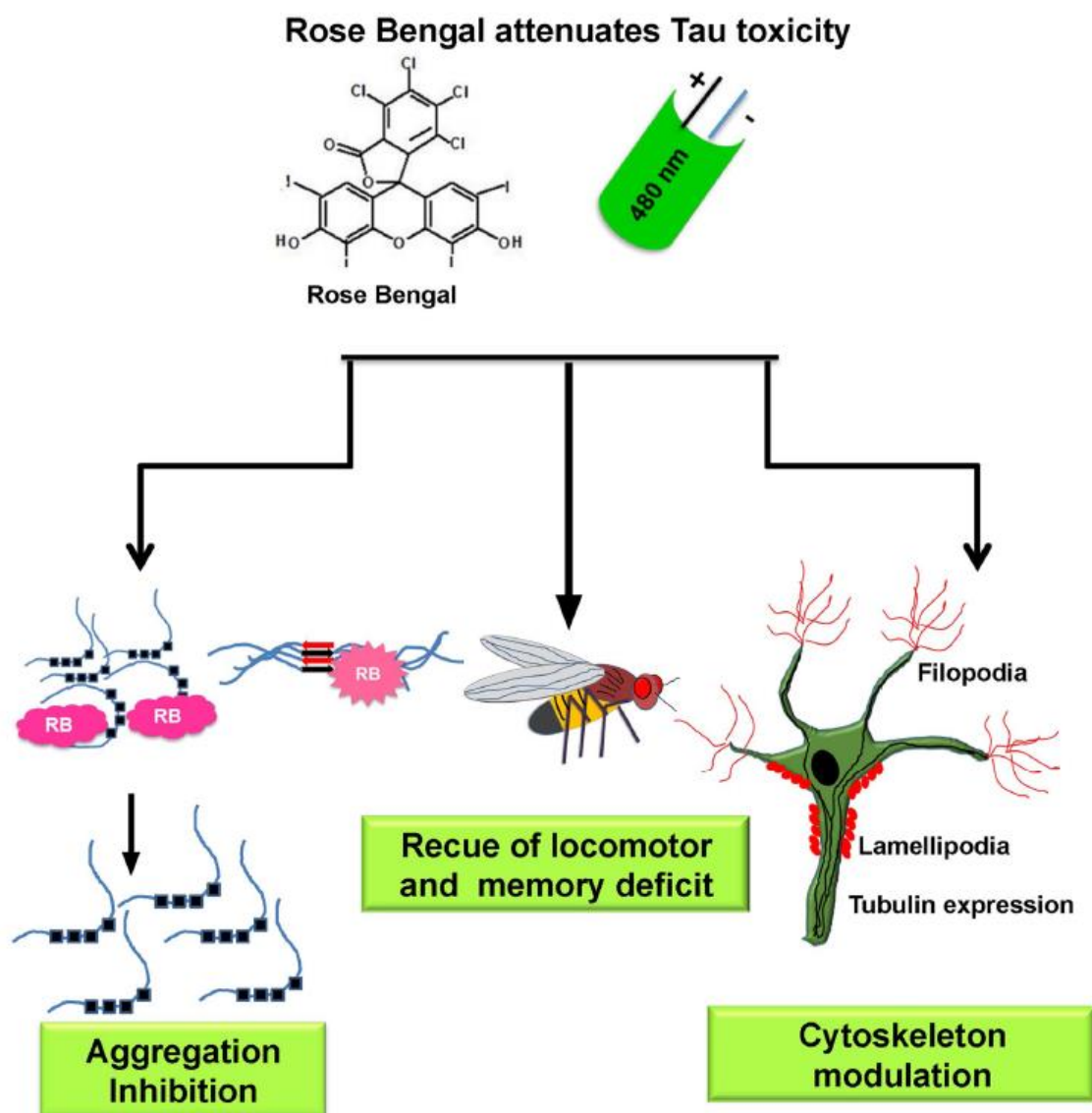


Figure 9. Rose Bengal attenuates the Tau toxicity. The RB attenuates Tau aggregation and photo-excited RB dissolves the Tau fibrils. The RB and PE-RB positively modulate the cytoskeleton. Memory and locomotor dysfunctions of UAS E14 Tau mutants were rescued after the RB and PE-RB treatment. Thus, RB was found effective against the various aspect of Tauopathy supporting it to be a neuroprotective molecule.

the Tau protein in nervous system³⁸. The screening of therapeutics have been done on the basis of their ability to restore the behavioural and memory deficits in flies²⁸. We found that 20 μ M RB and PE-RB efficiently restores the memory deficit and locomotor dysfunctions of mutant flies. The cumulative result of all the studies projects PE-RB and RB as a potential therapy against Tau aggregation and hence can be studied for further therapeutic property in AD (Fig. 9).

Conclusions

Tau aggregation is the major consequence of AD. The antagonist of Tau aggregation could be studied in the aspect of AD therapy. In our study, we observed that RB and PE-RB efficiently inhibit Tau fibrillization. The RB and PE-RB positively modulated the neuronal cytoskeleton. Additionally, in-vivo studies clearly suggested that RB and PE-RB have protective property against memory deficits and locomotor dysfunction in flies. Thus, it

could be suggested that RB and PE-RB are effective in in-vitro and in-vivo system against Tauopathy and could be studied as a lead molecule in the treatment of AD.

Materials and methods

Chemicals and reagents. MES (M3671), BSA (9048-46-8), BES (10191-18-1), BCA (B9643), CuSO₄ (C2284), ThS (T1892), MTT (M2128) and Rose Bengal (330000) were purchased from Sigma. IPTG (420322) and DTT (3870) were purchased from Calbiochem. Other chemicals such as Ampicillin (2007081), NaCl (194848), KCl (194844), Na₂HPO₄ (191437), KH₂PO₄ (19142), EGTA (194823), MgCl₂ (191421), PMSF (195381), Ammonium acetate (191404), Heparin (904108) and DMSO were from purchased from MP biomedical and protease inhibitor cocktail was from Roche (11697498001). Copper coated carbon grids were purchased from Ted Pella (01814.F, carbon type-B, 400 mesh Cu), DMEM advanced F12 media (12634010), Fetal Bovine Serum (16000044), Penstert cocktail (04693159001) and Anti-anti (15240062) were purchased from Gibco. Tubulin (Thermo PA1-41331), actin (Thermo MA5-15739) were procured from thermo, total Tau antibody K9JA was purchased from Dako (K9JA, Dako A0024). The secondary antibodies Alexa Fluor 488 (A11034) and Alexa Fluor 555 (A32727) were purchased from thermo.

Preparation of Tau. The recombinant full-length Tau was purified as per published protocol¹¹. The recombinant Tau was expressed in *E.coli* BL21* strain. The culture was incubated at 37 °C till OD₆₀₀ reached 0.5 to 0.6. It was then induced with 0.5 mM IPTG and was further incubated for 4 h. The cells were harvested by centrifugation at 4,000 rpm for 10 min. The cells were lysed using Constant Cell Disruption systems. The cells were resuspended in Buffer A composed of 50 mM MES, 1 mM EGTA, 2 mM MgCl₂, 5 mM DTT, 1 mM PMSF and 50 mM NaCl, this was subjected to homogenization at 15,000 psi pressure. The obtained lysate was heated at 90 °C for 20 min in presence of 0.5 M NaCl and 5 mM DTT. This was cooled and centrifuged at 40,000 rpm for 45 min. The supernatant was collected and dialyzed overnight against Buffer A before loading to the cation exchange column. Tau protein was eluted by applying ionic gradient of 1 M NaCl. The protein quality was analyzed by SDS-PAGE and further subjected to size-exclusion chromatography. The obtained fractions was analysed on SDS-PAGE, pooled and concentrated. The concentration was estimated by BCA assay and stored at -80 °C until further used.

In-vitro Tau aggregation. Tau aggregation was induced at 37 °C with heparin as previously described¹⁶. Tau in the presence of anionic inducer such as heparin, RNA, arachidonic acid, etc. undergoes aggregation. Among all these molecules heparin-induced Tau aggregation is the widely accepted model for in vitro Tauopathy studies. Previous observations suggested the heparin-mediated Tau aggregation demonstrates the transition of Tau from random coil to β-sheets. Taniguchi et al. demonstrated the inhibition of heparin-induced Tau filaments by phenothiazine, polyphenols, and porphyrins. In present study Tau aggregation was induced by heparin where the soluble full-length Tau was incubated with heparin (17,500 kDa) at a ratio of 4:1. The reaction was carried out in 20 mM BES buffer supplemented with 25 mM NaCl, 1 mM DTT, 0.01% NaN₃ and protease inhibitor cocktail mixtures.

Thioflavin S fluorescence assay. The effect of RB on aggregation of Tau was measured by Thioflavin S (ThS) fluorescence assay¹⁷. ThS is a mixture of methylated dehydrothioluidine and sulfonic acid and has a property to fluoresce to β-sheet structures. The fluorescence measurement was carried out by incubating 2 μM of Tau with ThS at a ratio of 1:4 for 15 min. All the reaction mixtures were measured in triplicate in TECAN Infinite M200 PRO spectrophotometer at an excitation of 440 nm and emission of 521 nm. Further, the data were analyzed using SigmaPlot 10.0.

Circular dichroism spectroscopy. The conformational changes of Tau were analyzed by using CD spectroscopy in the far-UV region. In native conditions, Tau has typical random coil conformation, but the aggregation causes its conformational change to β-sheet. The effect of RB on conformational changes of Tau was studied as described previously¹⁶. All the spectra were measured in Jasco J-815 spectrometer by diluting full-length Tau to 3 μM in 50 mM sodium phosphate buffer at pH 6.8 (Supplementary information 1).

Photodynamic treatment of Tau aggregates. For analyzing the effect of photo-excited RB on Tau aggregates, the aggregates were incubated for 1 h in dark with varying concentrations of RB (2, 5, 10, 20 and 40 μM). 200 μL of the reaction mixture was added in 96 black well plate (Eppendorf) and was irradiated in dark using green LED. After 1 h of incubation, the samples were analyzed by ThS fluorescence assay and SDS-PAGE for the presence of disintegrated Tau. The irradiation dose or irradiance was calculated by the formula

$$E = \frac{\text{Power}}{\text{Area}} * \text{Time of irradiation}$$

where E is irradiance, time was calculated in terms of seconds.

SDS-PAGE. The inhibitory effect of RB on Tau aggregation was observed by SDS-PAGE. Aggregates are resolved around 250 kDa as higher molecular weight species thus, the effect of RB on aggregation propensity of Tau can be observed by 10% SDS-PAGE. The experiments were done by using BIO-RAD Mini-PROTEAN electrophoresis unit.

Transmission electron microscopy. The morphological analysis of Tau fibrils were done by electron microscopy and the samples were prepared according to published protocol¹⁷. For electron microscopic analysis, 2 μM of Tau was incubated on carbon-coated copper grids. Following this, the samples were negatively stained with 2% uranyl acetate. The images were captured by TECNAI T20 at 120 kV.

Cytotoxicity assay. The cell viability was analyzed by methylthiazolyl-diphenyl-tetrazolium bromide (MTT) assay. The method was followed according to published protocol²⁰. Neuro2a cells (ATCC CCL-131) were cultured in advanced DMEM F-12 media supplemented with 10% FBS and glutamine. 10,000 cells/well were seeded in 96 well plates for the assays. After 24 h, the cells were treated with various concentrations of RB for 24 h; followed by the addition of MTT at a concentration of 0.5 mg/mL and incubated at 37 °C for 4 h. The formazan crystals formed were dissolved in 100 μL of 100% DMSO. Cell viability was evaluated by measuring the absorbance at 570 nm. Similarly, cells were incubated with 2.5 μM of full-length Tau aggregates to observe their cytotoxicity. Additionally, RB was also added to cells along with aggregates for analyzing its effect of RB in the presence of aggregates. RB treated cells were subjected to 10 min of irradiation for the cytotoxic analysis of photo-excited RB.

Immunofluorescence. Neuro2a cells were seeded at a density of 25,000 cells on glass coverslips. The cells were treated with 100 nM RB and incubated overnight at 37 °C. Similarly, another set of cells treated with 100 nM of RB were irradiated with green light for 10 min and incubated at 37 °C for 24 h. The cells were fixed with absolute methanol for 20 min at -20 °C. After fixation, cells were permeabilized by 0.2% Triton X-100 and after 3 subsequent PBS washes the cells were incubated with 5% horse serum for 1 h. Further primary antibodies against tubulin (Thermo PA1-41331), actin (Thermo MA5-15739) and Tau (K9JA, Dako A0024) were added and incubated overnight. The cells were incubated with Alexa Fluor 488 (A11034) and Alexa Fluor 555 (A32727) tagged secondary antibodies. The nucleus was stained with DAPI. The cells were scanned by Zeiss Axio observer 7.0, apotome 2.0 inverted microscope using 63X magnifications in oil emersion.

Fly stocks and genetics. The transgenic *Drosophila* strain used in this study was UAS-Tau E14. ELAV-Gal4 driver line was obtained from the National Drosophila Stock Centre at the University of Mysore, Mysore, Karnataka, India. *Drosophila* strains were raised on standard medium. Fly cultures and crosses were carried out at 25 °C. The stocks has been maintained as per published protocol^{20,64}.

Fly husbandry. Flies were maintained on standard banana-jaggery medium (SM) under standard laboratory conditions of 24 ± 1 °C temperature, $75 \pm 5\%$ relative humidity, and 12:12 light and dark cycle (SLC)⁶⁴. Flies were maintained in a 2 week discrete generation cycle for 10 generations before being used in this study. The adult density was regulated at about 100 flies per half-pint bottle with 25 mL of SM in 10 bottles. Flies from 10 bottles were combined into a single breeding cage, hereafter referred to as parental cage (PC).

Preparation of diet. A total of 2.5 L of SM was prepared and split into 5 batches of 500 mL each as described previously²⁸. For the control group, only SM was poured into the bottles. For the RB-supplemented media, 10, 20, 50, 100 and 500 μM of RB was added to SM and mixed thoroughly just before pouring into the bottles. All bottles were plugged with non-adsorbent cotton and the media was allowed to solidify under room temperature.

Larval feeding behaviour assay. The obtained eggs were transferred at a density of 50-eggs/6 mL of SM and allowed to develop till early third instar (as referred in²⁰). The early third instar larvae were removed from the SM vials and used in the feeding behaviour assay. Larvae were individually transferred to an assay Petri plate of 5 cm diameter containing 10 mL of either liquid SM (SM without agar) or liquid SM supplemented with different concentrations of RB and allowed for 5 s for acclimation. The feeding rate was measured as the mean number of sclerite retractions in 2 consecutive 30 s intervals. The average of the 2 rates was taken as the feeding rate of that larva. 20 larvae were assayed for each of the 2 treatment groups. The feeding rate of assays were replicated 4 times. A total of 160 larvae were assayed for the feeding rate.

Negative geotaxis assay. The ability to move against gravity and climb indicates the level of physical fitness of test animals (as referred in²⁰). The vertical climbing ability of male flies that emerged from different treatment bottles were assessed. 20 male flies per treatment group were collected and transferred to empty, 0–15 cm graduated vial. The vial was gently tapped and placed in a vertical position. The number of flies that crossed the 15 cm mark in 30 s were counted. Three trials were conducted on each set of 20 flies. The data were expressed as the percentage of flies that crossed 15 cm mark.

Larval olfactory behaviour. The olfactory test was carried out by employing the previous method with minor modifications (as referred in²⁰). Larvae were briefly dried on a filter paper before being placed at the centre of the Petri dish. The Petri dish containing 20 μL of Quinine sulphate dispensed on each of the 2 0.5 cm radius filter discs were placed in the diametrically opposite position to Quinine zones. After 2 min of placing the larvae and covering the petri dish, the numbers of larvae in different zones were counted to calculate the percentage of larvae avoiding the bad odour after training.

Statistical analysis. The statistical analysis was done using unpaired Student's *t*-test. Untransformed (raw) data were analyzed and plotted by SigmaPlot 10.0 software. The statistical analysis were represented as *, ** and *** where * $p < 0.05$, ** $p < 0.001$, *** $p < 0.0001$.

Data availability

All the data generated during various experiments are available from the authors on reasonable request.

Received: 23 January 2020; Accepted: 29 June 2020

Published online: 23 July 2020

References

- Association, A. s. 2018 Alzheimer's disease facts and figures. *Alzheimer's Dementia* **14**, 367–429 (2018).
- Gorantla, N. V. & Chinnathambi, S. Tau protein squired by molecular chaperones during Alzheimer's disease. *J. Mol. Neurosci.* **66**, 356–368 (2018).
- Ballatore, C., Lee, V.M.-Y. & Trojanowski, J. Q. Tau-mediated neurodegeneration in Alzheimer's disease and related disorders. *Nat. Rev. Neurosci.* **8**, 663 (2007).
- Wang, Y. & Mandelkow, E. Tau in physiology and pathology. *Nat. Rev. Neurosci.* **17**, 22 (2016).
- Iqbal, K. *et al.* Tau pathology in Alzheimer disease and other tauopathies. *Biochimica et Biophysica Acta (BBA)-Molecular Basis of Disease* **1739**, 198–210 (2005).
- Das, R. & Chinnathambi, S. Microglial priming of antigen presentation and adaptive stimulation in Alzheimer's disease. *Cell. Mol. Life Sci.* **1**, 1–14 (2019).
- Lee, V.M.-Y. & Trojanowski, J. Q. The disordered neuronal cytoskeleton in Alzheimer's disease. *Curr. Opin. Neurobiol.* **2**, 653–656 (1992).
- Calcul, L., Zhang, B., Jinwal, U. K., Dickey, C. A. & Baker, B. J. Natural products as a rich source of tau-targeting drugs for Alzheimer's disease. *Future Med. Chem.* **4**, 1751–1761 (2012).
- Li, W. *et al.* Inhibition of tau fibrillization by oleocanthal via reaction with the amino groups of tau. *J. Neurochem.* **110**, 1339–1351 (2009).
- Pickhardt, M. *et al.* Anthraquinones inhibit tau aggregation and dissolve Alzheimer's paired helical filaments in vitro and in cells. *J. Biol. Chem.* **280**, 3628–3635 (2005).
- Gorantla, N. V., Das, R., Mulani, F. A., Thulasiram, H. V. & Chinnathambi, S. Neem derivatives inhibits tau aggregation. *J. Alzheimer's Dis. Rep.* **3**, 169–178 (2019).
- Necula, M., Chirita, C. N. & Kuret, J. Cyanine dye N744 inhibits tau fibrillization by blocking filament extension: implications for the treatment of tauopathic neurodegenerative diseases. *Biochemistry* **44**, 10227–10237 (2005).
- Oz, M., Lorke, D. E. & Petroianu, G. A. Methylene blue and Alzheimer's disease. *Biochem. Pharmacol.* **78**, 927–932 (2009).
- Li, Q. Q., Chu, T. T., Chen, Y. X. & Li, Y. M. Tau protein associated inhibitors in Alzheimer disease. *Chin. J. Chem.* **32**, 964–968 (2014).
- Bulic, B. *et al.* Development of tau aggregation inhibitors for Alzheimer's disease. *Angew. Chem. Int. Ed.* **48**, 1740–1752 (2009).
- Gorantla, N. V. *et al.* Molecular complexes for effective inhibition of tau aggregation. *bioRxiv*. <https://doi.org/10.1101/363572> (2018).
- Sonawane, S. K., Ahmad, A. & Chinnathambi, S. Protein-capped metal nanoparticles inhibit tau aggregation in Alzheimer's disease. *ACS Omega* **4**, 12833–12840 (2019).
- Dias-Santagata, D., Fulga, T. A., Duttaroy, A. & Feany, M. B. Oxidative stress mediates tau-induced neurodegeneration in *Drosophila*. *J. Clin. Investig.* **117**, 236–245 (2007).
- Taniguchi, S. *et al.* Inhibition of heparin-induced tau filament formation by phenothiazines, polyphenols, and porphyrins. *J. Biol. Chem.* **280**, 7614–7623 (2005).
- Dubey, T., Gorantla, N. V., Chandrashekar, K. T. & Chinnathambi, S. Photoexcited toluidine blue inhibits Tau aggregation in Alzheimer's disease. *ACS Omega* **4**, 18793–18802 (2019).
- Costa, A. C. B. P. *et al.* The effects of rose bengal-and erythrosine-mediated photodynamic therapy on *Candida albicans*. *Mycoses* **55**, 56–63 (2012).
- Shrestha, A., Hamblin, M. R. & Kishen, A. Photoactivated rose bengal functionalized chitosan nanoparticles produce antibacterial/biofilm activity and stabilize dentin-collagen. *Nanomed. Nanotechnol. Biol. Med.* **10**, 491–501 (2014).
- Wang, B. *et al.* Rose-bengal-conjugated gold nanorods for in vivo photodynamic and photothermal oral cancer therapies. *Biomaterials* **35**, 1954–1966 (2014).
- Lee, J. S., Lee, B. I. & Park, C. B. Photo-induced inhibition of Alzheimer's β -amyloid aggregation in vitro by rose bengal. *Biomaterials* **38**, 43–49 (2015).
- Gorantla, N. V., Shkumatov, A. V. & Chinnathambi, S. Conformational dynamics of intracellular tau protein revealed by CD and SAXS. *Methods Mol Biol.* **1523**, 3–20 (2018).
- Gorantla, N. V. *et al.* Molecular cobalt (II) complexes for tau polymerization in Alzheimer's disease. *ACS Omega* **4**, 16702–16714 (2019).
- Dubey, T. & Chinnathambi, S. Brahmi (*Bacopa monnieri*): An ayurvedic herb against the Alzheimer's disease. *Arch. Biochem. Biophys.* **1**, 108153 (2019).
- Dubey, T., Gorantla, N., Chandrashekar, K. & Chinnathambi, S. Photo-excited Toluidine Blue inhibits full-length Tau aggregation in Alzheimer's disease. (2019).
- Bamburg, J. R. & Bloom, G. S. Cytoskeletal pathologies of Alzheimer disease. *Cell Motil. Cytoskelet.* **66**, 635 (2009).
- Howard, J. Mechanics of motor proteins and the cytoskeleton. (2001).
- Hammond, J. W., Cai, D. & Verhey, K. J. Tubulin modifications and their cellular functions. *Curr. Opin. Cell Biol.* **20**, 71–76 (2008).
- Pollard, T. D., Blanchoin, L. & Mullins, R. D. Actin dynamics. *J. Cell Sci.* **114**, 3 (2001).
- Mitchison, T. & Cramer, L. Actin-based cell motility and cell locomotion. *Cell* **84**, 371–379 (1996).
- Simon, V. & Pon, L. Actin-based organelle movement. *Experientia* **52**, 1117–1122 (1996).
- Dillon, C. & Goda, Y. The actin cytoskeleton: integrating form and function at the synapse. *Annu. Rev. Neurosci.* **28**, 25–55 (2005).
- Machesky, L. M. Lamellipodia and filopodia in metastasis and invasion. *FEBS Lett.* **582**, 2102–2111 (2008).
- Cottrell, W. J., Paquette, A. D., Keymel, K. R., Foster, T. H. & Oseroff, A. R. Irradiance-dependent photobleaching and pain in δ -aminolevulinic acid-photodynamic therapy of superficial basal cell carcinomas. *Clin. Cancer Res.* **14**, 4475–4483 (2008).
- Nezis, I. P. *et al.* Ref (2) P, the *Drosophila melanogaster* homologue of mammalian p62, is required for the formation of protein aggregates in adult brain. *J. Cell Biol.* **180**, 1065–1071 (2008).
- Alzheimer, A. Alzheimer's disease facts and figures. *Alzheimer's Dementia J. Alzheimer's Assoc.* **11**, 332 (2015).
- Avila, J., Lucas, J. J., Perez, M. & Hernandez, F. Role of tau protein in both physiological and pathological conditions. *Physiol. Rev.* **84**, 361–384 (2004).

41. Sultan, A. *et al.* Nuclear tau, a key player in neuronal DNA protection. *J. Biol. Chem.* **286**, 4566–4575 (2011).
42. Iqbal, K., Liu, F. & Gong, C.-X. Tau and neurodegenerative disease: the story so far. *Nat. Rev. Neurol.* **12**, 15 (2016).
43. Crowe, A. *et al.* Aminothienopyridazines and methylene blue affect Tau fibrillization via cysteine oxidation. *J. Biol. Chem.* **288**, 11024–11037 (2013).
44. Moghimi, S. M. *et al.* A two-stage poly (ethylenimine)-mediated cytotoxicity: implications for gene transfer/therapy. *Mol. Ther.* **11**, 990–995 (2005).
45. Desai, A. & Mitchison, T. J. Microtubule polymerization dynamics. *Annu. Rev. Cell Dev. Biol.* **13**, 83–117 (1997).
46. Rao, J. Y. & Li, N. Microfilament actin remodeling as a potential target for cancer drug development. *Curr. Cancer Drug Targets* **4**, 345–354 (2004).
47. Eira, J., Silva, C. S., Sousa, M. M. & Liz, M. A. The cytoskeleton as a novel therapeutic target for old neurodegenerative disorders. *Prog. Neurobiol.* **141**, 61–82 (2016).
48. Ramaekers, F. C. & Bosman, F. T. The cytoskeleton and disease. *J. Pathol. J. Pathol. Soc. Great Br. Ireland* **204**, 351–354 (2004).
49. Giganti, A. & Friederich, E. The actin cytoskeleton as a therapeutic target: state of the art and future directions. *Prog. Cell Cycle Res.* **5**, 511–525 (2003).
50. Marques-da-Silva, C., Chaves, M., Castro, N., Coutinho-Silva, R. & Guimaraes, M. Colchicine inhibits cationic dye uptake induced by ATP in P2X2 and P2X7 receptor-expressing cells: implications for its therapeutic action. *Br. J. Pharmacol.* **163**, 912–926 (2011).
51. Behrang, N., Hashemi, M., Borna, H. & Akbarzadeh, A. Microtubules and tubulins as target for some natural anticancer agents extracted from marines, bacterium, and fungus. *Adv. Stud. Biol.* **4**, 1–9 (2012).
52. Lacey, E. The role of the cytoskeletal protein, tubulin, in the mode of action and mechanism of drug resistance to benzimidazoles. *Int. J. Parasitol.* **18**, 885–936 (1988).
53. Delmonte, A. & Sessa, C. AVE8062: a new combretastatin derivative vascular disrupting agent. *Expert Opin. Investig. Drugs* **18**, 1541–1548 (2009).
54. Etminan, N. *et al.* Modulation of migratory activity and invasiveness of human glioma spheroids following 5-aminolevulinic acid-based photodynamic treatment. *J. Neurosurg.* **115**, 281–288 (2011).
55. Soldani, C. *et al.* Apoptosis in tumour cells photosensitized with Rose Bengal acetate is induced by multiple organelle photodamage. *Histochem. Cell Biol.* **128**, 485–495 (2007).
56. Forscher, P. & Smith, S. J. Actions of cytochalasins on the organization of actin filaments and microtubules in a neuronal growth cone. *J. Cell Biol.* **107**, 1505–1516 (1988).
57. Toni, N. *et al.* Synapse formation on neurons born in the adult hippocampus. *Nat. Neurosci.* **10**, 727 (2007).
58. Svitkina, T. The actin cytoskeleton and actin-based motility. *Cold Spring Harbor Perspect. Biol.* **10**, a018267 (2018).
59. Ohnishi, Y., Yasui, H., Kakudo, K. & Nozaki, M. Regulation of cell migration via the EGFR signaling pathway in oral squamous cell carcinoma cells. *Oncol. Lett.* **13**, 930–936 (2017).
60. Feng, H. *et al.* Calumenin-15 facilitates filopodia formation by promoting TGF- β superfamily cytokine GDF-15 transcription. *Cell Death Dis.* **4**, e870 (2013).
61. Reddy, P., Deguchi, M., Cheng, Y. & Hsueh, A. J. Actin cytoskeleton regulates Hippo signaling. *PLoS ONE* **8**, e73763 (2013).
62. Guo, J., Walss-Bass, C. & Ludueña, R. F. The β isotypes of tubulin in neuronal differentiation. *Cytoskeleton* **67**, 431–441 (2010).
63. Rijsewijk, F. *et al.* The *Drosophila* homology of the mouse mammary oncogene int-1 is identical to the segment polarity gene wingless. *Cell* **50**, 649–657 (1987).
64. Chandrashekar, K., Popli, S. & Shakarad, M. Curcumin enhances parental reproductive lifespan and progeny viability in *Drosophila melanogaster*. *Age* **36**, 9702 (2014).

Acknowledgements

This project is supported by grants from the in-house, National Chemical Laboratory-Council of Scientific Industrial Research-(CSIR-NCL) Grant MLP029526. Tau constructs were kindly gifted by Prof. Roland Brandt from the University of Osnabruck, Germany. Tushar Dubey and Nalini Vijay Gorantla acknowledge the fellowship from the University of Grant Commission (UGC), India.

Author contributions

S.C. designed the experiments, T.D., N.V. and S.C. carried out the experiments, T.D. and S.C. analyzed the data and wrote the article. *Drosophila* studies were carried out by K.T.C. S.C. conceived the idea of the project, provided resources, supervised the project and wrote the manuscript. All authors contributed to the discussions and manuscript review.

Competing interests

The authors declare no competing interests.

Additional information

Supplementary information is available for this paper at <https://doi.org/10.1038/s41598-020-69403-2>.

Correspondence and requests for materials should be addressed to S.C.

Reprints and permissions information is available at www.nature.com/reprints.

Publisher's note Springer Nature remains neutral with regard to jurisdictional claims in published maps and institutional affiliations.



Open Access This article is licensed under a Creative Commons Attribution 4.0 International License, which permits use, sharing, adaptation, distribution and reproduction in any medium or format, as long as you give appropriate credit to the original author(s) and the source, provide a link to the Creative Commons license, and indicate if changes were made. The images or other third party material in this article are included in the article's Creative Commons license, unless indicated otherwise in a credit line to the material. If material is not included in the article's Creative Commons license and your intended use is not permitted by statutory regulation or exceeds the permitted use, you will need to obtain permission directly from the copyright holder. To view a copy of this license, visit <http://creativecommons.org/licenses/by/4.0/>.

© The Author(s) 2020



Received: 21 January 2021 | Revised: 19 February 2021 | Accepted: 21 February 2021

DOI: 10.1002/cm.21655

REVIEW ARTICLE



Photodynamic sensitizers modulate cytoskeleton structural dynamics in neuronal cells

Tushar Dubey^{1,2} | Subashchandra Chinnathambi^{1,2} ¹Neurobiology Group, Division of Biochemical Sciences, CSIR-National Chemical Laboratory, Pune, India²Academy of Scientific and Innovative Research (AcSIR), Ghaziabad, India**Correspondence**Subashchandra Chinnathambi, Neurobiology group, Division of Biochemical Sciences, CSIR-National Chemical Laboratory (CSIR-NCL), Dr. Homi Bhabha Road, 411008 Pune, India.
Email: s.chinnathambi@ncl.res.in**Funding information**

CSIR-National Chemical Laboratory, Grant/Award Number: MLP029526

Abstract

The neuronal cytoskeleton plays a crucial role in maintaining cell integrity and functioning of neurons. Cytoskeleton deformities have been reported to be associated with neurodegenerative diseases thus; cytoskeleton can be targeted for therapeutic strategies. The therapeutic application of photosensitive molecule is termed as photodynamic therapy (PDT). PDT has been applied in the field of dermatology, cancer biology, and antimicrobial therapy. PDT induces several changes in cells, which include induction of apoptosis, DNA damage, and induction of inflammatory response. PDT has been also reported to modulate cytoskeleton such as actin dynamics. The *in vitro* studies suggested that PDT using dyes such as Toluidine Blue and Rose Bengal effectively modulated the actin cytoskeleton, neurite outgrowth, tubulin, and Tau aggregation. In this review, we focused on the effect of photosensitized molecules on various cytoskeleton proteins. We hypothesize that PDT could have potency against Alzheimer's disease and other neurodegenerative disorders.

KEYWORDS

actin, Alzheimer's disease, cytoskeleton modulation, neuronal cytoskeleton, photodynamic therapy, tubulin

1 | OVERVIEW OF PHOTODYNAMIC THERAPY: THE EMERGING THERAPY FOR VARIOUS DISEASES

Photodynamic therapy (PDT) is the novel strategy for the application of photoexcited molecules to the target, which leads to the generation of singlet oxygen species (Gold, 2007). PDT involves two main steps, first is the absorption of light by the photosensitizer and second is the transfer of energy by the excited state of the photosensitizer molecule to the oxygen molecule. In the first step, the photosensitizer upon absorption of light undergoes the transition from the ground

state to the singlet excited state. Since the excited singlet state is short-lived, it gets converted to a triplet state via a process known as "intersystem crossing" (Juarranz, Jaén, Sanz-Rodríguez, Cuevas, & González, 2008). This triplet state is relatively long-lived and participates in two types of reaction called Type I and II reactions. In Type I reaction, it reacts with a substrate and molecular oxygen to form free radicals. In Type II reaction, the triplet state transfers its energy to oxygen directly and converts to a singlet state. The singlet oxygen species is considered to be responsible for the effect of PDT (Castano, Demidova, & Hamblin, 2004) (Figure 1). PDT involves the application of various light sensitive molecules termed as "photosensitizer." These photosensitizers upon irradiation with a characteristic wavelength of light leads to the generation of singlet oxygen species (Levy, 1994). The molecules having tetrapyrrole structures belonging to classes porphyrin, choline, bacteriochlorin, phthalocyanin, and so forth, are generally considered as photosensitizers (Chilakamarthi & Giribabu, 2017). The tetrapyrrole photosensitizers generally follow

Abbreviations: AD, Alzheimer's disease; Arp2/3 complex, actin-related protein 2/3 complex; CDC 42, cell division control protein 42 homolog; DAAM, Dishevelled-associated activator of morphogenesis; F-actin, filamentous actin; G-actin, globular actin; LPA, lysophosphatidic acid; MAPs, microtubule-associated proteins; MB, Methylene Blue; MTOC, microtubule organization center; PDT, photodynamic therapy; PTMs, posttranslational modifications; RB, Rose Bengal; Rho, Ras homologous (Rho) protein; Sirt2, Sirtuinins; TB, Toluidine Blue; WASP, Wiskott-Aldrich syndrome family protein.

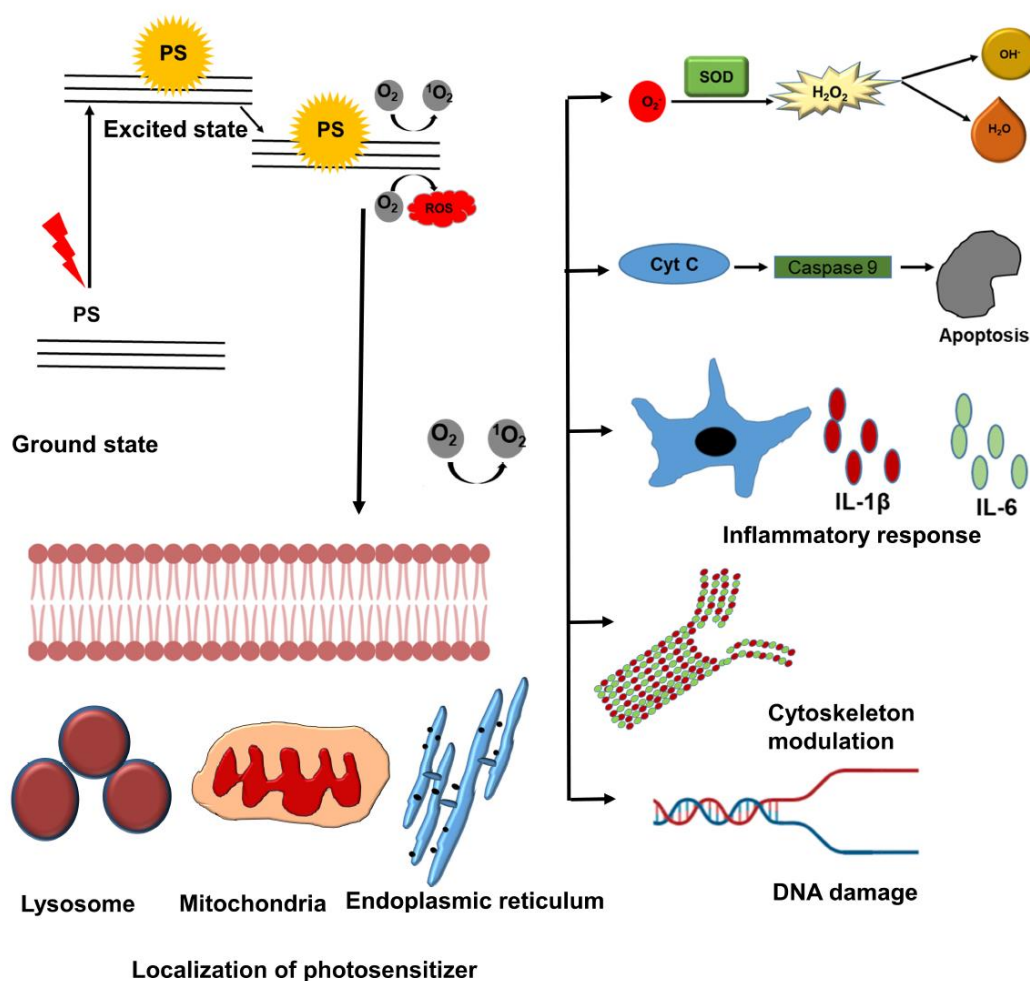


FIGURE 1 The effect of photodynamic therapy (PDT) in cells. PDT involves the excitation of photosensitizer after irradiation, which generates singlet oxygen species. In cells, photosensitizer accumulates in various organelles as lysosomes, endoplasmic reticulum, and mitochondria. PDT targets several components of cells, cytoskeleton modulation, DNA damage, and induction of inflammation

Type I reaction for the generation of singlet oxygen species. The porphyrinoid compounds, including chlorins, bacteriochlorins, phthalocyanines, and other related structures are majorly used as photosensitizer (Abrahamse & Hamblin, 2016). The porphyrin compounds such as meta-tetra(hydroxyphenyl) porphyrin, the meta isomer of 5,10,15,20-tetra(hydroxyphenyl)porphyrin, and 5,10,15,20-tetrakis (4-sulfonatophenyl)-21H,23H-porphyrin are considered as second-generation photosensitizer (Wilson, 2007). The methyl ester of aminolevulinic acid (ALA), methyl aminolevulinate, and the *n*-hexyl ester of ALA “hexaminolevulinate” have been approved as therapeutic agents for the treatment of carcinomas (Stepp et al., 2007). Several compounds belonging to the cholin family have been applied as photosensitizers. Meta-tetra(hydroxyphenyl)chlorin, tin ethyl etiopurpurin, *N*-aspartyl chlorin e6 are examples of cholin-based photosensitizer isolated from chlorophyll A. Pheophorbides are another class of

pyrrole-based photosensitizer, which is derived from chlorophyll. WST09 and WST11 are the bacterial origin pyrrole-based photosensitizer derived from bacteriochlorophyll A (Beems et al., 1987). Phthalocyanines are the class of photosensitizer having metal ions at the core. Most of the porphyrin-based photosensitizers have λ_{max} between 630 and 700 nm (Bonnett, 1995). In addition to porphyrinoid-based photosensitizers, the non-porphyrinoid compounds including anthraquinones, phenothiazines, xanthenes, cyanines, and curcuminoids are also used as photosensitizers (Sobotta, Skupin-Mrugalska, Piskorz, & Mielcarek, 2019). A variety of synthetic photosensitizers are available which belong to various classes of dyes such as phenothiazine, xanthene, benzophenothiazinium salt, and so forth (Kwiatkowski et al., 2018). Phenothiazines dyes Methylene Blue and Toluidine Blue (TB) have λ_{max} at 666 and 630 nm, respectively (Rice, Wainwright, & Phoenix, 2000). Methylene Blue is known to be

effective in the treatment of carcinomas and microbial biofilms. TB (tolonium chloride) is the acidophilic metachromatic dye with IUPAC name (7-amino-8-methylphenothiazin-3-ylidene)-dimethylammonium chloride. The dye has the chemical formula $C_{15}H_{16}N_3S^+$ and a molecular mass 270.374 g/mol (Sridharan & Shankar, 2012). The cationic dye TB is known to have high affinity for sulfates, carboxylates, and phosphate radicals of mammalian tissues, hence widely used in histology (Gandolfo et al., 2006). The potency of photoexcited TB has been reported against pathological microbes such as *Candida albicans*, *Pseudomonas aeruginosa*, *Acinetobacter baumannii*, and *Staphylococcus epidermidis* (Pourhajbagher et al., 2016; Sharma et al., 2008; Sharma, Bansal, & Gupta, 2005). Rose Bengal is another photosensitizer belonging to xanthene dye. It is the salt of 2,3,4,5-tetrachloro-6-(2,4,5,7-tetraiodo-6-hydroxy-3-oxoxanthen-9-yl)benzoic acid, which is widely used as fluorochrome and a histological dye. The dyes are readily soluble in water and have a molecular mass of 973.67 g/mol. Rose Bengal is known to behave potency of photoexcitation at λ_{max} of 546 nm (Vanerio, Stijnen, de Mol, & Kock, 2019). Rose Bengal has been known for its inhibitory property against several carcinoma and microbial infections. Silica nanoparticles decorated with Rose Bengal are reported to inactivate the methicillin-resistant *Staphylococcus aureus* (Guo, Rogelj, & Zhang, 2010). The gold nanorods conjugated with Rose Bengal has been proven to be effective against the oral carcinomas (Wang et al., 2014). Rose Bengal PDT was observed to inhibit the *P. aeruginosa keratitis* isolates (Durkee et al., 2020). Hence, TB and RB are two emerging non-porphyrin photosensitizer having potency against several diseases. The dyes belonging to squaraine, BODIPY, phenalenone are also studied for their potency against microbes and carcinomas (D'Alessandro & Priefer, 2020). Along with dyes, the transition metal complexes such as ruthenium, rhodium and iridium were observed to be good photosensitizers against microbes and carcinoma cells in vitro (Li & Chen, 2020). The natural compounds have been reported to be a potent photosensitizer. Hypericum-derived "Hypericin" belongs to perylenequinone class, which is known to have potency against microbial infection and cancerous cells (Waser & Falk, 2007). Similarly, hypocrellin is another perylenequinone isolated from fungi *Hypocrella bambuase sacc* has the property of photoexcitation (Zhenjun & Lown, 1990). The food supplements riboflavin and curcumin have been recently used as photosensitizer (Cardoso, Libardi, & Skibsted, 2012; Crivello & Bulut, 2005).

Recent studies suggested that PDT also has potency against neurodegenerative diseases (Aghaie et al., 2019). PDT using ALA has been reported to be effective against squamous carcinoma and basal cell carcinomas. Similarly, PDT was also found to be potent against cutaneous T-cell lymphoma (Sando et al., 2020). Photosensitizer such as chlorin 6 and photofrins showed anticancer activity against esophageal and lung carcinomas (Qiu, Kim, Penjweini, & Zhu, 2016; Srdanović et al., 2018). Whereas the dyes such as RB and TB were observed to have inhibitory efficiency against various microbial biofilms formation (Li, Yuan, Jia, Qin, & Wang, 2020; Parasuraman et al., 2019). The porphyrin photosensitizer ALA has been studied to have an inhibitory effect against papillomaviruses, leishmaniasis, and onychomycosis (Souza et al., 2017; Xie et al., 2019). Hence, the

overall studies suggest that PDT is an emerging therapy that could be applied in the treatment of wide range of diseases.

2 | NEURONAL CYTOSKELETON: THE CRUCIAL COMPONENTS FOR MAINTAINING CELL MORPHOLOGY

The cytoskeleton is the network of polymerized proteins, mainly comprised of microfilaments, microtubules and intermediate filaments (Kast & Dominguez, 2017). Each filamentous protein comprises of distinct globular protein that acts as the basic unit of these structures (Sheetz, 2001). In neuronal cells, the cytoskeleton plays various roles including transport, neurites extension, axon elongation, growth cone elongation, and maintaining the integrity of intracellular compartments (Gordon-Weeks & Fournier, 2014). Microtubules are one of the important cytoskeleton components of the neuron. The studies have suggested the contribution of microtubules in various aspects of neuronal integrity and intracellular transport. Neurite outgrowth formation is the initial phenomenon of neuronal polarization. The neurite outgrowths are known to have an abundance of bundled microtubule and actin-rich growth cones (Kapitein & Hoogenraad, 2015). Microtubules also play a crucial role in neuronal differentiation. Studies have suggested that the modulation of microtubule dynamics, for example, taxol treatment leads to the generation of multiple axons in neurons (Subramanian & Kapoor, 2012). Microtubules have also known to be associated with axonal elongation. The migration of neurons in the initial stages of brain development assisted by microtubules and actin (Suter & Miller, 2011). Another unit of neuronal architecture is the actin cytoskeleton. The migration, synaptic connection, and axonal polarization are the basic functions governed by the actin cytoskeleton (Morris & Hollenbeck, 1995). The cytoskeleton is being considered to be a crucial component in the neuron, thus any deformities in the microtubule functioning result in neurodegeneration. Cytoskeleton has been considered a potent target for studying therapeutics against neurodegenerative diseases. The microtubule stabilization drug epothilone D was reported to reduce axonal dysfunction and protect the neurons from toxicity (Zhang et al., 2012). The microtubule targeting agent such as paclitaxel was reported to have a protective mechanism against brain injury and neurodegeneration (Hur & Lee, 2014). Similarly, the treatment of nocodazole, vinblastine, and taxol was studied to protect the neurons from axonal swellings in spastin knockout (KO) mice (Fassier et al., 2013). Hence, the cytoskeleton has been considered as a major aspect in studying the therapeutics of neurodegeneration and neuronal development (Figure 2) (Table 1).

3 | TAU PROTEIN: THE CYTOSKELETON PROTEIN IN MAINTENANCE OF NEURONAL DIFFERENTIATION AND INTEGRITY

Tubulin is an acidic globular protein of molecular weight 50 kDa, which polymerizes to form microtubules. The α - and β -tubulin polymerize with help of GTP, where the tubulin rods are arranged in a

FIGURE 2 The neuronal cytoskeleton. The globular proteins α -tubulin and β -tubulin polymerize and form the microtubules. The microtubules assist the neurons in the maintenance of growth axonal growth and axonal guidance. The G-actin polymerizes to F-actin. The actin cytoskeleton assists the neurons in the formation of dendritic spines, the establishment of connections, endocytosis, and so forth. Actin filaments and microtubules both contribute to the growth and polarity of the growth cone

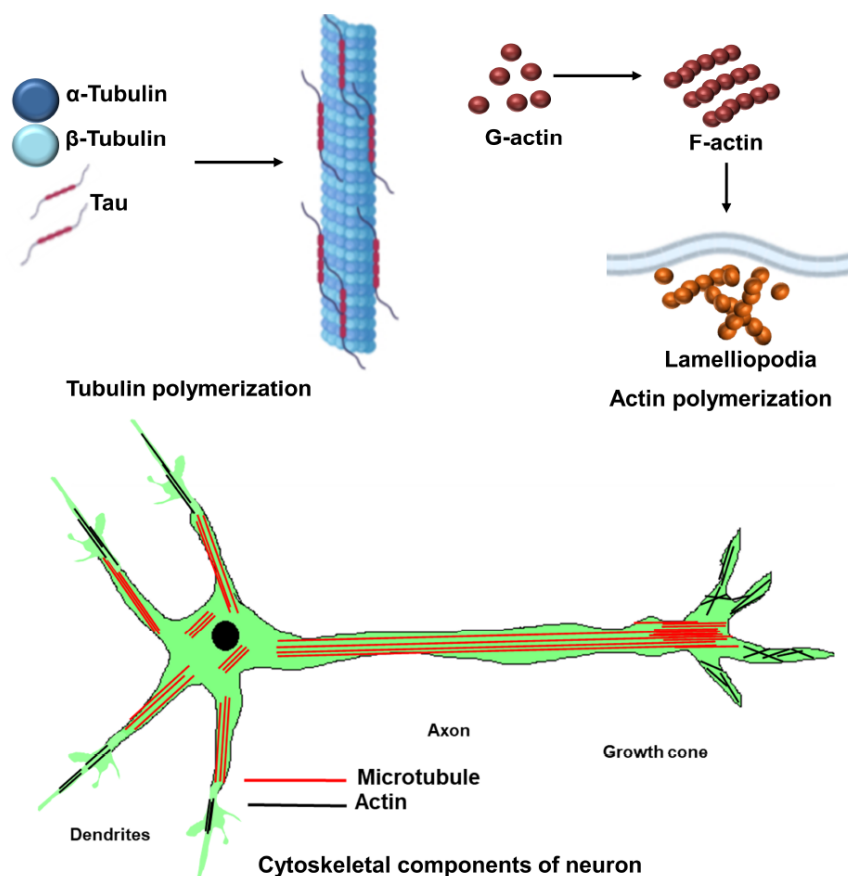


TABLE 1 The component of neuronal cytoskeleton. Neuronal cytoskeleton includes mainly the tubulin and actin protein. Several associated protein assist actin and tubulin polymerization and stabilization of cytoskeleton

S. No.	Cytoskeleton structure	Function	Localization
1.	α -Tubulin	Monomer unit of microtubule	All the cells including neurons
2.	β -Tubulin	Monomer unit of microtubule	All the cells including neurons
3.	MAP 2a, MAP 2b, MAP 2c	Stabilization of microtubule	Dendrites of neurons
4.	Tau	Stabilization of microtubule	Predominantly in axon
5.	Vimentin (IF Type 3)	Stabilization of neuronal cytoskeleton	Precursors of neurons and glia cells
6.	Type 4 IF (NFH, NFM, NFL)	Stabilization of neuronal cytoskeleton	Abundantly found in neurons
7.	Actin	The monomeric subunit of microfilaments	Predominantly in neurons and microglia
8.	Fimbrin	Cross-linking of actin filaments	Predominantly in neurons and microglia
9.	Ankyrin	Connects the microfilament to membrane	Neurons
10.	Tropomyosin	Stabilizing of microfilaments	Neurons

9 + 2 arrangement to form a hollow cylindrical structure, termed as microtubules (Rosenbaum, 2000). The end where the tubulin dimer is added is referred to as the plus end of microtubules, whereas the opposite end is designated as the minus end (Howard & Hyman, 2003). Minus end of microtubules is attached to the pericentriolar complex termed as microtubule organization center (MTOC). The axonal microtubules have a length of ≥ 100 nm and it

appears not to be associated with MTOC (Sanchez & Feldman, 2017). The axonal cytoskeleton was found mostly oriented toward the distal end of cells (Kirkpatrick & Brady, 1994). On contrary, the dendritic microtubules have a short length and mixed polarity (Kapitein & Hoogenraad, 2015). Several proteins are involved in stabilizing the microtubules. The stability of microtubules is assisted by the interaction of several microtubule-associated proteins (MAPs) (Drewes,

Ebnet, & Mandelkow, 1998). Various classes of MAPs such as MAP1A, MAP1B, MAP2A, and MAP2B have been reported. Tau is one of the MAPs that stabilize microtubules (Drewes et al., 1998). The *Tau* gene is present at chromosome 17q21, which results in the generation of six isoforms by alternative splicing (Andreadis, 2005). Tau plays a crucial role in pathology related to neurodegenerative diseases such as Alzheimer's disease (AD) (Dixit, Ross, Goldman, & Holzbaur, 2008). Several studies have demonstrated that the modulation of microtubule affects neuronal morphology in various aspects (Adamo et al., 2010). The treatment of lysophosphatidic acid (LPA) is known to cause neurite retractions. The studies suggested that the LPA treatment causes modulation of tubulin and elevated the phosphorylation of Tau protein by GSK-3 β (Sayas, Moreno-Flores, Avila, & Wandosell, 1999). The posttranslational modifications (PTMs) of tubulin play a crucial role in the maintenance of microtubule stability, where the tyrosinated tubulin induces the remodeling of neuronal growth cone (Gordon-Weeks, 1991). Similarly, the acetylation of tubulin contributes to the stability of microtubules and guides the kinesin proteins (KIF5A) in neurons (Janke & Kneussel, 2010). The mutant Phr1 associate with the microtubule cytoskeleton leads to defects in spinal cord development and motor neuron development (Lewcock, Genoud, Lettieri, & Pfaff, 2007). The deacetylase Sirtunins (Sirt2) is considered to be involved in neuronal differentiation, the acetylation level of tubulin was observed to be altered during neuronal differentiation (Tang & Chua, 2008). Similarly, another protein PAX 3 reported to inhibit the expression of β -III tubulin and neuronal differentiation in neuronal stem cells (Enzmann, Tamó, Trepp, & Wolf, 2014). The mutant Wnt and PI3K signaling affect the microtubule cytoskeleton by elevating the phosphorylation of Tau protein (Park et al., 2019). The destabilized microtubule structure results in alterations in the neuronal morphology of cortical neurons (Gavet, el Messari, Ozon, & Sobel, 2002). The exposure to 4-hydroxy-2(E)-nonenal, a major product of lipid peroxidation reduced the growth of neurite by disintegrating the microtubules (Neely, Sidell, Graham, & Montine, 1999). Similarly, the mercury treatment-induced neuronal membrane degeneration by affecting the microtubule integrity (Leong, Syed, & Lorscheider, 2001). The N-homocysteinylation Tau was observed to have a reduced affinity for tubulin which leads to neurodegeneration (Karima et al., 2012). The treatment of neuropeptide cerebrolysin affects the microtubules network of the neuron and enhances the neurogenesis and neuronal elongation (Maslah & Diez-Tejedor, 2012). In the same way, the proteins which promote disassembly of tubulin ultimately promote the loss of neuronal integrity and neurodegeneration. SCG 10 is a protein, which is involved in microtubule stabilization and the phosphorylation of SCG 10 accelerated the microtubule disassembly (Grenningloh, Soehrman, Bondallaz, Ruchti, & Cadas, 2004). Spastin is another MAP, the studies suggested that spastin deletion elevated the tubulin polyglutamylation which induced the impaired neuronal transport (Lopes et al., 2020). Hence, the earlier studies advocated that tubulin and microtubules are closely associated with maintaining neuronal integrity.

4 | THE CYTOSKELETAL COMPONENTS INVOLVED IN THE ESTABLISHMENT AND THE MAINTENANCE OF NEURONAL POLARITY

Microfilaments or actin cytoskeleton is one of the classes which has the most diverse arrangement and distribution in neurons (Luo, 2002). Actin is the monomeric unit of microfilaments. The globular actin (G-actin) has a molecular weight of 42 kDa (Schmidt & Hall, 1998). The G-actin polymerizes and leads to the formation of filamentous actin (F-actin) (Dominguez & Holmes, 2011). Although actin microfilaments are distributed through the neuron, their presence is prominently observed in a neuronal membrane having presynaptic terminals, dendritic spines and growth cones (Spooner & Holladay, 1981). F-actin is known to be involved in the formation of several membrane-associated structures such as filopodia, lamellipodia, podosome, and so forth. Filopodia are hair-like projections that facilitate synapse formation (Mattila & Lappalainen, 2008). Lamellipodia (lamina-sheet, pod-foot) are actin-rich fan-like structures, which are considered to have a role in endocytosis (Machesky, 2008). Several proteins have been reported to be associated with the actin cytoskeleton which aid in its stability (Schmidt & Hall, 1998). Proteins such as fimbrin and spectrins are involved in the crosslinking of actin filaments, tropomyosin, and β -thymosins contribute in stabilizing the actin filaments, whereas ankyrin bridges between actin filaments and the plasma membrane (Baines, 1990; Gunning, O'Neill, & Hardeman, 2008; Höfer & Drenckhahn, 1999). The actin cytoskeleton has a variety of crucial roles in the neuron, which includes plasma membrane proteins distribution, maintenance of cell morphologies, and segregation of axonal and dendritic proteins into respective cellular compartments (Luo, 2002; Sekino, Kojima, & Shirao, 2007). The growing end of polymerizing actin is called the "barbed end." Dishevelled-associated activator of morphogenesis, Ena/VASP proteins, MRL proteins are examples of such protein, which binds to barbed end (Barkó et al., 2010; Barzik et al., 2005; Hansen & Mullins, 2015). On contrary, proteins-like Mical causes the depolymerization of F-actin (Giridharan & Caplan, 2014). The actin cytoskeleton is reported to be arranged in dendrites in the form of branched F-actin-rich patches, longitudinal actin fibers and actin rings (Nicholson-Dykstra, Higgs, & Harris, 2005). The dendritic actin is involved in synapse formation (Toni et al., 2007). Protein such as Rho GTPase, Wiskott-Aldrich syndrome family protein (WASP), and CDC42 regulate the localization of actin in dendrites (Blanchoin et al., 2000; Higgs & Pollard, 2000; Newey, Velamoor, Govek, & van Aelst, 2005). The actin-rich presynaptic and postsynaptic dendritic spines contribute to the formation and maintenance of synapse (Allison, Chervin, Gelfand, & Craig, 2000; Gordon-Weeks & Fournier, 2014). The Ca²⁺ also plays important role in the regulation and maintenance dendritic actin cytoskeleton (Oertner & Matus, 2005). The axonal growth cone consists of a "fan-shaped" actin-rich structure, having the central dense core of actin and fine figure-like structures protruding from it (Kater, Mattson, Cohan, & Connor, 1988). Growth cone has an important role in the initiation and growth of the axon. The leading microfilament of the

growth cone forms the axon, while others contribute to the formation of dendrites (Kalil, Szebenyi, & Dent, 2000). Thus, it could be stated that the actin cytoskeleton dynamics have a crucial role in establishing the polarity of the neuron. The modulation of the actin cytoskeleton directly affects axonal growth and guidance (Gallo & Letourneau, 1999). The mutation of *Unc-115* gene, which codes for the actin-binding protein, modulated the actin polymerization and growth cone development (Gitai, Timothy, Lundquist, Tessier-Lavigne, & Bargmann, 2003). Similarly, the Plexin-B semaphorin receptor which regulates actin dynamics via interacting with Rac, ultimately induce changes in axonal growth (Driessens et al., 2001). The guidance of axon is also considered to be associated with actin cytoskeleton (Lykissas, Batistatou, Charalabopoulos, & Beris, 2007). Hence, the actin cytoskeleton plays a vital role in the generation of the growth cone and axonal development. The deregulation in cytoskeleton integrity is being considered to be associated with neurodegeneration (Figure 2).

5 | THE MICROTUBULE-ACTIN CROSS TALK FACILITATE THE AXONAL GROWTH

The actin cytoskeleton is known to be directly involved in axonal growth and guidance, but the studies suggested that the involvement of microtubule in the axon, which leads to the generation of the concept of microtubule-actin cross talk in neuronal development (Coles & Bradke, 2015). The cross talk is mediated via several microtubules and actin-associated protein, which serves as a link between the proteins (Seetharaman & Etienne-Manneville, 2020). The actin network act as a physical barrier for the microtubule, which retard their growth and promotes catastrophe (Walczak, 2000). The growth cone is considered to be an actin-rich structure in the neuron, but the presence of microtubule has also been reported in previous studies (Gordon-Weeks, 2004). In the growth cone, the bundles of microtubules are found to be arranged longitudinally to the actin rods (Williamson, Gordon-Weeks, Schachner, & Taylor, 1996). The significance of microtubule in growth is considered to the turning of the growth cone (Tanaka & Kirschner, 1991). The microtubules facilitate the nucleation of actin protein. The binding of growth arrest-specific 2-like 1 (Gas2L1) to the microtubule induces the stabilization of actin and thus contributes to maintaining ace of axonal morphology (van de Willige et al., 2019). The studies suggested that microtubule plus end-directed protein-like CLIP170 induces the polymerization of actin (Lewkowicz et al., 2008). The drebrin acts as a cross linker between EB-3 of microtubules and actin protein (Oh et al., 2006). ACF7 is another protein, which bridges the actin and EB-1, which helps the microtubule invasion to the growth cone (D'Souza-Schorey, 2005). p140Cap-Cortactin is a protein, which interacts with EB-3 of the microtubule, also known to mediate the actin polymerization (Repetto et al., 2014). The MAP2 also interacts with actin, which assists in the initiation of neurite formation (Dehmelt & Halpain, 2004). The actin-binding protein, formins also have an affinity for microtubule thus it contributes to the crosstalk of actin-microtubules (Bartolini &

Gundersen, 2010). The protein complex Doublecortin (Dcx)-spinophilin (Spn, or neurabin 2) reported to interact with both microtubule and actin, which leads to microtubule organization in the growth cone (Bielas et al., 2007; Fu et al., 2013). Thus, the recent studies suggested that the crosstalk between microtubule-actin plays a pivotal role in axonal development, guidance, and stability of neurons (Figure 2).

6 | THE SIGNALING CASCADES CONTROL THE CYTOSKELETON DYNAMICS IN CELLS

The cellular cytoskeleton dynamics are governed by complex signaling cascades, which include several crucial proteins. Rho GTPase family including Rho, Rac, and CDC42 play a crucial role in actin dynamics and signaling (Machesky & Insall, 1999). Rho is a family of signaling proteins, which include small GTPase. Rho protein has been reported to be involved in neuronal morphogenesis, axon growth, guidance, and dendritic formation via modulation of the cytoskeleton (Luo, 2000). Several studies have demonstrated that the crucial role of Rho GTPase in cytoskeleton modulation. The mutation in Nogo-A was found to alter the development of the growth cone, modulation of Rho-GTP/LIMK1/cofilin pathways in C57BL/6 Nogo-A KO mice (Montani et al., 2009). Similarly, the overexpression of cRac 1B increases the neurite formation in neuronal cells, on the contrary, the inhibition of cRac 1B causes a reduction in neurite numbers. The norepinephrine-mediated stress response targets the Rac 1, which results in a change in neuronal morphology (Swinny & Valentino, 2006). The Amyloid- β 42-mediated stress has stimulated the activity of Rac1/Cdc42 Rho GTPases. The upregulation of Rac 1 induces the formation of F-actin in hippocampal neurons (Mendoza-Naranjo, Gonzalez-Billault, & Maccioni, 2007). Cell division control protein 42(CDC42) is another protein of Rho GTPase family involved in actin cytoskeleton regulation. CDC42 is known to retard the actin polymerization (Ma, Rohatgi, & Kirschner, 1998). The neuropeptide galanin has stimulated the neurite outgrowth in the sensory neuron by attenuating CDC42 (Hobson, Vanderplank, Pope, Kerr, & Wynick, 2013). The Ca^{2+} -mediated interaction of Lis1 to scaffolding proteins activates CDC42 which causes retardation of actin polymerization (Kholmanskikh et al., 2006). ROCK is a ser/Thr kinase that plays a key role in the maintenance of actin polymerization. ROCK kinase upregulates the activity of LIM kinase, where LIM kinase phosphorylates cofilin-1 and hence it facilitates the polymerization of G-actin to F-actin (Maekawa et al., 1999). In the thrombin and nocodazole-treated cells, the downregulation of LIM-1 was observed which ultimately results in destabilization of microtubules and inhibition of actin polymerization (Gorovoy et al., 2005; Leonard, Marando, Rahman, & Fazal, 2013). Similarly, PAK-1 protein activates the LIM kinase, which induces alterations in actin cytoskeleton dynamics (Edwards, Sanders, Bokoch, & Gill, 1999). Cofilin-1 is a neuronal-specific protein, which binds to G-actin and attenuates the further polymerization of actin (Wioland et al., 2017). Cofilin-1 is known to present in two forms in cells, phosphorylated form, and non-phosphorylated form. In

phosphorylated form, cofilin-1 loses its affinity for actin, and hence the polymerization of G-actin to F-actin took place in presence of phosphorylated cofilin (Ono, 2003). Reelin is a matrix protein, which regulates the radial migration of cortical neurons. Reelin induces the phosphorylation of cofilin at Ser-3, which causes the stabilization of the actin cytoskeleton (Chai, Förster, Zhao, Bock, & Frotscher, 2009). Whereas the mutation in cofilin results in impaired neuronal migration leading to brain deformities (Bellenchi et al., 2007). The mutation of cofilin results in impaired neuronal tube development in defective embryos (Gurniak, Perlas, & Witke, 2005). The inactivation of cofilin also results in the deregulation of AMPA receptors which reduces the synaptic plasticity in cortical neurons (Gu et al., 2010). Several proteins such as Arp 2/3 complex induces the crosslinking of F-actin. Arp 2/3 complex is composed of seven subunits, the complex induces the branching and polymerization of actin (Goley & Welch, 2006). The binding of Arp 2/3 complex induces the nucleation of actin which in turn induces the activity of other proteins such as WASP (Yamaguchi et al., 2005). Activation of the Arp 2/3 complex results in the

generation of lamellipodia and filopodia structures in the cell membrane. The inhibition of Arp 2/3 complex by protein interacting with C Kinase-1 causes the attenuation of actin polymerization (Nakamura et al., 2011). Similarly, cortactin directly binds to Arp 2/3 complex which leads to activation of actin polymerization (Urano et al., 2001). Phosphatidylinositol 4,5-bisphosphate causes the movement of lipid raft which further modulating the actin cytoskeleton by Arp 2/3 complex (Rozelle et al., 2000) (Figure 3). Thus, the involvement of various signaling proteins makes the cytoskeleton an interesting and potential therapeutic target for studying the diseases.

7 | THE CYTOSKELETON DEFORMITIES IN NEURODEGENERATION

Cytoskeleton deformities are considered to be associated with neurodegeneration. α -Synuclein aggregates are one of the characteristics of Parkinson's disease. The aggregates of α -synuclein induce

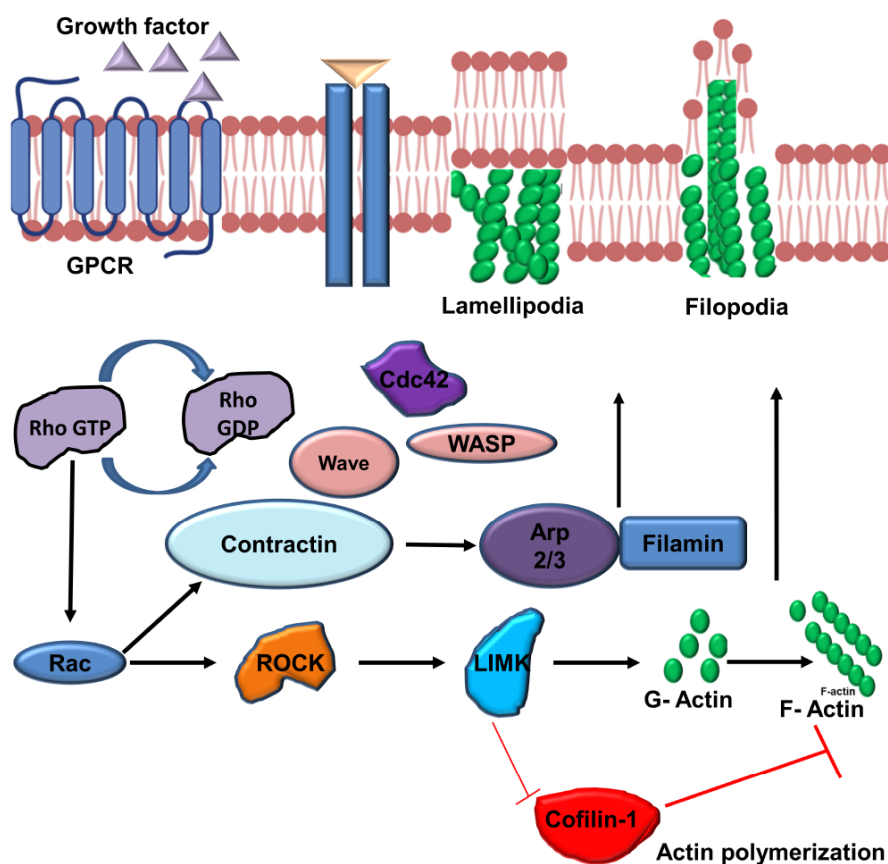


FIGURE 3 The signaling cascades involved in actin polymerization. Several proteins are involved in actin polymerization. Rho GTPase are closely known to be related to actin polymerization. The ROCK protein phosphorylates LIMK kinase, which in turn causes the inactivation of cofilin-1. Proteins such as Arp 2/3 complex and Wiskott-Aldrich syndrome family protein (WASP) facilitate the cross-linking of F-actin

mitochondria dysfunction via actin-mediated mislocalization of Drp-1 (Ordonez, Lee, & Feany, 2018). In AD conditions, the cofilin protein is reported to be associated with actin rods formation, which contributes to AD pathology (Bamburg et al., 2010). A β -42 aggregates are reported to induce the collapse of the actin network in neuronal cells ultimately resulting in dendritic spine degeneration. The presence of A β -42 aggregates is known to induce the phosphorylation of cofilin protein, which leads to destabilization of actin filaments causing the impairment in synaptic plasticity (Penzes & VanLeeuwen, 2011). Hirano bodies are the intraneuronal structures observed in AD conditions. Recent studies have suggested that these inclusions are rich in actin, thus it was stated that they are formed as a result of mislocalization of the actin cytoskeleton (Galloway, Perry, & Gambetti, 1987). The neurodegenerative disease-like AD was found to have impairment in actin-microtubule cross talk. Recent studies suggest the accumulation of F-actin in the Tauopathy model of *Drosophila*, which indicates the cross talk of Tau and actin cytoskeleton (Fulga et al., 2007). The PTMs of tubulin, for example, acetylation, polyglutamylation, tyrosination, and detyrosination were observed to be associated with AD pathology (Baird & Bennett, 2013; Sonawane, Raina, Majumdar, & Chinnathambi, 2020). Recent studies suggested that microtubule contributes to the dendritic spine formation and maturation, thus it was stated that the abnormality in microtubule dynamics leads to the deformities in neuronal spine formation in AD (Gu, Firestein, & Zheng, 2008). CCP1, CCP4, and CCP6 are the proteins belonging to tubulin deglutamylation, which are reported to play crucial role in neurodegeneration (Rogowski et al., 2010). In the diagnosis, patient with neurodegeneration observed to have mutation in deglutamylase CCP1 which causes the accumulation of glutamylated tubulin in cells (Shashi et al., 2018). Current studies indicated that tubulin polyglutamylation modulated the dynein motor activity. HDAC6 is another enzyme associated with tubulin acetylation, the studies suggested that downregulation of HDAC6 improves the cognitive defect in mouse (Govindarajan et al., 2013). The stabilization of microtubules by epothilone B initiated the axon regeneration, which assist in recovering the neuronal injury (Ruschel et al., 2015). The overall studies suggest that cytoskeleton plays a crucial role in neurodegeneration and hence it could be targeted for studying the therapeutic strategy against AD.

8 | THE EFFECT OF PDT ON CELL ORGANELLES AND CYTOSKELETON

The cytoskeleton plays a crucial role in maintaining the integrity of neurons which include maintenance of cell morphologies and segregation of axonal and dendritic proteins into respective cellular compartments. PDT is reported to target the cytoskeleton. PDT targeting prostate-specific membrane antigen was observed to induce the disruption of tubulin network, actin cytoskeleton, and intermediate filaments in tumor cells (Liu, Wu, & Berkman, 2010). The ALA-mediated PDT on glioblastoma cells shown a change in cell morphology associated with alteration of the actin cytoskeleton (Karmakar, Banik,

Patel, & Ray, 2007). Similarly, the PDT of Sinoporphyrin sodium has inhibited the migration of MDA-MB-231 cells by attenuating the F-actin formation (Wu et al., 2016). In colon adenocarcinoma cells, the treatment of hypericin was reported to alter the organization of F-actin (Süloğlu, Selmanoğlu, & Akay, 2015). Furthermore, PDT using TMPyP-porphyrine photosensitizer leads to microtubules disorganization and mitotic catastrophe in G361 cells (Cenklová, 2017). The photofrin-mediated PDT has induced an increase in intracellular Ca²⁺, which ultimately leads to microtubule depolymerization (Sporn & Foster, 1992). The use of 3,3'-dihexyloxacarbocyanine iodide as photosensitizer causes the damage of microtubule, but the other cytoskeleton element including actin stress fibers, vimentins, and intermediate filaments were not affected by PDT (Lee, Wu, & Chen, 1995). Thiazine dyes were also reported to cause damage to the microtubule network in HeLa cells (Stockert, Juarranz, Villanueva, & Cañete, 1996). Thus, the previous studies suggest that cytoskeletal elements act as a prominent target by various photosensitizers which ultimately results in alteration and reorganization of the cytoskeleton. PDT has been shown to affect various cellular components in different forms. Various photosensitizers accumulate specifically in different cell organelles, for example, RB is known to be accumulated in mitochondria whereas, phosphoindole oxide-based photosensitizer accumulates in the endoplasmic reticulum and leads to the generation of autophagy (Zhuang et al., 2020). Nile blue accumulates in lysosomes, while the Chlorin 6 and its derivative accumulate in mitochondria, endoplasmic reticulum, and lysosome and induces photo-oxidative damage to cell (Brilkina et al., 2019; Kang, 2018). Generally, PDT is known to induce several responses in the cell, which include induction of apoptosis and caspase activation are the common responses (Figure 3) (Qi et al., 2019). PDT using ALA induces apoptosis in lesioned T-lymphocytes of psoriatic plaques and malignant T-cells (Du et al., 2017). Similarly, PDT using a pheophorbide-based photosensitizer induces apoptosis by targeting a mitochondrial pathway in human uterine carcinoma (Tang, Liu, Zhang, Fong, & Fung, 2009). Another photosensitizer protoporphyrin IX reported inducing apoptosis in HeLa cells (Bednarz, Zawacka-Pankau, & Kowalska, 2007). The induction of inflammatory pathways is also reported as a response to PDT. Photofrin and benzoporphyrin derivative-mediated PDT were reported to induce cytokine release in cells (Firczuk, Nowis, & Gołab, 2011). The treatment of photoexcited photosensitizer 2-[1-hexyloxyethyl]-2-devinyl pyropheophorbide-a was observed to initiate the expression of pro-cytokines and chemokines, which ultimately lead to the secretion of interleukins such as IL-6 (Castano, Mroz, & Hamblin, 2006). PDT in the BALB/c mouse model showed the altered expression of IL-6 and IL-10. The PDT-treated dendritic cells were observed to have increased secretion of IL-1 and IL-6, whereas the expression of TNF- α was reduced (Gollnick, Liu, Owczarczak, Musser, & Henderson, 1997). PDT has also been reported to induce DNA damage in cells. The photosensitizer based on β -carboline derivatives was found to intercalate between DNA and caused DNA damage (Guan et al., 2006). The PDT of liposomal zinc phthalocyanine induces cell death by damaging the DNA of tumor cells (Broekgaarden et al., 2017) (Figure 1).

9 | EFFECT OF PDT ON THE NEURONAL CYTOSKELETON

The crucial role of the cytoskeleton in maintaining neuronal integrity and cognition has been already reported (Hirokawa, 1993). Cytoskeletal element such as microtubule helps the neuron to maintain cell structure, whereas the microfilaments and actin cytoskeleton assist the neurons in establishing the neuronal network via facilitating the synapse formation (Witte & Bradke, 2008). The PDT has been studied to modulate the cytoskeleton of neuronal cells. Several photosensitizers have been reported which target the neuronal cells (Table 2). ALA/PDT was observed to suppress the matrix formation and migration of glioblastoma cells (Etrinan et al., 2011). Exposure to PDT induced morphological alterations in glioma cells. This alteration of morphology and cell migration was associated with the modulation of the actin cytoskeleton (Kamoshima, Terasaka, Kuroda, & Iwasaki, 2011). The sub-lethal treatment of ALA/PDT of D54Mg glioma cells causes the changes in actin cytoskeleton in growth cones resulting in retraction of protrusions, and surface blebbing (Uzdensky, Kolpakova, Juzeniene, Juzenas, & Moan, 2005). The PDT-mediated with meta-tetrahydroxyphenyl chlorin causes the reduction in neurite length, which indicated the modulation of the microtubule network (Wright et al., 2009). Tau is one of the important cytoskeleton proteins of neurons, which is known to be associated with the maintenance of assemblies and microtubules stability (Gorantla, Shkumatov, & Chinnathambi, 2017). The 441 amino acid protein Tau is considered to be natively unfolded. Under pathological conditions, Tau loses its affinity for microtubules and undergoes several conformational changes in structure, which leads to the formation of intracellular Tau aggregates (Sonawane & Chinnathambi, 2018). The four tandem repeats of Tau are considered to be responsible for Tau aggregation, VQIINK in R2 and VQIVYK of R3 are the sequences that initiate Tau aggregation (Sonawane, Balmik, Boral, Ramasamy, & Chinnathambi, 2019). The aggregates of Tau are considered to be closely involved with several diseases including progressive supranuclear palsy, cortico-basal syndrome, pick's a disease and chronic traumatic encephalopathy, and AD (Spillantini & Goedert, 1998). Tau aggregates are considered a major hallmark of AD. The oligomers and aggregates of Tau lead to several metabolic and signaling defects in

neurons such as the generation of intracellular ROS, apoptosis, mitochondrial dysfunction, abrupt nuclear transport, and so forth (Iqbal, Liu, & Gong, 2016). Hence, several studies target the cytoskeletal-associated protein Tau for evaluating the potency of therapeutic molecules against AD. Some recent studies have suggested that the application of photoexcited dyes have potency modulate the Tau aggregation. TB is a basic phenothiazine dye having the potency to generate the singlet oxygen species when excited at a wavelength of 630 nm. TB was observed to inhibit the aggregation of in vitro Tau, whereas when the premature aggregates of Tau were exposed to photoexcited TB, a potent disaggregation of Tau fibrils was observed. The study also claims that the exposure of photoexcited TB modulated the tubulin cytoskeleton as the TB treated neurons were observed to have longer neurite extensions than untreated cells (Dubey, Gorantla, Chandrashekar, & Chinnathambi, 2019). Rose Bengal is well-known photosensitizer known to be effective against various targets including the microbial biofilms to extracellular neuronal aggregates of Amyloid- β (Lee, Lee, & Park, 2015). In recent studies, the efficiency of photoexcited RB to modulate various neuronal cytoskeleton components has been reported. As mentioned earlier that, Tau is one of the cytoskeletal protein, which forms the pathological aggregates in AD (Balmik et al., 2019). The studies suggested that photoexcited RB has the potency to induce the conformational changes and disaggregate the mature Tau fibrils. Tubulin is the monomeric unit of microtubules, the α - and β -tubulin polymerizes leading to the formation of microtubules (Parness & Horwitz, 1981). The photo-excited RB was observed to induce the neurotic extensions, which indicated that the RB might have the potency to modulate tubulin assembly in neurons. Thus, from these studies, it is evidence that photoexcited RB might have an effect on microtubule dynamic as it was two microtubule related proteins, namely, tubulin and Tau (Dubey, Gorantla, Chandrashekar, & Chinnathambi, 2020). Furthermore, photoexcited RB was found to induce changes in the actin cytoskeleton. The neurons exposed to photoexcited RB were observed to have an increased number of filopodia and lamellipodia. Filopodia and lamellipodia are the structures that form by the accumulation of F-actin (Nobes & Hall, 1995). The increased number of filopodia and lamellipodia indicated that photoexcited RB might have the efficiency to accelerate the polymerization of G-actin to

TABLE 2 Various classes of photosensitizers and their application

S. No.	Photosensitizer	Class	λ_{max} (nm)	Application
1.	Methylene Blue	Phenothiazine	665	Anti-biofilm, disaggregation of A β plaques
2.	Toluidine Blue	Phenothiazine	630	Inhibition of microbial biofilm, disaggregates Tau filaments
3.	Acridine orange	Aminoacridines	488	
4.	Rose Bengal	Xanthene	585	Anti-biofilms, reduces the carcinomas, disaggregates Tau and A β filaments
5.	Photofrins	Porphyryns	630	Treatment of esophageal and lung carcinomas
6.	Aminolevulinic acid	Porphyryns	456	Treatment of actinic keratosis, carcinomas
7.	Temoporfrins	Porphyryns	652	Treatment of esophageal and lung carcinomas
8.	Chlorin 6	Chlorin	406.5	Treatment of malignant tumors
9.	Azulene	Monoterpenes	304	—

F-actin. The studies suggested that shorter durations of light exposure (up to 30 min) induced the formation of filopodia but the longer exposure (60 min) reduced the filopodia numbers in cells. Interestingly the treatment of photoexcited RB was found to induce the actin-rich podosome-like structures in cells (Figure 4) (Dubey et al., 2020). Although the effect of photoexcited RB on the actin signaling dynamics was not reported yet. It would be interesting to observe the effect of photoexcited RB on signaling molecules involved in actin polymerization such as Arp 2/3, WASP, CDC-42, LIMPK, and Cofilin-1 (Figure 5). The studies gave hint about the potency of photoexcited RB in altering the cytoskeleton in vivo as the locomotory behavior of the Tau mutant *Drosophila* was improved after exposure to photoexcited RB. Hence, the recent results suggested that PDT has the potency to modulate the neuronal cytoskeleton in various aspects.

10 | PHOTODYNAMIC TREATMENT AS AN EMERGING THERAPY IN NEURODEGENERATION

PDT has emerged as a novel and promising therapeutic strategy in the treatment of neurodegenerative disorders that involve the misfolded protein aggregates. AD is one of the major neurodegenerative

diseases which is known to be associated with the accumulation of extracellular A β aggregates and intracellular aggregates of MAP Tau (Dubey & Chinnathambi, 2019). Recently, these protein aggregates have been targeted for studying the neuroprotective potency of several therapeutic molecules (Calcul, Zhang, Jinwal, Dickey, & Baker, 2012). Methylene blue (MB) is a phenothiazine dye that is already known to be effective against Tau aggregation (Schirmer, Adler, Pickhardt, & Mandelkow, 2011). MB and *N*-demethylated derivatives azure A and azure B induces the intermolecular crosslinking of two cysteine residues via reversible oxidation mechanism, the modification in C291 and C322 leads to inhibition of Tau aggregation (Akoury et al., 2013). Similarly, MB-induced autophagy and attenuated the Tau induced toxicity in FTD mice model (Sun et al., 2016). In recent studies, MB irradiated with 686 nm of red light was found to have potency against in vitro A β aggregation and A β -induced cytotoxicity. The treatment of photoexcited MB has reduced the damage to the neuromuscular junction by suppressing the synaptic toxicity in the *Drosophila* model of AD (Lee, Suh, Chung, Yu, & Park, 2017). Another dye RB from the xanthene family have the potency to photoexcited after irradiating at 570 nm, RB was also reported to be effective in the photoexcited state against A β aggregates mediated toxicity and aggregation (Lee et al., 2015). Additionally, the photoexcited TB and RB are reported to disintegrate the mature Tau fibrils and reduce the

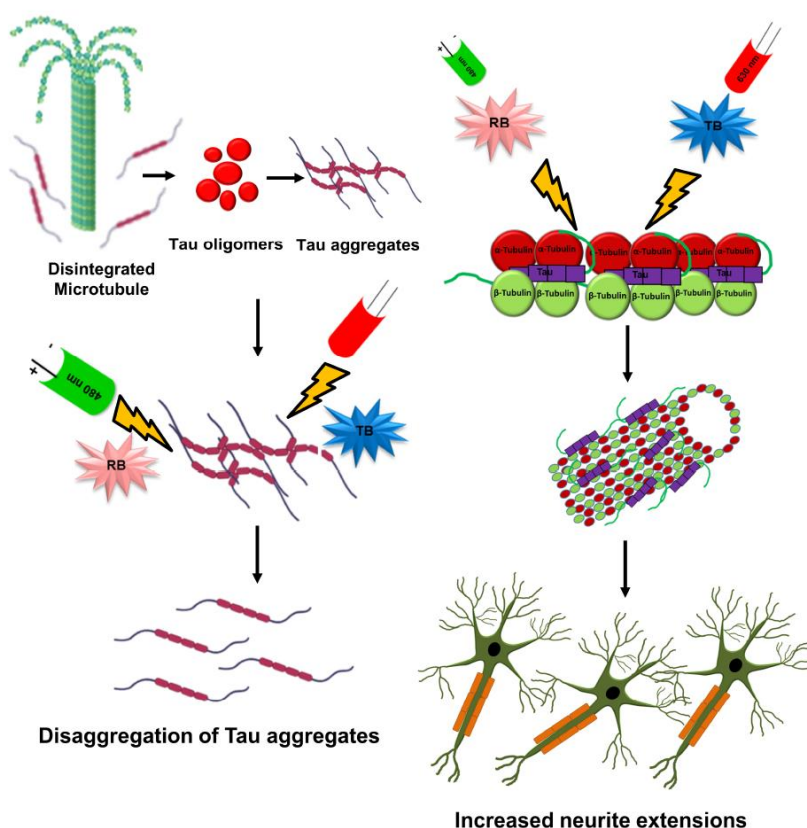


FIGURE 4 Photoexcited dyes modulate microtubule cytoskeleton. Tau is one of the microtubules-associated protein, the treatment of photoexcited Toluidine Blue (tolonium chloride) (TB) and RB disintegrate the Tau fibrils. The neuron exposed to photoexcited RB and TB was observed to have extended neurites indicating the modulation of the tubulin network

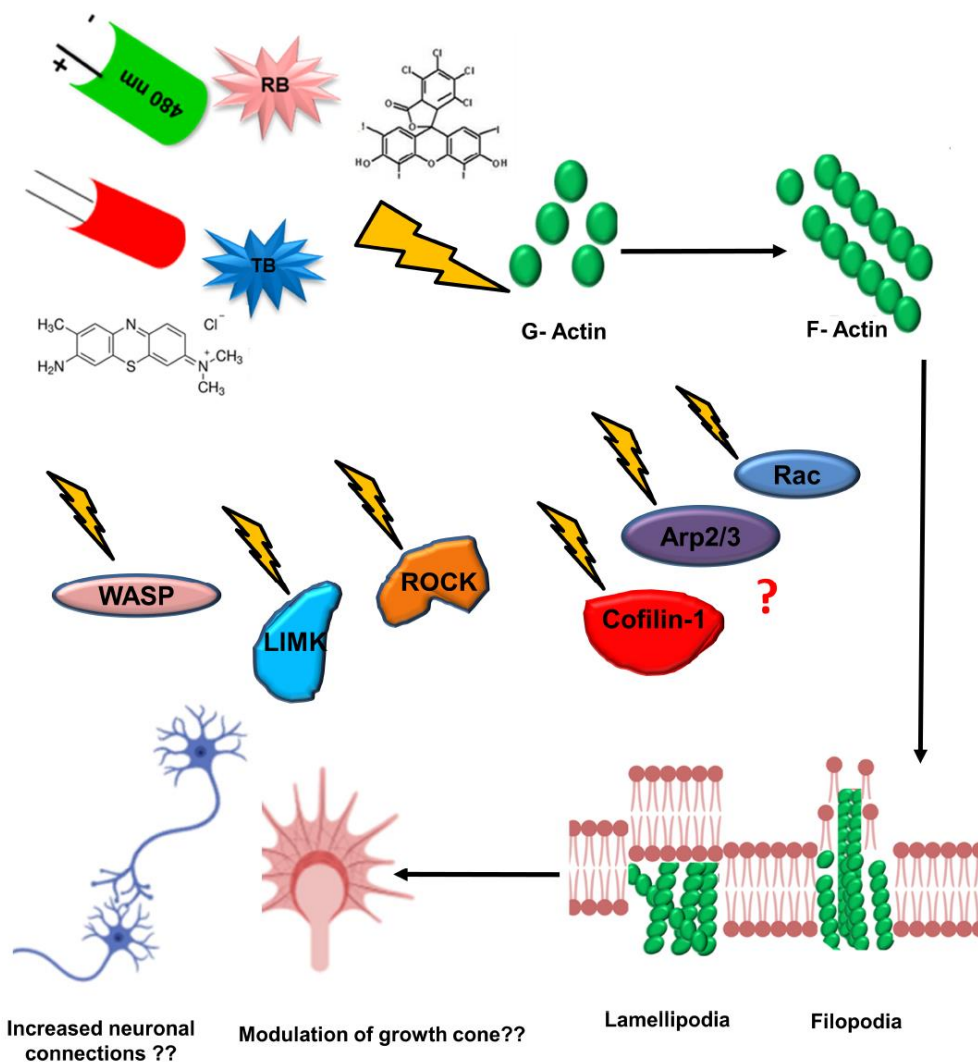


FIGURE 5 The effect of photodynamic therapy (PDT) on the actin cytoskeleton. Rose Bengal (RB)-mediated PDT induces the formation of filopodia and lamellipodia in neurons. The mechanism of action is still needed to be described. PDT could have an effect on the activity of LIMK, Rho, ARP 2/3 complex, and cofilin-1 which are involved in the actin polymerization

Tau-mediated toxicity (Dubey et al., 2019; Dubey et al., 2020). Creutzfeldt-Jakob disease is the human transmissible spongiform encephalopathies or human Prion diseases which is a rare neurodegenerative disease (Collinge, 1999). The disease is known to be associated with the spread of misfolded protein commonly termed as Prion protein. The normal protein PrP^C is found on the membranes of cells, but the misfolded protein PrP^{Sc} has the potency to convert the conformation of normal PrP^C into the infectious PrP^{Sc}. Thus, several investigations have been carried out to inhibit the spread of PrP^{Sc} protein (Glatzel, Abela, Maissen, & Aguzzi, 2003). Sulfonated phthalocyanines (Pcs) are cyclic teroles that are also used as photosensitizers (Janouskova, Rakusan, Karaskova, & Holada, 2012). The studies suggested that Pcs treatment inactivated the prion protein in brain

homogenate. Hence, the recent studies evidenced that the photoexcited molecule could be an effective strategy in the treatment of various neurodegenerative disorders (Table 3).

11 | ADVANTAGES OF PDT

Though several questions have to be answered for PDT, the technique has multiple benefits that support its application. The technique of PDT requires a light source and photosensitizers this reduces the cost of treatment which gives this technique an edge (Taylor & Brown, 2002). Another benefit of PDT is the low degree of invasiveness, for the delivery of photosensitizers, the patient has to face

TABLE 3 The effect of photosensitizers on neurodegeneration-related proteins

S. No.	Name of photosensitizer	Targeted neuronal protein	Effect
1.	Methylene Blue	A β	Inhibition of aggregation
2.	Toluidine Blue	Tau Tubulin	Disaggregation of Tau aggregates, Increased neurotic extension by modulating disaggregation of Amyloid- β aggregates tubulin
3.	Rose Bengal	Tau Tubulin Actin A β	Disaggregation of Tau aggregates, increased neurotic extension by modulating tubulin, modulation of the actin cytoskeleton and increased in filopodia, disaggregation of Amyloid- β aggregates
4.	Phthalocyanines	Prion	Inhibits the spread of prion protein

minimum surgery (Choudhary, Nouri, & Elsaie, 2009). Additionally, PDT was found to have fewer side effects as compared to other radiation therapies (Borgia et al., 2018). The technique has the advantage of a shorter duration of treatment; unlike other radiation therapies, the shorter duration of light exposure has shown the potent effect on a target. The photosensitizers, which are used for the treatment are reported to have a low degree of toxicity and high specificity which support the therapeutic application of PDT (Tabish et al., 2018). Thus based on above-mentioned point we can state that PDT could emerge as a better therapeutic method in the future.

12 | CHALLENGES IN PDT

PDT is one of the emerging strategies in several fields of treatment. The therapy has several advantages which include slight invasiveness, shorter duration of treatment, and low cost of therapy. Several points need to be considered for justifying the in vivo application of PDT on neuronal cells. The first and most important question regarding the therapy is the extent of invasiveness, how the neuronal cells would be irradiated in vivo?? The challenge of irradiating the brain cells hurdles its application in the field of neuronal treatment. In the initial studies, prototypes have of intranasal irradiation probes have been proposed but the applicability still needs to be elucidated in the case of the human brain (Dimauro, Attawia, Lilienfeld, & Holy, 2008). The next challenge in the field of PDT is to deliver the photosensitizer to the brain, the question arises whether the photosensitizer will be able to cross the blood-brain barrier and reach the targeted area of the brain? The next challenge is the photosensitivity of cells post-treatment? The therapy should include the application of a photosensitizer that would not produce any photosensitivity and toxicity after the treatment. Despite several questions, there is hope in further research to answer the drawbacks of PDT.

13 | CONCLUSION

The effect of PDT has been tested in various areas including cancer, microbial infections and dermatological diseases. In the case

of neurodegenerative disease, PDT showed promising results under in vitro conditions. Several neurodegenerative disorders are related to misfolded protein aggregation, in recent studies, PDT has shown the potency to disaggregate the protein filaments. Additionally, the cytoskeleton deformities are also considered as the consequence of neurodegeneration. In primary studies, PDT was observed to have potency in modulating various cytoskeleton components such as actin and tubulin network. However, various questions are still to be answered under in vivo conditions. Thus, it could be said that PDT might have the potency to emerge as a novel therapeutic strategy against AD and other neurodegenerative disorders.

ACKNOWLEDGMENTS

T. D. acknowledges the fellowship from University Grant Commission (UGC), India. Both authors thank Chinnathambi's lab people for their fruitful discussion on manuscript. This project is supported in part by grant from in-house CSIR-National Chemical Laboratory grant MLP029526 and MLP101726.

CONFLICT OF INTEREST

Both authors declare no conflict of interests.

AUTHOR CONTRIBUTIONS

Tushar Dubey and **Subashchandrabose Chinnathambi**: Collected and reviewed the literature and wrote the manuscript. **Subashchandrabose Chinnathambi**: Conceived the idea for the project, resource provided, supervised and wrote the manuscript. Both the authors read and approved the final manuscript.


DATA AVAILABILITY STATEMENT

Data sharing is not applicable to this article as no new data were created or analyzed in this study.

CONSENT FOR PUBLICATION

All authors consent to the publication.

ORCID

Subashchandrabose Chinnathambi  <https://orcid.org/0000-0002-5468-2129>



Small GTPases

ISSN: (Print) (Online) Journal homepage: <https://www.tandfonline.com/loi/ksgt20>

Photodynamic treatment modulates various GTPase and cellular signalling pathways in Tauopathy

Tushar Dubey & Subashchandraboese Chinnathambi

To cite this article: Tushar Dubey & Subashchandraboese Chinnathambi (2021): Photodynamic treatment modulates various GTPase and cellular signalling pathways in Tauopathy, Small GTPases, DOI: [10.1080/21541248.2021.1940722](https://doi.org/10.1080/21541248.2021.1940722)

To link to this article: <https://doi.org/10.1080/21541248.2021.1940722>



Published online: 17 Jun 2021.

Submit your article to this journal [↗](#)

Article views: 28


View related articles [↗](#)View Crossmark data [↗](#)

Full Terms & Conditions of access and use can be found at
<https://www.tandfonline.com/action/journalInformation?journalCode=ksgt20>

REVIEW



Photodynamic treatment modulates various GTPase and cellular signalling pathways in Tauopathy

Tushar Dubey and Subashchandra Chinnathambi 

Neurobiology Group, Division of Biochemical Sciences, CSIR-National Chemical Laboratory, Pune, India; Academy of Scientific and Innovative Research (Acsir), Ghaziabad, India

ABSTRACT

The application of photo-excited dyes for treatment is known as photodynamic therapy (PDT). PDT is known to target GTPase proteins in cells, which are the key proteins of diverse signalling cascades which ultimately modulate cell proliferation and death. Cytoskeletal proteins play critical roles in maintaining cell integrity and cell division. Whereas, it was also observed that in neuronal cells PDT modulated actin and tubulin resulting in increased neurite growth and filopodia. Recent studies supported the role of PDT in dissolving the extracellular amyloid beta aggregates and intracellular Tau aggregates, which indicated the potential role of PDT in neurodegeneration. The advancement in the field of PDT led to its clinical approval in treatment of cancers, brain tumour, and dermatological acne. Although several questions need to be answered for application of PDT in neuronal cells, but the primary studies gave a hint that it can emerge as potential therapy in neural cells.

ARTICLE HISTORY

Received 28 January 2021
Revised 12 May 2021
Accepted 4 June 2021

KEYWORDS

Photodynamic therapy; photosensitizers; GTPase; neurodegeneration; clinical application

Overview of photodynamic therapy: the principle and components of PDT

Photodynamic therapy (PDT) involves the use of photo-excited molecules against target cells or tissues. The main components of PDT are the photosensitizers and light source [1]. Photosensitizers are molecules that get excited on irradiation of specific wavelength of light leading to the generation of singlet oxygen species [2]. Several molecules have the potency of photo-excitation but all photo-excited molecules cannot be chosen for treatment. (i) The ideal photosensitizers should have a characteristic high quantum yield, and should be able to generate singlet oxygen. (ii) The localization of photosensitizer plays a crucial role in its selection, which should specifically localize to the target tissue. (iii) Photosensitizers should not produce dark toxicity to cells and upon treatment, should be released out of cell rapidly. (iv) The photosensitizers should be cost effective, easily available for the treatment of patients [3]. Various classes of chemicals have been reported to have the property of photo-excitation. The compounds containing tetrapyrrole ring such as haem, chlorophyll and bacteriochlorophyll are widely present in the nature. Derivative of these compounds such as Photofrin, Chlorin(e6), talaporfin sodium, LUZ11, Chloroaluminium sulphonated phthalocyanine

(CASP), Silicon phthalocyanine (PC4) are the examples of commonly known photosensitizers [4–6]. Apart from natural compounds, synthetic compounds are reported to have photo-excitation properties. The phenothiazine dye methylene blue, toluidine blue, xanthene dye rose bengal, DIMPY-BODIPY, Zinc(II)-dipicolylamine di-iodo-BODIPY, transition metal complex iridium, rhodium, ruthenium are well-known photosensitizers [7–10]. The mechanism of PDT involves two steps. In the first step, the photosensitizer absorbs the energy and in the second step, the absorbed energy is transferred for the generation of singlet oxygen species. The excited state is short lived and it follows the intersystem crossing after which the triplet oxygen either follows type 1 or type 2 reaction. In type 1 reaction, the triplet oxygen species form free oxygen radical and in type 2 reaction, it directly gets converted into singlet oxygen species (Figure 1) [11].

PDT induces the cell death via activation of various pathways

Apoptosis is the programmed cell death, which includes series of events like nuclear fragmentation, shrinking of cell, and change in their morphology

CONTACT Subashchandra Chinnathambi  s.chinnathambi@ncl.res.in  Neurobiology Group, Division of Biochemical Sciences, CSIR-National Chemical Laboratory, Pune 411008, India

© 2021 Informa UK Limited, trading as Taylor & Francis Group

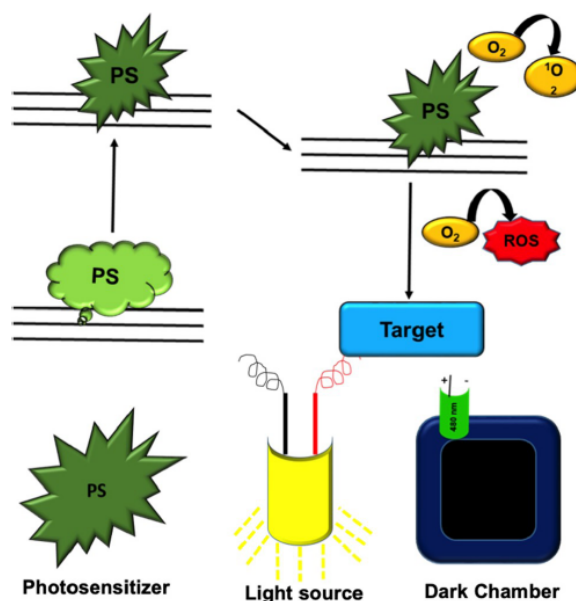


Figure 1. The principle and component of PDT. PDT involves the excitation of photosensitizer (PS) after exposure of specific wavelength of light. In the excited PS either follows type 1 and type 2 mechanism after intersystem crossing. The excited PS generated triplet and singlet oxygen species return to ground state. The singlet oxygen species act on target tissues to produce the effect. The basic components of PDT involve the photosensitive dye (photosensitizer), the light source to irradiate the photosensitizer and dark chamber to avoid exposure of undesirable light.

[12]. Generally apoptosis follows two pathways, intrinsic and extrinsic pathways, which include the formation of the death-inducing signalling cascades assisted by Caspases and other signalling molecules, e.g. Bcl-2 [13]. On other hand, necrosis is the traumatic cell death induced due to cell injury. The exposure of cells to PDT induces the cell death by initiating apoptosis, necrosis, and autophagy (Figure 2). PDT treatment induces the release of cytochrome C from mitochondria, which leads to triggering of Caspase-9-mediated apoptotic response. Bcl-2 is a known anti-apoptotic protein and it is observed that PDT inhibits Bcl-2 activity and initiates cell apoptosis. Sinoporphyrin sodium-mediated photodynamic therapy was studied to induce apoptosis and the levels of cleaved caspase-3 and Bax protein were higher in PDT-treated cells [14]. Phenalenone mediated photodynamic therapy induced the apoptosis *via* activation of caspase-8 and p38-MAPK (mitogen-activated protein kinase). Similarly, the oxidative stress generated by indocyanine-mediated PDT also induced the apoptosis [15]. Berberine is a photosensitizer, which is known to cause apoptosis caspase-3 activation [16]. The phosphindole oxide containing photosensitizers were observed to induce the endoplasmic stress in cells

leading to initiation of apoptosis. The activation of tumour necrosis factor after PDT treatment led to induction of necrosis [17]. Further, RIP1 binds with RIP3 leading to formation of necrosome after the PDT treatment [18]. As PDT damages Bcl-2, it also helps to stimulate the protein such as Beclin1, Atg5 and Atg7 which ultimately leads to autophagy response in cells [19].

The effect of photodynamic therapy on GTPase

The proteins belonging to GTPase family have property to hydrolyse GTP (Guanosine triphosphate) to GDP (Guanosine diphosphate) [20]. GTPases are known to be involved in several cellular mechanisms such as signal transduction, differentiation, translocation, division, nuclear transport, etc. [20]. Thus, these small GTPases have crucial role in cell division, embryogenesis, cytoskeleton dynamics, neurotic development and cell proliferation [21]. The general structure of GTPase has three subunits alpha, beta, and gamma. The alpha subunit has the GTPase activity while the dimer of beta-gamma subunits has several distinct roles [22]. The binding of activator molecules leads to dissociation

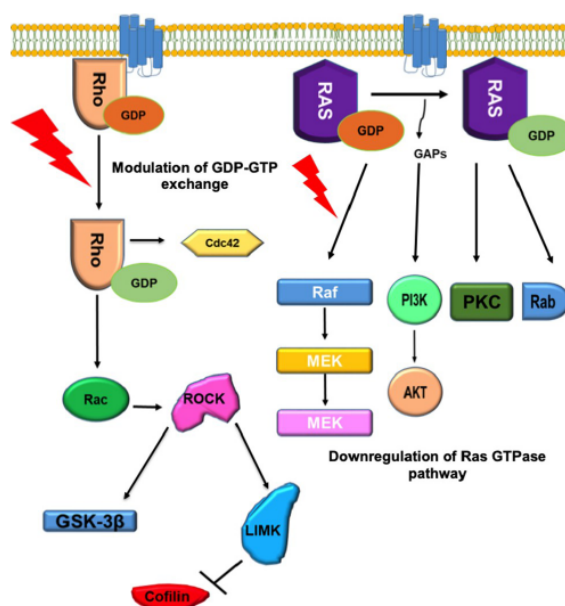


Figure 2. Induction of cell death after PDT. PDT is known to induce the cell death. PDT induces cell death via initiating apoptosis, necrosis and autophagy pathways. PDT upregulated the cytochrome C release from mitochondria, which leads to caspase-9-mediated apoptosis of cell. Similarly the ROS produces after PDT induces necrosis in the cells. PDT also causes inhibition of anti-apoptotic protein Bcl-2, which facilitates the apoptosis.

of GDP from alpha subunit with the help of GEFs (Guanine nucleotide exchange factor) and facilitates GTP binding. Whereas GAPs (GTPase-activating proteins) lead to release of GTP resulting in signal termination [23]. The modulation of GTPase signalling has been associated with various pathological conditions. Rho GTPase has been reported to be associated with several pathologies such as inflammation and cancer [24,25]. Rho is known to be involved in cell apoptosis, whereas the activation of Rac pathway elevated the cell survival. Rac GTPase activates the PAK kinase, which ultimately generates the survival signal via MAPK [25,26]. On contrary, Rho GTPase stimulates the ROCK pathways, which facilitates caspase-3-mediated apoptosis [27].

GTPase plays a key role in Cytoskeleton network

Rho GTPase is known to promote actin modulation in neurons. The Rho-mediated activation of LIMK induces the downregulation of cofilin-1, which results in polymerization of G-actin to F-actin [28]. The impairment of Rho GTPase leads to generation of several neurodegenerative disorders [29]. The studies on brain from AD patients suggested that Rac and PAK levels were depleted as compared to normal brain [30].

Similarly the aberrant increase of Rho GTPases were observed in the neuroblastoma cells, which leads to neurite retraction [31]. Gene silencing studies of topo II β resulted in downregulation of CDC42, Rac 1 and upregulation of Rho A, which leads to Parkinson's disease-like symptoms [30]. Similarly RhoA/ROCK, Rac1, and Cdc42 signalling cascades have been reported to be involved in various aspects of AD. Extracellular treatment of A β aggregates leads to localization of Rho A, which upregulated the phosphorylation of collapsin response mediator protein-2 (CRMP-2) in SH-SY5Y cells [32]. In myeloid precursor protein transgenic mice (J20) it was observed that the activity of caspase-2 downregulated due to the presence of amyloid aggregates. Rho GTPase plays key role in dendrites formation, the activity of Rho GTPase is modulated by Caspase-2. The studies suggested that the downregulation of caspase leads to reduced dendrites [33]. The studies carried on AD patients suggested that Rac and Cdc activity were downregulated whereas Rho was found to be co-localized with phosphorylated Tau [34]. Ran GTPase is the class which is known to be involved in the nucleocytoplasmic transport. It was observed that presence of Tau aggregates downregulated the expression of Ran leading to impaired nuclear transport [35]. Other neurodegenerative diseases such as Parkinson's disease (PD), Huntington's Disease

(HD), are reported to be associated with deregulation of Rho and Rac pathways. The Rac activity was reduced in HD fibroblast cells, whereas the modulation of Rac activity was restored after lowering of huntingtin in cells. In HD140Q/140Q primary neurons, the Rac activity was observed to be higher than wild type, which causes the upregulation of NOX (NADPH oxidase). The upregulation of NOX increased the production of reactive oxygen species [24]. The enhanced PAK expression enhanced the Htt aggregation *in-vitro* [36]. In PD, Rac plays a crucial role and rotenone is known to induce the PD like symptoms. The neurons exposed to rotenone were observed to have increased and decreased levels of Rho and Rac respectively [37]. LRRK2 (Leucine-rich repeat serine/threonine-protein kinase 2) phosphorylates several signalling protein and thus is known to be involved in processes like neuronal plasticity, autophagy, and vesicle trafficking, *etc.* The LRRK2 mutant SH-SY5Y cells observed to have retracted neurites. When Rac1 was overexpressed in cells the neurite retraction was rescued [38].

The involvement of deregulated of GTPase machinery in cancer

Cancer is another disease which has an extensive involvement of small GTPase as it has a major function in cell differentiation and migration [39]. The Rac GTPase and Rab35 are the common GTPases known to be involved in cell migration and proliferation [29,40]. Recent studies have demonstrated that the proliferation of cancerous cells is closely associated with the deregulation of Rab35. Hence, these small GTPases have been widely studied in various aspects of therapeutic strategies [41]. The recent studies have indicated the effect of PDT on various GTPase pathways (Figure 3). Talaporfin sodium is an improved photosensitizer belonging to second generation, which activated the Rho/ROCK signalling pathways resulting in blockage of tumour vessels [42]. The treatment of pancreatic cancer cells with alkyl modified cationic porphyrins downregulates the expression of KRAS and NRAS (Neuroblastoma RAS viral oncogene homolog) [43]. Ras/MEK is an important signalling cascade involved in cell proliferation and division. The inhibition of

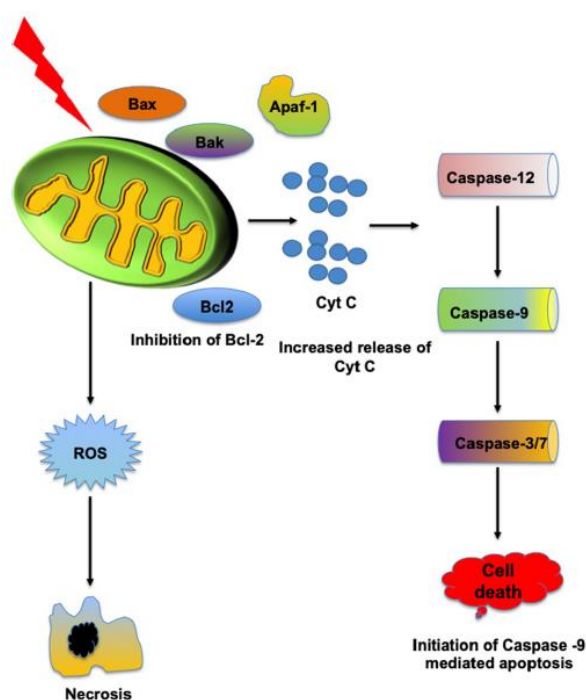


Figure 3. The modulation of key GTPase after PDT. PDT effects various signalling pathways in cell. The Rho and Ras GTPase are among the key GTPase protein which are known to involve in several cellular pathways. PDT is known to modulate the exchange of GTP and GDP which caused alternation in Rho GTPase function leading to downregulation several cellular pathways such as cytoskeleton modulation. Similarly PDT downregulated the Ras GTPase pathways leading to inhibition of cell division and proliferation. Apart from Rho and Ras, PDT also effects several other GTPase signalling cascades which results in modulation of various cellular functions.

MEK improved the potency of PDT in cancerous cells. The HeLa cells exposed to 5-aminolevulinic acid photodynamic therapy (ALA-PDT) was observed to have modulated Ras/Raf/MEK/ERK pathways, which ultimately reduced the papillomavirus load via induced autophagy [19]. Similarly, the combinatorial PDT treatment of natural isothiocyanate 'sulforaphene' and photofrin reduced the cell proliferation of FRO (human anaplastic thyroid carcinoma cells) cells by modulation of Ras/Raf/MEK/ERK pathways [44]. The potency of photo-active radachlorin was tested on HEC-1-A endometrial adenocarcinoma cell lines, and the results of these studies suggested that PDT showed efficiency against cancerous cells by downregulation of signalling molecules including VEGFR2 (Vascular endothelial growth factor receptor 2), EGFR (Epidermal growth factor receptor), Ras homolog gene family/ member A (RhoA) [45]. The effect of PDT has been reported to be associated with the inhibition of GTP-GDP exchange. Various studies carried on GTPase suggested that PDT modulated the exchange of GTP-GDP. Pheophorbide A (PhA) and delta-aminolevulinic acid-mediated PDT are known to hamper the GTP-GDP exchange in cancerous cells [46]. The studies have been done in context of the role of PDT in modulating GAP (GTPase-activating proteins). It was observed that in the presence of TAT-RasGAP (317–326) the effect of mTHPC-mediated photodynamic therapy (PDT) was increased [47]. Rac1/PAK1/LIMK1/cofilin signalling plays a crucial role in regulation of the cell migration by effecting actin dynamics. Chlorin e6 (Ce6-PDT)-mediated PDT downregulated the Rac1/PAK1/LIMK1/cofilin signalling, which retarded the migration of colon cancer SW620 cells [48]. Similarly Ce6-PDT was observed to destroy actin network of colon cancer SW480 cells which could be a consequence of downregulation of Rho GTPase pathway [49]. These studies indicated that proteins belonging to GTPase family are behaving as a preliminary target for PDT.

Photodynamic therapy in neurodegenera

Neurodegenerative disorders are characterized by progressive loss of neuron, memory deprivation, language dysfunction, impaired problem solving and thinking skills, motor nerves dysfunction. Parkinson's disease, Huntington's disease, Creutzfeldt – Jakob disease, Fronto-temporal dementia, and Alzheimer's disease are examples of neurodegenerative disorders [50]. Neurodegenerative diseases have been reported to be associated with protein misfolding, oligomerization and accumulation of protein aggregates [51]. Aggregates of

α -synuclein lead to generation of lewy bodies, which are considered as a cause for the progression of Parkinson's disease. Several studies suggest that mutation in α -synuclein locus leads to generation of familial Parkinson's disease [52,53]. Similarly, the misfolded prion protein leads to the generation of sporadic Prpsc (scrapie isoform of the prion protein), resulting in generation of Creutzfeldt-Jakob disease. The trinucleotide disorder such as Huntington's disease involves the aggregation of Huntingtin protein [53]. Intracellular Tau aggregates and extracellular senile plaques are known to be hallmarks of Alzheimer's disease. Alzheimer's disease is the neurodegenerative disease characterized by progressive memory loss and behavioural impairments [54]. PDT is widely used for the treatment of microbial infections, carcinomas, and dermatologic lesions (Figure 4). Several queries have been raised for the application of PDT on neuronal tissues. In recent years, advanced studies and techniques led to the hope that PDT could be used against neurodegenerative diseases (NDs). Several photosensitizers were tested for their efficiency against these pathological protein aggregates of NDs. Fullerene-sugar hybrid was designed and tested against A β aggregates of Alzheimer's disease. Fullerene-sugar photo activated by 365 nm UV light potentially inhibited the aggregation A β peptides [55]. Similarly, Polyoxometalate irradiated with 365 nm UV light degraded the A β fibrils [56]. 3-(4'-trifluoromethylphenyl)-5-(4'-methoxyphenyl)

-1,2,4-oxadiazole is another photosensitizer, which is reported to degrade A β fibrils and reduced the A β -mediated cytotoxicity in neuroblastoma cells [57]. Moreover, the photosensitizers having excitation in visible region are reported to have the potency against A β aggregates [58,59]. Tetra (4-sulfonatophenyl) porphyrin (TPPS), which is excited by blue light and Thioflavin T, are the compounds which are used against A β aggregation. The dyes such as Rose Bengal and methylene blue attenuated the A β aggregation upon irradiation with particular wavelength of light [60,61]. Additionally, the metal-based compounds such as Bismuth Vanadate and Zn phthalocyanine dis-aggregated A β aggregates efficiently. In recent studies, compounds having excitation in IR range are reported for their efficiency against A β . RB/UCNP@ROS and β NaYF₄:Yb/Er@SiO₂@RB are the compounds when irradiated with 980 nm of light lead to dissolution of A β aggregates [55]. Tau aggregation, which is a hallmark of several neurodegenerative diseases such as AD, progressive supranuclear palsy, corticobasal syndrome, pick's disease, chronic traumatic encephalopathy, *etc.* [62–64]. In some reported studies it was

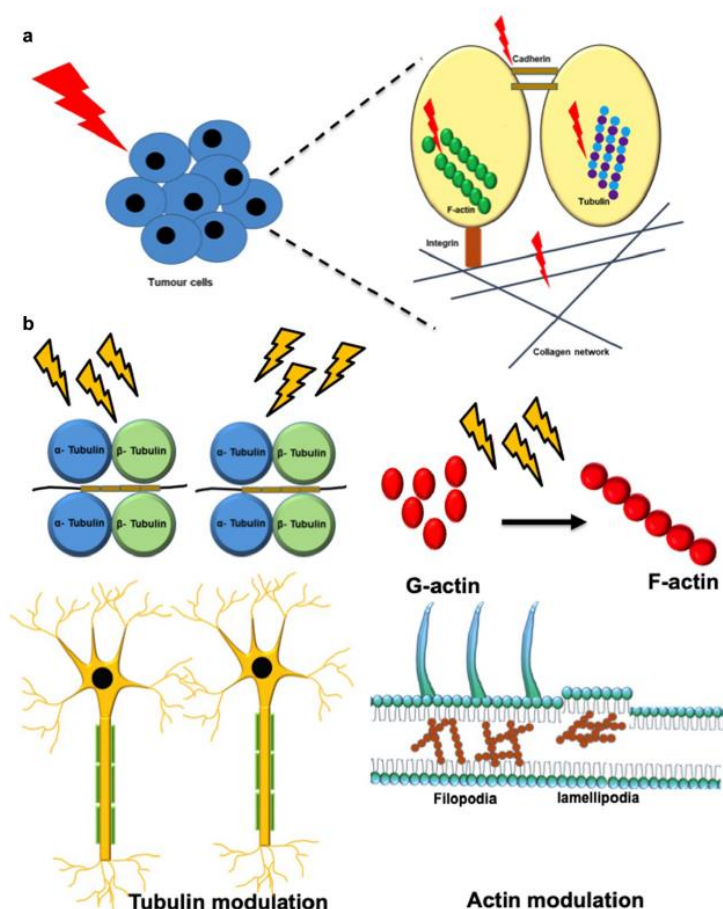


Figure 4. PDT modulates various cytoskeleton elements. The cytoskeleton is one of the primary targets of PDT. In cancerous cells PDT targets the cytoskeleton components such as actin, tubulin, and integrin the destruction of these elements ultimately leads to induction of cell death. In neuronal tissues PDT observed to modulate the cytoskeleton. The increased neurite extensions after PDT evidenced the effect of PDT on tubulin whereas cell exposed to PDT had increased actin-rich structures.

suggested that the photo-excited dyes could have therapeutic potential against Tau aggregation. The photo-active phenothiazine dye, Toluidine Blue (TB), induces the disaggregation of Tau fibrils. TB was found to attenuate the aggregation of soluble Tau *in-vitro*. The *in-vivo* studies on *Drosophila* model suggested that TB and PE-TB treatment improved the cognition, learning and survival of *Drosophila* [62]. Similarly, the effect of xanthene dye Rose Bengal (RB) was studied for its potency against Tau aggregation. The *in-vitro* studies suggested that RB efficiently attenuated the aggregation of Tau, whereas the treatment of photo-excited RB disrupted the mature Tau aggregates (Figure 5). The exposure to RB and PE-RB improved the cognition and survival of UAS Tau E14 transgenic *Drosophila* [65]. Apart from these studies, dyes which have the potential for photo-activation have been reported to attenuate Tau and A β aggregation. Erythrosine B (ER) is

a xanthene dye, which is used as food colouring agent. The dye has high lipid solubility and hence, can cross the blood-brain barrier. It was observed that ER modulated the aggregation of A β and helped in reducing A β -mediated toxicity [66]. Curcumin is the polyphenol isolated from *Curcuma longa*. Curcumin is known to attenuate the *in-vitro* aggregation of A β [67]. Although the studies are in preliminary phase but the data obtained from all the studies suggested that photodynamic therapy could emerge as a new strategy against neurodegenerative diseases.

Photodynamic therapy in neuroglial activation

Microglial cells are specialized type of macrophages, which have protective functions in nervous system. The microglia cells perform continuous surveillance

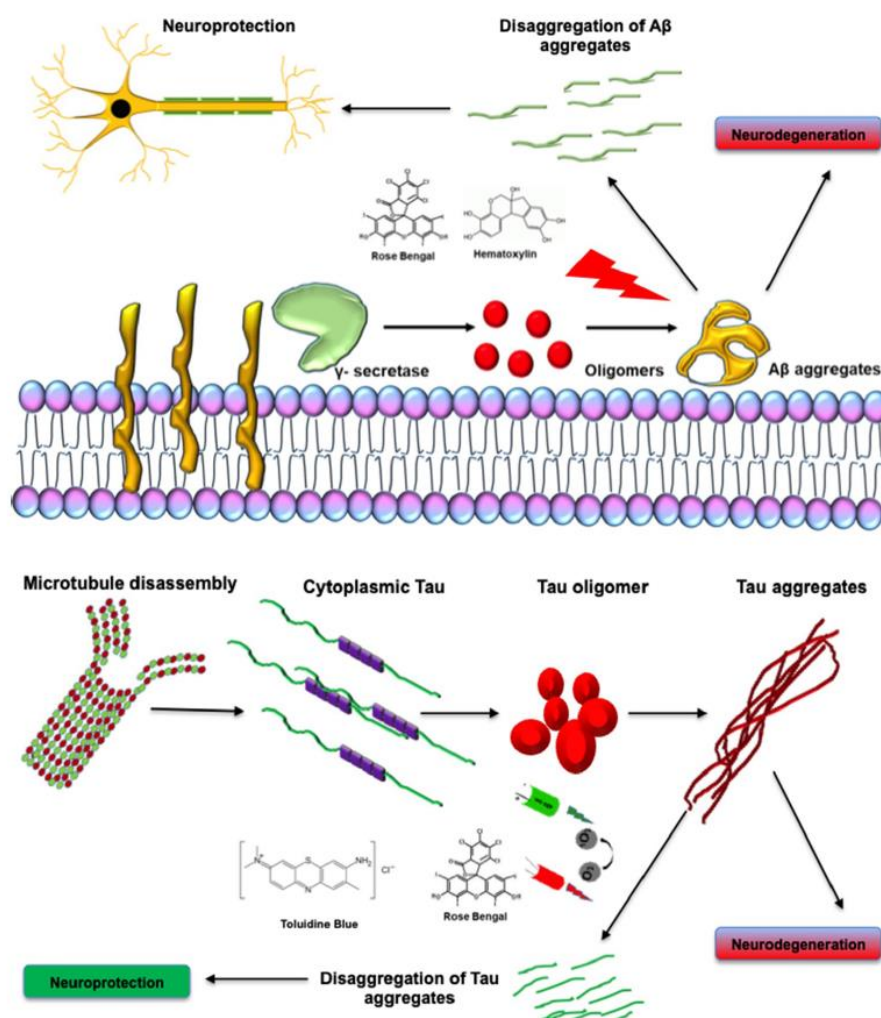


Figure 5. PDT attenuates the Alzheimer's disease-related amyloid aggregates. Extracellular amyloid beta and intracellular Tau protein aggregates are known to be closely associated with Alzheimer's disease. Several photo-excited molecules such as methylene blue, rose Bengal etc dissolve the mature amyloid beta aggregates and rescues the cells from toxicity. Similarly, photo-excited toluidine blue and rose Bengal improves the viability of Tau treated cells and disaggregates the matured Tau fibrils *in-vitro*.

of neuronal tissues and provide the first line of defence against invading pathogens. In resting state, microglia possesses ramified or branched morphology whereas, after activation microglia acquire an amoeboid morphology [68–70]. Actin modulation plays a crucial role in migration of microglia. The actin-rich structures such as fan like lamellipodia and figure like filopodia assist the microglia in migration [71]. The microglia cells deposit near the site of injury and release the pro-inflammatory cytokines such as TNF- γ , IL-1 β , TNF- α , etc which results in inflammation [72]. Microglia cells are known to be involved in homeostasis of neuronal tissues. The microglial specific receptors such as CX3CR1, CD11b, Iba1, and F4/80, P2ry12 and TREM2 are known to be involved in sensing,

autophagy, inflammation, and neurodegeneration [73,74]. Microglia are known to clear the A β plaques from neurons and deregulation of microglial machinery leads to elevated amyloid beta deposits and Tau hyperphosphorylation [75]. Hence, it was observed that microglia has a wide functional aspect which could be further studied. In 1980s the photofrin-mediated PDT was first tested against glioma [76]. The oxidative stress generated by PDT led to apoptotic responses in neurons and glial cells. The studies carried on using THPC-PDT on rat neurons and satellite glia, compared with human adenocarcinoma cells (MCF-7) suggested that MCF-7s and satellite glia were more sensitive to PDT than neurons. The ALA-PpIX-mediated PDT improved the survival and reduced the inflammation

in glioblastoma rat cells [77]. The PDT leads to generation of nitric oxide and various studies have evidenced that the NO generated after PDT leads to death of glial cells [78]. The study carried on crayfish suggested that the radachlorin-mediated PDT induced the autophagy response in sensory neurons of glial envelope. Another study on crayfish model indicated that PDT induces the nitric oxide stress in glial cells, which ultimately causes death of cells [79]. The glial death after PDT was studied to be associated with several signalling cascades such as phospholipase C/Ca²⁺, Ca²⁺/calmodulin/CaMKII, Ca²⁺/PKC, Akt/mTOR, MEK/p38, and protein kinase G *etc.* It was observed that alumophthalocyanine-mediated PDT reduced the release of natural neuroglial mediator N-acetylaspartylglutamate resulting in generation of apoptosis [80]. The treatment of phospholipid-conjugated indocyanine green (LP-iDOPE) in rat 9 L glioblastoma model enhanced the immune response by accumulation of CD8 + T-cells and HSP70, which helped in improving survival [81]. It was observed that the Photofrin-mediated treatment induced transient proliferation of microglia, which indicated the modulation on glioma microenvironment [82]. The evidence generated by various studies indicated that PDT effects glial cells significantly.

Photodynamic therapy in clinical use

The recent research advancements in PDT led to its clinical implication against several diseases. The PDT has been found to be effective against pre-cancerous lesions, non-melanoma skin cancers, skin infections, acne, and microbial infections (Table 1). The first clinical approval of PDT was reported in year 1993 which includes the application of Hematoporphyrin-derived photosensitizers [83]. Photofrin is one of the early photosensitizer that was used clinically for treatment of carcinomas. Photofrin was used in the treatment of head and neck tumours. Subsequently, UK, USA, and Canada approved porfimer sodium for the treatment of various carcinomas like lung and oesophageal cancer [84,85]. After 2000, various new photosensitizers have

been approved for the clinical use such as Temoporfin and Talaporfin, which have been used for treatment of lung and oesophageal cancers [86,87]. Another class of photosensitizer, Motexafin Lutetium (MLu), was found to be effective on patient suffering from prostate cancer [88]. After the year 2010 the advancements in field of PDT led to approval of some more photosensitizers such as Hexaminolevulinic acid and Padeliporfin in USA, Sweden and Mexico for the treatment of prostate and oesophageal cancer. Verteporfin is another clinically approved photosensitizer which is used in the treatment of age related macular degeneration (AMD). In recent years, PDT has been used as a combinatorial therapy for treatment of cancer [89]. This combinatorial strategy helped to overcome several side effects of chemotherapy and radiotherapy. The application of platinum (IV) complex-based prodrug monomer (PPM) and 2-methacryloyloxy ethyl phosphorylcholine (MPC) observed to facilitate the drug delivery and helped in overcoming the problem of multidrug resistance in tumour [90]. Similarly, the combination of doxorubicin and chlorin e6 loaded (Dox@MSNs-Ce6) on silica nanoparticles efficiently entered A549 lung cancer cells and increased the potency of the drug [91]. In 2000, USA approved the use of ALA-PDT for the treatment of dermatological conditions. In 2003, ALA-PDT got the approval for the treatment of Acne [92]. Addition to ALA-PDT, MLA based PDT were also approved for clinical use in the treatment of dermatological problems such as actinic keratosis (AK) [93]. Additionally, PDT has also been used for the treatment of microbial infections such as *streptococci* and *Lactobacillus* (Figure 6). Hence, PDT has emerged as a potent therapeutic approach in several fields and the recent researches on PDT provides a strong hint that PDT application would be increased in all other clinical areas as well.

PDT has advantages over classical therapies

PDT is emerging therapy in several areas. Various photosensitizers have been approved for clinical use and some of them are showing promising leads in pre-

Table 1.

S.No.	Name of photosensitizer	Target	Year of clinical approval
1.	Photofrin	Head and neck carcinoma and lung cancer	1993 In Canada, 1995 In USA, 1998 In UK
2.	Temoporfin	Oesophageal cancer	2001 In china
3.	Talaporfin	Lung cancer	2003 In Japan
4.	Chlorin e6	Ladder cancer	2006 In Russia
5.	ALA	Brain tumour	2017
6.	Padelliporfin	Prostate cancer	2018 In Mexico

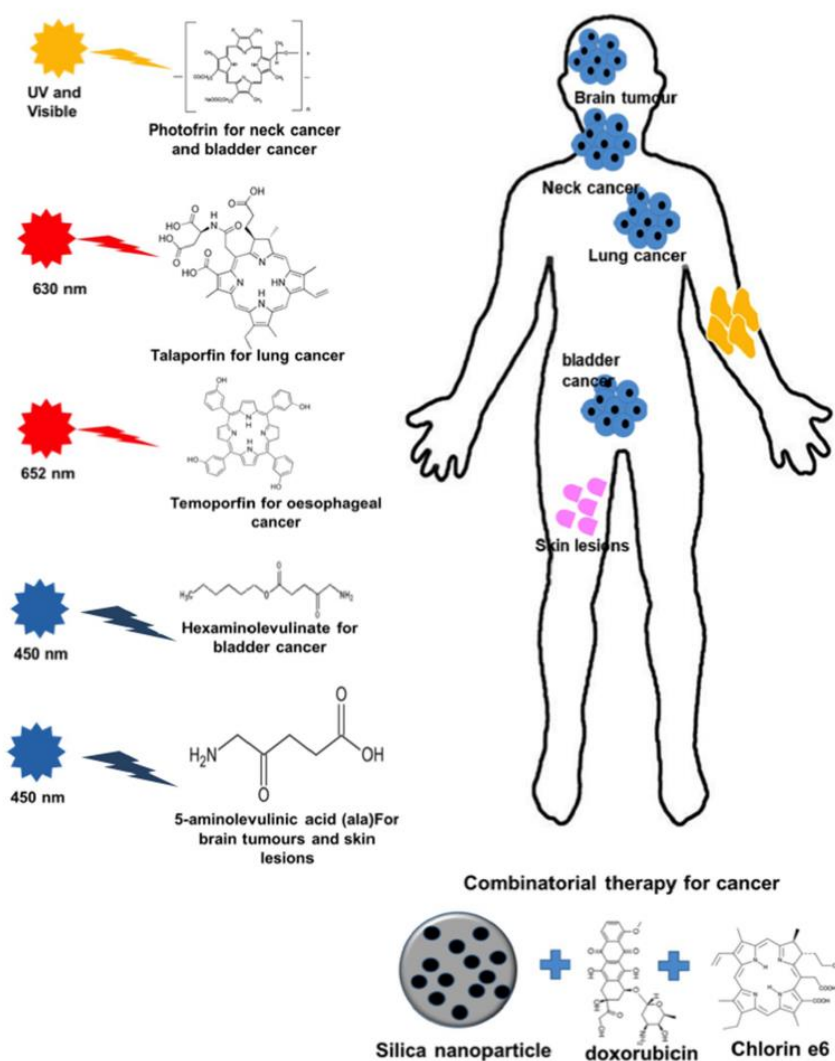


Figure 6. The clinical application of PDT against various disease. Several advancements have been made in field of PDT which facilitated its clinical application. The involvement of new generation of photosensitizer and combinatorial therapies have supported the use of PDT against several diseases which are showing promising results.

clinical trials. The advantages of PDT which gives it edge over other therapies include-

- PDT has a limited long-term side effects and the degree of side-effects is certainly low as compared to other techniques such as chemotherapy.
- Low degree of invasiveness- PDT treatment requires very less or no invasive surgery. In several cases, the topical irradiation showed the effect while surgery is required only for internal tissues present under the skin.
- PDT is cost effective and affordable therapy as compared to other techniques like chemo and radio therapy. The photosensitizer and irradiation are easy to setup thus the cost of treatment reduces to appreciable extent.
- Post PDT, the treated area recovered rapidly leaving very little scars.
- The therapeutic strategies such as chemotherapy or radiotherapy require multiple rounds of treatment while in PDT single exposure causes the desired effect on target tissues.

The challenges of PDT

- PDT can only be applied to cells which are present on surface since the irradiation of cells plays a challenging role for deep tissues.
- Another key drawback is that the PDT can only be applied to localized tissues. The metastatic tissues cannot be treated with PDT efficiently.
- The dark toxicity is one of the major concern, as the molecules applied for PDT are very sensitive to light thus it is very important for a patient not to expose to light after the treatment.
- The most important question arises when we wish to apply PDT in neuronal cells. The choice of photosensitizer which can cross blood brain barrier and the delivery of light to neuronal tissues are two major challenges arises in case of PDT.
- Another challenge is in choosing the photosensitizer which will not accumulate in body for long time. If the body will not be able excrete these photosensitizers they may lead to cytotoxicity.

Consent for publication

All authors consent to the publication.

Acknowledgments

Tushar Dubey acknowledges the fellowship from University Grant Commission (UGC), India. We thank Chinnathambi's lab people for their fruitful discussion on manuscript.

Disclosure statement

The authors declare that they have no competing interests.


Funding

This project is supported in part by grant from in-house CSIR-National Chemical Laboratory grant MLP101726.

Author contributions

TD and SC collected and reviewed the literature and wrote the manuscript. SC conceived the idea for the project, resource provided, supervised and wrote the manuscript. Both the authors read and approved the final manuscript.

ORCID

Subashchandrabose Chinnathambi  <http://orcid.org/0000-0002-5468-2129>

References

- [1] Zhao J, Duan L, Wang A, et al. Insight into the efficiency of oxygen introduced photodynamic therapy (PDT) and deep PDT against cancers with various assembled nanocarriers. *Wiley Interdiscip Rev Nanomed Nanobiotechnol.* 2020;12:e1583.
- [2] Meimandi M, Ardakani MRT, Nejad AE, et al. The effect of photodynamic therapy in the treatment of chronic periodontitis: a review of literature. *J Lasers Med Sci.* 2017;8:S7.
- [3] Lan M, Zhao S, Liu W, et al. Photosensitizers for photodynamic therapy. *Adv Healthc Mater.* 2019;8:1900132.
- [4] Abrahamse H, Hamblin MR. New photosensitizers for photodynamic therapy. *Biochem J.* 2016;473:347–364.
- [5] Agostinis P, Berg K, Cengel KA, et al. Photodynamic therapy of cancer: an update. *CA Cancer J Clin.* 2011;61:250–281.
- [6] Kou J, Dou D, Yang L. Porphyrin photosensitizers in photodynamic therapy and its applications. *Oncotarget.* 2017;8:81591.
- [7] Kamkaew A, Lim SH, Lee HB, et al. BODIPY dyes in photodynamic therapy. *Chem Soc Rev.* 2013;42:77–88.
- [8] Ormond AB, Freeman HS. Dye sensitizers for photodynamic therapy. *Materials.* 2013;6:817–840.
- [9] Shi C, Wu JB, Pan D. Review on near-infrared heptamethine cyanine dyes as theranostic agents for tumor imaging, targeting, and photodynamic therapy. *J Biomed Opt.* 2016;21:050901.
- [10] Li L, Chen Y, Chen W, et al. Photodynamic therapy based on organic small molecular fluorescent dyes. *Chin Chem Lett.* 2019;30:1689–1703.
- [11] Allison RR, Moghissi K. Photodynamic therapy (PDT): PDT mechanisms. *Clin Endosc.* 2013;46:24.
- [12] Lawen A. Apoptosis—an introduction. *Bioessays.* 2003;25:888–896.
- [13] Cohen GM. Caspases: the executioners of apoptosis. *Biochem J.* 1997;326:1–16.
- [14] Wang H, Wang X, Zhang S, et al. Sinoporphyrin sodium, a novel sensitizer, triggers mitochondrial-dependent apoptosis in ECA-109 cells via production of reactive oxygen species. *Int J Nanomedicine.* 2014;9:3077.
- [15] Salmerón ML, Quintana-Aguilar J, De La Rosa JV, et al. Phenalenone-photodynamic therapy induces apoptosis on human tumor cells mediated by caspase-8 and p38-MAPK activation. *Mol Carcinog.* 2018;57:1525–1539.
- [16] Wang X, Gong Q, Song C, et al. Berberine-photodynamic therapy sensitizes melanoma cells to cisplatin-induced apoptosis through ROS-mediated P38 MAPK pathways. *Toxicol Appl Pharmacol.* 2021;418:115484.
- [17] Wang H, Xiong L, Xia Y, et al. 5-aminolevulinic acid-based photodynamic therapy induces both necrosis and apoptosis of keratinocytes in plantar warts. *J Cosmet Laser Ther.* 2020;22:165–170.
- [18] Bin L, Xu G, Wang Z-Q, et al. Shikonin induces glioma cell necroptosis in vitro by ROS overproduction and promoting RIP1/RIP3 necrosome formation. *Acta Pharmacol Sin.* 2017;38:1543–1553.



Contents lists available at ScienceDirect

Archives of Biochemistry and Biophysics

journal homepage: www.elsevier.com/locate/yabbi

Review article

Brahmi (*Bacopa monnieri*): An ayurvedic herb against the Alzheimer's diseaseTushar Dubey^{a,b}, Subashchandra Bose Chinnathambi^{a,b,*}^a Neurobiology Group, Division of Biochemical Sciences, CSIR-National Chemical Laboratory, Dr. Homi Bhabha Road, 411008, Pune, India^b Academy of Scientific and Innovative Research (AcSIR), 411008, Pune, India

ARTICLE INFO

Keywords:

Brahmi
Reactive oxygen species
Neuroinflammation
Neurodegeneration
Antioxidant
Tau
Amyloid beta
Alzheimer's disease

ABSTRACT

Ayurveda is the medicinal science, dealing with utilization of naturally available plant products for treatment. A wide variety of neuroprotective herbs have been reported in Ayurveda. Brahmi, *Bacopa monnieri* is a nootropic ayurvedic herb known to be effective in neurological disorders from ancient times. Numerous approaches including natural and synthetic compounds have been applied against Alzheimer's disease. Amyloid- β and Tau are the hallmarks proteins of several neuronal dysfunctions resulting in Alzheimer's disease. Tau is a microtubule-associated protein known to be involved in progression of Alzheimer's disease. The generation of reactive oxygen species, increased neuroinflammation and neurotoxicity are the major physiological dysfunctions associated with Tau aggregates, which leads to dementia and behavioural deficits. Bacoside A, Bacoside B, Bacosaponins, Betulinic acid, etc; are the bioactive component of Brahmi belonging to various chemical families. Each chemical component known have its significant role in neuroprotection. The neuroprotective properties of Brahmi and its bioactive components including reduction of ROS, neuroinflammation, aggregation inhibition of Amyloid- β and improvement of cognitive and learning behaviour. Here on basis of earlier studies we hypothesize the inhibitory role of Brahmi against Tau-mediated toxicity. The overall studies have concluded that Brahmi can be used as a lead formulation for treatment of Alzheimer's disease and other neurological disorders.

1. Introduction

Ayurveda is an ancient science, dealing with understanding, screening the medicinal property of naturally available plant products and their role in treatment of various diseases [1]. According to Ayurveda, the human body influenced by three energies or doshas viz "Vata", "Pitta", and "Kapha". The imbalance between these components would lead to generation of diseases [2]. The predominance of "Vata" dosh generates neurological disorders, symptomized as memory loss, poor blood circulation, anxiety etc. The "Pitta" imbalance leads to gastric troubles and imbalanced "Kapha" correlates to cholesterol related diseases in body. Thus, ayurveda implies the medicines and formulations of herbal origin to balance dosha aiming to cure the diseases [3]. Imbalanced "Vata" results in neurodegenerative diseases, hence the prescribed herbal formulations to patients targets stabilization of the "Vata" component of body [4]. Brahmi (*Bacopa monnieri*), Shankhpushpi (*Convolvulus pluricaulis*), Jatamansi (*Nardostachys jatamansi*), Ashwagandha (*Withania somanifera*), Sargandha (*Rauwolfia serpentina*), are herbs of ayurveda, which are regularly administered for

rehabilitating the neurological problem in various formulations such as Kwath, Churna, Asav, Vati etc., [5] (Fig. 1). Ayurveda has been remarkably noticed in from past few years by modern science as various extract of these medicines have been shown neuroprotective potency against various neurological disorders (Table 1) [6]. The extract of ayurvedic herbs known to comprises of several bioactive component belonging to different categories. A total of 20 phytochemical have been reported to be present in ethanolic extract of Brahmi. Similarly chemical belonging to alkaloids, saponins, alcohols etc. are also present in extract of other ayurvedic herbs.

1.1. Neurodegeneration and Alzheimer's disease

Neurodegeneration is characterised by gradual loss of neurons, impairment of memory, locomotion and cognition are the prominent consequences of neurodegeneration [7]. The neuronal disorders such as Alzheimer's, Parkinson's, Huntington's disease, Schizophrenia etc., have been categorized under neurodegeneration [8]. The risk factor for neurodegeneration include increased load of amyloid aggregates,

Abbreviations: AD, Alzheimer's disease; Nrf2, Nuclear factor erythroid 2-related factor 2; ERK, Extra cellular signal regulated kinase; CCAP, Caspase cysteine aspartic protease; CDK5, Cyclin dependent kinase 5; TNF, tumour necrosis factor; IL-1, interleukin 1; ROS, reactive oxygen species

* Corresponding author. Neurobiology group, Division of Biochemical Sciences, CSIR-National Chemical Laboratory (CSIR-NCL), Dr. Homi Bhabha Road, 411008, Pune, India.

E-mail address: s.chinnathambi@ncl.res.in (S. Chinnathambi).

<https://doi.org/10.1016/j.ab.2019.108153>

Received 1 September 2019; Received in revised form 8 October 2019; Accepted 11 October 2019

Available online 14 October 2019

0003-9861/ © 2019 Elsevier Inc. All rights reserved.

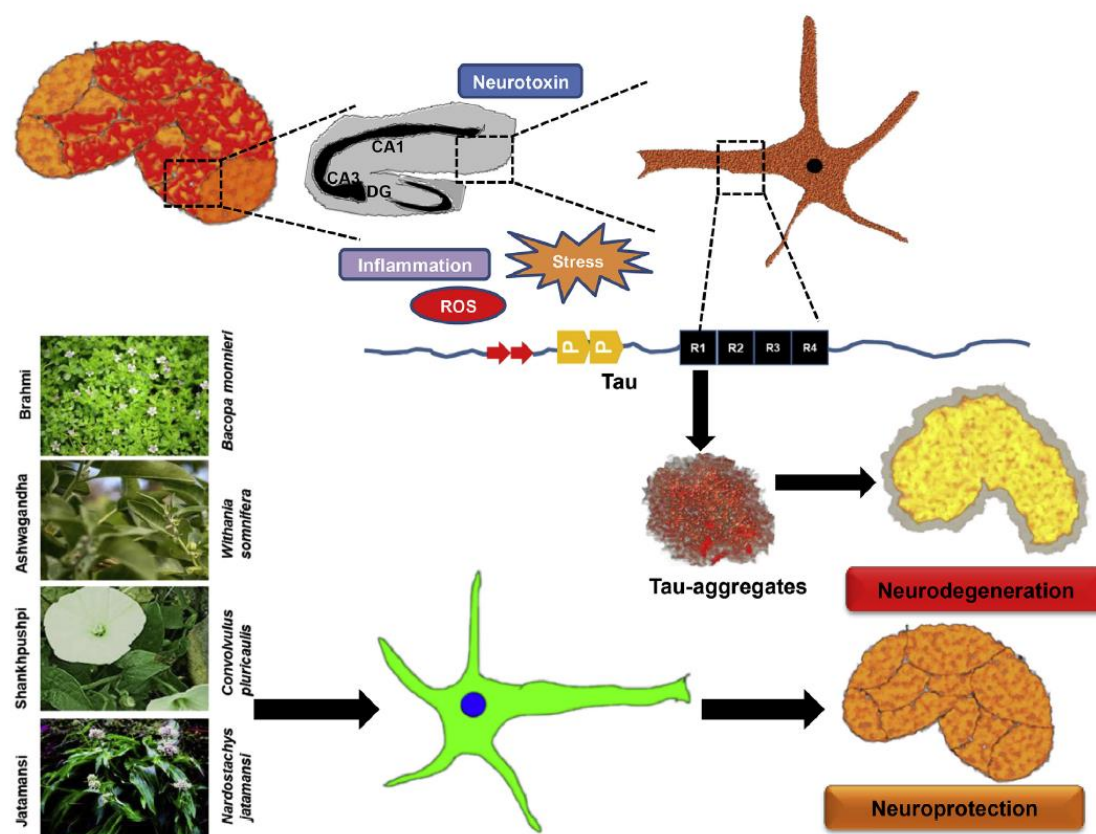


Fig. 1. The broader overview of Neurodegeneration. The hippocampal region is involved in generation of episodic memory. CA1, CA3 and dentate gyrus are the region which are preliminary effected in AD. Several stress factors as neurotoxin, hypertension, ROS leads to the aggregation of microtubule-associated Tau protein resulting in neurodegeneration. In ayurveda a spectrum of herbs have been reported are administered in various formulation so as to recover brain from degeneration. Brahmi, Shankpushpi, Jatamansi and Ashwagandha are the common herbs, which are reported to have neuroprotective properties.

elevated oxidative stress and genetic mutations [9,10]. AD is prominent dementia emerging worldwide at an exponential rate [11]. An estimate of 46.8 million people worldwide have been reported for suffering from AD in 2015, this number would increase to a 75 million till 2030 [12]. The statistical data suggested that by 2050 prevalence of AD would be increase to an intensity that at every 33 s one person would be diagnosed for AD [13]. The definite cause of AD is still debatable, but three hypothesis viz. protein aggregation, cholinergic neuron and gene mutation hypothesis are being given more consideration. The cholinergic neuron hypothesis states that the loss of acetyl choline transmission leads to neurodegeneration in AD [14,15]. The genetic risk factors of AD include the mutation in ApoE, APP, PS1 genes, which leads to impaired protein metabolism resulting in neuronal loss [16,17]. The deposition of protein aggregates extensively studied as a cause for generation of AD and this would be an emerging cause of AD [18,19].

1.2. Ayurvedic herbs in Alzheimer's disease

AD is neurological disorder, which generally reported in patients of above the age of 60 years. The worldwide increased rate of AD emergence directed the researches for studying the remedy for the disease [12]. The approaches for treatment of AD include application of various molecules of natural as well as synthetic origin. Ayurvedic herbs have diverse chemical composition that gives liberty to test numerous formulations against various aspects of AD. Ashwagandha, the Indian ginseng is known to be effective against AD, the alkaloids of

Ashwagandha is known to increase the cognitive function by modulating the acetyl choline levels and attenuating the amyloid- β aggregation [20]. Similarly *Curcuma longa* reported to reduce the Amyloid- β -induced oxidative stress and neuroinflammation in cells. *In-vitro* the down regulation of peroxidase activity after *Curcuma longa* treatment has been reported [21]. Shankpushpi is an Indian herb, which has been known to reduce the cognitive dysfunction by altering acetylcholine esterase activity in CA1 and CA3 region of rats [22]. Similarly Ghotu kola, Jatamansi and Guggulu are the distinguished herbs, which reduce oxidative stress in brain and act as neuroprotective agent [23,24]. *Ginkgo biloba* showed neuroprotective activity similar to common AD drug Donepezil, which increases the cholinergic neuron activity in brain [25,26]. *Rosmarinus officinalis* contains numerous cyclooxygenase-2 (COX-2) inhibitors such as Apigenin, Eugenol thus it is considered to be beneficial in Alzheimer-related pathology [27]. Moreover *Acronis calamus* is also been reported for its property to improve the memory. The asarone present in *Acorus* inhibits the acetylcholine esterase activity and thus reduces the risk of AD [28]. Reserpine obtained from *Rauvolfia serpentina* possess antipsychotic and anti-depressant activity, which designate it as a neuroprotective herb [29,30]. Among all these herbs Brahmi and its active component have been exclusively studies in context of neurodegeneration. Brahmi have been proven to possess antioxidant and neuroprotective activity, thus making it most promising herb in treatment of AD [31].

Table 1
Neuroprotective herbs in Ayurveda. Ayurveda implements the use of many herbs for the treatment of various diseases. Each part of plant has a characteristic medicinal use which is extensively explored in Ayurveda. The table suggests the nootropic herbs regularly used in Ayurveda to treat neurological disorders.

S.No.	Name of Herb	Medicinal part of plant	Bioactive component	Model System	Function	Reference
1.	Ashwagandha (<i>Withania somnifera</i>)	Roots	withanine, withananine, somniferine, somnifone, somnifone	Male Wistar rat	Reduction of neuroinflammation, Depression, Memory deficit	Kumar et al., 2009
2.	Jatamansi (<i>Nardostachys jatamansi</i>)	Roots	sesquiterpenoids, valeriananoids	Streptozotocin- induced cognitive impaired rats	Memory deficit, Insomnia	Khan M et al., 2012
3.	Sarpagandha (<i>Rauwolfia serpentina</i>)	Roots	Reserpine	Human patients of hypertension	Hypertension, Insomnia, Depression	Lobay et al., 2015
4.	Turmeric (<i>Curcuma Longa</i>)	Roots	Curcumin	<i>C. elegans</i> (R406W Tau model)	Reduction of Neuroinflammation, neurodegeneration, memory deficit	Monroy et al., 2013
5.	Shankhpushpi (<i>Convolvulus pluricaulis</i>)	Leaves	Shankhpushpine, convolamine, convoline,	Drosophila model (V337M/FM7a; GMR/CyO)	Improvement of memory and learning ability, Reducing Tau- mediated toxicity	Khizhakkie A et al., 2019
6.	Brahmi (<i>Bacopa monnieri</i>)	Leaves	Bacoside A, Betulinic acid, Bacosposide	AF64A-induced AD model of Wistar rats	Improvement in memory and cognitive function	Uabundit N et al., 2019
7.	Awla (<i>Embllica officinalis</i>)	Fruit	Pyrogallol	Swiss albino mice	Improvement of memory	Vasudevan et al., 2007
8.	Guggul (<i>Commiphora mukul</i>)	Gum	Guggulsterones	<i>In-vitro</i> biochemical assays	Antioxidant	Khan et al., 2001 Dubey et al., 2009
9.	Gotu kola (<i>Centella asiatica</i>)	Leaves	Asiaticoside A, Asiaticoside B, Asiatic acid	Sprague-Dawley rats, SHSY-5Y cell lines	Improvement of memory and learning	Shah et al., 2012 Dey et al., 2015
10.	Jyotishmati (<i>Celastrus paniculatus</i>)	Seed/Seed oil	Pristimerin	Restraint stressed male Wistar rats	Antioxidant	Xu Y et al., 2008
11.	Gloy (<i>Tinospora cordifolia</i>)	Leaves	Timocordioside	Swiss albino mice	Memory enhancer Anti-depressant	Bhagya V et al., 2016
12.	Tulsi (<i>Ocimum sanctum</i>)	Leaves	Cordiosides	Male Wistar rats	Acetyl choline inhibition	Girdharan V et al., 2010
13.	Neem (<i>Azadirachta indica</i>)	Leaves	Eugenol	Charles-Foster albino rats	Improvement of cognition	Raghvendra et al., 2013
14.	Bringraj (<i>Eclipta alba</i>)	Leaves	Limonoids Wedelolactone	Cerebral ischemia stressed male Wistar rat	Antioxidant	Mansoorali et al., 2012
15.	Vacha (<i>Acorus calamus</i>)	Rizome	Asarone, Asaraldehyde	Middle cerebral artery occlusion induced Wistar rat	Improves learning Improves the learning	Shukla PK et al., 2013
16.	Shatavar (<i>Asparagus racemosus</i>)	Rizome	Shatavarin IV	Female Swiss albino mice	Antioxidant Anti-Parkinson's herb	Parihar M et al., 2004
17.	Vidari Kanda (<i>Pueraria tuberosa</i>)	Rizome	Tuberosin	scopolamine-induced amnesia in Wister mice	Antioxidant Nootropic	Rao et al., 2008
18.	Kesar (<i>Crocus sativus</i>)	Stigma, style of flower	Crocins	6-OHDA- stressed Wistar rat	Antioxidant, Anti-Parkinson effect	Shaterzadeh H et al., 2018
19.	Almond (<i>Prunus amygdalus</i>)	Seed	Morin	<i>In-vitro</i> model of recombinant A β aggregates. PC 12 cells	Destabilises the Amyloid- β Fibrils	Lamkul JA et al., 2010
20.	Garlic (<i>Allium sativum</i>)	Cloves	Crude extract	A β (1–42) rat model of AD	Downregulation of Amyloid- β induced apoptosis in PC12 cells.	Guo JP et al., 2010
21.	Pepper (<i>Piper nigrum</i>)	Seeds	Piperine		Protective action against neurodegeneration and memory impairment	Chonpathompikunlert et al., 2010
22.	Ginger (<i>Zingier officinalis</i>)	Rizome	Crude extract	PC 12 cells	Inhibition of Amyloid- β aggregation	Guo JP et al., 2010
23.	Clove (<i>Syzygium aromaticum</i>)	Cloves	Eugenol	Wistar rat model	Protective action in rat models against depression	Song J et al., 2007

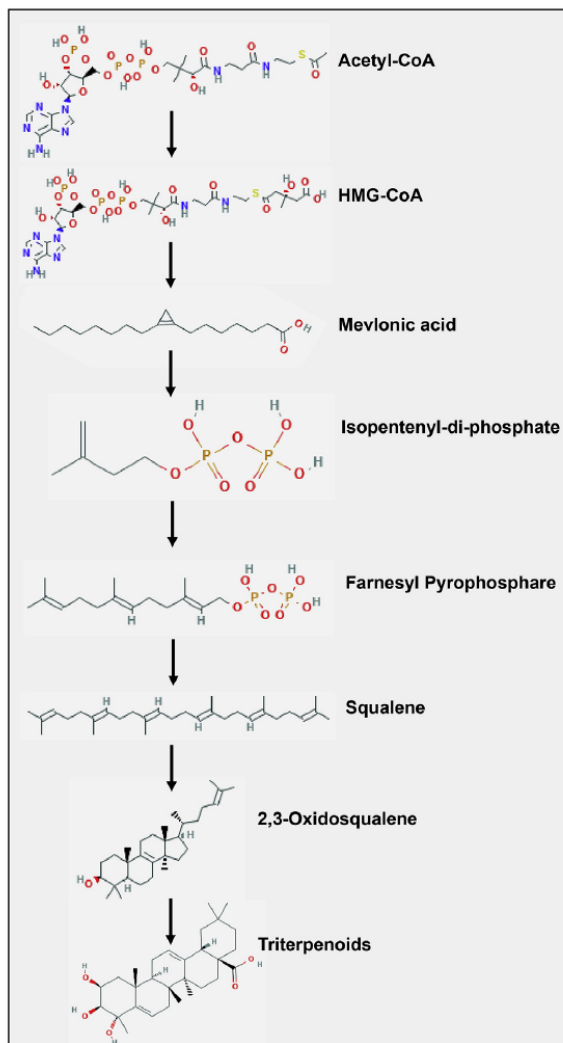


Fig. 2. The MVA pathway. The triterpenoids Bacoside is generated as an end products of Mevalonate pathway (MVA) in Brahmi. The MVA pathway starts with Acetyl Co-A. Acetyl Co-A converted to HMG-CoA via reaction catalysed by HMG-CoA synthase. Further HMG-CoA converted to Mevlonic acid via action of HMG-CoA reductase. IPP formed by Mevlonic acid via action of variety of enzyme such as mevalonate-5-phosphatase kinase. The final product of MVA cycle results in generation Triterpenoids from Isopentenyl di-phosphate (IPP).

1.3. Tau and its role

Tau is a microtubule-associated protein (MAP), functioning as a stabilizer of microtubule integrity. The pathological conditions, leads to downregulation of Tau affinity for microtubules ultimately resulting in formation of toxic aggregates [32–35]. Tau is encoded by gene located at 17q21 chromosome, six isoforms of Tau are being reported so far, which are generated as a result of alternative splicing. Tau aggregates generates of neurotoxicity that causes neurodegeneration, thus the aggregation inhibition of Tau is considered as important target for studying the therapeutic potency of molecules [36–38]. The repeat region of Tau have two hexapeptides VQIINK and VQIVYK, which are considered to be responsible for its aggregation. Physiological role of Tau is to stabilize the microtubules whereas; in several post-

translational modifications (PTMs) of Tau including phosphorylation, glycation, ubiquitination, glycosylation, etc., leads to the pathological Tau. Phosphorylation of Tau protein is the important PTM reported to be associated with AD pathology [39,40]. GSK3 β , CDK5/p25, MAPK are the kinase involved in the hyperphosphorylation of Tau leading to generation of Tau aggregates [41,42]. Various synthetic as well as natural compounds have been studied for inhibition of neurotoxic Tau aggregation. Compounds extracted from natural origin e.g. Galantamine, Curcumin, EGCG, limonoids, Homotaurine., have also been tested for their potency against Tau [43–47]. Flavonoid of *Hibiscus* Cinnamaldehyde from *Cinnamomum zelanicum* and Procynadines also been reported to inhibit Tau aggregation [48]. Likewise β -sitosterol and β -estradiol from tender coconut juice and ginsenoside from ginseng also exhibits the protective potency against Tauopathy [49]. The effect of Brahmi extract has not been studied in case of Tauopathies yet. Henceforth, the studies related to role of Brahmi extract against Tau aggregation would lead the researches in a way to investigate the cure for AD. The nootropic herb Brahmi is known to up regulate the cell metabolism by decreasing many of risk factors, Hence, the neuroprotective efficiency of Brahmi in context of various neurodegenerative conditions and future applications of Brahmi in Alzheimer's disease are the key points that are addressed in the present review.

2. Brahmi and its active components

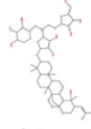
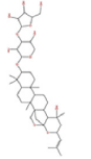
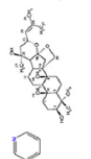
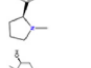
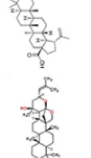
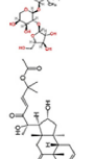
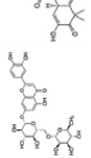
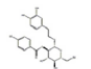
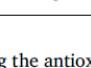
Brahmi is a creeper plant of height 2–3 feet with branched leaves and purple flowers, inhabiting the damp and marshy areas. It was previously addressed in Ayurveda as a 'medhya rasayana', or "the memory booster herb" [50,51]. The phytochemical analysis of Brahmi extract revealed the presence of several bioactive component in the extract [52]. The Brahmi extract reported to contain compounds belonging to triterpenoids saponins, alkaloids, glycoside and alcohols. The Brahmi extract contains alkaloids such as "Brahmine", Nicotine and Herpestine. The dammarane type triterpenoids saponins such as Bacoside A [3-(α -L-arabinopyranosyl)-O- β -D-glucopyranoside, 20-dihydroxy-16-keto-dammar-24-ene] is considered as a major bioactive component of Brahmi. Further studies have reported presence of triterpenoid saponin 3- β -[O- β -D-glucopyranosyl (1-3)-O-(α -L-arabinofuranosyl (1-2))-O- β -D-glucopyranosyl]oxy], which is named as Bacoside A3. The glycoside component of Brahmi extract contain chemicals such as pseudojубogenin, which is chemically identified as 3-O-(α -1-arabinofuranosyl (1-2) β -D-glucopyranosyl]. The methanolic extract of Brahmi yielded two pseudojубogenin glycoside identified as 3-O- α -1-arabinofuranosyl-1(1-2)-[6-O-sulphonyl- β -D-glucopyranosil-(1-3)]- α -1-arabinopyranosyl pseudojубogenin and 3-O- α -1-arabinofuranosyl-1(1-2)-[β -D-glucopyranosil-1(1-3)] β -D-glucopyranosyl pseudojубogenin [53]. One of noval saponin named bacopasaponin G was isolated from ethanolic extract of Brahmi, which chemically identified as 3-O-(α -1-arabinofuranosyl-1(1-2))- α -L-arabino-pyrosyl jубogenin [54]. A, phenylethanoid glycoside, 3,4-dihydroxyphenylethyl alcohol (2-O-feruloyl)- β -D-glucopyranoside and phenylethyl alcohol [5-O-p-hydroxybenzoyl- β -D-apifuranosyl-(1-2)- β -D-glucopyranoside [55] "Bacoside A" and "Bacoside B" are the main components reported to be responsible for Brahmi's neuroprotective efficiency. Bacoside A is a mixture of various saponins as Bacoside A3, bacopaside, jубogenin, bacopasaponin C. The synthesis of bacoside took place by mevalonate (MVA) and methyl-D-erythritol-4-phosphate (MEP) pathway [56] (Fig. 2 and Table 2).

3. Brahmi as an antioxidant

Reactive oxygen species are the oxygen-derived free radicals, which have short half-life and unpaired electron in their valence shells. Excessive ROS accumulation in cells leads to damage of cellular machinery resulting in diseases such as inflammation, cancer, and neurodegeneration [57,58]. Oxidative stress or ROS generates numerous

Table 2

The bioactive component of Brahmi extract. Brahmi extract comprises of a variety of bioactive component belonging to different chemical families. Most of the bioactive component of Brahmi are identified as Triterpanoids. All the chemical structures were adapted from Pubchem-data base.

S.No.	Bioactive component	IUPAC Name	Chemical Formula	Chemical Structure	Category
1	Bacoside A2	2-[2-[3,4-Dihydroxy-5-(hydroxymethyl)oxolan-2-yl]oxy-1-[3,4-dihydroxy-5-[[16-hydroxy-2,6,6,10,16-pentamethyl-17-(2-methylprop-1-enyl)-19,21-dioxahexacyclo[18.2.1.01,14.02,11.05,10.015,20]tricosan-7-yl]oxy]oxolan-2-yl]ethoxy]oxane-3,4,5-triol	C46H74O17		Triterpanoids saponins
2	Bacoside A	[3-(α -L-arabinopyronyl)-O- β -D-glucopyronaside, 20-dihydroxy-16-keto-dammar-24-ene]	C40H64O12		Triterpanoids saponins
3	Bacoside A3	3- β -[O- β -D-glucopyronosyl (1-3)-O-(α -L-arabinofuranosyl (1-2))-O- β -D-glucopyronosyl]oxy]	C47H76O18		Triterpanoids saponins
4	Pseudojubilogenin	3-O-(α -1-arabinofuranosyl (1-2) β -D-glucopyronosyl]	C46H74O17		Glycoside
5	Nicotine	(S)-3-[1-Methylpyrrolidin-2-yl]pyridine	C10H14N2		Alkaloid
6	Betulinic acid	(3 β)-3-hydroxy-lup-20(29)-en-28-oic acid	C30H48O3		triterpanoid
7	Bacopasaponin G	3-O-(α -1-arabinofuranosyl(1-2))- α -L-arabino-pyrosyl jujubogenin	C46H74O17		Saponins
8	Cucurbitacin E	[(E,6R)-6-[8S,9R,10R,13R,14S,16R,17R)-2,16-dihydroxy-4,4,9,13,14-pentamethyl-3,11-dioxo-8,10,12,15,16,17-hexahydro-7H-cyclopenta[a]phenantren-17-yl]-6-hydroxy-2-methyl-5-oxohept-3-en-2-yl] acetate	C32H44O8		triterpene
9	Luteolin-7-rutinoside	2-(3,4-dihydroxyphenyl)-5-hydroxy-7-[(2S,4S,5S)-3,4,5-trihydroxy-6-[[2R,4S,5R)-3,4,5-trihydroxy-6-methyl-oxan-2-yl]oxymethyl]oxan-2-yl]oxychromen-4-one	C27H30O15		Triterpanoids
10	Monnieraside III	(((2R,3R,4S,5S,6R)-2-[2-(3,4-Dihydroxyphenyl)ethoxy]-4,5-dihydroxy-6-(hydroxymethyl)oxan-3-yl] 4-hydroxybenzoate)	C21H24O10		Triterpanoids

neurological dysfunctions, including oxidation of enzymes, protein aggregation and membrane disruption, resulting in gradual loss of neurons [59]. To overcome the oxidative stress neurons have the antioxidant machinery, comprises of enzymatic as well as non-enzymatic pathways. The enzymatic machinery of cell to overcome oxidative stress includes the proteins like-SOD, catalase, GSH peroxidase. Glutathione (GSH) is a tripeptide of Glutamate, Cysteine and Glycine majorly act as defence mechanism in cells [60]. Oxidative stress activates

transcription factors Nrf2, triggering the antioxidant response elements (AREs) in nucleus [61]. NF Kappa- β is a transcription factor known to be activated by ROS [62]. The downregulation of cellular defense machinery against oxidative stress results in generation of neuronal toxicity and neurodegeneration [63]. ROS accumulate in mitochondria, which leads to generation of several mitochondrial dysfunction as it damages the cytochrome IV and V complexes resulting in increased oxidative burden in cells [64]. Hence several antioxidant molecules

have been studied for their therapeutic potential in AD. The antioxidant property of Brahmi have been evidenced by several studies. Brahmi treatment found to upregulate expression of various antioxidant molecules as SOD and GSH. Furthermore, Brahmi studied to quench the H_2O_2 -mediated oxidative stress *in-vitro* as well as *in-vivo* [65]. Lipoygenase enzyme degrade the cell membrane by deoxygenation of polyunsaturated fatty acids leading to degeneration of cell. Brahmi reportedly down regulate the lipoygenase activity in mouse brain and facilitates the rescue from oxidative stress [66]. Furthermore, oral administration of Brahmi extract in streptozotocin-induced diabetic mouse, increases the activity of SOD, glutathione peroxidase and reduce glutathione [67]. Additionally administration of Brahmi down regulated the catalase activity in diabetic mice [68]. Nrf2 and NF-kappa β are two major transcription factor involved in antioxidant machinery of cells. Low doses of Brahmi found to increase Nrf2 and NF-kappa- β expression in okadaic acid treated *wistar* rat [69]. The aqueous and ethanolic extract of Brahmi showed a potent free radical scavenging activity [70]. Moreover, the *in-vitro* studies evidenced Brahmi to be a potent free radical scavenger [71]. In addition to cellular studies, *in-vitro* studies also supported the free radicle quenching potency of Brahmi [72]. Reactive nitrogen species (RNS) also contribute in producing stress to cells as ROS, arginine-derived nitric oxide induces cell damage by deactivating many enzymes required for cellular metabolism. Recent studies suggested that in addition to oxygen stress, Brahmi

also found to reduce S-nitroso-N-acetyl-DL-penicillamine (SNAP) induced NO stress in cells [73] (Fig. 3).

4. Brahmi in neuroinflammation

A number of factors such as brain injuries, exposure to toxins, deposition of protein aggregates trigger the inflammatory responses in central nervous system (CNS). The microglia residing in CNS are the principle immune cells, which leads to neuroinflammation via several signalling proteins predominantly the interleukins IL-6, IL-10 and TNF- α , and cytokines [74,75]. The exposure of LPS, Amyloid- β fibres *etc.*, are the immunogenic factor, which triggers the activation of microglia from resting to activated stage. M1 microglia secretes pro-inflammatory protein including IL-1 β , IL-6 and TNF- α , which leads to neuroinflammation [76,77]. Mesodermal hematopoietic cell-derived microglia enters in brain at developmental stages and ultimately forms 5–20% of total glial cells population [78]. Microglia obtains variety of shapes and morphology *viz.* ramified, activated and amoeboid microglial cells [79]. Immunological pathways are known to be involved in AD, where activated microglia secretes pro-inflammatory cytokines causing neurotoxicity [80]. As a neuroprotective herb, the effect of Brahmi has been studied illustratively in context of downregulating neuroinflammation. Lower doses of Brahmi extract treatment was found to reduces the interleukin and TNF- α levels in LPS-induced N9 microglial cells [81].

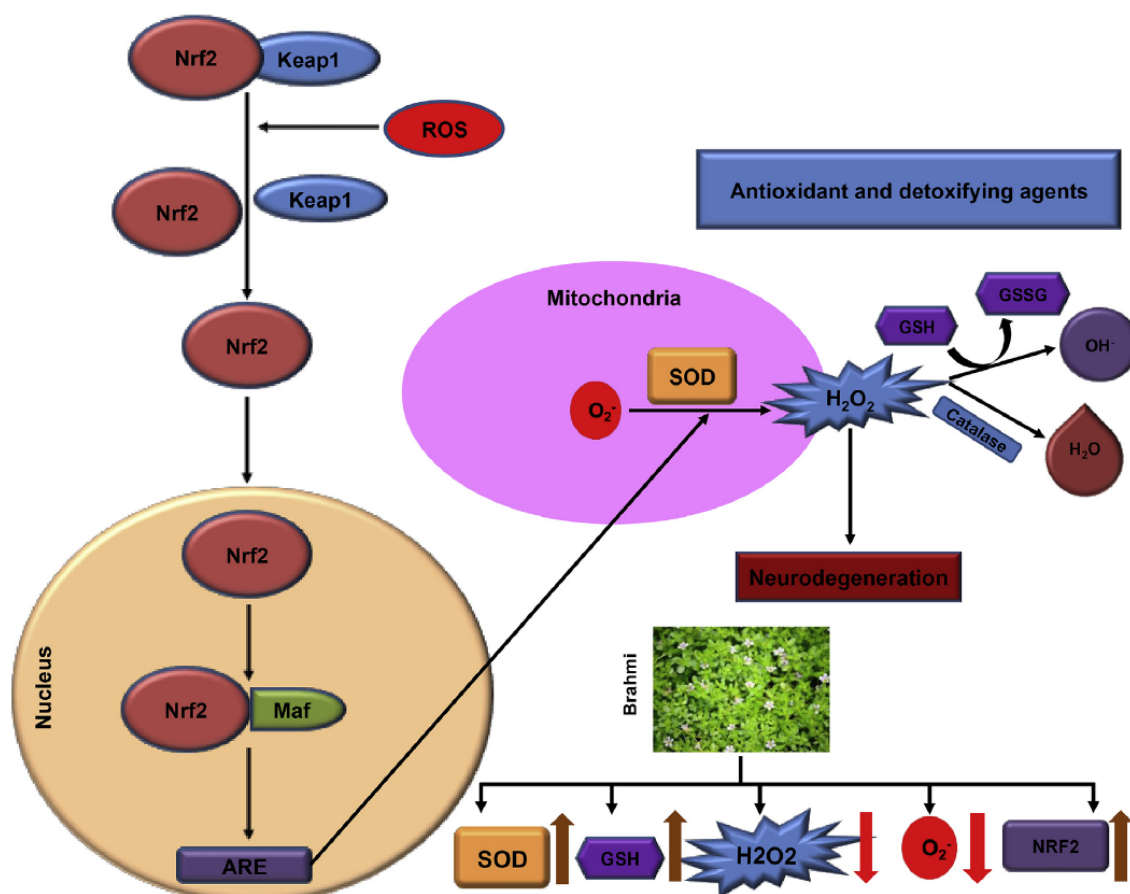


Fig. 3. Brahmi possess antioxidant properties and reduces oxidative stress in cells. The cell have defence machinery to overcome the oxidative stress. Nrf2 is a transcription factor which under oxidative stress translocate to nucleus. The binding of Nrf2 to antioxidant response element (ARE) leads to translation of enzymes as SOD, Catalase and GSH, which provides shield to cells against oxidative stress. Accumulation of ROS in cells leads to generation of mitochondrial fragmentation in AD. Brahmi found to possess the antioxidant property as exposure of Brahmi in cells increases the levels of Nrf2, SOD and GSH in cells. On contrary the levels of H_2O_2 , peroxide ions downregulated in presence of Brahmi. Thus, Brahmi is considered as a potent antioxidant herb.

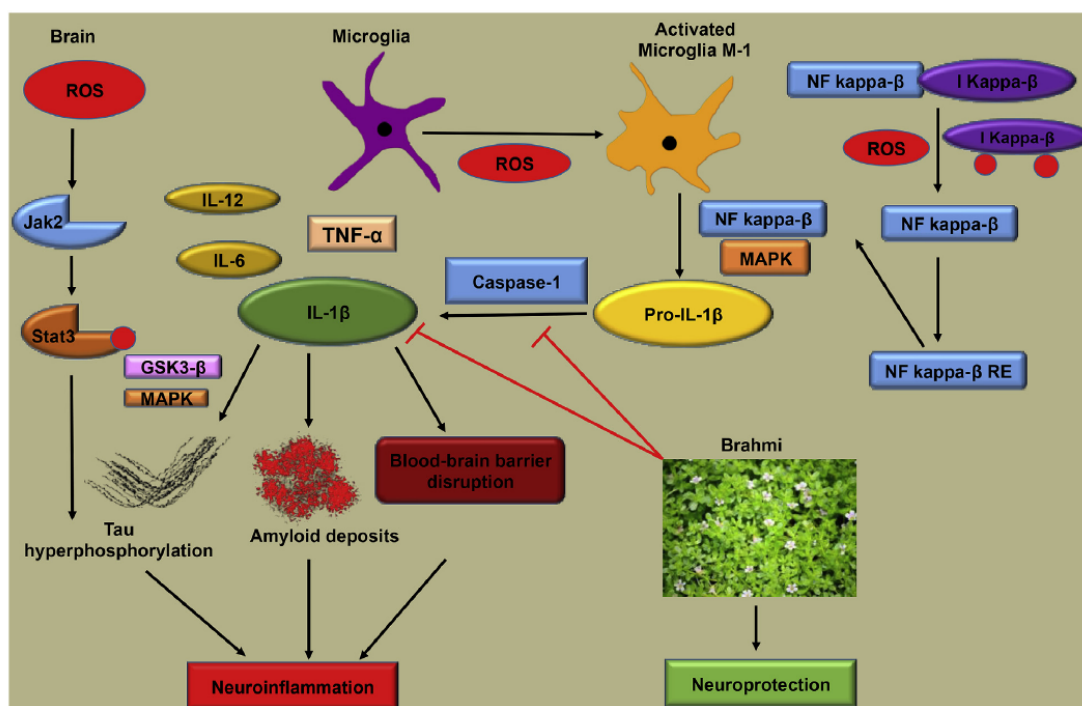


Fig. 4. Brahmi attenuate the neuroinflammation and leads to neuroprotection. Neuroinflammation is majorly related to activation M1 microglia. Under conditions as inflammation, the triggered microglial activation lead to release of pro-inflammatory cytokines. ROS is the prominent factor which activate NF-Kappa B and MAPK signalling cascades. Caspase 1 accelerate the secretion of inflammatory cytokines like IL-12, IL-6, IL-1 β and TNF- α ultimately resulting in neuroinflammation. Tau hyperphosphorylation and amyloid plaques formation are the prominent consequences of neuroinflammation. Recent studies demonstrated anti inflammation property of Brahmi which involved downregulating inflammatory cytokines-like IL-1 β , IL-6 and TNF- α and attenuated caspase-1 activity leading to protection of neurons from inflammation.

Caspase are the cysteine aspartate proteases, which are majorly involved in apoptosis and inflammatory pathways. Caspase-10 is an interleukin converting enzyme (ICE), involved in proteolytic cleavage of precursor protein interleukins precursor protein. Brahmi reportedly down regulated the caspase-10 level in cells and reverberated in reduction of neuroinflammation [82,83]. Furthermore, Brahmi-derived peptide found to increase the caspase-3 activity, the leaf extract of Brahmi was found to downregulate caspase-3 levels in sodium nitroprusside treated human embryonic lung epithelial cell line (L132) [73,84]. Betulinic acid (BA) is one of bioactive component of Brahmi BA was found to reduce the LPS-mediated pro-inflammatory response in cells as it reduced the COX-2 expression and prostaglandin E2 production. Additionally it also attenuates the Akt and ERK signalling cascade [85] (Fig. 4). The assessment of all previous studies suggested that Brahmi could be designated as a potent anti-inflammatory herb protecting the cells from the neurodegeneration.

5. Role of Brahmi in Tau and Amyloid- β

Inhibition of Amyloid- β and Tau aggregation is an emerging strategy for attenuation of AD. Numerous ayurvedic extracts such as *Withania Somanifera* (ashwagandha) and Brahmi have been reported for their potency in inhibiting the Amyloid- β -mediated toxicity [86,87]. Amyloid- β oligomers are the extracellular aggregates of Amyloid- β 42 peptides. The cleaving of amyloid precursor protein (APP) by action of β -secretase and γ -secretase leads to generation of Amyloid- β peptide monomers [88,88,89]. These soluble monomer aggregates in cholesterol-rich region of neuronal membrane leading to formation of soluble Amyloid- β oligomers, which could obtain diverse β -sheet rich

structures. The interaction of these oligomers with various receptors eg. NMDA, NGF, insulin, frizzled *etc*; leads to generation various metabolic impairments such as increased GSK-3 β kinase activity, impaired insulin signalling, increased ROS, which ultimately results in cytotoxicity [90]. Amyloid- β oligomers and Tau oligomers are being reported as a major cause of mitochondrial dysfunction, which leads to neuronal toxicity resulting in Alzheimer's disease [91]. One of the cause of mitochondrial dysfunction is the inhibition of Cytochrome C by Amyloid- β oligomers, additionally Dynamin-related protein 1(Drp1) was observed to mediate the Amyloid- β 42 related mitochondrial dysfunction in AD [92,93]. Thus Amyloid β oligomers are considered as a main target for AD treatment. Recent studies advocated the defensive property of Brahmi against A β -mediated toxicity in primary cultures. Brahmi treatment also found to reduce amyloid- β -induced acetylcholine levels in cells. The bioactive component of Brahmi, Bacoside A showed neuroprotective activity against Amyloid- β -induced cytotoxicity in SH-SY5Y cells. The rescue of Amyloid- β -induced neuronal toxicity in presence of Bacoside A has been well reported in earlier [31] Bacoside A dissolves the matured aggregates of Amyloid- β and hence it was suggested that Bacoside could act in revising the amyloid- β -mediated toxicity in cells [94]. Furthermore Bacoside A reportedly reduced the amyloid levels in PSAPP mouse supporting the feasibility of Bacoside A in crossing the blood-brain barrier [95]. Unlike bacoside, betulinic acid (BA) induces the rapid fibrilization of Amyloid- β and reduces the oligomer formation of Amyloid- β [96] (Fig. 5). In contrast to extracellular Amyloid- β aggregates, intracellular aggregates of Tau are also considered as a cause of AD. However the effect of Brahmi against Tauopathy has not been studied illustratively, some of the recent studies of Brahmi extract on Tau protein suggested that the Brahmi extract treatment in NGF-

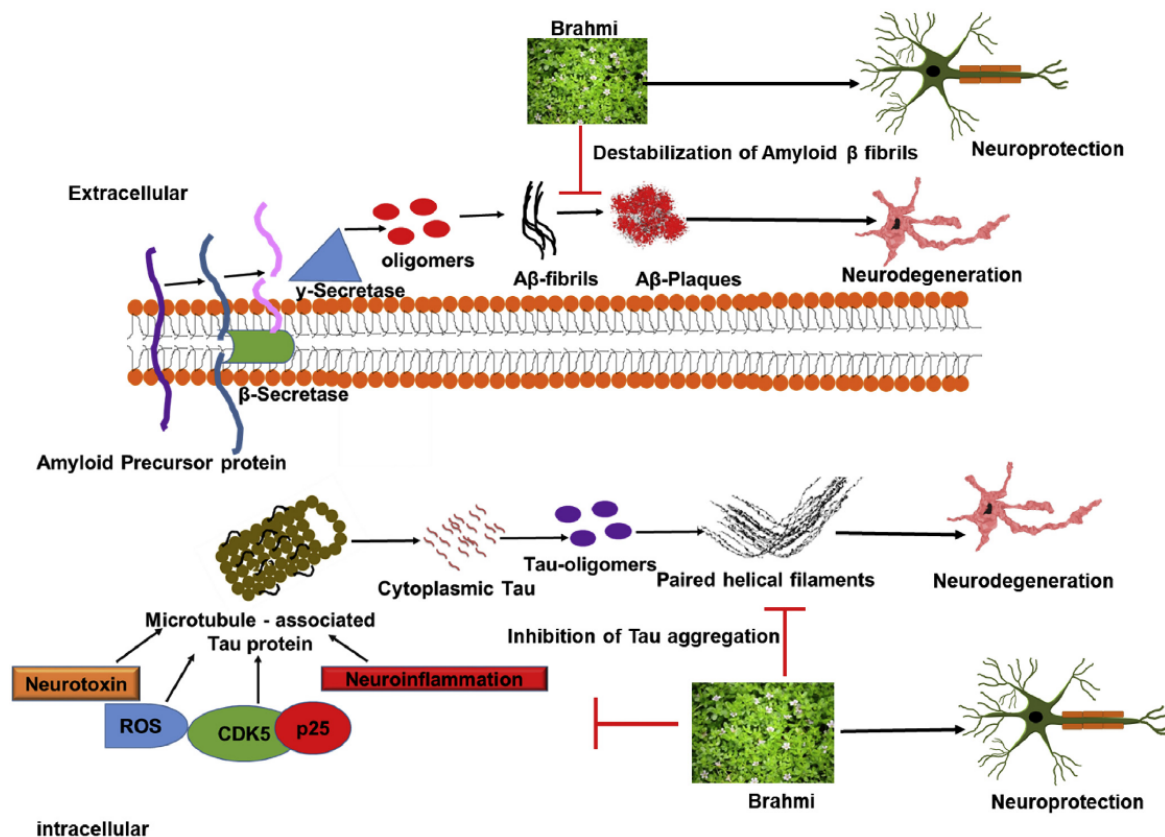


Fig. 5. The role of Brahmi in reducing the Protein aggregate related pathology. Extracellular amyloid plaques and intracellular tangles are the two hallmarks of AD. γ -Secretase mediated cleavage of APP led to generation of Amyloid- β 42 peptides which self-aggregate in shape of plaques and leads to neurotoxicity. A β -42 oligomers leads to mitochondrial dysfunction resulting in cytotoxicity. Brahmi is reported to inhibit the Amyloid- β -mediated toxicity in neuron ultimately protecting the neurons. Microtubule-associated protein Tau is another AD related protein, which under pathological condition as exposure to neurotoxin, ROS or PTMs as phosphorylation led to generation of toxic intracellular PHFs. Here we are hypothesizing that Brahmi could rescue the Tau-mediated pathology by down regulating the Tau hyperphosphorylation, neuroinflammation, and ROS production. The effect of Brahmi would be studied in context of Tau phosphorylation, ROS production, and neuroinflammation.

deprived PC12 cells reduces the phospho-Tau levels and attenuates Tau-mediated toxicity [97]. The role of Brahmi in context of rescuing the Tau-mediated toxicity is still need to be studied illustratively as several aspects such as phosphorylation, generation of oxidative stress, inhibition of aggregation have not been investigated.

Cognition is the ability of individual to acquire knowledge, logical thinking and analysing the facts which include judgment, language and problem solving [63]. Neurodegenerative conditions lead to declination of learning and memorizing ability of individual in great extent. Henceforth, medications are being targeted to improve the cognitive function of brain. Brahmi is a designated memory booster herb, hence it is regularly administered for various neurological disabilities. Recent studies proved Brahmi as a nootropic drug, *i.e.* it restores the cognitive and learning efficiency of brain [52]. The ethylcholine aziridium induced *Wistar* rat model of AD, Brahmi showed rescuing of cognitive efficiency. Oral administration of Brahmi extract showed improved escape latency time in *morris water maze* test indicating improved cognitive behaviour [68,98]. Moreover, the Brahmi treatment of 100–200 mg/kg showed the revision of scopolamine-induced amnesia and natural aging in mice [99]. Epilepsy leads to deregulation of NMDA receptors, whereas Brahmi treatment brings back the NMDA receptors near to control level. Apart from animal models, clinical trials also carried out using standardized Brahmi extract. The reported results

suggest that Brahmi has mild effect in improving the cognitive behaviours of humans [100].

6. Downside of ayurvedic formulations

Ayurvedic formulations despite of being plant origin known to have side-effect. If the standardized protocol have not followed for synthesis, the errors including contamination of heavy metals, excessive alcohol generation in formulations leads to unexpected ill effects in patient [101,102]. Furthermore, the bioavailability of ayurvedic herbs also need to be increased as the course for these medicine extent for months [103]. Thus the current studies needs to be focused more on improving the bioavailability of these herbs with generation of minimum side-effects.

7. Poly-pharmacological evaluation of Brahmi

The researches have been strongly focussed on formulating the therapeutic molecules against AD. Despite of illustrate studies no prominent remedy of AD have been invested. Till date three drugs, Donepezil, Rivastigmine, Galantamine are being widely accepted and prescribed by medical practitioners [104–106]. Here on the basis of all the current studies we can hypothesize that poly-pharmacological

formulations of brahmi along with classical anti-dementia drug could increase the pharco kinetic property of drugs. The combination of these drugs with Brahmi could result in stable recovery the AD patient.

8. Conclusion and perspectives

Alzheimer's disease is associated with various neurodegenerative symptoms. The aggregates of Tau protein are the predominant cause of AD. The current pharmacological approaches are mildly effective in attenuating AD. Thus, certain new approaches have been tested for AD, which prominently includes application of natural products. Brahmi (*Bacopa Monnerei*) is a well-known neuroprotective herb. The effect of Brahmi is well elucidated in various aspects of neurodegeneration. Previous studies have suggested the antioxidant, anti-inflammatory, viability and proliferative effect of Brahmi. Here we are hypothesizing that Brahmi could be effective in overcoming the Tau-mediated pathology in neurons. Henceforth, nootropic herb Brahmi could be beneficial in overcoming the AD symptoms and pathology.

Author contributions

T.D contributed to design and drafting the manuscript; in acquisition, analysis and interpretation of the data. T.D and S.C wrote the manuscript. S.C. in conception or design, revising manuscript critically for important intellectual content and the final approval of the version to be submitted.

Declaration of competing interest

The authors listed this article certifies that they have no conflict of interest and competing financial interest.

Acknowledgements

This project is supported in part by grant from the in-house, National Chemical Laboratory-Council of Scientific Industrial Research-(CSIR-NCL) grant MLP029526. Tushar Dubey acknowledges the fellowship from University of Grant Commission (UGC), India.

References

- C.P. Khare, Indian Herbal Remedies: Rational Western Therapy, Ayurvedic, and Other Traditional Usage, Springer science & business media, Botany, 2004.
- V. Lad, Textbook of Ayurveda, Ayurvedic Press, 2002.
- A. Hankey, Ayurvedic physiology and etiology: ayurveda Amritanaam. The doshas and their functioning in terms of contemporary biology and physical chemistry, J. Altern. Complement. Med. 7 (5) (2001) 567–574.
- A. Hankey, The scientific value of Ayurveda, J. Altern. Complement. Med. 11 (2) (2005) 221–225.
- P.K. Mukherjee, A. Wahile, Integrated approaches towards drug development from Ayurveda and other Indian system of medicines, J. Ethnopharmacol. 103 (1) (2006) 25–35.
- K.G. Ramawat, S. Dass, M. Mathur, Herbal Drugs: Ethnomedicine to Modern Medicine, Springer, 2009.
- S. Przedborski, M. Vila, V. Jackson-Lewis, Series Introduction: neurodegeneration: what is it and where are we? J. Clin. Investig. 111 (1) (2003) 3–10.
- B.S. Shastry, Neurodegenerative disorders of protein aggregation, Neurochem. Int. 43 (1) (2003) 1–7.
- J.K. Andersen, Oxidative stress in neurodegeneration: cause or consequence? Nat. Med. 10 (7s) (2004) S18.
- H. Khanam, A. Ali, M. Asif, Neurodegenerative diseases linked to misfolded proteins and their therapeutic approaches: a review, Eur. J. Med. Chem. 124 (2016) 1121–1141.
- M.B. Feany, D.W. Dickson, Neurodegenerative disorders with extensive tau pathology: a comparative study and review, Ann. Neurol.: Off. J. Am. Neurol. Assoc. Child Neurol. Soc. 40 (2) (1996) 139–148.
- A.s. Association, 2018 Alzheimer's disease facts and figures, Alzheimer's Dementia 14 (3) (2018) 367–429.
- A. Alzheimer's, 2015 Alzheimer's disease facts and figures, Alzheimer's Dementia: J. Alzheimer's Assoc. 11 (3) (2015) 332.
- A. Bordon, Molecular mechanisms of Alzheimer's disease, The Sci. J. Lander Coll. Arts Sci. 10 (2) (2017) 2.
- P.T. Francis, A.M. Palmer, M. Snape, G.K. Wilcock, The cholinergic hypothesis of Alzheimer's disease: a review of progress, J. Neurol. Neurosurg. Psychiatry 66 (2) (1999) 137–147.
- J. Loring, X. Wen, J. Lee, J. Seilhamer, R. Somogyi, A gene expression profile of Alzheimer's disease, DNA Cell Biol. 20 (11) (2001) 683–695.
- E. Rogaeve, R. Sherrington, E. Rogaeve, G. Levesque, M. Ikeda, Y. Liang, H. Chi, C. Lin, K. Holman, T. Tsuda, Familial Alzheimer's disease in kindreds with missense mutations in a gene on chromosome 1 related to the Alzheimer's disease type 3 gene, Nature 376 (6543) (1995) 775.
- Y.S. Eisele, C. Monteiro, C. Fearn, S.E. Encalada, R.L. Wiseman, E.T. Powers, J.W. Kelly, Targeting protein aggregation for the treatment of degenerative diseases, Nat. Rev. Drug Discov. 14 (11) (2015) 759.
- J. Hardy, D.J. Selkoe, The amyloid hypothesis of Alzheimer's disease: progress and problems on the road to therapeutics, Science 297 (5580) (2002) 353–356.
- N. Sehgal, A. Gupta, R.K. Valli, S.D. Joshi, J.T. Mills, E. Hamel, P. Khanna, S.C. Jain, S.S. Thakur, V. Ravindranath, Withania somnifera reverses Alzheimer's disease pathology by enhancing low-density lipoprotein receptor-related protein in liver, Proc. Natl. Acad. Sci. 109 (9) (2012) 3510–3515.
- D.S. Kim, S.-Y. Park, J.-Y. Kim, Curcuminoids from Curcuma longa L. (Zingiberaceae) that protect PC12 rat pheochromocytoma and normal human umbilical vein endothelial cells from β A (1–42) insult, Neurosci. Lett. 303 (1) (2001) 57–61.
- J. Malik, M. Karan, K. Vasiht, Nootropic, anxiolytic and CNS-depressant studies on different plant sources of shankpushpi, Pharm. Biol. 49 (12) (2011) 1234–1242.
- H. Joshi, M. Parle, Nardostachys jatamansi improves learning and memory in mice, J. Med. Food 9 (1) (2006) 113–118.
- R.V. Rao, O. Descamps, V. John, D.E. Bredesen, Ayurvedic medicinal plants for Alzheimer's disease: a review, Alzheimer's Res. Ther. 4 (3) (2012) 22.
- M. Mazza, A. Capuano, P. Bria, S. Mazza, Ginkgo biloba and donepezil: a comparison in the treatment of Alzheimer's dementia in a randomized placebo-controlled double-blind study, Eur. J. Neurol. 13 (9) (2006) 981–985.
- X. Zhang, M. Shi, R. Ye, W. Wang, X. Liu, G. Zhang, J. Han, Y. Zhang, B. Wang, J. Zhao, Ginsenoside Rd attenuates Tau protein phosphorylation via the PI3K/AKT/GSK-3 β pathway after transient forebrain ischemia, Neurochem. Res. 39 (7) (2014) 1363–1373.
- E.S. Mengoni, G. Vichera, L.A. Rigano, M.L. Rodriguez-Puebla, S.R. Galliano, E.E. Cafferata, O.H. Pivetta, S. Moreno, A.A. Vojnov, Suppression of COX-2, IL-1 β and TNF- α expression and leukocyte infiltration in inflamed skin by bioactive compounds from Rosmarinus officinalis L, Fitoterapia 82 (3) (2011) 414–421.
- P.K. Mukherjee, V. Kumar, M. Mal, P.J. Houghton, In vitro acetylcholinesterase inhibitory activity of the essential oil from Acorus calamus and its main constituents, Planta Med. 73 (03) (2007) 283–285.
- T. Crow, A. Cross, S. Cooper, J. Deakin, I. Ferrier, J. Johnson, M. Joseph, F. Owen, M. Poulter, R. Lofthouse, Neurotransmitter receptors and monoamine metabolites in the brains of patients with Alzheimer-type dementia and depression, and suicides, Neuropharmacology 23 (12) (1984) 1561–1569.
- D. Khare, P. Savanur, Understanding of unmadia in ayurveda and rational application of herbal drugs-A review, J. Ayurveda Integr. Med. Sci. 4 (4) (2019) 279–288 2456–3110.
- N. Limpeanchob, S. Jaipan, S. Rattanakaruna, W. Phrompittayarat, K. Ingkaninan, Neuroprotective effect of Bacopa monnieri on beta-amyloid-induced cell death in primary cortical culture, J. Ethnopharmacol. 120 (1) (2008) 112–117.
- L. Buée, T. Bussièrè, V. Buée-Scherrer, A. Delacourte, P.R. Hof, Tau protein isoforms, phosphorylation and role in neurodegenerative disorders, Brain Res. Rev. 33 (1) (2000) 95–130.
- N.V. Gorantla, V.G. Landge, P.G. Nagaraju, L.P. Sunny, A. Nair, S.P. Midya, P. Priyadarshini, B. Ekambaram, S. Chinnathambi, Molecular Complexes for Effective Inhibition of Tau Aggregation, bioRxiv, 2018, p. 363572.
- Y. Wang, E. Mandelkow, Tau in physiology and pathology, Nat. Rev. Neurosci. 17 (1) (2016) 22.
- T. Dubey, N.V. gorantala, k.T. Chandrashekara, S. Chinnathambi, Photo-excited Toluidine blue inhibits Tau aggregation in Alzheimers disease, ACS Omega (2019), <https://doi.org/10.1021/acsomega.9b02792>.
- A.A. Balmik, S. Chinnathambi, Multi-faceted role of melatonin in neuroprotection and amelioration of Tau aggregates in Alzheimer's disease, J. Alzheimer's Dis. 62 (4) (2018) 1481–1493.
- N.V. Gorantla, S. Chinnathambi, Tau protein squired by molecular chaperones during Alzheimer's disease, J. Mol. Neurosci. 66 (3) (2018) 356–368.
- E.-M. Mandelkow, E. Mandelkow, Biochemistry and cell biology of tau protein in neurofibrillary degeneration, Cold Spring Harb. Perspect. Med. (2012) a006247.
- J. Avila, J.J. Lucas, M. Perez, F. Hernandez, Role of tau protein in both physiological and pathological conditions, Physiol. Rev. 84 (2) (2004) 361–384.
- S.K. Sonawane, S. Chinnathambi, Prion-like propagation of post-translationally modified tau in Alzheimer's disease: a hypothesis, J. Mol. Neurosci. 65 (4) (2018) 480–490.
- G. Šimić, M. Babić Leko, S. Wray, C. Harrington, I. Delalle, N. Jovanov-Milošević, D. Bažadona, L. Buée, R. De Silva, G. Di Giovanni, Tau protein hyperphosphorylation and aggregation in Alzheimer's disease and other tauopathies, and possible neuroprotective strategies, Biomolecules 6 (1) (2016) 6.
- S.K. Sonawane, A. Ahmad, S. Chinnathambi, Protein-capped metal nanoparticles inhibit tau aggregation in Alzheimer's disease, ACS Omega 4 (7) (2019) 12833–12840.
- B. Bulic, M. Pickhardt, B. Schmidt, E.M. Mandelkow, H. Waldmann, E. Mandelkow, Development of tau aggregation inhibitors for Alzheimer's disease, Angew. Chem. Int. Ed. 48 (10) (2009) 1740–1752.
- C. Caltagirone, L. Ferrannini, N. Marchionni, G. Nappi, G. Scapagnini, M. Trabucchi, The potential protective effect of tramiprosate (homotaurine) against Alzheimer's disease: a review, Aging Clin. Exp. Res. 24 (6) (2012) 580–587.
- H. Geerts, Indicators of neuroprotection with galantamine, Brain Res. Bull. 64 (6) (2005) 519–524.
- N.V. Gorantla, R. Das, F.A. Mulani, H.V. Thulasiram, S. Chinnathambi, Neem